Reprogramming Human Keratinocytes: A Non-Viral, MicroRNA Approach

Thesis submitted in accordance with the requirements of the University of Liverpool for the degree of Doctor in Philosophy

By

Fiona Christine Lewis

July 2012

ABSTRACT

The ability to reprogram somatic cells toward a stem cell phenotype has created a powerful method of reversing the fate of lineage restricted cells. If the potential of reprogramming is realised we will be able to provide a source of autologous, functional cells circumventing many of the issues associated with donor transplantation and provide a source of stem cells free from the controversy surrounding derivation from embryos.

MicroRNA (miRNAs) are an attractive substitute to foreign DNA for induction of reprogramming. This thesis focused on a specific miRNA, miR-145 due to its role as a repressor of pluripotency during embryogenesis. The majority of reprogramming approaches to date have utilised viral vectors to deliver inducing stimuli however a considerable amount of literature strongly suggests that cells reprogrammed using viral vectors are unsuitable from a clinical perspective due to risks associated with insertional mutagenesis and potential immunogenicity. Therefore this investigation sought a non-viral method of delivering inducing stimuli and an electroporation based technique, known as nucleofection was identified. This non-viral delivery method was evaluated in terms of its efficiency and cell viability and was found to be highly effective in its capacity to deliver both plasmid DNA and miRNA inhibitors to human epidermal keratinocytes (hEKs).

Nucleofection of hEKs with an antisense oligonucleotide, which effectively inhibits miR-145 was shown to significantly increase the expression of *Oct4, Sox2, Klf4* and *c-Myc* all of which are required for the successful reprogramming of somatic cells. MiR-145 inhibited hEKs were subsequently subjected to modified culture conditions in an attempt to further promote the expression of pluripotency-associated transcription factors. hESC media containing growth factors, known to promote a

human embryonic stem cell phenotype, lead to a distinctive change in cell morphology with cells clustering together to form colonies and also further stimulated the expression of pluripotency associated genes. While hEKs did exhibited re-expression of normally silenced pluripotency genes they had not undergone full cellular reprogramming however now presented a more ‘plastic’ phenotype.

A direct reprogramming approach was formulated where miR-145 inhibition of hEKs was performed and post-nucleofection cells were incubated using either standard hEK media or growth factor supplemented hESC media for 5 days. Defined osteogenic, chondrogenic or adipogenic differentiation media were then applied to stimulate reprogramming towards ‘tri-lineage’ fates, whilst crucially demonstrating transgermal differentiation of hEKs. A defined neurogenic media was also applied to further validate their differentiation potential and together this provided further evidence for acquisition of a ‘plastic’ phenotype with identification of lineage specific markers following directed differentiation.

Taken together this investigation details a novel, miRNA mediated strategy for the direct reprogramming of hEKs in the absence of foreign DNA or viral vectors whilst facilitating re-differentiation into a number of desirable lineages offering significant advances for clinical translation.

ACKNOWLEDGEMENTS

First and foremost I would like to thank my supervisors Prof. John Hunt and Dr. Nicholas Rhodes for their ideas, support and for allowing my PhD to be a productive and stimulating experience. I also gratefully acknowledge the EPSRC for funding, as without their monetary support this PhD would not have been possible.

I would like to extend my gratitude to Prof. David Edgar and Dr. Deepak Kalaskar for kindly providing a source of human embryonic stem cells and the technical expertise to culture these cells. This was an important resource throughout my PhD and your willingness to aid this research is greatly appreciated.

To everyone at the Department of Clinical Engineering who made my time here so enjoyable and fulfilling. This group has been a source of friendships as well as support and collaboration and I feel privileged to have been part of a team with such enthusiasm and expertise in this field. I would like to extend my gratitude to everyone here for their support, which took a number of forms and in particular to Dr. Judith Curran for both encouraging me to pursue a PhD and along with Dr. Nicholas Bryan, providing invaluable molecular biology advice. Finally I would like to thank the many friends here that became a part of my life, brightening even the dullest of days - I couldn't have done it without you!

Lastly, I would like to thank my friends and family for their continued love and encouragement in whatever I choose to pursue and most of all to Graham for his faithful support and confidence in me throughout.

CONTENTS

ABBREVIATIONS

ANOVA	Analysis of variance
BSA	Bovine serum albumin
CBFA1	**C**ore binding factor α1
Col I	Type-I collagen
Col II	Type-II collagen
DAPI	4',6'-diamidino-2-phenylindole
ECM	Extracellular Matrix
EDTA	Ethyenediaminetetraacetic acid
EthD-1	Ethidium homodimer-1
ESCs	Embryonic stem cells
FCS	Fetal calf serum
GFP-P	PmaxGFP plasmid
H&E	Haematoxylin and Eosin
HA	Hydroxyapatite
HCl	Hydrochloric acid
HFN	Human plasma fibronectin
IPSCs	Induced pluripotent stem cells
MEFs	Mouse embryonic fibroblasts
MiRNA	MicroRNA
MSCs	Mesenchymal stem cells
PBS	Phosphate buffered saline
PPARγ	Periosome proliferator-activated receptor γ
PPP	Platelet-Poor Plasma
qRT-PCR	Real-Time Polymerase Chain Reaction
SCNT	**S**omatic cell nuclear transfer
TCP	Tissue culture polystyrene

LIST OF FIGURES

Chapter 1 – INTRODUCTION

CHAPTER 2 – MATERIALS & METHODS

CHAPTER 3 – RESULTS

LIST OF TABLES

CHAPTER 2 – MATERIALS & METHODS

CHAPTER 3 - RESULTS

1.0 Introduction

1.1 Stem Cells in Tissue Engineering

Tissue engineering is the development of functional substitutes that restore, maintain or improve tissue function [1]. This field has progressed rapidly over the last decade with development of functional replacements for many tissues of the human body. The requirement for improved tissue engineered products remains evident nevertheless with transplantation of tissues and organs considerably limited by the number of compatible donors while alternative strategies, such as mechanical devices or artificial prostheses, fail to completely restore tissue function. If the promise of tissue engineering is realised it will provide an alternative solution to replace or repair tissue and ultimately patient quality of life, thus providing both economic and health benefits for the population.

In order to develop functional alternatives for use in tissue engineering human cells are often manipulated either by modifying their extracellular environment or by altering the cell's own genetic program to direct it towards a desired tissue type. In the search for a suitable source of cells for tissue engineering various candidates have been identified, each with benefits and limitations.

Autologous, lineage committed cells were initially thought to be an ideal candidate for tissue replacement strategies due to the functional benefits of these cells. However large numbers of cells are often required to repair damaged tissue, which must be generated either by extensive tissue harvesting or through expansion of smaller cell populations *ex vivo*. Investigations into lineage committed cells, such as osteoblasts and chondrocytes, revealed the cellular damage, incurred during harvesting, which contradicts the aim of tissue engineering in the first instance and

while smaller populations can be propagated *in vitro* this is often accompanied by loss of cellular function, rendering this approach inappropriate for tissue engineering.

Lineage uncommitted stem cells have caught the public and scientific imagination as they have been identified as an attractive alternative to autologous, lineage committed somatic cells. In terms of plasticity and self-renewal capabilities they offer many advantages while still presenting a patient-specific source of cells thus avoiding many of the complications associated with immune rejection. Their self-renewal characteristics are particularly important as this suggested these cells can be expanded indefinitely without loss of functionality [2]. The search for sources of adult stem cells has been one of the most prolific aspects in the field of tissue engineering with an abundance of sources identified within the human body. Stem cells reside within specific niches and are found amongst differentiated cells within a tissue or organ. They are characterised primarily by their ability to self renew, through mitotic cell division and differentiate into a diverse range of specialised cell types, to maintain or repair the tissue in which they reside [3-7]. Despite the initial hypothesis that lineage uncommitted stem cells derived from adult sources were restricted in their differentiation capacity to mesoderm-derived cells, this has now been widely disproved with adult stem cells forming tissues derived from the three germ layers with some tissue sources displaying more plasticity than others [8, 9].

Stem cells isolated from adult tissues have been extensively investigated as potential cell therapies for a wide range of diseases. One area that has received much interest is the treatment of cardiovascular disease, which is a leading cause of death worldwide. The majority of clinical trials aimed at treating cardiovascular disease have used bone marrow-derived

mononuclear cells however while there have been no reports of adverse side effects to these cells the improvement reported appears only marginal with no obvious long term improvements in heart function [10-12]. Promisingly recent clinical trials suggest that the progression of heart failure can be prevented or even reversed using resident cardiac stem cell based therapy with initial reports indicating that intracoronary infusion of autologous cardiac stem cells (CSCs) can significantly improve heart function and reduce infarct size in patients with heart failure after myocardial infarction [13]. This illustrates why we need to understand the basic biology of stem cells in order to unlock their potential in a clinical setting.

Diabetes mellitus, another debilitating disease affecting millions of people worldwide, has also been extensively targeted by adult stem cell therapy. Diabetes develops when the insulin-producing beta-cells are destroyed, resulting in an accumulation of glucose in the body, which produces an array of complications. Stem cell therapy was proposed as an attractive strategy to replace beta-cells to restore normal insulin levels, which has proven to be an achievable target with varying success rates. One study that demonstrates the potency of stem cell therapy as a treatment for diabetes reports autologous, non-myeloablative hematopoietic stem cell (HSC) transplantation in 15 newly diagnosed type I diabetes mellitus patients. This clinical trial resulted in the majority of patients becoming insulin free after 18 months [14] while a later follow-up study after 30 months confirmed an increase in beta-cell function [15].

Perhaps one of the greatest success stories of adult stem cells (ASCs) to date is the identification and clinical application of HSCs. These multipotent stem cells can be isolated from peripheral blood, bone marrow or cord blood and were first identified in mice in 1961 [16]. By 1999 over 50 diseases had been treated using bone marrow and stem cell therapy in humans including

leukaemia, inflammatory bowel disease and osteogenesis imperfecta [17]. The first global survey of HSC transplantation revealed that it has now become an accepted cell therapy worldwide with over 50,000 transplantations undertaken in 2006, providing one of the best examples of stem biology translated into the clinical arena [18].

Despite ASCs being identified as an attractive cell for therapeutic purposes they do generally represent a more lineage restricted source of cells compared to pluripotent embryonic stem cells (ESCs). Pluripotency is the term applied to a cell, which has the capacity to become any cell of an organism and was initially thought to be an exclusive property of early embryonic cells or their *in vitro* proxy, embryonic stem cells. As these cells differentiate to become more specialised their pluripotent characteristics are diminished and unless disrupted by disease these cells become restricted to their ultimate cell fate. Pluripotent ASCs, although rare and generally small in number, have been reported in the brain and umbilical cord blood [19, 20] however, these cell sources are not readily accessible and difficult to isolate therefore it is unlikely that stem cells isolated from these sources would be suitable for tissue engineering. While ASCs can be isolated from more accessible tissues, such as adipose [21] and dental pulp [22], their potential faces greater restrictions and cannot match the pluripotent differentiation capabilities of ESCs.

ESCs are derived from embryos, specifically epiblast tissue of the inner cell mass during the blastocyst stage of development. This group of cells are recognised as the most pluripotent of all stem cells and as a result of their distinctive cellular biology have an indefinite capacity to self-renew and give rise to all cell types within the three germ layers of the developing organism [23, 24]. Despite their huge potential there are also major drawbacks associated with ESCs as a source of cells for tissue engineering. As ESCs are derived from donor embryos they are non-autologous therefore

tissues derived from these stem cells would likely be rejected by the host's immune system upon transplantation [25].

Research into human embryonic stem cells (hESCs) has also been fraught with ethical concerns primarily due to the destruction of human blastocysts during isolation however it appeared there may be potential for the development of hESC therapies with the approval of the first human clinical trials using hESC-derived oligodendrocyte progenitor cells in patients with spinal cord injuries in 2010. Unfortunately the coordinators of this project have recently halted these trials due to financial issues [26] therefore it appears that the translation of hESC biology to a clinical setting still faces some major hurdles. In terms of the therapeutic use of hESCs on a large scale, the number of hESC lines required to provide a good match for specific patient populations would be vast, with the number of embryos required far exceeding the number available from assisted reproductive clinics, thus requiring both oocytes and sperm to be donated; in turn, having its own set of ethical and practical concerns. These issues have led the research community to investigate other cell sources as alternatives to both ASCs and ESCs, which possess many of their desirable characteristics, such as pluripotency, patient specificity and accessibility from adult tissue.

1.2 Reprogramming

The differentiation of pluripotent cells along increasingly defined lineages involves considerable genetic and epigenetic changes and it was initially uncertain if it would ever be possible to completely reverse these changes in adult somatic cells.

The reprogramming of somatic cells has been developed based on principles and techniques, which have been formulated over the last six decades. The

first step towards overcoming restrictions imposed during development came in the 1950s, with Briggs and King establishing the technique of somatic cell nuclear transfer (SCNT). This involves introducing nuclei of somatic cells into genetically inactivated oocytes, with nuclei consequently reprogrammed by the host oocyte. Using this technique they investigated the developmental potential of cell nuclei isolated from late-stage embryos or tadpoles by transferring them into enucleated oocytes and were able to successfully generate viable offspring [27]. Gurdon *et al.* examined the capacity of differentiated nuclei, in this instance isolated from the intestinal epithelium of an adult frog, to be reprogrammed by the recipient oocyte, which also resulted in production of viable organisms [28]. This research established that differentiated cells contain a full complement of genes to support the generation of cloned offspring.

Despite the success of SCNT using amphibian cells, transferring this knowledge to mammalian cells was not as simple as first anticipated, primarily due to the small size of mammalian oocytes. The development of micromanipulation techniques facilitated SCNT using mammalian cells; Wilmut *et al* performed nuclear transfer of cultured mammary gland cells by electrofusing them into enucleated sheep eggs. This experiment resulted in the generation of a single cloned sheep, known as 'Dolly' [29]. This study demonstrated that fully differentiated mammalian cells remain genetically totipotent therefore it could be concluded that development imposes reversible genetic modifications rather than irreversible genetic changes. Despite the success of cloning mammalian cells, the majority of cloned animals exhibit genetic abnormalities, suggesting that SCNT results in defective epigenetic reprogramming. Therefore the proposal to use this technique in human stem cell research was deemed unethical and as a result no human stem cell lines have been generated using SCNT. This research

did however lead researchers to consider what factors contained within the cytoplasm of oocytes had enabled reprogramming of somatic nuclei.

Due to the technical expertise involved in SCNT, researchers sought alternative methods to probe cell developmental potential. An important step came with the establishment of immortal cell lines from tumours of germ cell origin, known as teratocarcinomas, which provided a source of cells that could be clonally expanded in culture whilst retaining their pluripotent characteristics [30]. These cells are termed embryonal carcinoma cells (ECCs) and provide an ideal model for studying the pluripotency network in more detail. A number of laboratories went on to use ECCs to successfully reprogram both murine and human somatic cells using cell fusion. However these cells contain two sets of chromosomes and with normal cell function depending on innumerable interactions between genes, altering the numbers of chromosomes effect these interactions, rendering this approach unsuitable for clinical application [31-33]. This research demonstrated the dominance of the pluripotent state over the somatic state while the factors responsible still remained unidentified.

It was these efforts, which stimulated the isolation of ESCs initially from the inner cell mass of mouse blastocysts [34] and later from human embryos [23]. Pluripotent cell lines have also been generated from a variety of other sources, such as embryonic germ cells (EGCs) isolated from primordial germ cells of the middle gestation embryo [35] and epiblast stem cells (EpiSCs) isolated from post-implantation embryos [36]. One characteristic that they all share is that they are all derived from early embryos or germ lineage cells, however only ESCs are capable of tetraploid embryo complementation as a result of balanced parental imprints, which are required for normal development.

Investigations into reprogramming continued through a series of experiments incubating somatic cells with extracts of pluripotent cells. This involved permeabilising somatic cells and exposing them to nuclear and cytoplasmic extracts derived from pluripotent cells from various origins including hESCs [37], xenopus oocytes [38] and ECCs [37]. While these studies provided some interesting findings with many cell lines showing re-expression of the pluripotency marker *Oct4* many reprogrammed cells only regained restricted pluripotency properties. Ultimately the results obtained were not conclusive that expression of these characteristics was due to cellular extracts.

Meanwhile attention had turned to lineage associated transcription factors, which would later prove to be the most influential factor in establishing fully reprogrammed somatic cells. Lineage associated transcription factors were known to maintain cellular identity through inducing expression of lineage specific genes whilst inhibiting expression of plasticity associated genes. The use of these transcription factors as a tool to dedifferentiate somatic cells was first demonstrated through the conversion of mouse embryonic fibroblasts (MEFs) to myoblasts through the over expression of the myogenic regulatory factor, MyoD [39]. Later researchers successfully converted B lymphocytes into macrophages through over expression of the myeloid transcription factor C/EBPα [40] demonstrating the versatility of using transcription factors to alter cell fate.

1.3 Induced Pluripotent Stem Cells

Although much research into the reprogramming of somatic cells had been undertaken, it was in 2006 that a major breakthrough occurred when Yamanaka *et al* determined four specific factors, which were sufficient to reprogram somatic cells to a pluripotent state [41]. Yamanaka and colleagues had devised an elegant screen for transcription factors capable of

reprogramming somatic cells from a pool of 24 thought to be implicated in pluripotency. Each of these factors was retrovirally transfected into ESC-specific *Fbx15* reporter fibroblasts and selected according to expression of this marker gene. Successive rounds of elimination narrowed down the initial number of 24 to four defined factors, *Oct4*, *Sox2*, *c-Myc* and *Klf4 (OKSM)*, which on their own were sufficient to induce pluripotency [42]. Since Yamanaka's discovery, this four factor cocktail has been shown to reprogram both murine and human cells to a pluripotent stage, termed induced pluripotent stem cells (iPSCs) [41, 43-45]. IPSCs were capable of producing colonies morphologically similar to ESCs and displayed many markers typically associated with pluripotency including *SSEA1* and *Nanog*. When iPSCs were injected subcutaneously into immunocompromised mice, teratoma formation occurred and furthermore upon blastocyst injection were found to contribute to a number of different tissues of the developing embryo [41].

Despite the "first generation iPSCs" generated in Yamanka's initial studies displaying many pluripotency markers, these cells appeared only partially reprogrammed. These cells were unable to produce viable chimeras or contribute to the germ-line and also displayed incomplete promoter demethylation of ESC regulators, such as *Oct4*, strongly suggesting incomplete reprogramming. The isolation procedure was thus modified, replacing the *Fbx15* reporter with a reporter associated with either *Nanog* or *Oct4* [46, 47], both of which are more closely associated with pluripotency. IPSCs isolated using this method were germline competent and represented a population of cells functionally indistinguishable from hESCs. Since then, iPSCs have been generated from a number of different species including humans [45], rats [48] and rhesus monkeys [49] through expression of OKSM, demonstrating that key factors governing the pluripotency network remain conserved during evolution.

Variations of the four-factor cocktail have been used to successfully reprogram somatic cells. Factors can be substituted by family members with *Sox1* or *Sox3* capable of replacing their counterpart *Sox2*. *Klf2* and *Klf5* are able to replace *Klf4* and *c-Myc* can be substituted by *l-Myc* and *n-Myc* suggesting that proteins recognise similar DNA-binding motifs [50]. It should also be noted that *Oct4*, *Sox2*, *c-Myc* and *Klf4* are not the only four factor combination that can reprogram somatic cells. Another group of factors *Oct4, Sox2, Nanog* and *Lin-28* have also been used by several groups to successfully generate iPSCs [51]. This suggests that there is more than one route to pluripotency or that different transcription factors can activate the same route through promoting each other's expression. In the case of *Lin-28* this transcription represses let-7 miRNAs [52], which negatively regulate *c-Myc* expression [53] therefore likely functioning to indirectly increase levels of endogenous *c-Myc*. In an attempt to reduce the number of factors required to induce pluripotency, successful reprogramming has also been achieved in the absence of both *c-Myc* and *Klf4* [54] suggesting that *Oct4* and *Sox2* play a more pivotal role in this process, whereas *c-Myc* and *Klf4* are thought to enhance reprogramming.

In the vast majority of cases *Oct4* is required to induce pluripotency. In fact iPSCs have been generated from human neural stem cells (NSCs) using *Oct4* alone [55] providing further evidence that *Oct4* may be the master regulator of pluripotency in mammalian cells. Until recently *Oct4* remained the only factor that was irreplaceable with other transcription factors, including close family members *Oct1* and *Oct6* [56], until the discovery that the nuclear receptor Nr5a2 was capable of replacing exogenous *Oct4* and in conjunction with *Sox2* and *Klf4* was capable of reprogramming MEFs [57]. Nr5a2 is an upstream activator of *Oct4*; therefore it is likely that in this case indirect activation of endogenous *Oct4* expression has driven the

reprogramming process. The orchestration of pluripotency involves many gene interactions and just a few of these are detailed in Figure 1.1.

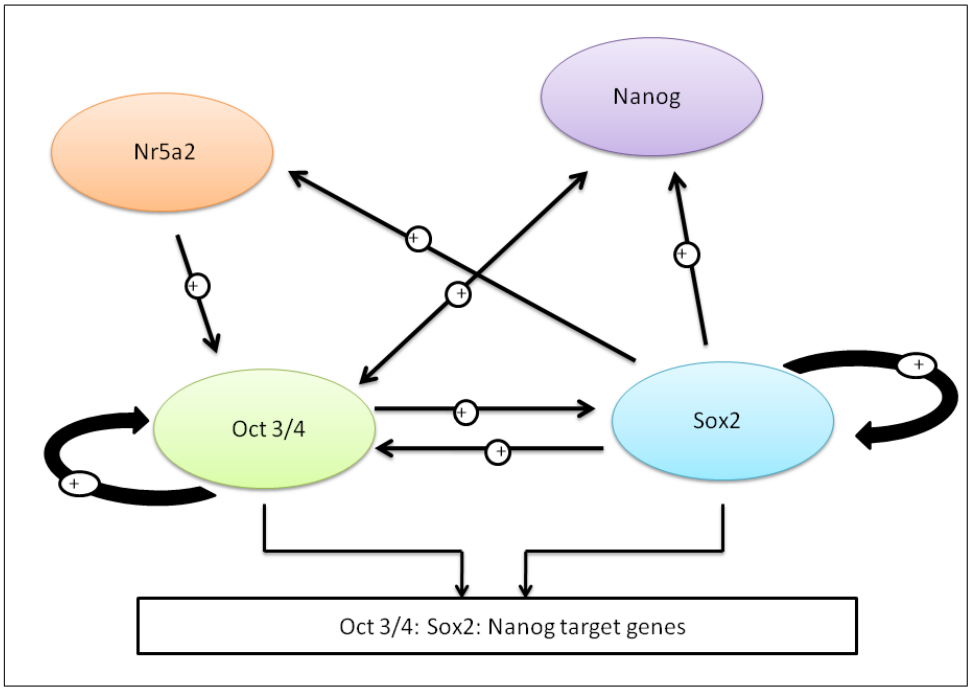

Figure 1.1 Schematic of gene regulatory network in pluripotent stem cells

1.4 Reprogramming Factors

1.4.1 *Oct4*

The four factors initially identified by Yamanaka *et al* have been widely used for inducing pluripotency. The transcription factor *Oct4* is strongly implicated in maintenance of pluripotency and has become somewhat of a proxy for stemness. *Oct4* belongs to the Pit-Oct-Unc (POU) family of transcription factors [58] and appears to be almost exclusively expressed in ESCs and germline cells playing a vital role in ontogenesis [58, 59]. *Oct4* is expressed in all blastomeres initially with expression becoming

progressively downregulated in the trophoectoderm and more profuse in the inner cell mass. In late blastocysts, *Oct4* becomes most abundant in the primitive endoderm [60] and eventually at maturity *Oct4* expression becomes limited to germ cells [61].

Niwa *et al* measured levels of *Oct4* expression at various ESC states to understand its role in more detail [62, 63]. This work demonstrates that repression of *Oct4* leads ESCs to differentiate into cells resembling trophoectoderm whilst over expression of *Oct4* results in differentiation into several lineages, including extra-embryonic mesoderm and primitive endoderm lineages [62, 63]. This suggests *Oct4* differs from many regulatory transcription factors in that it does not function in an on/off manner, with fluctuations in expression having profound effects on cell fate.

Genome studies of human and murine ESCs using chromatin-immunoprecipitation (ChIP)-on-chip assays have highlighted a large number of genes with *Oct* regulatory elements. In hESCs 581 genes have been identified as *Oct4* targets, whereas 963 genes have been identified in the case of mESCs [64, 65]. *Oct4* can act either as a suppressor of genes responsible for ESC differentiation or as an activator of genes known to retain the pluripotency of ESCs while many of these genes also express regulatory elements for *Sox2* and *Nanog*, which provides evidence for the existence of co-regulation of numerous genes in a positive regulatory loop [64].

1.4.2 *Sox2*

The transcription factor SRY-type high mobility group box 2, also known as *Sox2* is part of a large family of 20 proteins strongly implicated in maintenance of pluripotency. Downregulation of *Sox2* promotes ESC differentiation in mESCs demonstrating the importance of *Sox2* in

pluripotency regulation [66]. *Sox2* is initially expressed in all blastomeres and later becomes restricted to the inner cell mass and epiblast and then germ cells. However, unlike *Oct4*, *Sox2* is also expressed in multipotential cells of the extra embryonic ectoderm and in precursor cells of the developing central nervous system [66]. In terms of regulating pluripotency *Sox2* acts in combination with *Oct4* to activate Oct–Sox enhancers, which regulates the expression of pluripotent stem cell-specific genes, including *Nanog*, *Oct4* and *Sox2* itself [67]. It was originally thought that *Sox2* maintained pluripotency through Oct-Sox enhancer activity however *Sox2* is in fact dispensable for activation of these enhancers although it is required to stabilise ESCs in a pluripotent state by maintaining the appropriate level of *Oct4* expression indirectly through regulation of multiple transcription factors [68].

1.4.3 *C-Myc*

The helix-loop-helix/leucine zipper transcription factor, *c-Myc*, is a known oncogene responsible for a number of cellular functions including cell growth, differentiation and proliferation [69]. Like the other transcription factors previously described, *c-Myc* interacts with a considerable number of genes acting as both a repressor and activator of its targets [69]. In terms of its role inducing pluripotency, it has been suggested that *c-Myc* serves as a major downstream target of two pathways known to promote pluripotency, the LIF/STAT3 and Wnt signalling pathways [70]. The LIF/STAT3 pathway stimulates pluripotency in mESCs however, activation of this pathway is not required for hESC pluripotency [71]. In mESCs, LIF binds to hetero-dimeric LIF receptor stimulating a cascade of signalling events, eventually resulting in translocation of the transcription factor STAT3, required to maintain pluripotency. The Wnt pathway on the other hand maintains pluripotency of both mESCs and hESCs. Activation of the Wnt

pathway promotes pluripotency through inhibition of glycogen synthase kinase-3ß (GSK3β), which in turn results in a cascade of signalling events, including an increase in *c-Myc* expression [70]. While research has revealed that *c-Myc* is not strictly required for generation of iPSCs, its absence often makes the reprogramming process more inefficient. One way in which *c-Myc* is thought to aid the reprogramming process is through its ability to open the chromatin structure by binding various genome sites and recruiting histone acetylase complexes [72]. To exploit the attributes of *c-Myc*, many groups have explored reprogramming cells which endogenously express high levels of *c-Myc* and small molecules, such as Wnt3a, to promote reprogramming without exogenous *c-Myc* [73].

1.4.4 *Klf4*

The Kruppel-type zinc-finger transcription factor Klf4 is also a downstream target of STAT3 and over expression leads to sustained expression of *Oct4* and inhibition of differentiation in ESCs [74]. Relatively speaking *Klf4* is not required to the same degree as *Oct4* and *Sox2* in maintaining pluripotency, although its activation can also improve the efficiency of the reprogramming process. *Klf4* has also shown to exhibit cofactor regulation of gene transcription along with *Oct4* in a similar way to *Sox2*, however *Klf4* acts on a much smaller scale with only a small number of genes regulated [75]. *Klf4* may also serve to upregulate *Nanog* by suppressing p53, a negative regulator of *Nanog* [76, 77].

1.5 Mechanisms of Inducing Pluripotency

Despite the identification of numerous factors, which are able to initiate pluripotency, the nature and sequence of events occurring during reprogramming remain unclear. A number of studies have focused on the stochiometry of reprogramming and provide further insight into mechanisms responsible for this remarkable event. One particular study, which provides a clearer indication of the molecular and cellular changes during reprogramming, makes use of a doxycycline-dependent lentiviral system, which is able to transiently express OKSM. This system allowed for the self-selection of iPSCs upon the removal of doxycycline from culture media, with surviving cells demonstrating pluripotent characteristics. This study demonstrated that exogenous expression of the four factors is required for approximately 10 days and after this point the somatic genome is ready for conversion to pluripotency suggesting that reprogramming follows a defined set of events rather than a random sequence of reprogramming [78].

MacArthur *et al* also provided further insight into processes underlying reprogramming by putting forward a fundamental theory suggesting that in order to reprogram somatic cells it is necessary to supply them with enough energy to overcome barriers maintaining their differentiated state. This switch is often induced by *Oct4* and *Sox2* and many studies have achieved reprogramming by inducing high levels of these genes using viruses. This study demonstrates that low level, transient fluctuations of *Oct4* and *Sox2* are adequate to induce expression of endogenous gene expression [79] suggesting considerably less invasive methods may be used to induce reprogramming. Another important conclusion drawn from this study is that a general increase in transcriptional noise may assist reprogramming. Rather than specifically targeting the pluripotency regulatory circuit, non-specific widespread gene amplification is thought to shake the system into pluripotency [79].

1.6 Reprogramming Efficiency

Despite improvements in somatic cell reprogramming, induction of pluripotency largely remains an inefficient process. Low efficiency and slow kinetics are evident when compared to the relatively efficient method of cell lineage switching. In the case of B lymphocyte conversion to macrophages through forced expression of C/EBPα, the process is almost 100% efficient with a switch in cell fate occurring after around 48 hours [40] compared to the reprogramming of somatic cells to a pluripotent state with the highest efficiencies reported at around 3% [80]. This suggests that induction of pluripotency faces greater restrictions due to decreased transcription and epigenetic similarity between somatic cells and pluripotent stem cells. In addition to the inefficient nature of reprogramming, acquisition of a fully pluripotent phenotype is not necessarily complete upon endogenous expression of key pluripotency genes. It may require several rounds of cell division to reach this stage as illustrated by distinct differences in telomere length [81], global transcription [82] and DNA methylation patterns [83] between early and late passage iPSCs.

Reprogramming efficiency can largely be attributed to the method used for delivery of reprogramming factors with the greatest efficiency achieved using integrating viruses. Lentiviruses generate the highest efficiencies of ~0.1%-1% [51] closely followed by retroviruses at ~0.01%-0.05% [45]. Excisable vectors, such as the piggyBac transposon system have also demonstrated relatively high efficiency levels of ~0.1% [84] whilst non-integrating systems using adenoviruses or plasmids produce lower efficiencies of ~0.001% [85]. DNA free systems also produce low efficiencies with proteins and RNA reporting reprogramming efficiencies of ~0.001% [86]. The efficiency of reprogramming also largely depends on inducing factors and the somatic cell type, which will be discussed in more detail later in this chapter.

1.6.1 Cooperative Factors

The slow kinetics of reprogramming compared to cell fusion or SCNT suggests that a number of cooperative factors, which target *Oct4, Sox2, Klf4, c-Myc*, must exist. In an attempt to improve efficiency of this process and identify novel molecules that may provide alternatives to existing factors, a number of antagonists have been identified. The use of chromatin-modifying agents to enhance the overall efficiency of reprogramming is well documented and can often be used as replacements for one or more inducing factors.

All cells of the mammalian embryo prior to the eight-cell stage have potential to form all somatic and germ cells of the organism in addition to all extra-embryonic tissues and therefore are termed totipotent [87]. This potential is progressively restricted during development through epigenetic reprogramming of the cell nucleus to prevent the re-expression of undesired genes. The epigenome of each cell is subsequently determined by the histone code, DNA methylation patterns and chromatin remodelling. These modifications make up the epigenetic code, which is a series of specific changes in each eukaryotic cell, which adds an additional level of specificity above that of genes [88]. In addition, packaging of nucleosomes into higher orders of structure creates a physical barrier, which prevents molecular machinery from accessing information encoded in DNA for gene expression, replication and chromosome stability [89] .

The histone code itself is generated by post-translational modifications to histone tails, which include acetylation, methylation, phosphorylation, ADP-ribosylation, ubiquitination and sumoylation [90]. These modifications affect the electrostatic charge of the nucleosomes, which in turn affects the structure of chromatin, altering silencing or activation of chromatin domains [88]. The more open the chromatin structure, the more transcriptionally active it becomes, illustrated in Figure 1.2, where ESCs have an open, active

chromatin structure compared to somatic cells whose comparatively closed structure leads to a lack of plasticity [91].

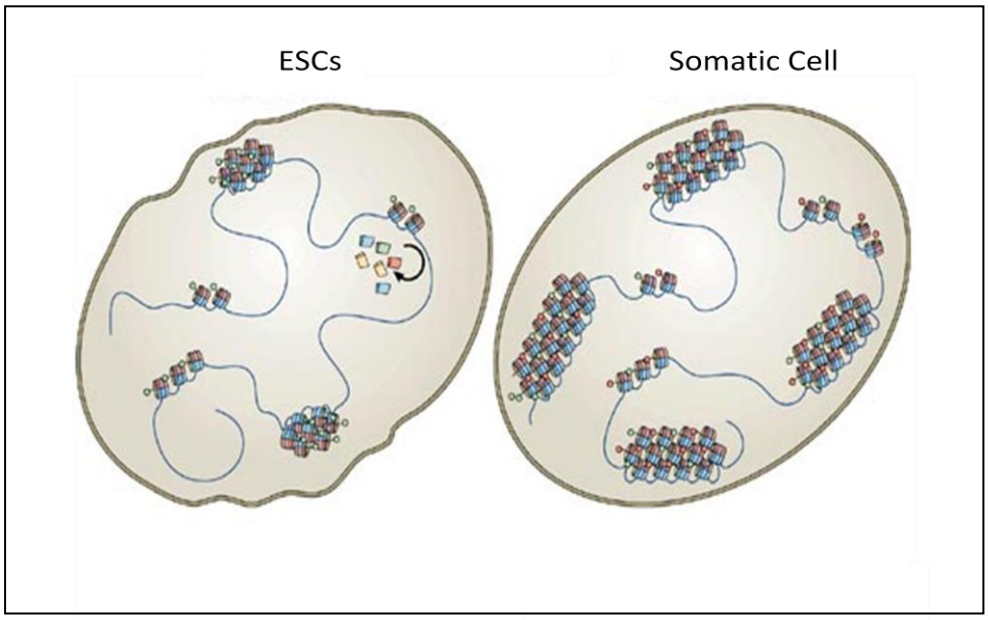

Figure 1.2 Schematic representing chromatin structure of ESCs and somatic cells. In ESCs chromatin is decondensed while in somatic cells regions of condensed heterochromatin form. Green circles represent active histone marks while red circles represent silencing histone marks. Adapted from [91]

Although these changes are epigenetic and heritable they are also reversible and form part of the core regulatory machinery in cellular reprogramming. In order for somatic cells to be reprogrammed they must be converted from a differentiated cell to a default nuclear state. This involves genome-wide epigenetic reprogramming, which is required in order to stimulate erasure of the somatic epigenetic memory, generating relatively naive chromatin with a broader developmental potential, known as the erase and re-build strategy [92].

One example of using chromatin-modifying agents to enhance reprogramming is inhibition of histone deacetylases (HDACs) using valproic acid (VPA), which results in reprogramming of human fibroblasts in the absence of *Sox2* and *c-Myc* [93]. Similarly, inhibition of the histone methyltransferase G9a, using a small molecule BIX-01924, successfully reprogrammed mouse neural progenitors (NPCs) in the absence of *Sox2* or *c-Myc*, at the same efficiency reported for four factor reprogramming. Inhibition of G9a can also successfully replace *Oct4*, which is consistent with events occurring during development; G9a functions to epigenetically silence *Oct4* therefore subsequent inhibition allows reversal of this modification in somatic cells [94]. In an attempt to identify other small molecules that could synergise with BIX to improve the low efficiency of reprogramming, Shi *et al*. discovered a novel compound now recognised as BayK. This calcium channel agonist does not demonstrate any identifiable reprogramming activity in the absence of BIX and rather than acting at the epigenetic level this molecule affects the cell at the signal transduction level. However in combination with BIX this small molecule can further improve reprogramming efficiency and effectively compensate for *Sox2* enabling reprogramming of MEFs using *Oct4* and *Klf4* [95]. Together this demonstrates that erasure of a somatic epigenetic state is preferable in order to establish pluripotency.

Modification of key signalling pathways, such as Wnt signalling, can also improve efficiency of reprogramming. Activation of this pathway is initiated by binding of Wnt proteins to frizzled and LRP cell surface receptors leading to signal transduction. Wnt signalling inhibits the amino-terminal phosphorylation of β-catenin mediated by GSK-3, which prevents β-catenin degradation. Unphosphorylated β-catenin is able to translocate to the nucleus, where it interacts with members of the Lef1/Tcf family of HMG domain-containing DNA-binding proteins to activate target genes. These DNA-binding transcription factors activate transcription in the

presence of a Wnt signal and repress expression of target genes in the absence of a Wnt signal [96].

Exploiting this pathway, chemical inhibition of GSK-3 has been shown to facilitate reprogramming of human fibroblasts [48]. An aminopyrimidine: CHIR99021, is the most selective inhibitor of GSK-3 reported to date with 350-fold selectivity toward GSK-3 compared with other potent inhibitors [97]. Combined inhibition of GSK-3 and mitogen activated protein kinase (MAPK) signalling also enhances reprogramming of NSCs and drives conversion of partially reprogrammed cells to pluripotency [98]. This is consistent with research demonstrating GSK-3 and MAPK inhibition are sufficient to maintain undifferentiated mESCs [99]. Inhibition of differentiation pathways enhancing reprogramming provides further evidence that reprogramming requires inhibition of lineage-specific genes and induction of a more primitive state. In addition it should be noted that small molecules offer low host immunogenicity and lack permanent genome modification. In addition, large scale production of small molecules is much simpler compared with viral vectors therefore offering a number of advantages.

1.7 Direct Reprogramming

Direct reprogramming of one specific cell type to another is one way of tackling autologous cell replacement therapies without establishing pluripotency. Through circumventing the pluripotent state, issues associated with tumorigenesis are largely removed while on the whole direct conversion of a mature somatic cell to another is altogether a much simpler process that can be acquired using fewer exogenous factors.

The first examples of direct reprogramming were reported in the 1980s with direct conversion of MEFs into muscle cells through forced expression of MyoD as previously described [39]. MyoD was subsequently used in many reprogramming studies and it was discovered that this transcription factor could convert many different cell types into myoblasts including dermal fibroblasts, chondroblasts, smooth muscle and retinal epithelial cells [100].

The first report that lineage committed cells could be transdifferentiated using transcription factors came in 2004 with B lymphocytes being converted to macrophages using the transcription factor C/EBPα [40]. Since then, large numbers of cells have been converted into a variety of lineages using combinations of transcription factors. One example of this is the conversion of fibroblasts into excitatory neurones, termed induced neurones (iNs) using a three factor combination of Ascl, Brn2 and Mytl1. iNs were generated using lentiviruses encoding the three reprogramming factors and upon expression of Tau, a microtubule-associated protein, cells co-expressed green fluorescent protein enabling neuronal identification. Extensive electrophysiological studies confirmed that iNs function as neurons *in vitro* [101].

Fibroblasts have also been directly reprogrammed into induced cardiomyocytes (iCMs) using Gata4, Mef2c and Tbx5, identified from a pool of 14 factors. iCMs exhibit spontaneous contractions *in vitro* and when injected into mouse hearts, differentiate to form small isolated cardiomyocyte-like cells *in vivo* [102]. This further supports the argument that cells need not be fully reverted to pluripotency and instead directly reprogrammed to yield desirable, functional phenotypes.

Unlike multi-factor reprogramming demonstrated in previous studies Szabo *et al.* detailed conversion of human fibroblasts into multilineage hematopoietic precursors using over expression of a single factor. In this example expression of *Oct4* initiated haematopoiesis without reverting cells

through a pluripotent intermediate or activating mesodermal pathways. This report is somewhat unusual as *Oct4* is not typically required for haematopoietic cell maintenance however it was proposed that in this case *Oct4* binds the regulatory loci of haematopoietic-specific genes stimulating the expression of transcription factors required for a multipotent blood cell progenitor phenotype [103]. It has also been suggested that over expression of *Oct4* allows cells to reach a near multipotent state so that in the presence of haematopoietic cytokines they could then differentiate towards a haematopoietic lineage. Driving cells towards an intermediate pluripotent state has also been explored by Kim *et al* who induced murine fibroblasts into neural progenitors (NPCs) through transient expression of OKSM before exposure to neuronal cell culture conditions [104]. A similar investigation exposed MEFs to transgenic expression of OKSM for 4 days to gain a transient, plastic developmental state before directly differentiating into cardiomyocytes [105].

Directing reprogramming of somatic cells is clearly feasible however the molecular mechanisms underpinning this dedifferentiation process remain largely unknown. Specifically, it remains unclear whether a cell reverts to a progenitor before undergoing differentiation or rather directly differentiates into the terminal phenotype. However, dedifferentiation of somatic cells into desirable lineages undoubtedly presents a more elegant approach to reprogramming than the more robust method of reversing cell fate to pluripotency followed by differentiation to yield functional lineages.

1.8 MicroRNA

More than a decade since discovery of the first MicroRNA (miRNA), *lin-4* [106], we now know that miRNAs constitute ~1% of the eukaryote genome, however the cellular functions of many miRNAs remain unknown.

MiRNAs are non-coding RNAs, typically 20-22 nucleotides in length, which significantly impact almost every aspect of cellular biology [107]. Their primary function is to control gene expression through regulation of specific messenger RNAs (mRNA) mediated by base-pairing interactions. The majority of miRNA-mRNA targeting occurs between a short sequence located at the 5' end of the miRNA, known as the seed sequence and the complementary sequences within the 3' untranslated region of the corresponding target mRNA. Binding leads to destabilisation of mRNA or inhibition of protein synthesis [108] as illustrated in Figure 1.3.

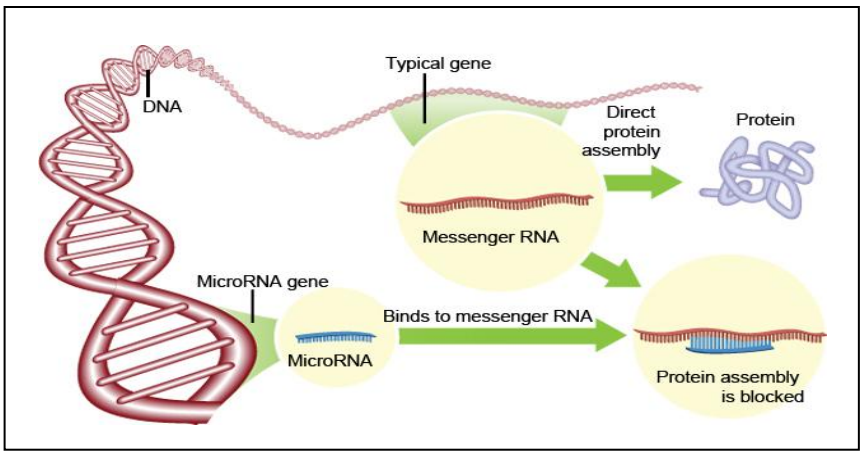

Figure 1.3 Schematic of protein inhibition with miRNA [109]

MiRNA processing is crucial for production of mature miRNAs and is clearly illustrated in Figure 1.4. Initial cleavage of primary miRNA transcripts (pri-miRNAs) is catalysed by the nuclear RNase III Drosha together with the double stranded RNA binding protein DGCR8/Pasha, to produce an imperfect stem-loop precursor miRNA (pre-miRNA) [110]. Step 2 involves Exportin 5, which transports pre-miRNA across the nuclear membrane into the cytoplasm [111] where the cytoplasmic RNase III, Dicer, along with the transactivator RNA-binding protein (TRBP) produces imperfect double-stranded RNA duplexes. The double-stranded RNA

consists of a mature miRNA strand and a complementary sequence. During the final stage, the double stranded RNA is unwound and one strand enters an RNA-induced silencing complex (RISC) where argonautes are recruited for mRNA recognition and silencing [112]. The mature miRNA goes on to target mRNA either through mRNA cleavage or translational repression.

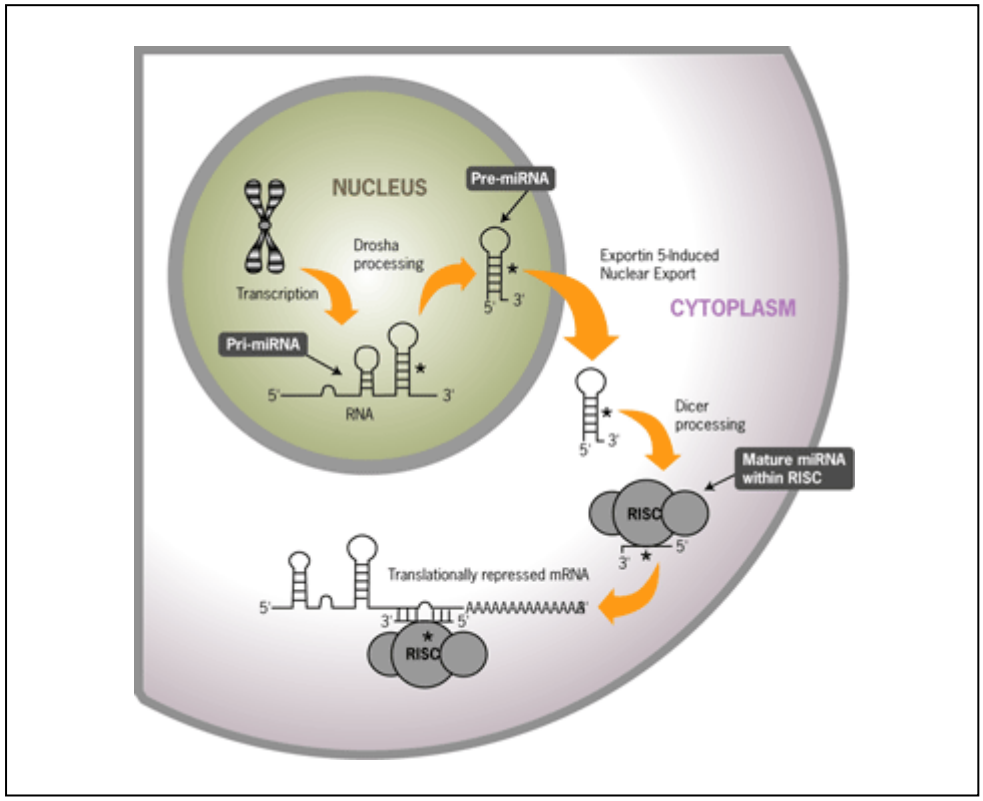

Figure 1.4 MiRNA biogenesis and processing [113]

Traditionally, miRNA phenotypic studies have focused on small numbers of targets regulated by a specific miRNA. However, it is becoming increasingly apparent that miRNAs influence cell fate decisions through suppressing hundreds of mRNAs contributing to many pathways. A classic example is introduction of miR-124 into HeLa cells, a cervical cancer cell line, which results in a complete shift in their expression profile towards a

neural lineage. Further investigation has now identified that a number of miR-124s targets are functionally associated with neuronal differentiation [114].

A subset of the miR-290 cluster, known as the embryonic stem cell cycle (ESCC) regulating miRNAs have been shown to improve efficiency of reprogramming. An example of this is introduction of miR-291-3p, miR-294 and miR-295 to MEFs along with *Oct4*, *Sox2* and *Klf4*, which were able to effectively replace *c-Myc* in promoting reprogramming [115].

MiRNAs have also been shown to facilitate reprogramming of somatic cells in the absence of further inducing stimuli. Lentiviral over expression of the *miRNA302/367* cluster, which was first identified as a direct target of *Oct4* and *Sox2*, can successfully reprogram mouse and human cells. Moreover, this miRNA-mediated reprogramming is up to 100x more efficient than traditional four factor over expression [116].

Another similar study demonstrated that transfection of mature, synthetic miRNAs, mir200c, mir302s and mir-369, at 48 hour intervals also successfully produced iPSCs from mouse and human somatic cells. Despite demonstrating lower efficiency, the numbers of iPSCs produced remained comparable to four-factor retroviral over expression systems [117]. Interestingly, only mir302s are common between this study and the lentiviral-mediated strategy performed by Anokye-Danso *et al*.

The promoters of the miR-290 and miR-302 clusters are bound by Yamanaka's four original factors and it is already known that increasing or decreasing expression of specific miRNAs results in fluctuations in corresponding mRNA expression [118]. Therefore, it is likely that these miRNAs are acting through their corresponding mRNAs to activate pluripotency. The high efficiency experienced using miRNA for

reprogramming is also likely due to the fact that miRNA targets hundreds of mRNAs, compared to providing one mRNA at a time.

One miRNA of particular interest is miR-145, due to its association with major pluripotency regulators; *Oct4, Sox2* and *Klf4*, all of which feature in Yamanaka's classic combination of reprogramming factors. miRNA profiling of embryoid body differentiation by Xu *et al.* uncovered a large increase in miR-145 expression upon hESC differentiation. Reporter studies were able to pinpoint transcripts encoding *Oct4, Sox2* and *Klf4* as targets of miR-145 while gain- and loss-of-function experiments were able to demonstrate that forced expression of miR-145 prevented self-renewal of hESCs and inhibition of mir-145 had the opposite effect. Another important finding of this study was identification of an *Oct4* binding site upstream of miR-145 which together with reporter assays suggested that *Oct4* occupies this site repressing transcription of miR-145 [119]. Given the role miR-145 plays in the switch between pluripotent and committed cell lineages this miRNA may be exploited to enhance reprogramming of somatic cells.

Researchers have long suspected a strong link between the molecular signature of cancer and stem cells; however this still remains largely unknown. Neveu *et al.* developed a miRNA map through examining miRNA expression profiles of numerous cancer and stem cells, identifying almost 330 miRNAs in over 50 human cell lines and highlighting 11 miRNAs shared by all cancer cells and a subset of pluripotent stem cells. Interestingly, each of these miRNAs targets genes responsible for down-regulating proliferation or upregulating the p53 network [120] .

The p53 pathway plays an important role in impeding cellular reprogramming. Exemplified by inhibition of this pathway, which enhances efficiency of this process up to 100-fold [121]. Alternatively, using p53 null cells, up-regulating a negative regulator of p53, knocking down p53 or knocking down one of its targets, such as p21, also increases efficiency of

reprogramming up to 25-fold. One example is the conversion of mouse fibroblasts to pluripotency using *Oct4* and *Sox2* alone in the presence of decreased levels of p53. Interestingly keratinocytes, which have a higher reprogramming efficiency than fibroblasts, display lower protein levels of p53 and p21 than other cell types providing further evidence for the influential role of this pathway [122] . Importantly p53 acts as a checkpoint to prevent cells with damaged DNA and chromosomal abnormalities prevailing [121] therefore cells reprogrammed by directly manipulating the p53 pathway would not be suitable for clinical use due to risks associated with mutated DNA.

The role of p53 during reprogramming raises important questions about how p53 knockdown can exert such a pronounced effect. If we consider miR-145, we already know that this miRNA is essential for differentiation of ESCs by modifying the translation of *Oct4*, *Sox2* and *Klf4*. Interestingly p53 promotes the maturation of precursor miR-145 to the mature miR-145 [123] so may provide a possible mechanism for the ability of p53 to alter reprogramming. Specifically, disruption of p53 may lead to a decrease in mature miR-145, which in turn increases pluripotency gene transcripts as illustrated in Figure 1.5. It is therefore possible to speculate that miR-145 itself may influence the reprogramming of somatic cells.

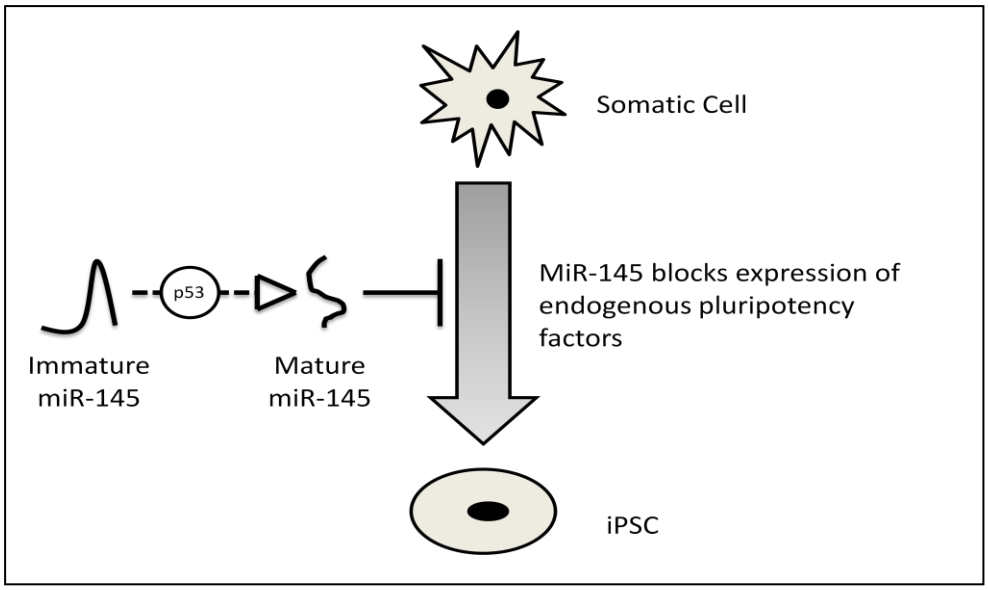

Figure 1.5 proposed roles for miR-145 in reprogramming

1.9 The Donor Cell

The list of donor cells that have given rise to iPSCs continues to increase and to date iPSCs have been derived from a diverse range of cell type including CD34+ peripheral blood cells [124], kidney mesangial cells [125], amniocytes [126] and T lymphocytes [127] to name but a few.

As detailed earlier, reprogramming can be achieved with different efficiencies and outcomes. This is largely dependent on donor cell type with some cells being more amenable to reprogramming than others. To exemplify this, using the same process it can take between 8-12 days to reprogram MEFs, while human foreskin fibroblasts (HFFs) can take between 20-25 days to undergo the same transformation. Many studies have compared the reprogramming capacity of alternative cell types, such as human fibroblasts and keratinocytes, with keratinocytes being reprogrammed up to 100 times more efficiently and two-fold faster [128].

Human umbilical vein endothelial cells (HUVECs) have been identified as one of the most efficiently reprogrammed cells to date with the fastest kinetics and highest efficiencies. HUVEC-derived iPSCs appear as early as 6 days after a single retroviral infection of *Oct4, Sox2, Klf4* and *c-Myc* whilst demonstrating 2.5–3% efficiency. Furthermore, when HUVEC reprogramming was performed under hypoxia in the presence of a TGF-β family signalling inhibitor, colony formation increased an additional 2.5-fold over standard conditions [80].

Other cell types, which require reduced numbers of factors are cord blood CD133+ cells that have been successfully reprogrammed using just *Oct4* and *Sox2* [129] and NPCs, which can be reprogrammed through forced expression of *Oct4* alone [55]. Differences in efficiency, kinetics and factor requirements can largely be attributed to higher endogenous levels of pluripotency factors, for example the high levels of *Sox2* endogenously expressed by NPCs, which removes requirement for exogenous *Sox2*.

1.10 Delivery of Inducing Stimuli

1.10.1 Retroviruses

Viruses have proven extremely useful tools in providing an efficient gene delivery system to primary cells, which are typically difficult to transfect. Retroviruses are infectious particles consisting of an RNA genome packaged within a protein capsid contained within a lipid envelope [130] as illustrated in Figure 1.6.

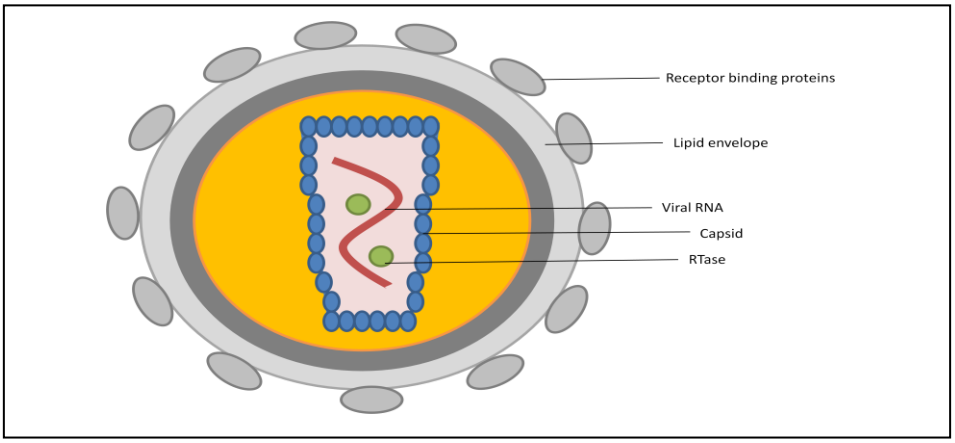

Figure 1.6 Structure of a retrovirus

While transcription typically refers to conversion of DNA to RNA, retroviruses carry out this process in reverse hence the prefix 'retro'. Packaged within the protein capsid along with the viral RNA is the enzyme reverse transcriptase (RTase), which is able to synthesise complementary DNA (cDNA) from the RNA template in the cytosol of host cells upon infection [130].

One of the characteristics of stem cells that distinguish them from somatic cells is their ability to silence retroviruses by *de novo* methylation [131]. Successfully reprogrammed cells demonstrate silencing of *Oct4*, *Sox2*, *c-Myc* and *Klf4* genes, while partially reprogrammed cells exhibit incomplete silencing. Silencing of retroviral genes during reprogramming is a gradual process that occurs as early as 4 days after induction of transcription factors and is only completed in cells that have reached a pluripotent state [78]. Therefore initial attempts at reprogramming somatic cells utilised Moloney murine leukaemia-based retroviral vectors, which were known to undergo silencing in the pluripotent state [132]. It was due to their self-silencing properties that they became established as an attractive means of delivering transcription factors because the temporal requirement for factor expression was at the time undefined.

To facilitate delivery of inducing stimuli, genes encoding required transcription factors are artificially added to viral RNA so that they too are copied. This integration step enables these genes to be inserted into host DNA however it is also this integration step, which makes these viruses unsuitable for clinical use due to risks associated with insertional mutagenesis [133]. Reverse transcription lacks the usual proofreading step that occurs during DNA replication, therefore mutations occur more frequently. Also new genes are inserted at arbitrary points in the host DNA, which can harmfully affect the function of native genes while viral transgene reactivation may occur in reprogrammed cells leading to tumorigenesis as demonstrated in iPSC-derived chimeric mice [50]. These risks present a major limitation in deriving cells generated by retroviral infection to a pharmacopeia grade therefore suitable alternatives need to be sought.

1.10.2 Lentiviruses

Drug inducible lentiviruses share similar characteristics to retroviruses, with respect to genomic integration. They provide an effective means of investigating events occurring during reprogramming as they allow temporal control over gene expression [51]. Lentiviruses have also proved useful by generating secondary systems, which involves production of iPSC-derived differentiated cells that have proviral integrations in their genomes in the same pattern that allowed primary iPSC production. Upon secondary induction, the viral transgenes are reactivated leading to a 100-fold increase in secondary iPSC generation [134]. This system has provided a means of screening chemicals and genes that enhance reprogramming.

The low efficiency of reprogramming using viral vectors suggests that viral integration into specific genomic sites may be essential for reprogramming.

Viral integration sites were subsequently mapped in several mouse iPSC lines with no common integration sites identified [135]. Although a wider study would need to be performed to rule out the effect of insertional mutagenesis completely it does suggest that reprogramming is due to specific factors introduced irrespective of their integration sites. The ability of adenoviruses to reprogram differentiated cells without viral integration into the genome also provides strong evidence against the idea that reprogramming is dependent upon viral integration into specific genomic loci leading researchers to conclude that it may be feasible to develop non-integrative measures to stimulate cellular reprogramming.

1.10.3 Non-Integrating Gene Delivery

Non-integrating gene delivery techniques have been developed over recent years to overcome complications associated with sustained transgene expression and insertional mutagenesis. The first integration-free iPSCs were generated using non-integrating adenoviruses combined with transient transfection [136]. As well as demonstrating feasibility of non-viral methods for reprogramming this also provided proof of principle that transient expression of the four classical reprogramming factors was sufficient to generate iPSCs.

A significant difference between adenoviruses and retroviruses is that genetic material of the former consists of double-stranded DNA, like the DNA of the host. When an adenovirus infects a cell, its DNA is transcribed within the host cell's nucleus before being translated using the same processes used by the host cell. This lack of integration is the reason that adenoviruses are favored for reprogramming compared to retroviruses [137]. Despite obvious advantages, a major drawback using adenoviruses is their low rate of efficiency, with 0.0001% to 0.001% of cells successfully

reprogrammed [85]. Another concern is that in one study, 3 out of 13 adeno-iPSC lines were identified as tetraploid, which has not been observed using retroviruses or lentiviruses [136].

Another non-integrating method makes use of Epstein-Barr virus to generate an Epstein-Barr nuclear antigen-1 based episomal (oriP/EBNA1) vector. This vector can be transfected into somatic cells without viral packaging and later removed through drug selection. As such, exogenous DNA is not integrated into resulting iPSCs producing vector- and transgene- free iPSCs after multiple rounds of cell division. Despite the clear advantages of this system, the reported efficiency using this non-integrating method is very low with only 0.0003-0.0006% of cells successfully reprogrammed [138].

Research to date suggests that non-integrating methods of reprogramming are of typically extremely low efficiency, as insufficient factor expression results in a failure to induce complete epigenetic remodelling. Attempts to overcome this led to the generation of integration dependent delivery vectors. Doxycycline (DOX)-inducible lentiviral vectors containing a loxP site within the 3' long terminal repeat were developed so that transgenes could be subsequently removed following complete reprogramming using Cre-recombinase-mediated excision [139]. Despite the complete removal of transgenes using this method, residual vector sequences remain, therefore not completely removing risks associated with insertional mutations.

Transgene-free reprogramming has also been achieved using piggyBac (PB) transposition. PB transposon is a mobile genetic element that efficiently transposes between vectors and chromosomes via a 'cut and paste' mechanism. During this process transposase, an enzyme that catalyses this insertion or excision, recognises inverted terminal repeat sequences located at both ends of the transposon vector and efficiently integrates them into chromosomal sites. The unique feature of this system is that the PB vector can be re-excised using transposase, leaving the genome transgene-free.

Successful and efficient reprogramming of murine and human fibroblasts has been reported using doxycycline-inducible transcription factors delivered using PB transposition. However, like many non-integrating systems PB transposition also suffers from low efficiency of ~0.001% and may also leave behind residual vector sequences [84].

1.10.4 Proteins

Successful reprogramming has recently been achieved in the absence of vectors through delivery of inducing factors as purified recombinant proteins or as whole cell extracts isolated from ESCs [86, 140, 141]. While this presents an attractive approach to reprogramming with the generation of transgene-free protein induced pluripotent stem cells (piPSCs), the efficiency of this process is extremely low and requires addition of small molecules, such as VPA to stimulate reprogramming [86]. Overcoming this has been demonstrated by delivery of synthetic mRNA molecules encoding reprogramming factors into somatic cells, which led to multiple cell lines termed RNA induced pluripotent stem cells (RiPSCs) [142].

1.10.5 Lipofection

Lipofection is another non-viral method, which has been successfully used to deliver plasmids to induce reprogramming of somatic cells [143, 144]. Lipofection is a lipid-based transfection technique, which can be effectively used to deliver DNA. Lipofection was developed when scientists discovered that mixing lipids with DNA in water formed spheres known as liposomes containing a DNA core. These liposomes were able to fuse with plasma membranes and internalised via endocytosis [145]. There are three types of lipids: anionic, neutral, or cationic; which are negative, neutral and

positively-charged respectively. Initially, anionic lipids were used to produce liposomes; however they proved complex and time consuming to create. Therefore attention turned to cationic lipids, which easily combine with negatively-charged DNA due to their positive charge. When combined with DNA, cationic lipids spontaneously change to form structures known as lipoplexes, which are much more complex than simple liposomes. Once they are prepared under appropriate conditions, lipoplexes maintain an overall positive charge, enabling them to efficiently bind negatively charged cell membranes and are subsequently internalised by endocytosis [146]. Their organised structure helps protect DNA during transfection as DNA can become damaged upon entering the cell. Lipoplexes taken up via an endocytic pathway would usually result in fusion with lysosomes and subsequent DNA degradation would occur. Neutral helper lipids, such as dioleoylethanolamine (DOPE), are typically included with the cationic lipid, allowing entrapped DNA to escape the endosomes and migrate to the nucleus [147]. Although this method of gene delivery has fewer variables than alternative transfection techniques it does result in low efficiencies, therefore its application in reprogramming of somatic cells has been somewhat limited [144].

1.10.6 Nucleofection

Another non-viral transfection technique that may be used to deliver reprogramming factors to somatic cells is nucleofection. This electroporation-based technique enables efficient transfer of nucleic acids, such as DNA and RNA into cells. Nucleofection uses optimised electrical pulses generated by a device called a nucleofector with cell specific reagents to efficiently deliver nucleic acids to target cells [148]. Most transfection procedures transfer DNA to the cytoplasm and can only enter the nucleus upon disintegration of the nuclear envelope during cell division [149].

During nucleofection, the combination of cell-specific nucleofection solution and electrical pulses enables DNA to enter the nucleus. This is the only non-viral method of introducing DNA into nuclei directly, which greatly increases the chance of chromosomal integration [148]. Unlike viral vectors, which are integrated via viral genome integration mechanisms, the exact mechanism by which nucleofection integrates nucleic acids is unknown. However it has been hypothesised that integration into chromosomal DNA may occur through the cell's DNA repair and recombination enzymes [150].

As discussed previously, transfection of primary cells with common non-viral methods, such as liposome-mediated transfer has proved problematic with low efficiencies reported. This technique has been used successfully to transfect a variety of cell types including primary myoblasts [151], ESCs [152], NSCs [153] and of particular interest to this study, keratinocytes at relatively high efficiencies. One study reports transfection of primary human epidermal keratinocytes at an efficiency of 56%, the highest level of non-viral transfection reported [154]. Nucleofection has also been used to successfully reprogram human adipose stem cells (hADSc) through delivery of a minicircle vector containing a single cassette of *Oct4*, *Sox2*, *Lin-28* and *Nanog*. In addition, each transgene was separated by sequences encoding the self-cleaving peptide 2A, therefore generating transgene-free iPSCs in the absence of drug selection [144].

Optimal nucleofection conditions are not substrate dependent, therefore identical conditions are used for the nucleofection of DNA, RNA, siRNAs, shRNAs, mRNAs and other biologically active molecules. As such, switching between substrates or performing co-transfections is much simpler using this technique. Another benefit is that nucleofection can be used as a transient or stable transfection technique depending upon the desired outcome [148]. A transient approach is considered more attractive

with a view to clinical application as it excludes genomic integration, however this approach may involve the repeated transfection of inducing factors to stimulate reprogramming.

1.11 IPSC Differentiation

The major promise of iPSCs is that we can generate patient-specific cells for use in a vast array of cell therapies. Many consider iPSCs superior to other resident progenitor cells due to their pluripotent characteristics however in order to harness this potential it is necessary to develop defined differentiation strategies to ensure the homogenous differentiation of iPSCs. The majority of differentiation protocols thus far have been derived from our knowledge of hESC differentiation however this is far from defined therefore the same problems that researchers face in deriving lineage specific cells from hESCs also apply to iPSCs. Despite drawbacks a variety of functional cells have been derived from iPSCs including fetal-like red blood cells [155], retinal pigment epithelium (RPE) [156], MSCs [157] and hepatocytes [158] along with a number of disease-specific iPSCs including Parkinson's [139], lung disease [159] and acquired blood disorders [160]. One of the most widely investigated lineages is iPSC-derived cardiomyocytes [161, 162] , likely due to the well established protocols for hESC-derived cardiomyocyte differentiation. This rapid progression is exemplified with reports of large scale cardiomyocyte production with standardised, scalable processes able to manufacture hundreds of billions of cardiomyocytes for drug testing by the pharmaceutical industry [163]. This demonstrates that iPSCs are already able to provide a useful tool to efficiently select drug candidates and the focus for the future will be on developing safer ways of reprogramming to enable the development of cellular therapies.

1.11 Hypothesis

Reprogramming somatic cells circumvents not only the ethical issues associated with the use of human embryos for research but also provides a source of cells, which are patient specific. To date most reprogramming strategies have employed viral vectors for the delivery of foreign genetic material, rendering the resultant cells unsuitable for therapeutic purposes. Therefore reprogramming cells in the absence of viral vectors whilst reducing the amount of genetic material used will offer significant advances for regenerative medicine.

We hypothesised that a non-viral method of introducing both plasmid DNA and miRNA could provide an attractive alternative to viral reprogramming. In order to progress from traditional methods of reprogramming a novel, miRNA mediated approach was sought to revert the fate of differentiated hEKs isolated from the epidermis of normal adult donors. The subsequent biological and genomic effects of inhibiting a specific miRNA, miR-145, known to be implicated in the maintenance of a pluripotent phenotype would need to be investigated. In addition, we hypothesised that providing miR-145 inhibited hEKs with a microenvironment akin to that of hESCs would further stimulate the expression of endogenous pluripotency-associated genes therefore a combination of extracellular matrix protein and stimulatory growth factors known to maintain the expression of hESCs would be evaluated. In order to develop a clinically translatable approach it was hypothesised that a direct reprogramming strategy would be beneficial therefore one of the main drivers for this investigation was to direct the differentiation of miR-145 inhibited hEKs to derive functionally competent cells.

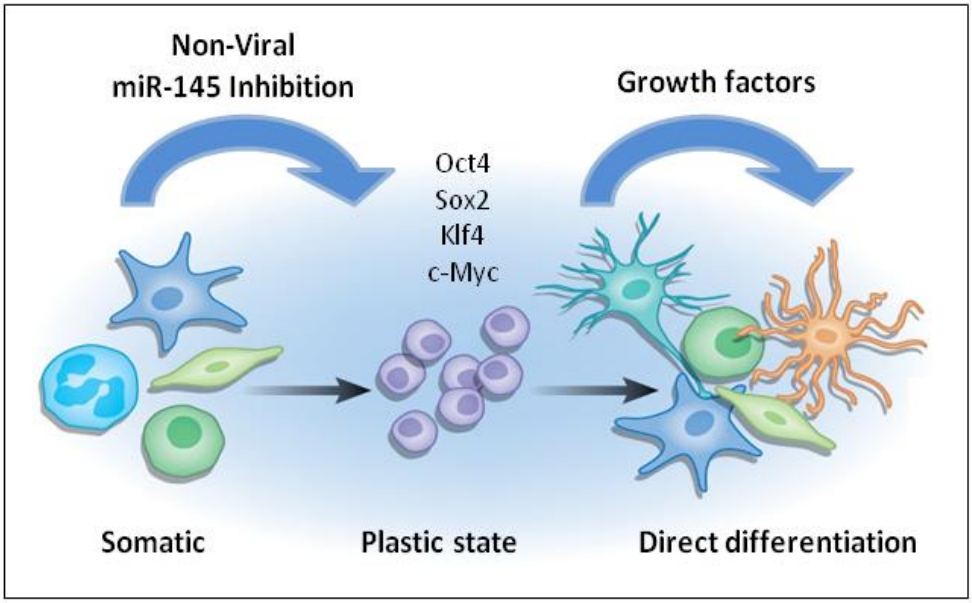

Figure 1.7 Reprogramming hEKs: A non-viral miRNA hypothesis

2.0 Materials & Methods

2.1 Cell Culture

2.1.1 Adherent Culture hEKs

Primary hEKs were isolated from normal adult skin from multiple donors of both sexes (Invitrogen) and maintained in an animal product-free environment on plasma-treated tissue culture polystyrene (TCP) (Scientific Laboratory Supplies, UK) pre-coated with 1% human Type-I collagen (hCol I) for 30 minutes at room temperature. hEKs were maintained in Epilife Media containing 1% S7 growth supplement, 1% 10,000 U/mL penicillin and 10mg/mL streptomycin. Cell culture reagents were purchased from Invitrogen, UK unless stated otherwise.

Upon reaching 75% confluence hEKs were passaged as follows: media was aspirated and the adherent cell monolayer washed with phosphate buffered saline (PBS) for 5 minutes at room temperature to remove residual protein which may inhibit enzymatic dissociation. PBS was replaced with recombinant trypsin 10x, 0.2% ethylenediaminetetraacetic acid (ETDA) (Sigma Aldrich, UK) and 0.5% trypsin diluted to a working concentration of 10% (v/v) in PBS. Trypsinisation was performed at 37°C for 3-5 minutes. Cell detachment was monitored using transmitted light microscopy until approximately 90% of cells had detached, at which point trypsinisation was neutralised by addition of an equal volume of sterile defined trypsin inhibitor containing 0.0125% purified soybean trypsin inhibitor in PBS. The trypsin/cell suspension was centrifuged at 2000g for 5 minutes at 4°C to retrieve cells. The resulting supernatant was aspirated and the remaining cell pellet resuspended in the required volume of Epilife media, pre-warmed to 37°C and reseeded at a density of 5.0 $x10^3$ cells/cm^2 before incubation at

37°C, in a humidified atmosphere, containing 5% CO_2. Culture media was refreshed 24 hours after seeding then every 3rd day until confluence.

2.1.1.1 Suspension Culture hEKs

hEKs were maintained on TCP pre-coated with hCol I in Epilife media and cells from passage 2-5 were used in subsequent experiments. Upon reaching 75% confluence hEKs were harvested as detailed in section 2.1.1 and enumerated. To induce terminal differentiation, hEKs were resuspended at a seeding density of $1x10^5$ cells/mL in DMEM (Invitrogen, UK) supplemented with 1.5% methyl cellulose (Sigma Aldrich, UK) (w/v), 10% fetal bovine serum (FBS) (Lonza, UK) (v/v), 1% 10,000 U/mL penicillin and 10mg/mL streptomycin. Cells were incubated at 37°C, in a humidified atmosphere, containing 5% CO_2.

2.1.2 Human Embryonic Stem Cells

Human embryonic stem cells (hESCs), derived from the HUES7 cell line, were obtained from Harvard University (hES Cell Facility/Melton Laboratory, MA, USA). hESCs were maintained on TCP, pre-coated for 1 hour with 50µg/mL of human plasma fibronectin (hFN) (Millipore, UK) in PBS (v/v), at 37°C. hESCs were sustained in 50:50 F12/DMEM media (Lonza, UK) supplemented with 10ng/mL Activin A (R&D, UK), 4ng/mL neurotrophin 4 (NT4) (Preprotech, UK), 40ng/mL basic fibroblast growth factor (bFGF) (Autogen Bioclear, UK), N-2 supplement (10g/L transferrin, 500mg/mL insulin, 0.63mg/L progesterone, 1.611g/L putrescine), B-27 supplement (components undisclosed), 2mM L-glutamine, 1% non-essential amino acids, 0.1mM β-mercaptoethanol (Invitrogen, UK) and 0.1% bovine serum albumin (BSA) (Sigma, UK).

When hESCs had reached approximately 75% confluence, media was removed and adherent cells washed with PBS for 5 minutes at room temperature. PBS was replaced with 5% recombinant trypsin, 2% ETDA (Sigma Aldrich, UK) diluted to a working concentration of 1% (v/v) in PBS, and detachment was performed at 37°C for less than 1 minute. Trypsinisation was monitored using transmitted light microscopy until approximately 90% of cells detached. At this point trypsinisation was neutralised by addition of an equal amount of Dulbecco's modified eagle medium (DMEM) (Invitrogen, UK) containing 10% FBS (Lonza, UK) (v/v). The trypsin/cell suspension was spun at 2500g for 3 minutes at 4°C to retrieve cells. The supernatant was aspirated from the cell pellet, which was then resuspended in culture media, pre-warmed to 37°C. Cell suspension was distributed into the required number of tissue culture vessels at a density of 1.0 x 10^4cells/cm^2 and incubated at 37°C, in a humidified atmosphere, containing 5% CO_2. Culture media was refreshed 24 hours after seeding then on alternate days with fresh media pre-warmed to 37°C until cells reached confluence.

2.1.3 Human Mesenchymal Stem Cells

Human mesenchymal stem cells (hMSCs) were maintained on conventional TCP in mesenchymal stem cell basal media (MSCBM) supplemented with SingleQuots Bulletkit containing 10% mesenchymal stem cell growth supplement (MSCGS), 2% L-glutamine and 0.1% gentamicin/amphotericin. All hMSC culture reagents were purchased from Lonza, UK unless stated otherwise.

Upon reaching 75% confluence hMSCs were passaged as follows. Media

was aspirated and the adherent cell monolayer washed with PBS for 5 minutes at room temperature. PBS was replaced with 5% recombinant trypsin, 2% ETDA (Sigma Aldrich, UK) diluted to a working concentration of 10% (v/v) in PBS. Detachment was carried out at 37°C for 3-5 minutes and monitored using transmitted light microscopy until approximately 90% of cells had detached at which point the reaction was neutralised by the addition of an equal volume of pre-warmed hMSC media. Trypsin/cell suspension was centrifuged at 2000g for 5 minutes at 4°C. The resulting supernatant was aspirated and the remaining cell pellet resuspended in the required volume of hMSC media, pre-warmed to 37°C. The cell suspension was distributed into the required number of tissue culture vessels at a density of 5.0 $x10^3$ cells/cm^2 diluted in sufficient media to permit long-term culture and incubated at 37°C, in a humidified atmosphere, containing 5% CO_2. Media was refreshed 24 hours after seeding then every 3rd day until confluence.

2.2 Nucleofection

hEKs were passaged 7 days preceding nucleofection, cultured until 75% confluent with daily media changes. Reagents were purchased from Lonza, UK unless otherwise stated. hEKs were dissociated using a 5% recombinant trypsin, 2% ETDA (Invitrogen, UK) diluted to 1% in PBS (v/v) and enumerated using a haemocytometer. An appropriate volume of cell suspension was aliquoted into sterile falcon tubes to a working concentration of $7x10^5$ cells/mL. Trypsin/cell suspension was centrifuged at 2000g for 5 minutes at 4°C and the resulting cell pellet was resuspended in 100µL keratinocyte nucleofector solution and transferred to a sterile cuvette. In addition, either 2µg pmaxGFP plasmid (GFP-P) (Lonza, Germany), 1.5µg miRNA hairpin inhibitor control labelled with Dy547 or hsa-miR-145 hairpin inhibitor antisense oligonucleotide sequence:

GUCCAGUUUUCCCAGGAAUCCCU (Dharmacon, USA) were added to each cuvette. Controls consisted of $7x10^5$ hEKs resuspended in 100µL keratinocyte nucleofector solution, minus the addition of either GFP-P or miRNA inhibitor. Cuvettes were immediately inserted into the nucleofector device and selecting the T-024 program, nucleofection was performed. Immediately after nucleofection, 500µL of pre-warmed media was added to each sample and the contents transferred onto TCP substrates, pre-coated with either hCol I or hFN, within wells containing cell culture media pre-warmed to 37°C. Samples were incubated at 37°C, in a humidified atmosphere, containing 5% CO_2. After 24 hours media was exchanged in order to remove dead cells and refreshed every 3rd day.

2.3 Immunohistochemistry

Cells were cultured on TCP cover slips and immunohistochemistry carried out *in situ*. Cells were fixed using 4% (w/v) paraformaldehyde solution (Sigma Aldrich, UK); 4g of paraformaldehyde was dissolved in 100mL ddH_2O at 60°C with continuous stirring for 10 minutes, solution was cleared using sodium hydroxide and pH adjusted to 7.2.

Culture media was aspirated and samples washed in PBS (without Ca^{2+} or Mg^{2+}) for 5 minutes at room temperature. Samples were fixed using 4% paraformaldehyde solution for 10 minutes at 37°C and washed with PBS for 5 minutes at room temperature. Non-specific antigens were blocked by the addition of 10% (v/v) animal serum (Invitrogen, UK) in PBS for 1 hour at room temperature. Specifically the blocking serum used was the same speciation as the desired secondary antibody. Where the detection of intracellular antigens was required, 0.1% Triton-X100 (v/v) (Sigma Aldrich, UK) was also added to the blocking solution to permeabilise samples.

Blocking solution was aspirated and primary antibodies added at working concentrations given in table 2.1. Primary antibodies were diluted in 1% animal serum (v/v)/PBS. For intracellular antigens 0.1% Triton-X100 (v/v) was also included. Incubations were performed overnight at 4°C. Negative controls to establish non-specific binding were setup by replacing primary antibodies with relevant isotype controls (Autogen Bioclear, UK).

Following incubation with primary antibodies samples were washed 3 times with PBS for 5 minutes at room temperature to remove unbound antibody. Samples were incubated with appropriate fluorescently conjugated secondary antibodies diluted to working concentrations, given in table 2.2, for 1 hour at 37°C. Secondary antibodies were diluted in 1% animal serum/ PBS and where intracellular staining was required, 0.1% Triton-X100 was included. Following incubation with secondary antibodies samples were washed 3 times with PBS for 5 minutes at room temperature to remove unbound antibody. Counter-staining was performed by illuminating f-actin using phalloidin (Invitrogen, UK) at a working dilution of 1:100. This phallotoxin is conjugated to an Oregon Green fluorochrome (Ex495, Em518nm) allowing visualisation of F-actin filaments. Prior to visualisation, cells were counterstained with vector shield mounting medium (Vector Laboratories, UK), containing the fluorescent 4',6'-diamidino-2-phenylindole (DAPI) (Ex358, Em461), which specifically stains cell nuclei. Immediately after mounting, samples were visualised using laser scanning confocal microscopy (LSM 510, Carl Zeiss).

Antigen	Speciation	Reactivity	Clonality	Supplier	Dilution
Oct4	Mouse	Human	Monoclonal	Santa Cruz	1:500
Nanog	Goat	Human	Monoclonal	R&D, UK	1:200
Sox2	Mouse	Human	Monoclonal	R&D,UK	1:100
TRA-1-81	Mouse	Human	Monoclonal	Abcam,UK	1:500
TRA-1-60	Mouse	Human	Monoclonal	Abcam,UK	1:500
SSEA3	Rat	Human	Monoclonal	R&D,UK	1:100
SSEA4	Mouse	Human	Monoclonal	Abcam,UK	1:100
Cytokeratin14	Mouse	Human	Monoclonal	Abcam,UK	1:500
Involucrin	Mouse	Human	Monoclonal	Abcam,UK	1:100
CBFA1	Rat	Human	Monoclonal	Abcam,UK	1:100
Osteocalcin	Mouse	Human	Monoclonal	Abcam,UK	1:100
Aggrecan	Mouse	Human	Monoclonal	Abcam,UK	1:100
Type II Collagen	Mouse	Human	Monoclonal	Abcam,UK	1:100
Leptin	Rabbit	Human	Monoclonal	Abcam,UK	1:50
Neurofilament	Mouse	Human	Monoclonal	Abcam,UK	1:50
B-III Tubulin	Mouse	Human	Monoclonal	Abcam,UK	1:50

Table 2.1 Primary antibodies used in immunohistochemical staining

Antigen	Speciation	Reactivity	Conjugate	Supplier	Dilution
IgG2b	Goat	Mouse	AlexaFluor 594	Invitrogen,UK	1:2000
IgG	Rabbit	Goat	AlexaFluor 488	Invitrogen,UK	1:500
IgG2a	Goat	Mouse	AlexaFluor 594	Invitrogen,UK	1:500
IgM	Goat	Mouse	AlexaFluor 633	Invitrogen,UK	1:100
IgM	Goat	Rat	AlexaFluor 488	Invitrogen,UK	1:500
IgG	Goat	Mouse	AlexaFluor 488	Invitrogen, UK	1:100
IgG	Goat	Rat	Texas Red	Invitrogen, UK	1:100
IgG	Donkey	Mouse	AlexaFluor 594	Invitrogen, UK	1:500
IgG	Chicken	Rabbit	AlexaFluor 594	Invitrogen, UK	1:500

Table 2.2 Secondary antibodies used in immunohistochemical staining

2.4 Live/Dead Staining

Live/dead reagents were supplied in kit form by Invitrogen, UK in combination with a Hoechst counter stain (Invitrogen, UK). The Live/Dead viability kit contains two dyes, calcein AM and ethidium homodimer-1 (EthD-1). Live cells can be identified with calcein AM due to their intracellular esterase activity. This enzyme converts non-fluorescent calcein AM into intensely fluorescent calcein (Ex494, Em520). Dead cells can be distinguished through EthD-1, which is exclusively taken up by cells with damaged membranes, binding double stranded DNA (Ex510, Em595). Hoechst was used to stain cell nuclei irrespective of their viability (Ex350, Em461).

Live/dead reagents were diluted in PBS to give working concentrations of 0.1mM EthD-1 and 0.1mM calcein AM. Hoechst was diluted in PBS to a working concentration of 3mg/mL. Media was aspirated and adherent cells washed with PBS for 5 minutes at room temperature to remove residual esterase activity resulting from serum-supplemented media. Equal amounts of each solution were added to the cells and incubated at 37°C for 30 minutes. Samples were then washed with PBS for 5 minutes at room temperature and visualised immediately using inverted fluorescent microscopy (Axiovert 200, Carl Zeiss) or quantified using flow cytometry.

2.5 Quantification of Cell Attachment to HFN

hFN was diluted in PBS and added to TCP substrates at defined concentrations and incubated at 37°C for 45 minutes to ensure complete coating. hFN solution was aspirated and replaced with cell suspension containing $5x10^4$ hEKs before incubation at 37°C, 5% CO_2. 24 hours post-seeding, the culture media was removed and the cells washed twice with PBS ensuring only hEKs that had successfully attached remained in the

culture system. hEKs were detached and enumerated using a haemocytometer.

2.6 Trypan-Blue Exclusion Assay

hEKs were harvested as detailed in section 2.1.1 and the resulting cell pellet resuspended in 1mL PBS. An aliquot of cell suspension was mixed with an equal volume of 0.4% trypan blue and incubated at room temperature for 3 minutes. 10µL of this mixture was then added to a haemocytometer and the stained (non-viable) and non-stained (viable) cells enumerated.

2.7 Von Kossa Staining for Visualisation of Mineralisation

Prior to Von Kossa staining the following solutions were prepared: 1% silver nitrate ($AgNO_3$) (w/v) (Sigma Aldrich) in ddH_2O, 2.5% sodium thiosulphate (w/v) (Sigma Aldrich, UK) in ddH_2O and 1% acid alcohol solution (v/v) generated by diluting 1% 1M HCl (hydrochloric acid) (Sigma Aldrich, UK) in ethanol.

Samples were fixed using 4% paraformaldehyde (w/v) (Sigma Aldrich, UK) for 10 minutes, followed by a 5 minute wash using PBS then 3 changes of ddH_2O for 5 minutes each: All reactions were carried out at room temperature. Samples were submersed in 1% $AgNO_3$ solution and subjected to UV light excitation for 1 hour. The 1% $AgNO_3$ solution was then replaced with 3 changes of ddH_2O for 5 minutes each. Samples were incubated with a 2.5% sodium thiosulphate solution for 5 minutes to remove any residual silver and subject to 3 changes of ddH_2O for 5 minutes each before counterstaining with Harris' haematoxylin (Sigma Aldrich, UK) for 5 minutes. Samples were 'blued' under running ddH_2O for 5 minutes,

differentiated in 1% acid alcohol for 3 seconds and finally washed using 3 changes of ddH_2O for 5 minutes each before mounting with aqueous mountant (Sigma Aldrich, UK) and immediately visualised using transmitted light microscopy. Positive staining of phosphates appeared as dark brown/black staining whilst nuclei appeared blue.

2.8 Alizarin Red S Staining for Visualisation of Calcification

Alizarin Red S can be used to identify calcium deposits, however it does not exclusively stain calcium since magnesium, manganese, barium, strontium and iron may also interfere with Alizarin Red S staining. The presence of calcium results in the formation of an Alizarin Red S-calcium complex in a chelation process.

Prior to staining, a 2% Alizarin Red S solution (w/v) was prepared by dissolving 2g of Alizarin Red S (w/v) (Sigma Aldrich, UK) in 100mL of ddH_2O. The pH of this solution was then adjusted to 4.1 through drop-wise addition of NaOH.

Samples were fixed using a 4% paraformaldehyde solution for 10 minutes: All reactions were carried out at room temperature. Post-fixation, this solution was aspirated and the samples washed 3 times with ddH_2O for 5 minutes each. Samples were incubated in 2% Alizarin Red S for 5 minutes and the reaction was observed microscopically. Excess Alizarin Red S was blotted from the samples using filter paper (Whattman, UK) and subsequently dehydrated through immersion in 100% acetone (Fisher Scientific, UK) for 1 minute, followed by 50% acetone-xylene solution for 1 minute before clearing in 100% xylene (VWR, UK). Finally, samples were mounted with DPX mounting medium (VWR, UK) before visualisation

using transmitted light microscopy. Positive staining of calcium deposits was observed as orange-red staining.

2.9 Van Gieson Staining for Visualisation of Collagen

Prior to Van Gieson staining the following solutions were prepared: 1% acid fuschin (w/v) (Sigma Aldrich, UK) in ddH_2O which was subsequently added to saturated aqueous picric acid (Sigma Aldrich, UK) (v/v) at a concentration of 10% to generate the Van Gieson stain. This solution was boiled for 3 minutes before filtering, cooling and adding 250µL 1M HCl. Weigert's iron haematoxylin was generated by mixing equal parts of A (1% haematoxylin in ethanol) & B (ferric chloride in dilute HCl) (Sigma Aldrich, UK) and a 1% acid alcohol solution (v/v) generated by diluting 1% 1M HCl in ethanol.

Samples were fixed in 4% paraformaldehyde for 10 minutes: All reactions were carried out at room temperature. The 4% paraformaldehyde solution was aspirated and samples washed in PBS for 5 minutes. Weigert's haematoxylin was applied to samples for 20 minutes before washing them in ddH_2O for 5 minutes. Samples were then differentiated in 1% acid alcohol for 3 seconds and again washed in ddH_2O for 5 minutes before applying Van Gieson stain for 5 minutes. Samples were blotted using filter paper and dehydrated through gradients of ethanol: 70%, 90% and 100% (v/v) for 2 minutes each. Finally samples were cleared in 100% xylene (VWR, UK) and mounted with DPX mounting medium (VWR, UK) before visualisation using transmitted light microscopy. Positive staining of collagen was observed as pink/red staining while nuclei appeared brown.

2.11 Oil Red O Staining for Visualisation of Lipid Droplets

Prior to Oil red O staining a 0.5% Oil red solution (w/v) (Sigma Aldrich, UK) was prepared by dissolving 0.5g of Oil red O powder in 100mL of 1,2,propandiol $CH_3(OH)CH_2OH$] (Sigma Aldrich, UK) at 95°C. Once the Oil red O had completely dissolved the resultant solution was then filtered through coarse 25µm filter paper (Whattman, UK) overnight.

Samples were air dried for 30 minutes before fixation in 4% paraformaldehyde for 10 minutes: All reactions were carried out at room temperature unless otherwise stated. Post-fixation samples were washed in ddH_2O for 5 minutes before being transferred to 100% 1,2,propanediol for 5 minutes to avoid carrying H_2O over into the Oil red O. Samples were stained in pre-warmed 0.5% Oil red O for 8 minutes at 60°C before being washed in 100% 1,2,propanediol for 5 minutes. Samples were washed in ddH_2O for 5 minutes before being counterstained in Gill's haematoxylin (Sigma Aldrich, UK) for 2 minutes. Samples were then 'blued' in ddH_2O for 5 minutes before mounting with aqueous mountant (Sigma Aldrich, UK) and visualised using transmitted light microscopy. Positive staining of lipid droplets can be observed as pink/red staining whilst nuclei appear blue.

2.12 Real-Time Polymerase Chain Reaction (qRT-PCR)

2.12.1 Primer Design

A series of steps were undertaken to design suitable primers for qRT-PCR reactions. Firstly, coding strand cDNA sequences (CDS) of genes of interest were identified using the genome search platform www.ncbi.nlm.nih.gov. The CDS sequence was copied into the primer design platform, Beacon Designer V.7.21 (Premier Biosoft International, USA). A basic local alignment search tool (BLAST) was then used to search human genome sequence databases to find regions of local similarity within sequences. Once a successful BLAST had been performed a primer search was carried out allowing the selection of regions of the coding strand sequence suitable for amplification. A final product size of 75-200bp was selected for optimal compliance with SYBR green chemistry, along with low guanine-cytosine (GC) content and an annealing temperature of 55.0 +/- 5.0°C. In addition, all primers were designed between 18-24bp in length. The proposed amplicons were verified for tertiary structures using the DNA mfold server provided by M. Zuker at http://frontend.bioinfo.rpi.edu/applications/mfold/cgi-bin/dna-form1.cgi. Primers that formed complex hairpin loops at the annealing temperature identified by the primer design platform were discarded as it was unlikely that they would anneal correctly. An example of a predicted tertiary structure of a target amplicon is illustrated in Figure 2.1.

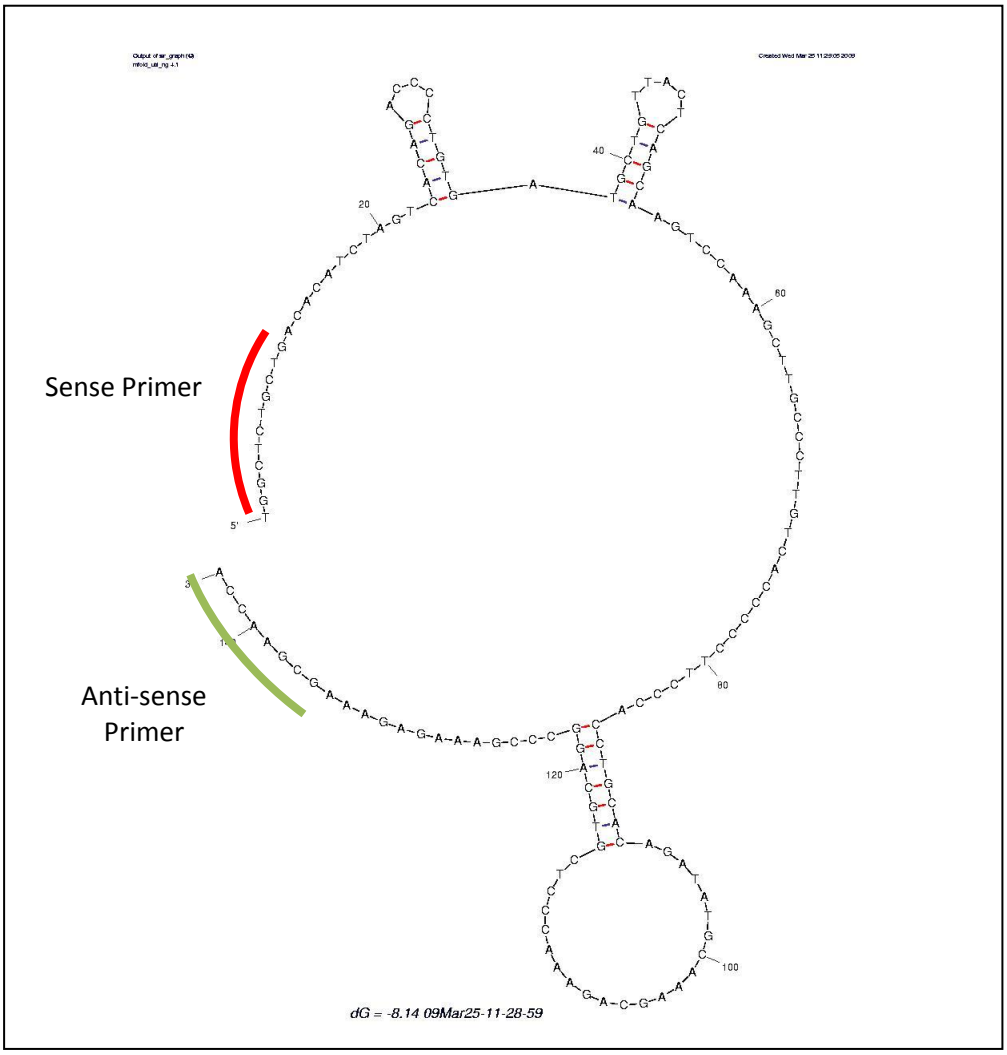

Figure 2.1 Predicted tertiary structure of target amplicon for *Oct4* generated using mfold application

After identification of suitable binding sequences at the annealing temperature specified, primers were synthesised at a production scale of 25nM by Invitrogen, UK. All primers (table 2.3) were designed in-house with the exception of Klf4 and Cytokeratin-14, which were purchased from Primer Design Ltd, UK.

Target Gene	Accession Number	Sense Primer	Antisense Primer	Tm
β-Actin	NM001101	GGACCTGACT GACTACCTC	GCCATCTCTTG CTCGAAG	53.9
GAPDH	NM002046	GAAGGTGAAG GTCGGAGT	CATGGTGGAA TCATGTTGGA A	53.5
18S rRNA	NR003286.1	CGT CTG CCC TAT CAA CTT TC	TGC CTT CCT TGG ATG TGG	53.3
Oct4	NM002701.4	TGGCTCTGCTG ACACATC	TGGTTCGCTTT CTCTTTCG	53.4
Sox2	NM003106.2	GAGAGAAAGA AAGGGAGAGA AG	GAGAGAGGCA AACTGGAATC	53.0
Nanog	NM024865.2	CTGGCTGAAT CCTTCCTCTCC	TGATTAGGCTC CAACCATACT CC	57.0
C-Myc	NM002467.3	CAC ATC AGC ACA ACT ACG	GTT CGC CTC TTG ACA TTC	50.1
Klf4	NM004235.3	Custom Design	Custom Design	60.0
Cytokeratin14	NM000526	Custom Design	Custom Design	60.0
CBFA1	AH005498	GGCAGTTCCC AAGCATTTC	GCAGGTAGGT GTGGTGTG	54.5
Osteonectin	BC008011	GCTGGATGAT GAGAACAACA C	AAGAAGTGGC AGGAAGAG	53.4
Osteocalcin	NM000711	AGCGAGGTAG TGAAGAGAC	GAAAGCCGAT GTGGTCAG	55.2
Collagen II	NM001844	GAGCAGCAAG AGCAAGGAGA AG	TGGACAGCAG GCGTAGGAAG	54.3
PPAR-γ	NM005037	GACCACTCCC ACTCCTTTG	GTGAATGGAA TGTCTCGTAAT G	50.7
Adiponectin	EU420013	ATATGAAGGA TGTGAAGGTC	CAGCATAGAG TCCATTACG	54.1
Nestin	NM006617	GGAAAGTCAA AGGAATCTG	CTTCTCCACCG TATCTTC	53.7
Neurofilament	NM006158	CTTCCAGAAG CCAAGACTCC AG	GAAGCAGATG TCGTAGAGC	55.0

Table 2.3 Details of primers used in qRT-PCR analysis

2.12.2 Primer Optimisation

Using this design process the most suitable primers were selected, however further optimisation was required to ensure correct efficiency. For each primer set a plate was prepared to include a no template control followed by serial dilutions of target cDNA. The Bio-Rad software was then used to calculate the efficiency of each primer set through selecting the appropriate annealing temperature, highlighting the wells to be detected and identifying the dilution factor for the defined standards. At the end of the qRT-PCR reaction a standard curve graph was produced and from this, the efficiency of the reaction calculated an example of this is illustrated in Figure 2.2. Only primers sets with an efficiency of 90% or more were used in subsequent qRT-PCR experiments.

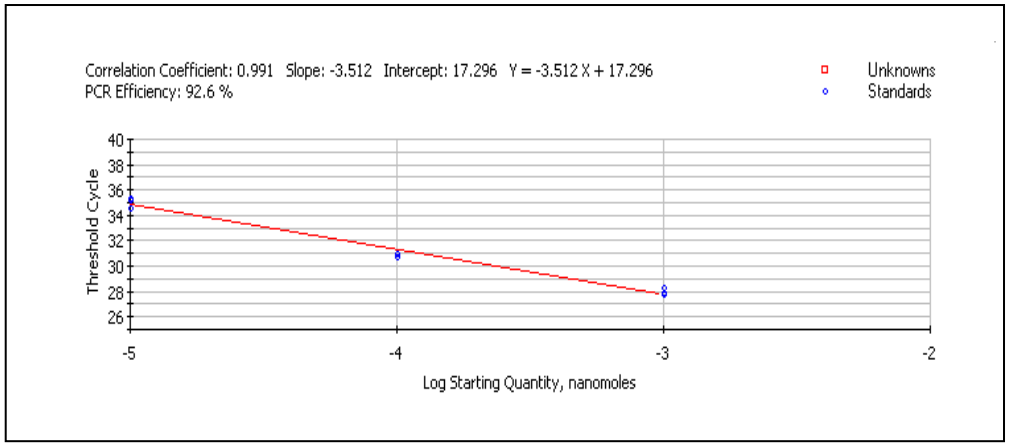

Figure 2.2 Efficiency standard curve for *Sox2* primers

2.12.3 RNA Isolation

The following solutions were prepared prior to total cellular RNA isolation with all reagents used purchased from Qiagen, UK unless stated otherwise. 44mL of ACS grade 100% ethanol were added to 6mL of wash buffer

(RPE), while 10µL of 1M β-mercaptoethanol (Sigma-Aldrich UK) were added to 1mL of lysis buffer (RLT).

Samples were washed for 5 minutes with PBS at room temperature: This was repeated three times to ensure complete removal of culture media. Following this, 350µL of buffer RLT was added to each sample and incubated for 5 minutes at room temperature. The resulting lysate was transferred to a QIAshredder column and spun at 13400g for 2 minutes. 250µL of 100% ethanol was added to the eluant, transferred to an RNeasy mini column and spun at 13400g for 15 seconds. 500µL of wash buffer (RW1) was then added to the column and incubated for 5 minutes at room temperature before being spun at 13400g for 15 seconds. Following this, 500µL of pre-warmed buffer RPE was added to the column and spun for 13400g for 15 seconds. This step was repeated a second time and spun at 13400g for 2 minutes. Finally, to elute RNA this column was transferred to an RNase free tube and 30µL of RNase free ddH_2O added, incubated at room temperature for 2 minutes then spun at 13400g for 1 minute. The quantity and purity of isolated RNA was determined by 260/280nm absorbance using a spectrophotometer and only samples that had a 260/280nm absorbance between 1.9 and 2.1 were used in subsequent experiments. Once the quantity and purity had been recorded RNA samples were stored at -80°C until required.

2.12.4 cDNA Synthesis

The following stock solutions were prepared prior to reverse transcription: All reagents were purchased from Invitrogen, UK unless otherwise stated. Stock 1 consisted of 1µL 50 µM Oligo $(dT)_{20}$, 1µL 10mM deoxyribonucleotide triphosphate (dNTP) and 9µL RNase free ddH_2O. Stock 2 consisted of 4µL 5x first-strand buffers, 1µL 0.1M dithiothreitol

(DTT), 1µL RNaseOUT recombinant RNase inhibitor (40U/µL) and 1µL SuperScript III RT (200U/µL). Each of these stock solutions was required for the reverse transcription of 2µg of RNA and was scaled up accordingly for larger sample numbers. Stock 1, with the addition of 2µL of RNA, was denatured at 65°C for 5 minutes, immediately followed by a 1 minute chill on ice. After this, stock 2 was added and heated for 40 minutes at 50°C, immediately followed by a further 15 minutes of heating at 70°C to terminate the reaction. The synthesised cDNA was stored at -20°C.

2.12.5 qRT-PCR

There are several variables that must be considered in order to produce accurate, reproducible qRT-PCR data. All reactions were carried out in triplicate with the inclusion of a no template control in all reactions, which included all reaction components except the cDNA of interest. This allowed the detection of any contaminated reaction components that might have reduced the relevance of the data collected. qRT-PCR offers the advantage of detecting inaccurate primer binding, such as the formation of primer dimers, through melt curve analysis. During melt curve analysis the temperature of each reaction was increased incrementally providing peak fluorescence at a specific temperature. As the temperature increments denature the double stranded PCR products the SYBR green dissociates with intricate kinetics dependant on the nucleotide sequence, with continuous luminescent monitoring. If target-specific binding has been carried out specifically, the dissociation temperature would be the same for each reaction due to the sequence homogeneity of the PCR products. Therefore as a final verification step melt curve analysis was conducted at the end of each amplification, allowing any anomalies to be eliminated based upon this analysis.

Prior to qRT-PCR the following solutions were prepared: Primer solutions were generated from 10µL sense primer and 10µL antisense primer (Invitrogen,UK) diluted in 80µL of Ultra Pure ddH_20 (Invitrogen, UK). A PCR reagent stock solution was prepared from 7.5µL SYBR Green single tube real time master mix (Bio-Rad, UK), 4.5µL ultraPURE ddH_2O and 1µL primer solution per reaction.

Where primers were designed and supplied by Primer Designs Ltd, UK the primer mix (Primer Designs Ltd, UK) was reconstituted with 660µL ultraPURE ddH_2O. A PCR reagent stock solution was prepared from 10µL SYBR Green single tube real time master mix (Bio-Rad, UK), 4µL ultraPURE ddH_2O and 1µL primer solution per well.

The cDNA synthesised from the reverse transcription reaction was diluted 10 fold with ultraPURE DNase, RNase free ddH_2O prior to undergoing the qRT-PCR reaction. All PCR reactions were carried out in RNase-free 96 well plates (Bio-Rad, UK). In PCR reactions, using in-house designed primers, the diluted cDNA was added to each well in triplicates of 2µL then 13µL of PCR reagent stock solution was added to each well to give a total reaction volume of 15µL. In the instance where PCR reactions utilised primers provided by Primer Designs, diluted cDNA was added to each well in triplicates of 5µL then 15µL of PCR reagent stock solution was added to each well to give a total reaction volume of 20µL. No template controls were included in each plate by replacing cDNA with ultraPURE ddH_2O to identify contaminant DNA in reaction reagents. At all stages of the experimental setup, filtered RNase-free pipette tips were used (Starlab, Germany).

qRT-PCR reactions were carried out using a Bio-Rad i-cycler and the standard i-cycler operating platform (Bio-Rad, UK). qRT-PCR was conducted as follows for reactions using primers designed in-house: Plates were denatured for 3 minutes at 95°C, 40 cycles of amplification at 95°C for

30 seconds, followed directly by 30 seconds of the optimum annealing temperature for the specific primer detailed in table 2.3. For reactions using primers supplied by Primer Designs Ltd, plates were denatured for 10 minutes at 95°C. Following this there were 40 cycles of amplification at 95°C for 15 seconds directly followed by 60 seconds at the annealing temperature of 60°C.

C_t values were calculated when fluorescence from SYBR Green binding to double stranded DNA entered its exponential phase during amplification. Once amplification had been performed melt curve analysis of the product was undertaken where plates were subject to an increase in temperature of 1°C per second starting at 55°C and terminating at 95°C. This quantified the decrease in fluorescence as the double stranded DNA dissociated. As the melting temperature of double stranded DNA varies depending upon its base composition, this analysis indicates the identity of the amplified products when compared against the melting temperature of an amplified product for a specific primer. Amplicons were stored at 4°C for further analysis using gel electrophoresis.

2.12.6 Agarose Gel Electrophoresis

qRT-PCR products were subject to electrophoresis using a 1.5% agarose gel to confirm the identity of an amplicon Firstly, a 10% Tris-Borate-EDTA (TBE) (Sigma Aldrich, UK) solution was prepared by diluting 100mL TBE in 900mL ddH_2O (v/v). Then a 1.5% agarose solution was prepared by dissolving 1.5g agarose powder (Sigma Aldrich, UK) in 100mL of 10% TBE buffer (w/v) and heated until the agarose had completely dissolved. Once the solution had cooled 2µL of ethidium bromide (Merck, Germany) was added and the gel was poured into a casting tray including the addition of a comb to allow the formation of individual wells. When the gel had

solidified, the comb marking the wells was removed from the gel tray, the gel was transferred to the electrophoresis basin and submerged in 1x TBE buffer. 5µL of each sample were loaded into each well along with 1µL 6x loading buffer (Promega, UK). One lane was also loaded with 5 µL of a 100bp DNA ladder (Promega, UK) along with 1µL 6x loading buffer (Promega, UK). An electrical current was then passed through the gel from negative to positive at a voltage of 90V for 45 minutes allowing separation of different sized DNA fragments. Once electrophoresis was complete the PCR products could be directly visualised, due to the incorporation of ethidium bromide into the gel, with UV light illumination using a Multi Image light cabinet (GRI LTD, UK). Images were captured using Alpha Imager 2200 software.

2.13 Flow Cytometric Analysis of Nucleofected hEKs

Quantification of hEKs nucleofected with either GFP-P (Lonza, Germany) or miRNA inhibitor (Dharmacon, USA) was performed using flow cytometry. Adherent cells were washed with PBS for 5 minutes at room temperature. This solution was replaced with 10% recombinant trypsin/EDTA (Invitrogen,UK) for approximately 5 minutes until 90% of cells had become detached, observed by transmitted light microscopy. The cell/trypsin solution was then diluted in an equal volume of defined trypsin inhibitor (Invitrogen,UK) to neutralise the reaction and cells collected using centrifugation at 2000g for 5 minutes at 4°C. The cell pellet was resuspended in 1mL of sheath fluid (BD-Biosciences, UK) and transferred into clean flow cytometry tubes (Elkay, UK) for subsequent analysis using a FACsort flow cytometer (BD-Biosciences, UK). Non-specific fluorescence was determined using control samples, which had previously been nucleofected in the absence of either GFP-P (Lonza, Germany) or miRNA inhibitor (Dharmacon, USA).

2.14 Differentiation Assay

Four cell types: miR-145 inhibited hEKs maintained in either hEK or hESC media for 5 days prior to directed differentiation, hEKs taken at passage 3 nucleofected without miR-145 inhibitor and hMSCs taken at passage 4 were subject to directed differentiation parameters.

hEKs were nucleofected as detailed in section 2.2 whilst hMSCs were seeded in a monolayer at a density of $5x10^4$ cells/cm^2 cultured under basal conditions for 24 hours before replacing the media with defined differentiation media (Table 2.4). All samples were incubated at 37°C, 5% CO_2 with media refreshment every 7^{th} day for 28 days.

Osteogenic Low Glucose DMEM (1g/L) + 10% FBS	**Chondrogenic** High Glucose DMEM (4.5g/L) + 1% FBS
Ascorbate 50µM	Pyruvate 1mM
Dexamethasone 100nm	Ascorbate 50µM
B-Glycerophosphate 10mM	Dexamethasone 100µm
	TGFβ1 10ng/mL
Adipogenic Low Glucose DMEM (1g/L) + 10% FBS	**Neurogenic** Low Glucose DMEM (1g/L) + 10% horse serum
Dexamethasone 1µm	All-trans retinoic Acid 300ng/mL
Hydrocortisone 50µm	

Table 2.4 Soluble factor composition of defined differentiation media

2.15 Platelet-Poor Plasma (PPP)-Derived Hydrogel Synthesis

2.15.1 Blood Plasma Isolation

20mL of peripheral blood was isolated from consenting healthy humans via venipuncture, collected in sterile plastic falcon tubes and anticoagulated using 10% 10mM sodium citrate (v/v) (Sigma Aldrich, UK), which inhibits clotting through the chelation of Ca^{2+}. Citrated blood samples were allowed to remain at room temperature for 2 hours before incubation at 4°C overnight. Blood was centrifuged at 1000g for 10 minutes and the resulting supernatant decanted. This supernatant was then centrifuged once more at 1000g for 10 minutes to largely remove blood cells. The citrated, platelet poor plasma was then stored at -20°C.

2.15.2 Stable Hydrogel Formation

A PPP-derived hydrogel was prepared from two distinct components: citrated, platelet poor human blood plasma and basal media containing calcium. Components were pre-warmed to 37°C and the blood plasma fraction added to the media component at a concentration of 10% (v/v). The combined liquids were incubated for 5 minutes at 37°C resulting in a stable hydrogel. The gellation process occurred as a result of the presence of Ca^{2+} in the media, which allows blood coagulation to proceed in combination with the liquid component of the media, forming a hydrogel.

2.16 Ectopic Bone Formation Model

All studies adhered to UK home office use of animals in scientific procedures guidelines. Subjects (NOD/SCID mice, male, 6 weeks old, 10-15g) were anaesthetised using a gas and air mix equal ratio of O_2/NO

supplemented with isofluorane at 2% (v/v). Once the subject was sedate (confirmed by the absence of a pedal withdraw reflex), the injection area was sterilised using surgical iodine. Buprenorphine (pain relief) and Baytril (prophylactic antibiotic) were administered by subcutaneous injection.

Subjects received four injections, 1 above each each shoulder and each hip. 4 human cell types were selected for validation: miR-145 inhibited hEKs maintained in hEK media, miR-145 inhibited hEKs maintained in hESC media, hMSCs maintained in MSCBM and hEKs nucleofected in the absence of miR-145 maintained in hEK media. Each cell type was injected both with and without 1% hydroxyapatite beads (w/v) (Biocomposites, Keele, UK).

Each implant site received $5x10^5$ cells, in the case of hEKs passage 2-4 while all hMSCs were passage 4, in a total injection volume of 300µL. Citrated PPP and culture media were pre-warmed then combined at a concentration of 10% PPP: media (v/v) immediately prior to implantation using a three-way stop cock system (Smiths Medical, UK), shown in Figure 2.3, before delivery through a 21 gauge needle.

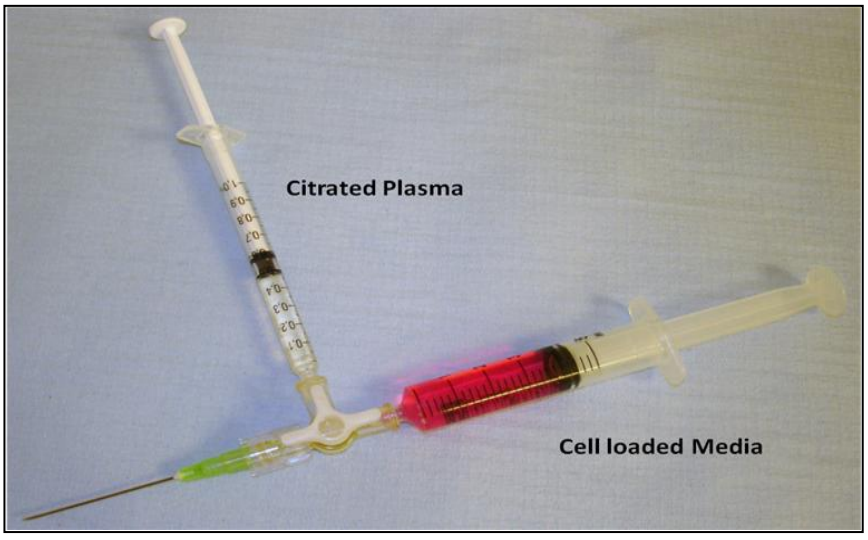

Figure 2.3 Implantation system used for the delivery of cell loaded hydrogel *in vivo*

Animals were sacrificed at 4 and 8 weeks post-implantation using asphyxiation with CO_2 and ectopic tissue explanted for analysis.

2.17 Histological Tissue Processing

Samples were placed directly into periodate-lysine-paraformaldehyde fixative, which was prepared as follows. A 0.2M lysine-HCl solution and a 0.1M solution of Na_2HPO_4 were prepared. 60mL of 0.1M Na_2HPO_4 was then added to 300mL of Lysine-HCl to result in a solution with a pH of 7.4. Next, a 0.1M NaH_2PO_4/ Na_2HPO_4 buffer was prepared. 240mL of this phosphate buffer was added to the Lysine-HCl/Na_2HPO_4 solution resulting in a 0.1M concentration of Lysine-HCl.

Immediately prior to use, 300mL of the phosphate buffered lysine-HCl solution was combined with 100mL of 2% (w/v) paraformaldehyde and to this was added sodium periodate resulting in a concentration of 0.1M. The fixative was then chilled to 4^{o}C prior to use. Samples were placed under periodate-lysine-paraformaldehyde fixation on a roller for 48hrs at 4^{o}C.

Fixative was aspirated from samples and replaced with a cold washing solution, which consisted of the previously described 0.1M phosphate buffer modified to contain 7% sucrose and 40mM NH_4Cl. Samples were gently rolled at 4^{o}C for 24 hours. After this time had elapsed, the cold washing solution was aspirated and replaced by ice-cold acetone to remove phosphate crystals and dehydrate the specimens, for 48 hours at 4^{o}C.

Once samples were suitably dehydrated they were immersed in 100% glycol methacrylate (GMA) (TAAB, UK) for 24 hours at 4^{o}C, after which, samples were moved to ice cold Technovit infiltration solution (TAAB, UK) for a further 24 hours at 4^{o}C. Specimens were then cast in place in an appropriately sized mould, orientated carefully for optimum cutting and

submersed in Technovit embedding solution (TAAB, UK). The pre-resin surface was covered with mineral oil to prevent oxidation and evaporation, sealed with aluminium foil and placed at -55^{o}C to infiltrate for 4 days. After this time had passed, the incubation temperature was then increased to -20^{o}C for 2 days to facilitate polymerisation of the resin.

After successful polymerisation followed by subsequent removal from the moulds, tissue blocks were sectioned (5µm thick sections) using a polycut microtome (Reichert-Jung, USA) and placed onto microscope slides coated with 3-aminopropyl triethoxysilane.

Unless stated otherwise, all reagents were purchased from Sigma Aldrich, UK.

2.18 Haematoxylin and Eosin Staining of Resin Embedded Tissue

Tissue samples were hydrated using ddH_2O before being submersed in Harris's haematoxylin (Sigma Aldrich, UK) for 5 minutes at room temperature. Samples were 'blued' under running ddH_2O for 3 minutes before differentiation using ethanol containing 0.01M HCl (v/v) for 10 seconds. Samples were washed in ddH_2O before being incubated with 1% eosin (w/v) (Sigma Aldrich, UK) in ddH_2O for 3 minutes at room temperature. Samples were then dehydrated through a gradient of ethanol: 70%, 90%, 100% (v/v) for 2 minutes each, then cleared using xylene (VWR, UK) before finally mounting in DPX mounting medium (VWR, UK). Samples were visualised using transmitted light microscopy where tissue structure could be differentiated by varying shades of red/pink whilst nuclei appeared blue.

2.19 Immunohistochemistry of Resin Embedded Tissue

Masked epitopes were exposed through digestion of 6µm resin-embedded tissue with 0.1% trypsin type III (Sigma Aldrich, UK) in 0.1% calcium chloride ($CaCl_2$) (Sigma Aldrich, UK) in ddH_2O, pH7.8, for 30 minutes at 37°C, followed by a 5 minute wash at room temperature using PBS. Non-specific binding was then blocked by incubating samples with 1mL horse serum (Sigma Aldrich, UK) diluted in 10mL of PBS for 30 minutes at 37°C.

Primary antibodies were diluted to working concentrations specified in table 2.1 using 1% BSA (w/v) (Sigma Aldrich, UK) in PBS. Samples were incubated with primary antibodies overnight at 4°C.

Following incubation with primary antibody, the samples were washed using PBS for 5 minutes at room temperature. Secondary biotin-conjugated antibodies (Dakocytomation, Denmark) were diluted to 1:200 using PBS and applied to samples for 60 minutes at 37°C.

Following incubation with secondary antibodies samples were washed in PBS for 5 minutes at room temperature before exposure to mouse avidin DH and biotinylated alkaline phosphatase H (ABC/AP) tertiary antibody kit (Vector Laboratories, UK) for 30 minutes at room temperature. This was immediately followed by a further wash in PBS then incubation with alkaline phosphatase substrate solution (Vector Laboratories, UK) diluted in 0.1M Tris-HCl (Sigma Aldrich, UK) pH8.2 for 20 minutes at room temperature. Finally, samples were washed in PBS then ddH_2O respectively for 5 minutes each at room temperature before being mounted in aqueous mountant (Sigma Aldrich, UK). Samples were visualised using a combination of fluorescent and transmitted light microscopy.

2.20 Statistical Analysis

Statistical analysis was performed using the SPSS statistical package (SYSTAT Software Inc.). Differences between samples were evaluated by performing Mann-Whitney U, one-way and two-way ANOVA tests with a *p*-value of <0.05 being considered statistically significant.

3.0 Results

3.1 Characterisation of HESCs

The hESC line (HUES7) was kindly donated by Harvard University and maintained without feeder cells in serum-free conditions (section 2.1.2). A number of techniques were used to establish the pluripotency exhibited by these cells, providing baseline data to determine the extent of reprogramming of hEKs throughout this investigation.

Transmitted light microscopic observations revealed that the hESCs had a high nucleus to cytoplasmic ratio with prominent nucleoli and displayed compact colony morphology (Figure 3.1) consistent undifferentiated hESC phenotype.

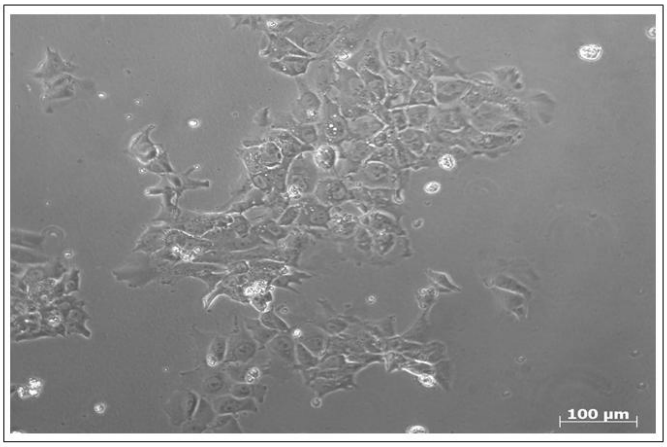

Figure 3.1 Phase contrast microscopic observation of passage 5 hESCs after 48 hours in culture, scale bar 100µm

An accumulating body of literature highlights key pluripotency regulators, identified primarily through studying the synergy between plasticity and gene expression. *Oct4, Nanog* and *Sox2* are now widely regarded as central regulators of plasticity and through cooperative interaction, have been shown to drive pluripotent-specific expression of a number of genes [164].

Initially, immunohistochemical staining of hESCs was performed to confirm the expression of these key pluripotency-associated genes. After 48 hours in culture, passage 8 hESCs demonstrated nuclear staining of each of these three markers (Figure 3.2). These proteins were found to be almost homogenously expressed, except for a small number of unstained hESCs typically found at the periphery of the colonies, suggesting these cells had spontaneously differentiated.

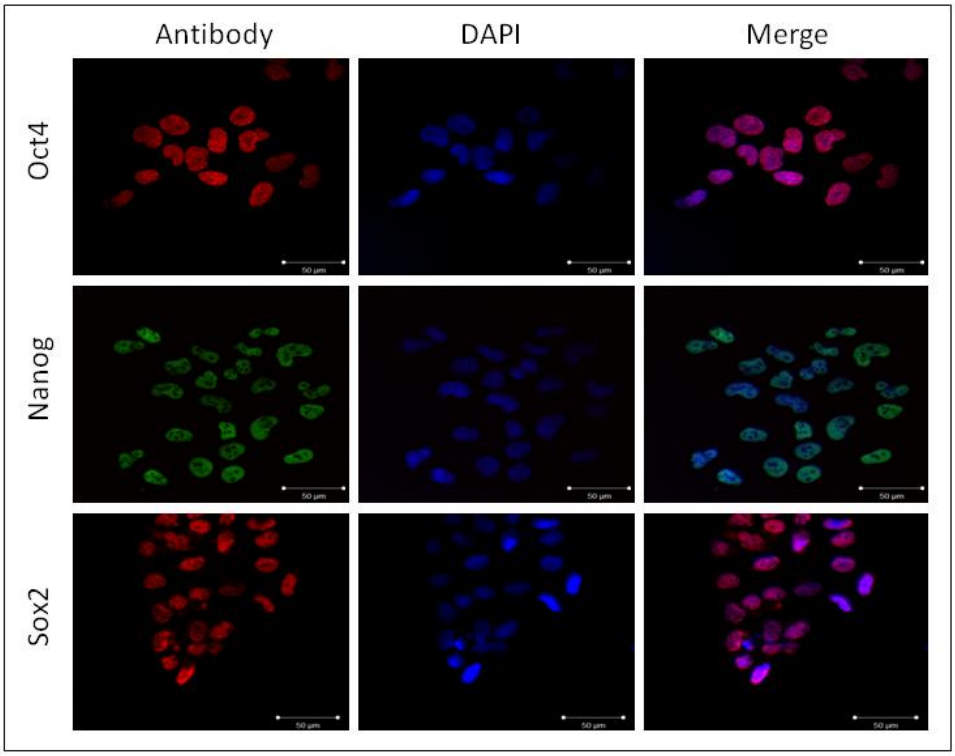

Figure 3.2 Immunohistochemical characterisation of passage 8 hESCs after 48 hours of *in vitro* culture. ***Oct4***, ***Nanog***, ***Sox2*** and **Nuclei, scale bar 50µm**

Pluripotent stem cells can also be characterised according to surface antigenicity, such as the stage specific embryonic antigens, SSEA3 and SSEA4. These antigens are synthesised during oogenesis and are present on

the surface of oocytes, zygotes and early cleavage stage embryos [165]. Other well established biomarkers of undifferentiated hESCs include the keratin sulphate-associated antigens, TRA-1-60 and TRA-1-81, which are highly expressed in hESCs and absent in lineage committed stromal cells [165]. After 48 hours of culture, hESCs showed strong immunoreactivity for SSEA3, SSEA4, TRA-1-60 and TRA-1-81, all of which were localised to the cell surface and absent in the nucleus (Figure 3.3).

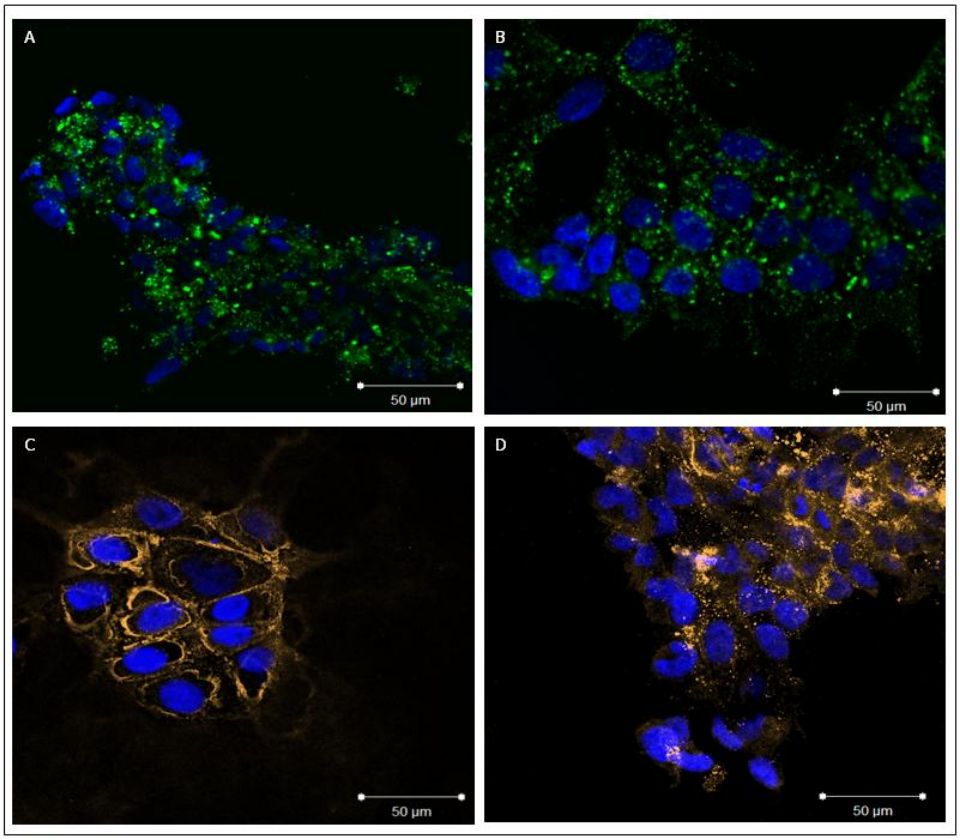

Figure 3.3 Immunohistochemical characterisation of passage 8 hESCs after 48 hours of *in vitro* culture. **A**: **SSEA3**, **Nuclei**. **B**: **SSEA4**, **Nuclei**. **C**: **TRA-1-60**, **Nuclei**. **D**: **TRA-1-81, Nuclei, scale bar 50 µm**

Another characteristic of pluripotent cells is the expression of alkaline phosphatase at high levels, which is known to decrease during differentiation [165]. HESCs were maintained under standard culture

conditions and stained for alkaline phosphatase after 1, 2, 3 and 5 days. Alkaline phosphatase was absent until day 2 and then largely increased after 3 days, persisting up to 5 days in culture (Figure 3.4).

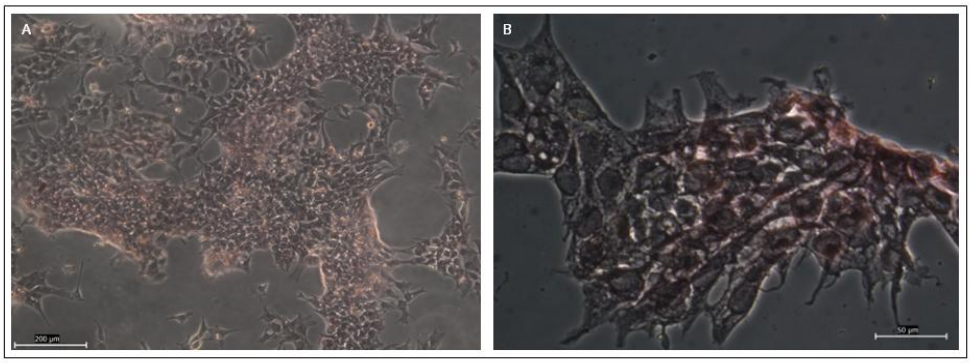

Figure 3.4 Phase contrast microscopic observation of hESCs stained for alkaline phosphatase **A**: 3 days. **B**: 5 days in culture. Scale bar represents **A**: 200µm. **B**: 50µm

To characterise hESCs at a transcriptomal level, qRT-PCR analysis of key pluripotency genes was performed. To meaningfully compare different samples, an appropriate reference gene needed to be identified and PCR reaction terminated when amplification kinetics of both internal controls and genes of interest were proceeding exponentially. Reference genes are used in qRT-PCR to normalise experimental data, such that relative expression levels of genes of interest can be quantified against a non-fluctuating internal standard. Therefore it was first necessary to identify an appropriate reference gene, which would maintain constitutive expression under the parameters of this investigation. Three of the most commonly used reference genes β-actin**,** Glyceraldehyde-3-phosphate-dehydrogenase (GAPDH) and 18s ribosomal RNAs (rRNAs) were considered as internal controls.

Primers for these reference genes were designed according to the methods detailed in section 2.10.1 and optimised against cDNA isolated from hESCs. All primer sets were found to have efficiencies exceeding 98%. To identify which reference gene would be the most appropriate for this investigation the experimental conditions hypothesised for the reprogramming of hEKs were replicated. hEKs were subject to nucleofection before quantifying each of the internal gene controls and comparing this data with hEKs maintained under standard culture conditions. Each reference gene was expressed in all samples, however analysis revealed that β-actin showed the least variation post-nucleofection and was therefore selected as the internal control for all subsequent gene expression studies.

Once an appropriate reference gene had been established hESCs were subject to qRT-PCR to determine expression of pluripotency associated genes. HESCs from passage 7 were cultured for 5 days (section 2.1.2), qRT-PCR analysis revealed expression of *Oct4*, *Sox2*, *Nanog*, *c-Myc* and *Klf4* all of which are associated with a pluripotent, self-renewing phenotype.

hEKs were also analysed using qRT-PCR to confirm absence of genes associated with pluripotency and identify expression of hEK lineage specific genes. hEKs taken from passage 4 were cultured for 5 days (section 2.1.1). hEKs did not express *Oct4*, *Sox2* or *Nanog* and were found to express *Cytokeratin14*, a hEK marker. Interestingly hEKs were found to express *Klf4* at comparatively high levels whilst also expressing *c-Myc*, at reduced levels compared with hESCs (Figure 3.5). It was therefore possible to conclude that this panel of primers is capable of distinguishing an undifferentiated hESC phenotype from differentiated hEKs.

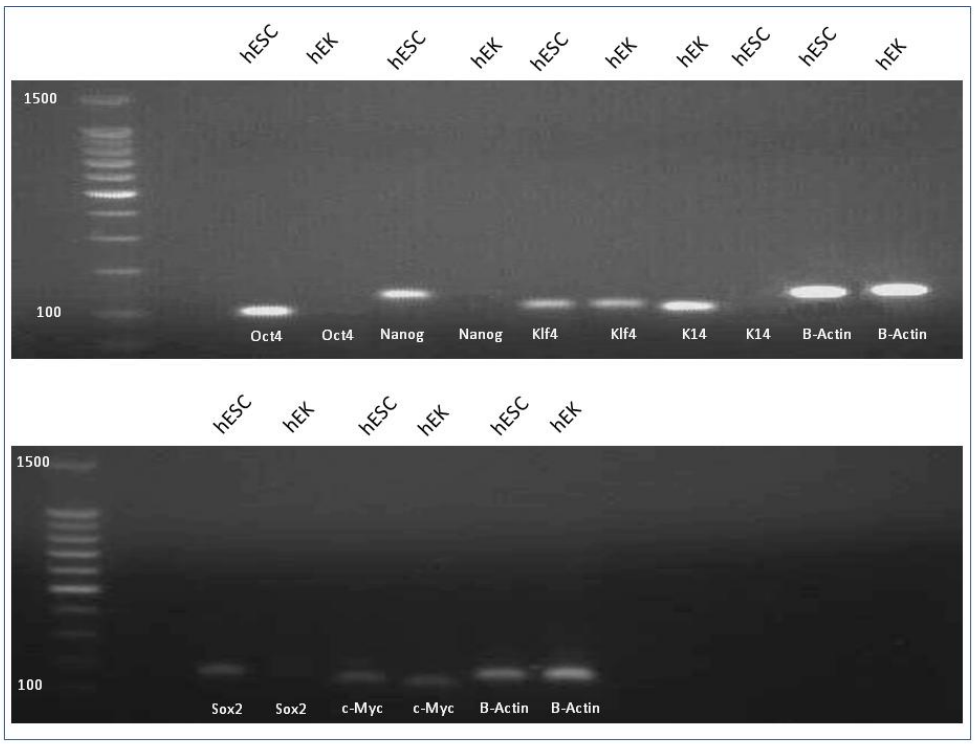

Figure 3.5 Comparison of hESC and hEK gene expression, passage 7 and 4 respectively, 5 days *in vitro* culture. Agarose gel electrophoresis of PCR products stained with ethidium bromide and visualised under UV light

3.2 Maintenance of hEKs on Human Fibronectin

The extracellular microenvironment provides specific cues to regulate cell function in both developing and adult organisms. It was hypothesised that an appropriate, well considered microenvironment may enhance cellular reprogramming. When considering the specifics of extracellular matrices (ECM) we find that they contain proteins and tethered soluble factors, which promote adhesion, proliferation, migration or differentiation of cells via transmembrane receptors, linking the ECM, intracellular cytoskeleton and nucleus. Evidence suggests that these components influence cell physiology [166] and suggests that cells *in vitro* only respond to certain signals when cultured in contact with an appropriate microenvironment.

hEKs possess extracellular matrix receptors of the integrin family, including $\alpha_5\beta_1$, a fibronectin receptor and $\alpha_2\beta_1$, a collagen receptor [167]. When considering the epidermis, proliferation is largely restricted to the basal layer, as hEKs move through the suprabasal tissues they undergo terminal differentiation. The role of these integrins is to mediate adhesion to the basement membrane and regulate the onset of lineage commitment. Thus it was hypothesised that hEK proliferation and differentiation may be affected as a direct result of the *in vitro* ECM microenvironment.

Similarly, hESCs require the support of appropriate substrata to maintain pluripotent, self renewing characteristics. During this investigation, human fibronectin (hFN) was used to maintain hESCs *in vitro* due to the superior proliferation and decreased spontaneous differentiation in comparison to other available substrates [168]. Therefore it is rational to predict that after induction by exogenous soluble stimuli, maintenance on a coating known to promote pluripotency may enhance this process.

Routine hEK culture involves seeding cells on tissue culture polystyrene, coated with matrix largely composed of recombinant human type-1 collagen (hCol I). To determine whether hFN could be utilised in our strategy for reprogramming hEKs, it was necessary to assess whether this protein could support hEK proliferation and phenotype. All concentrations of hFN supported varying degrees of hEK attachment, however a coating of $5\mu g/cm^2$ was found to provide optimal attachment (Figure 3.6).

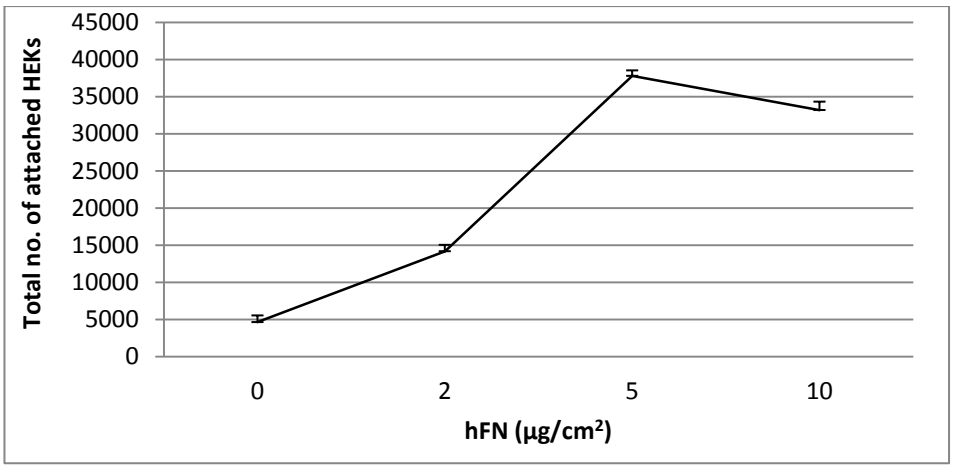

Figure 3.6 hEK attachment to hFN coated substrate. Total number of attached hEKs was quantified 24 hours post-seeding on a range of hFN concentrations. Points represent the mean, error bars represent standard error of the mean, n=3

hEKs attached to hFN coated dishes after 2 hours with the majority attaching as single cells (Figure 3.7).

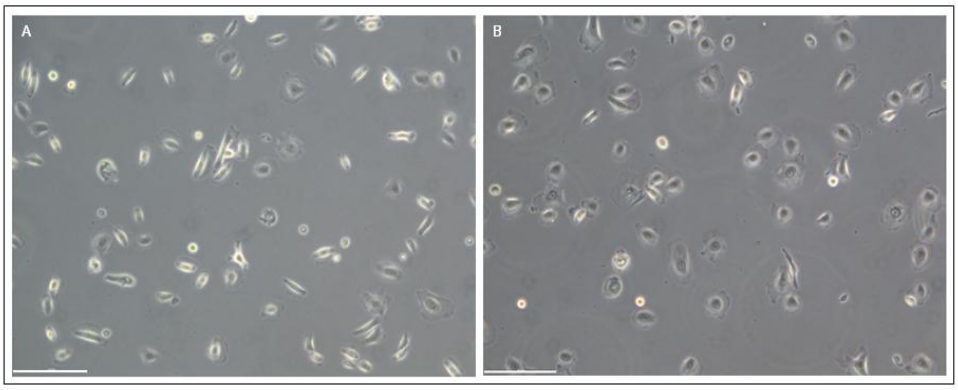

Figure 3.7 Phase contrast microscopic observation of hEKs 24 hours post-seeding on dishes coated with **A**: hFN. **B**: hCol I. Scale bar represents 200µm

Over a period of 7 days hEKs proliferated and exhibited typical hEK morphology (Figure 3.8).

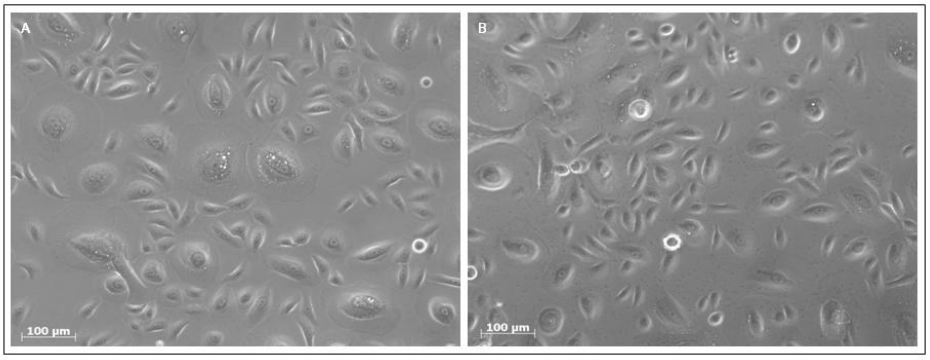

Figure 3.8 Phase contrast light microscopic observation of hEKs 7 days post-seeding on dishes coated with **A**: hFN. **B**: hCol I

Proliferation of hEKs maintained on either hCol I or hFN at a concentration 5µg/cm^2 were compared over 96 hours. hEKs were seeded at a density of 5 x10^4 per cm^2 and maintained using standard culture procedures (section 2.1.2). At each time point media was removed and wells washed twice with PBS leaving hEKs that had successfully attached. hEKs were detached and enumerated.

The number of hEKs attached to hFN-coated surfaces was reduced compared to hCol I-coated surfaces. Despite impaired attachment of hEKs to hFN, cells which had successfully attached proliferated with a comparable profile to those cultured on hCol I (Figure 3.9).

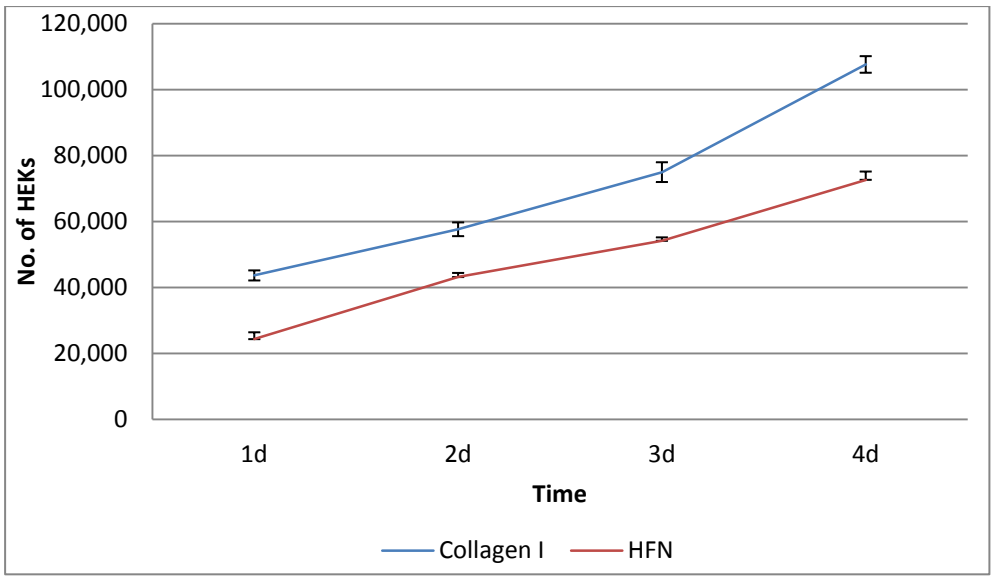

Figure 3.9 hEK growth on hCol I and hFN coated surfaces at 1, 2, 3 and 4 days post-seeding. Points represent the mean, error bars represent standard error of the mean, n=3

3.3 Nucleofection

Another of the major aims of this study was to identify a method of delivering factors capable of reprogramming hEKs at a high frequency without cytotoxicity. Although much research has focused on viral systems, which have proved an effective method of gene transfer, resultant cells face barriers in clinical translation due to complex viral biology associated with these vectors [136]. The future of reprogramming therefore lies with non-viral, non-toxic methods, which efficiently deliver inducing stimuli to somatic cells. At present non-viral methods are substandard demonstrating low transfection efficiencies or cytotoxicity [169]. Here we evaluate an electroporation technique termed nucleofection, which utilises low voltage electroporation in combination with cell-specific reagents to allow direct electro-transfer of nucleotides into target cell nuclei whilst maintaining high levels of viability, to directly reprogram hEKs [148].

Traditional electroporation methods often reduce viability. If electrical pulses are the incorrect length or intensity, pores caused may fail to close, causing loss of mechanical membrane integrity and subsequent apoptosis. Therefore it was necessary to establish the level of hEK cell viability post-nucleofection. An initial qualitative assessment was achieved by performing a live/dead assay 24 hours post-nucleofection. Observations from this assay indicated a high level of viability following nucleofection (Figure 3.10).

Figure 3.10 Fluorescent microscopic observation of hEKs 24 hours post nucleofection stained using live/dead cytotoxicity kit. **A**: **Live cells**. **B**: **Dead cells**. **C**: **Nuclei.** Same field of view, scale bars represent 200µm

In order to quantify the overall viability, whole well analysis was performed, including both the adherent monolayer and supernatant. Two assays were performed to quantify viability 24 hours post-nucleofection: trypan-blue dye exclusion (section 2.5) and live/dead staining quantified using flow cytometry (section 2.4). Viability of hEKs subject to a single round of nucleofection (section 2.2) and unmodified hEKs subject to identical trypsinisation and centrifugation procedures were quantified (Table 3.1).

Live/dead assay			Trypan-blue exclusion assay		
	Nucleofected	Non-nucleofected		Nucleofected	Non-nucleofected
Mean (%)	66.2% Non-viability	12.7% Non-viability	Mean (%)	25.63% Viability	88.38% Viability
SD	3.45	1.3	SD	0.03	2.5

Table 3.1 Summary of hEK percentage viability 24 hours post-nucleofection seeded onto hCol I coated dishes, n=3

To determine the attachment of nucleofected hEKs to either hCol I or hFN-coated surfaces, adherent cells were harvested 24 hours post-nucleofection, trypan-blue dye exclusion assay performed and the percentage viability calculated (table 3.2).

	hCol I		hFN	
	Total no. hEKs	Viability (%)	Total no. hEKs	Viability (%)
Mean	181,694	25.63	90,370	12.91
SD	21,032	3.00	19,565	2.79

Table 3.2 Summary of hEK viability post-nucleofection, n=9

These results confirm that hEKs undergoing nucleofection are subject to increased cell death compared to hEKs under identical experimental parameters without nucleofection. When considering hEKs seeded on hCol I approximately 25% successfully attached post-nucleofection indicating that a number of viable hEKs fail to adhere to the substrate post-nucleofection. In addition, an increased number of hEKs failed to adhere to hFN coated surfaces, with approximately 12% attachment post-nucleofection. Irrespective of coating, hEKs proliferated and exhibit typical hEK morphology following nucleofection indicating that the high seeding density of $7.0x10^5$ cells per sample (section 2.2) is a crucial factor in compensating for the significant number of cells which are non-viable or fail to adhere post-nucleofection.

A number of non-viral transfection techniques are known to differentiate hEKs, therefore it was important to assess the effect of nucleofection on hEK phenotype before commencing reprogramming. An established marker of hEK terminal differentiation is involucrin, a protein found in keratinocytes of the epidermis and other stratified squamous epithelia [170]. This protein first appears in the cytosol and eventually becomes cross-linked to membrane proteins to form an insoluble envelope beneath the plasma membrane [170]. Involucrin is synthesised after hEKs have left the basal layer and begun to enlarge before the onset of envelope cross-linking, which occurs only in the outermost cells. Therefore involucrin is considered to be the most reliable marker of the terminal differentiation of hEKs [171].

hEKs maintained under adherent culture, suspension culture or subject to nucleofection were immunohistochemically stained for cytokeratin14 and involucrin. Positive cytokeratin14 staining was identified in all samples, however it was considerably reduced in suspension cultures (Figure 3.11).

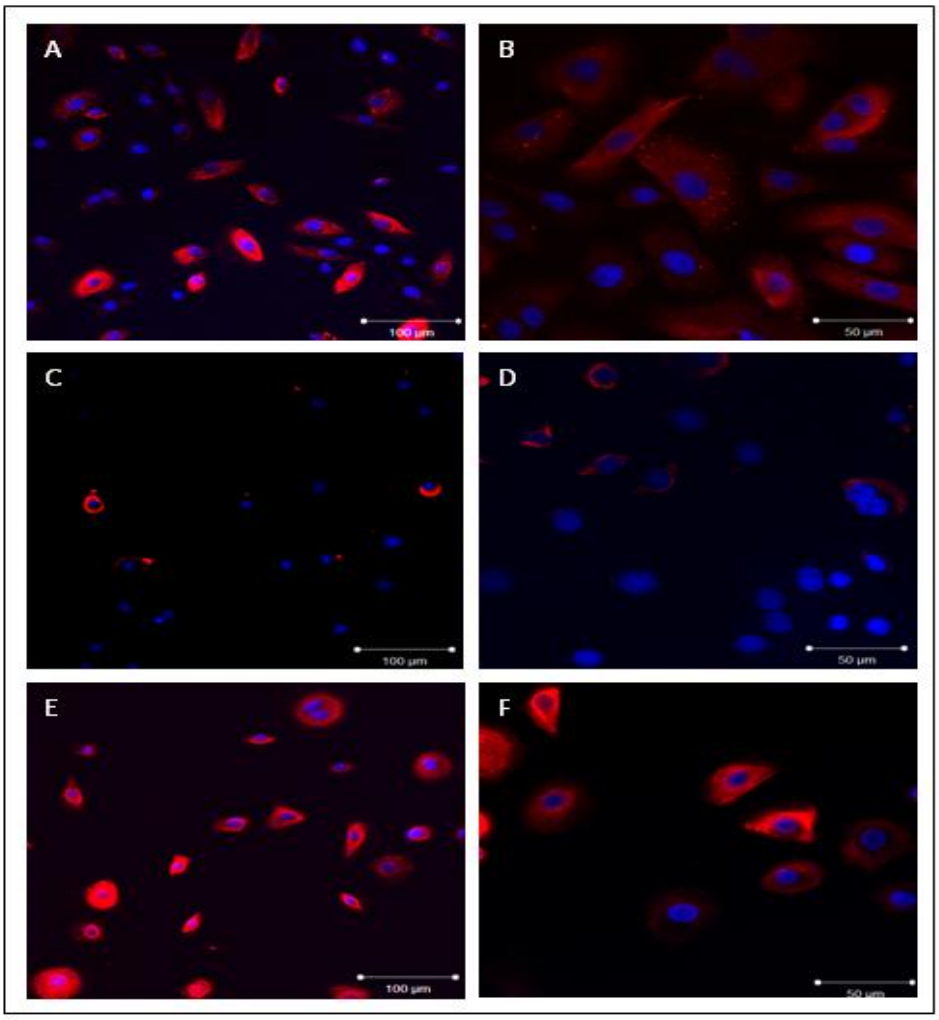

Figure 3.11 Assessment of hEK phenotype upon different culture conditions. Fluorescent microscopic observation of hEKs stained for **Cytokeratin14**, **DAPI**. (**A-B**): adherent culture (**C-D**): suspension culture. (**E-F**): 24 hours post-nucleofection, scale bars represent 50µm

Involucrin was absent in hEKs maintained in adherent culture, whilst being highly prevalent in hEKs maintained in suspension. Where samples had been nucleofected, only a few cells stained positive for involucrin (Figure 3.12).

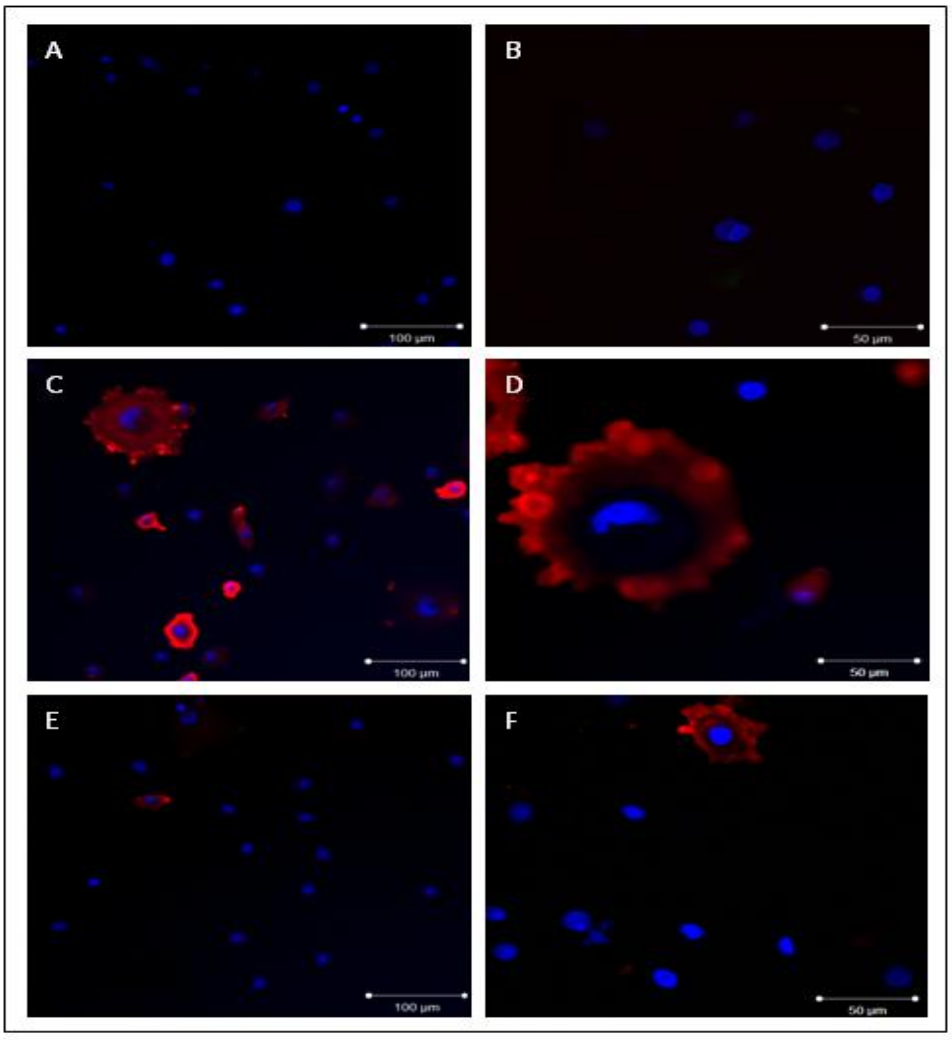

Figure 3.12 Assessment of terminal differentiation upon different culture conditions. Fluorescent microscopic characterisation of hEKs. **Involucrin**, **DAPI**. (**A-B**): adhesion culture. (**C-D**): suspension culture. (**E-F**): 24 hours post-nucleofection, scale bars represent 50µm

hEKs nucleofected with GFP-P (section 2.2) were also analysed using qRT-PCR to assess whether nucleofection had altered the expression of genes associated with lineage commitment and differentiation. Total RNA was isolated from hEKs after 1, 3, 5 and 7 days. qRT-PCR analysis revealed that expression of *Oct4, Sox2, Nanog, c-Myc, Klf4* and *cytokeratin-14* remained unchanged despite this intervention. Thus indicating nucleofection alone

does not modulate expression of sentinel plasticity associated genes outside of primary hEK basal levels.

3.3.1 Nucleofection Plasmid DNA

To develop a strategy for hEK reprogramming it was necessary to ascertain the delivery efficiency of inducing stimuli, such as plasmid DNA, miRNA inhibitors or a combination of both.

hEKs were nucleofected with pmaxGFP control plasmid (GFP-P) (section 2.2). Successful delivery was detected as early as 6 hours post-nucleofection using fluorescent microscopy. After 24 hours successful delivery of the plasmid to a large number of hEKs was clearly evident (Figure 3.13).

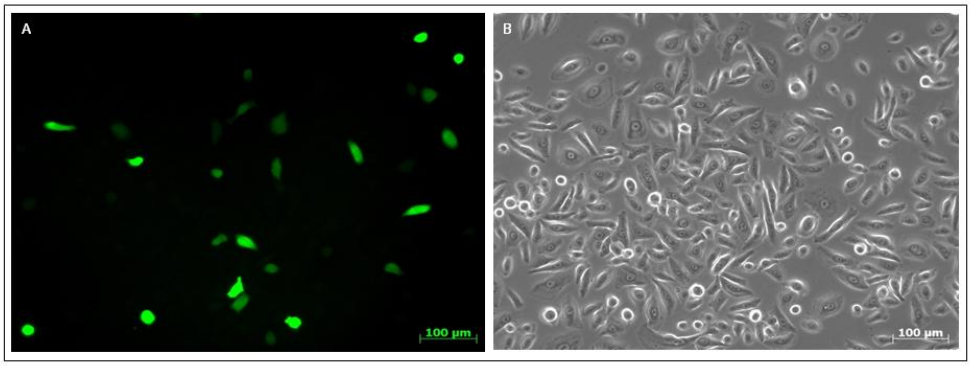

Figure 3.13 hEKs 24 hours post-nucleofection with GFP-P **A**: Fluorescent observation. **B**: Phase contrast microscopic observation. Same field of view, scale bar represents 200µm

To quantify the number of successfully nucleofected hEKs, flow cytometric analysis of hEKs nucleofected with GFP-P and seeded onto either hCol I or hFN, were performed 24 hours post-nucleofection. The histogram below shows flow cytometric data for hEKs nucleofected with GFP-P and seeded on hCol I (Figure 3.14). The marked area to the right of the peak reflects

the number of successfully nucleofected hEKs, with GFP fluorescence from the plasmid reporter as a smear rather than a defined peak or shoulder. This is a consequence of hEKs receiving differing intercellular concentrations of GFP-P thus producing a range of fluorescence intensities. This was confirmed by subtraction of control samples, which underwent the same experimental parameters in the absence of GFP-P to offset non-specific fluorescence.

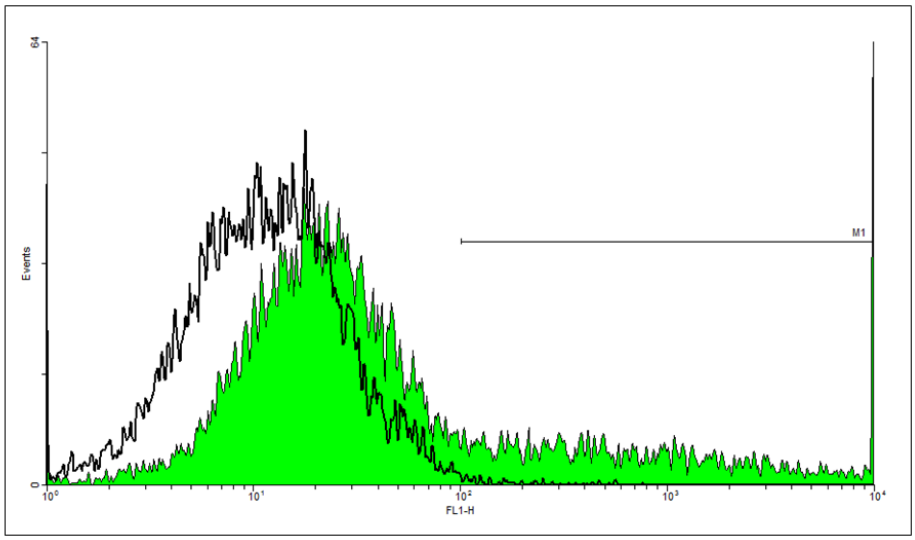

Figure 3.14 Histogram illustrating flow cytometric analysis of hEKs subject to nucleofection. Black line represents hEKs nucleofected without GFP-P. Green area represents hEKs nucleofected with GFP-P 24 hours post nucleofection

Post-nucleofection with GFP-P, hEKs were seeded on either hCol I or hFN. In order to quantify the transfection efficiency, flow cytometry was performed 24 hours post-nucleofection. Prior to analysis wells were washed with PBS in order to remove any non-adherent cells and the remaining adherent monolayer analysed (section 2.12).

Data indicated that the numbers of GFP^{bright} cells were reduced when seeded on hFN (table 3.3).

	hCol I	**hFN**
	GFP ^{bright} (%)	GFP ^{bright} (%)
Mean	19.82	8.01
SD	2.45	2.85

Table 3.3 Summary of nucleofection efficiency quantified using flow cytometry, n=6

Substrate coating is an independent variable and should not directly modulate transfection efficiency. However, as hFN is known to influence hEK attachment it was hypothesised that the reduced number of GFP^{bright} cells was due to a number of successfully nucleofected hEKs failing to attach. To confirm this, whole well contents including non-adherent hEKs, were analysed. Flow cytometric analysis of whole well contents revealed the mean number of GFP^{bright} cells to be equivalent for hEKs seeded on hCol I and hFN with a mean number of 29.23% ± 3.40% GFP^{bright} cells for both culture variables, n=6 (Figure 3.15).

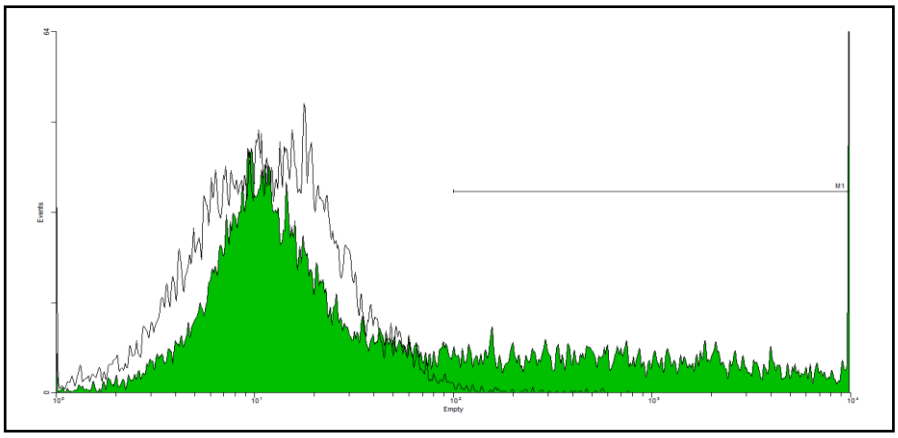

Figure 3.15 Histogram illustrating flow cytometric whole well analysis of hEKs seeded on hFN 24 hours post-nucleofection with GFP-P

While this procedure was able to successfully deliver GFP-P to almost 30% of hEKs, cells which had not attached to the given substrate after 24 hours were considered non-viable and were subsequently removed following replacement of media. Subsequent experiments therefore focused on seeding cells initially on hCol I post-nucleofection due to the superior attachment of successfully nucleofected hEKs compared to hFN.

To summarise, these results demonstrate that nucleofection is a reproducible, non-viral method of delivering plasmid DNA to hEKs. Within experimental groups little variation existed with total number of GFP^{bright} hEKs ranging between 17.40% and 22.56% ± 2.22 on hCol I and a range of 5.46% to 14.56 ± 2.85, n=6 on hFN, demonstrating the repeatability of this technique (Figure 3.16).

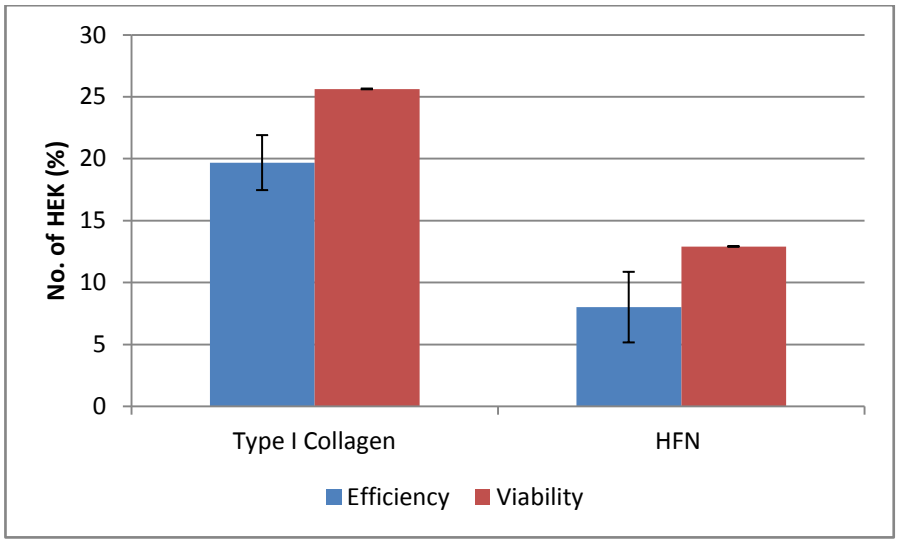

Figure 3.16 Summary of nucleofection efficiency 24 hours post-nucleofection quantified by flow cytometry, n=6 and cell viability calculated through trypan-dye exclusion assay, n=9

3.3.2 Stable or Transient Transfer?

Transfection is the introduction of foreign DNA into any eukaryotic cell and can be stable or transient. In the case of stable transfection foreign DNA is permanently integrated into the host genome while transient transfection imparts only transient expression of the transfected genetic material, which is subsequently diluted then lost through mitosis. hEKs successfully nucleofected with GFP-P were maintained *in vitro* for 10 days to study persistence of GFP-P. 3 days following nucleofection hEKs had proliferated and the number of GFP^{bright} cells had increased. After 5 days proliferation continued with hEKs forming a confluent monolayer; however GFP expression did not increase further although did persist in a number of hEKs. Transmitted light microscopy also showed hEKs maintained typical morphology during this period (Figure 3.17).

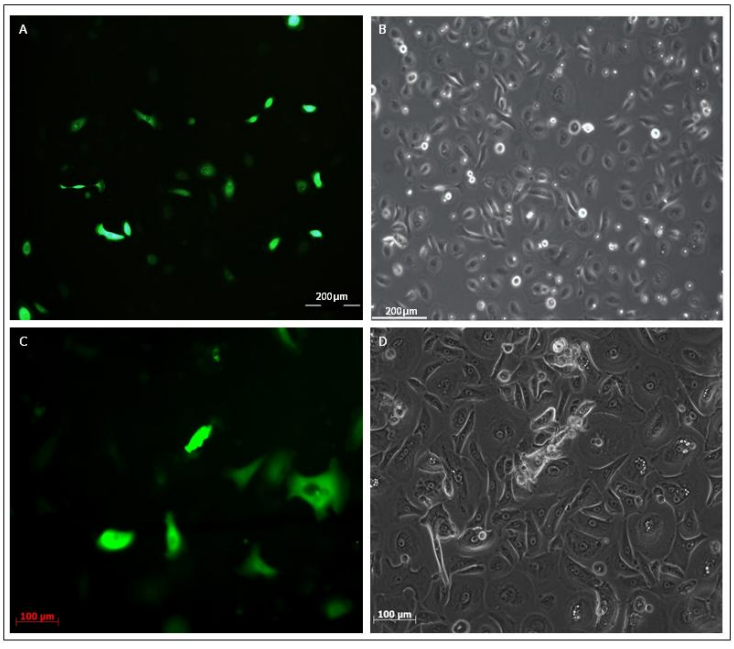

Figure 3.17 Fluorescent and phase contrast light microscopic observation of hEKs nucleofected with GFP-P (**A-B**) 3 days post-nucleofection, same field of view, scale bar represents 200µm. (**C-D**) 5 days post-nucleofection, same field of view, scale bar represents 100µm

hEKs maintained in their original wells up to 10 days post-nucleofection demonstrated a notable decrease in the number of GFP^{bright} hEKs. To quantify persistence of GFP-P, hEKs were subject to flow cytometry at 1, 3, 5, 7 and 10 days post-nucleofection. In order to enumerate the percentage of GFP^{bright} cells, non-GFP-P nucleofected cell fluorescence was subtracted from GFP-P nucleofected cell fluorescence. This revealed that despite a peak in the number of GFP bright hEKs, throughout the remainder of the experimental time course there was a decrease in fluorescence associated with the GFP-P (Figure 3.18).

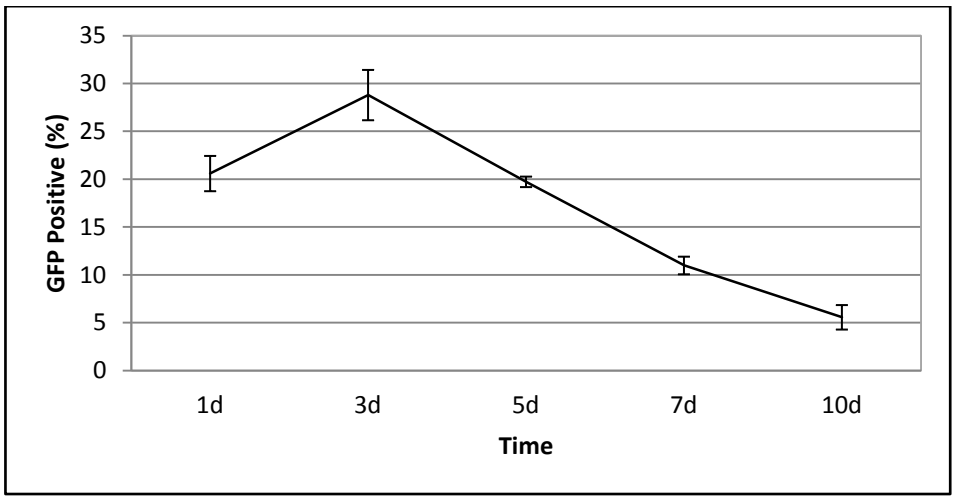

Figure 3.18 Nucleofection efficiency GFP-P. Points represent percentage of hEKs successfully nucleofected with GFP-P quantified using flow cytometry at time points post-nucleofection, error bars represent standard error of the mean, n=3

GFP^{bright} populations were passaged 7 days post-nucleofection and observed. GFP was found to be absent in successive populations therefore when hEKs were provided with sufficient space to proliferate GFP expression was rapidly lost, indicating transient expression persisting between 5-7 days. While stable transfection ensures long-term gene expression, transient transfection is attractive in terms of reprogramming

therapeutic somatic cells due to non-integration of foreign DNA into the nuclear genome leading to eventual clearing through routine mitosis. This data therefore highlights the possibility that multiple repeated transfection of hEKs may be required to sustain transgene expression over longer periods using the nucleofection technique.

3.3.3 Nucleofection MiRNA Inhibitors

It was hypothesised that a combination of plasmid DNA and miRNA inhibitors may provide a potent mixture for hEK reprogramming. One specific miRNA, miR-145, was highlighted during this investigation due to its association with major pluripotency regulators: *Oct4, Sox2* and *Klf4* [119], all of which feature in Yamanaka's classic combination of reprogramming factors. It was proposed that an inhibitor of miR-145 could provide a means of elevating expression of these pluripotency genes, facilitating hEK reprogramming.

Prior to delivering the miRNA inhibitor of interest a control miRNA inhibitor containing a fluorescent reporter, supplied by Dharmacon, was used to optimise delivery (section 2.2). All experimental conditions remained the same as for nucleofection of plasmid DNA, however a range of miRNA inhibitor control concentrations was evaluated, ranging between 10pM and 100nM. Fluorescent microscopy revealed a large number of hEKs successfully nucleofected with 100nM control miRNA inhibitor. Lower concentrations of 10nM also demonstrated high occurrence of nucleofection however the number of hEKs incorporating the miRNA inhibitor appeared reduced and the inhibitor was found to be distributed throughout the cell rather than the clear nuclear localisation observed in the case of 100nM. Lower concentrations of 100pM and 10pM were unsuccessfully delivered (Figure 3.19).

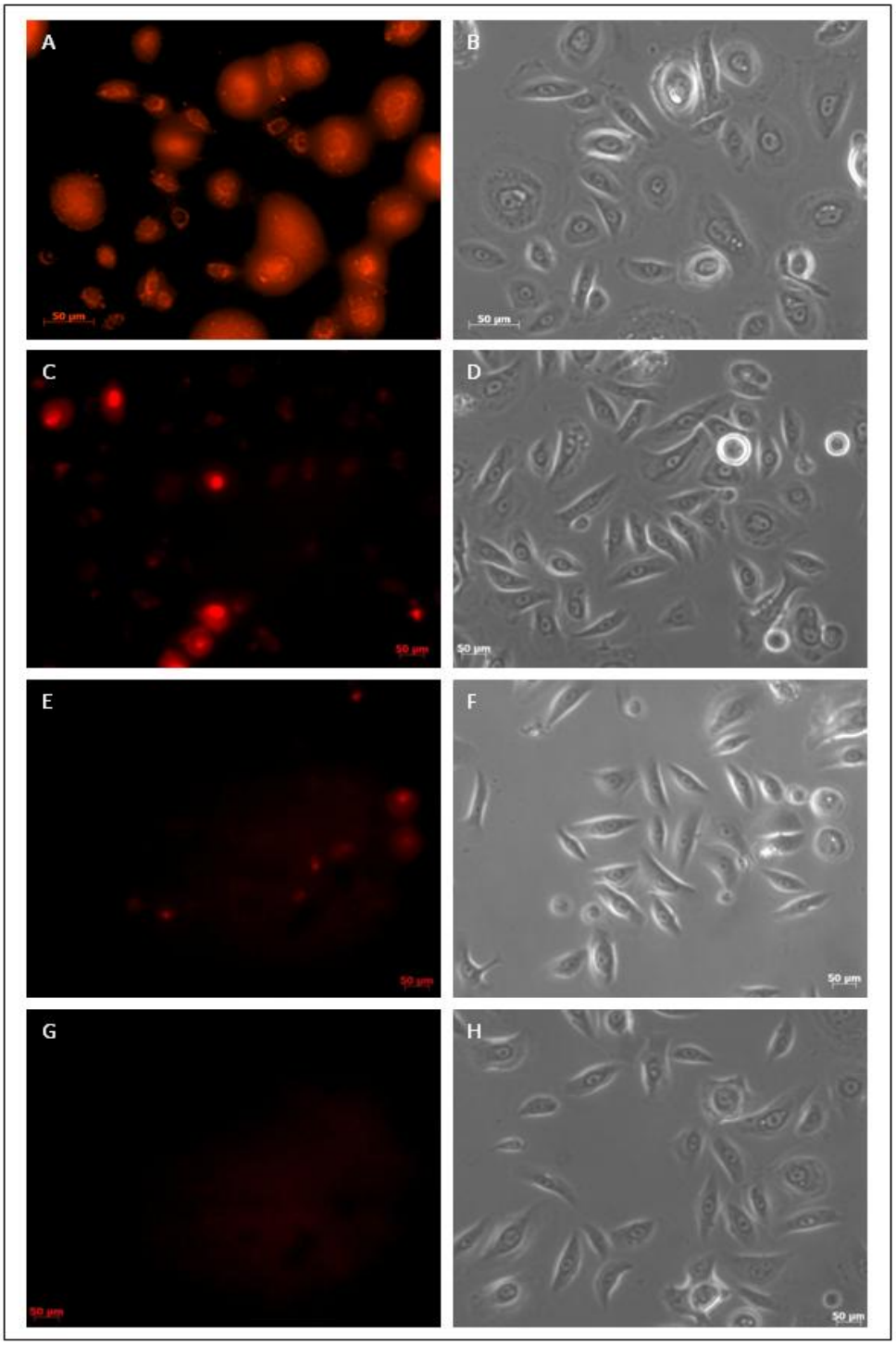

Figure 3.19 Fluorescent and phase contrast microscopic observations of hEKs 24 hours post-nucleofection with (**A-B**) 100nM; (**C-D**) 10nM; (**E-F**) 100pM; (**G-H**) 10pM miRNA inhibitor control, same field of view for each concentration assayed, scale bar represents 50µm

To optimise an appropriate concentration for delivery of miRNA inhibitors, varying miRNA inhibitor control concentrations were evaluated in terms of their effect on viability and delivery efficiency. Flow cytometry of hEKs nucleofected with different concentrations of miRNA inhibitor control were performed to quantify efficiency of delivery in conjunction with a trypan-blue exclusion assay to determine viability 24 hours post-nucleofection. Control samples consisted of hEKs nucleofected without miRNA inhibitor control. This revealed that altering the concentration of miRNA inhibitor control did not notably alter viability while delivery efficiency increased as a function of increasing the concentration of miRNA inhibitor control (Figure 3.20).

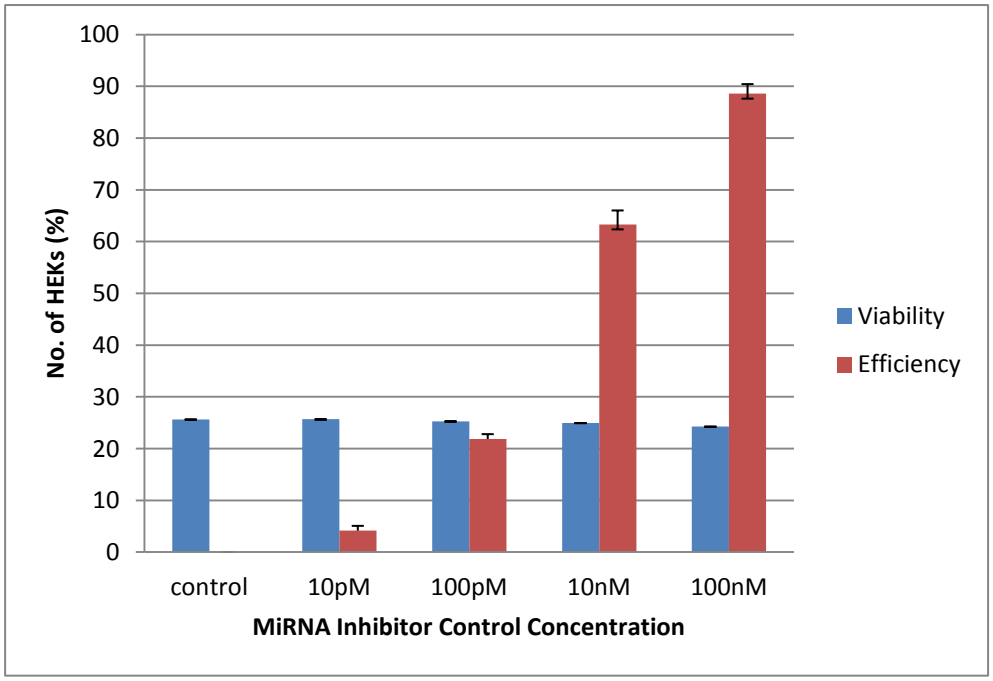

Figure 3.20 Effect of miRNA inhibitor control concentration on cell viability and nucleofection efficiency. Viability was quantified using trypan-blue exclusion assay and efficiency quantified using flow cytometry 24 hours post-nucleofection, n=3

The flow cytometric data obtained for hEKs, which had been nucleofected with 100nM of miRNA inhibitor control showed a distinct peak compared to the broader range of fluorescence observed for samples nucleofected with GFP-P (Figure 3.21). In addition, a significantly higher number of hEKs were nucleofected with miRNA inhibitor control than GFP-P, with a mean nucleofection efficiency of 88.58% ± 1.87, n=6 observed 24 hours post-nucleofection.

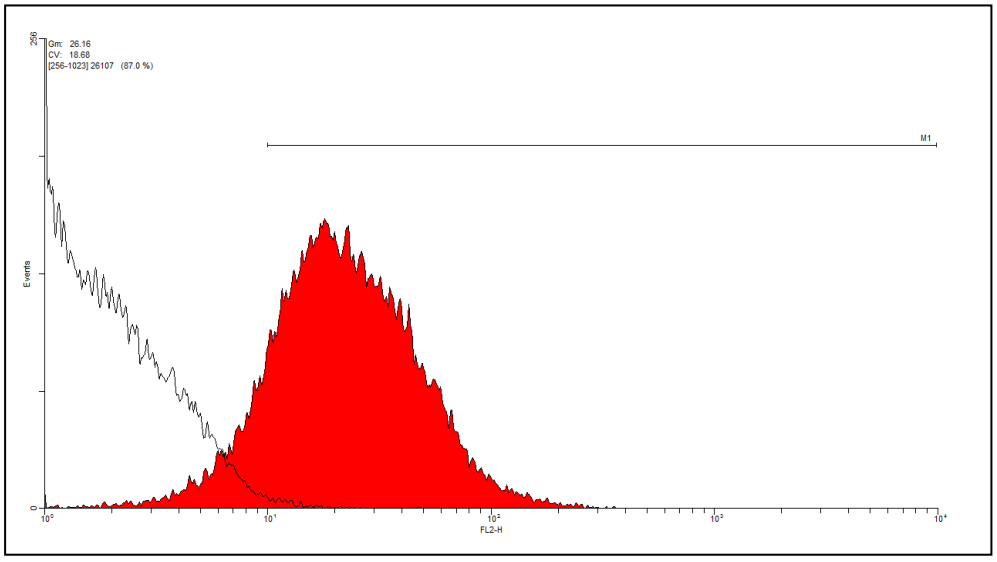

Figure 3.21 Flow cytometric analysis of hEKs nucleofected with miRNA inhibitor control 24 hours post-nucleofection

Therefore concurrent with initial visualisation, a concentration of 100nM miRNA inhibitor control demonstrated the highest level of nucleofection efficiency with no significant difference in viability compared to other concentrations investigated (Figure 3.20). This concentration was therefore selected for successive miRNA inhibitor functional investigations.

To assess the longevity of miRNA inhibitors over time, samples were nucleofected with 100nM miRNA inhibitor control, maintained under

standard culture conditions (section 2.2) and observed after 1, 3 and 5 days using fluorescent microscopy. hEKs had proliferated following nucleofection and the miRNA inhibitor control was observed throughout this culture period (Figure 3.22).

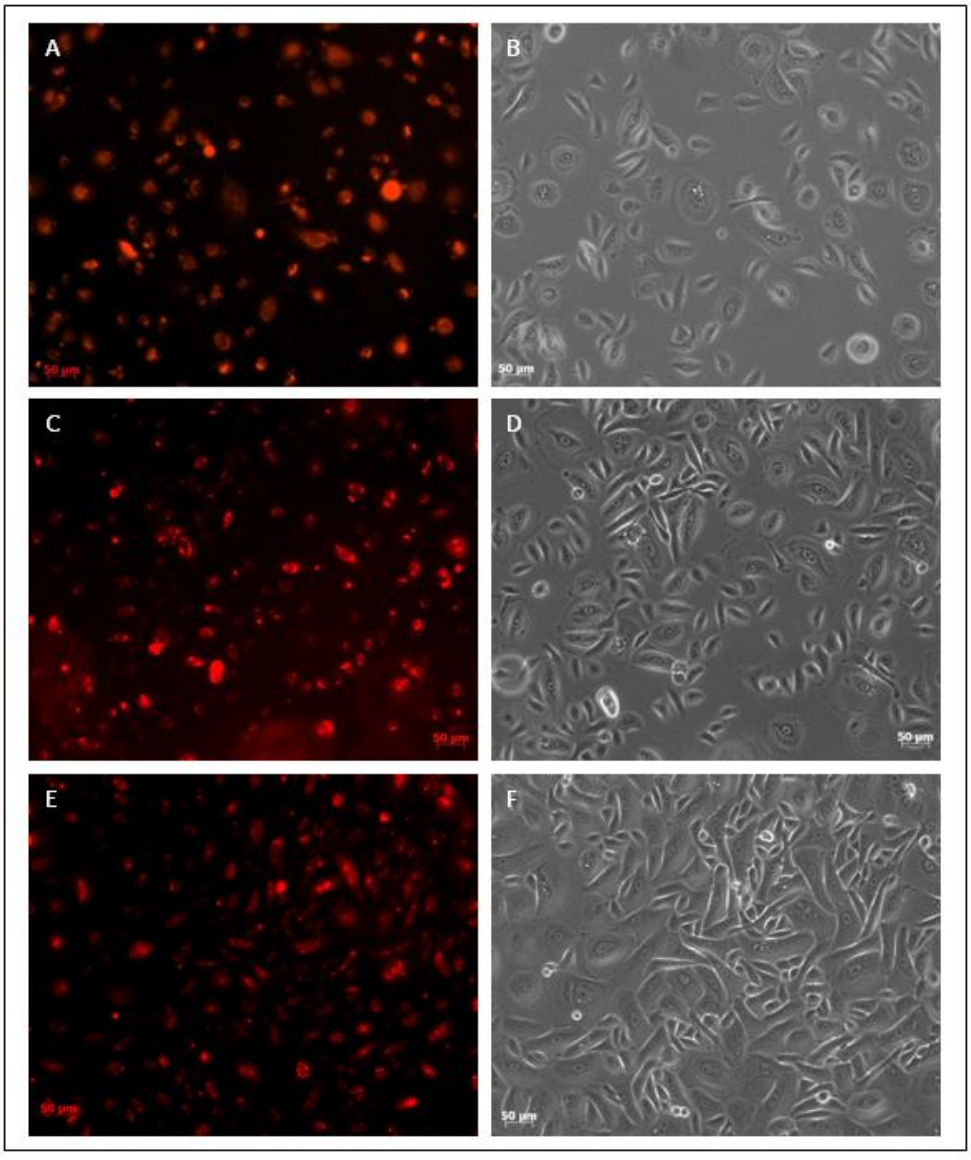

Figure 3.22 Fluorescent and phase contrast microscopic observation of hEKs (**A-B**) 1 day (**C-D**) 3 days (**E-F**) 5 days post-nucleofection with miRNA inhibitor control, same field of view for each given time point, scale bar represents 50µm

hEKs were maintained for 10 days post-nucleofection with a gradual decrease in the number of miRNA inhibitor control positive cells. To quantify persistence of the miRNA inhibitor control during this period, hEKs were subject to flow cytometry at 1, 3, 5, 7 and 10 days post-nucleofection. This confirmed that miRNA inhibitor delivery is considerably more efficient than plasmid DNA delivery. While miRNA inhibitor expression is also transient in nature and is found to gradually decrease over time it does however persist at much higher levels than GFP-P over the same time period (Figure 3.23).

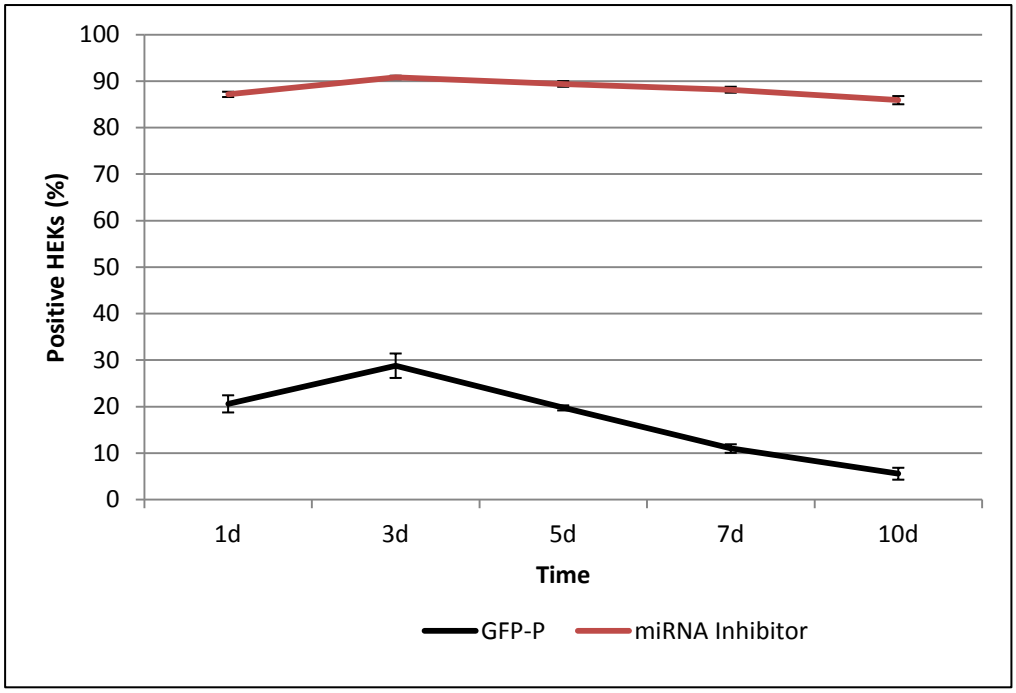

Figure 3.23 Comparison of GFP-P and miRNA inhibitor control nucleofection efficiency. Points plotted represent the mean number of hEKs successfully nucleofected with either miRNA inhibitor control (red) or GFP-P (black) quantified using flow cytometry at specific time points post-nucleofection, error bars represent standard error of the mean, n=3

3.3.4 Repeated Rounds of Nucleofection

Due to the transient nature of this technique it was hypothesised that, to sustain an appropriate level of stimulation to induce reprogramming, additional rounds of nucleofection may be required. To assess the feasibility of repeated rounds of nucleofection, hEKs were nucleofected with GFP-P or miRNA inhibitor control and maintained for 5 days. Each well then typically contained $3x10^4$ cells per cm^2, therefore the contents of three wells were harvested to yield the required number of hEKs for each additional round of nucleofection. After the second round of nucleofection, delivery of GFP-P or miRNA inhibitor control was observed. A comparison was made with samples nucleofected without inclusion of GFP-P or miRNA inhibitor control during the second round of nucleofection.

Samples subject to a second round of nucleofection with GFP-P resulted in a number of successfully nucleofected hEKs compared those without GFP-P, which failed to express GFP (Figure 3.24).

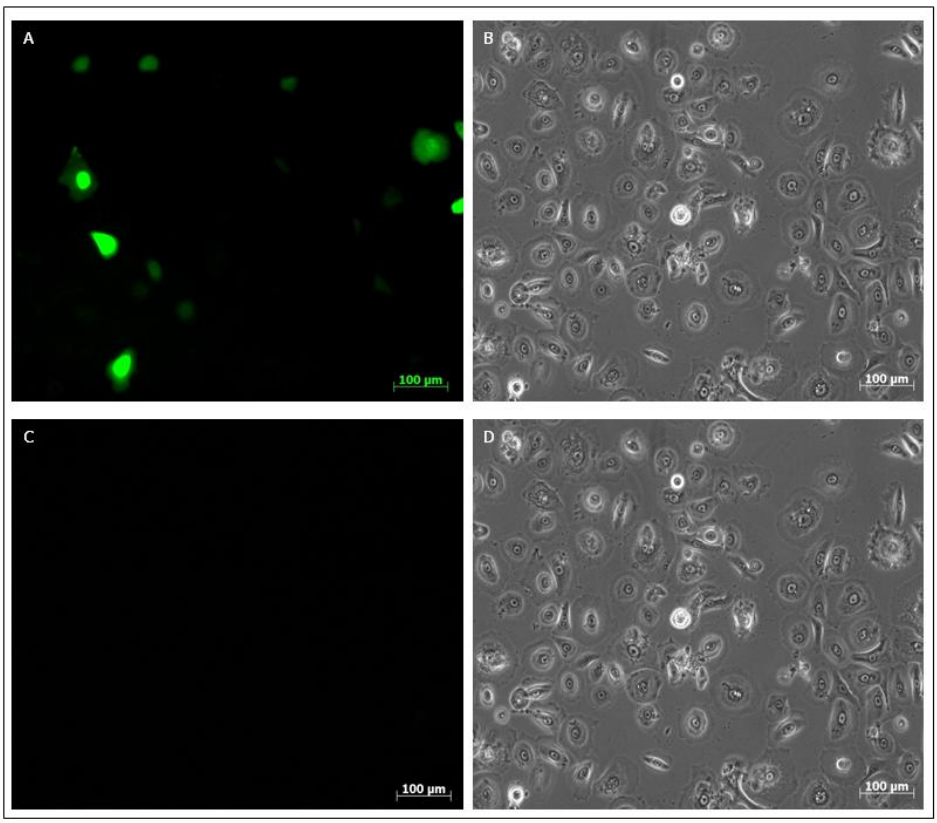

Figure 3.24 Fluorescent and phase contrast microscopic observations of hEKs subject to a second round of nucleofection (A–B) with GFP-P; (C-D) without GFP-P after 48 hours, same field of view, scale bar represents 100µm

hEKs subject to a second round of nucleofection with of GFP-P were maintained for a further 9 days, a total of 14 days since the initial round of nucleofection and observed using fluorescent and transmitted light microscopy after 5, 7 and 9 days. The GFP-P was observed in a number of hEKs during this culture period (Figure 3.25), thus highlighting the ability to sustain plasmid DNA expression through successive rounds of nucleofection.

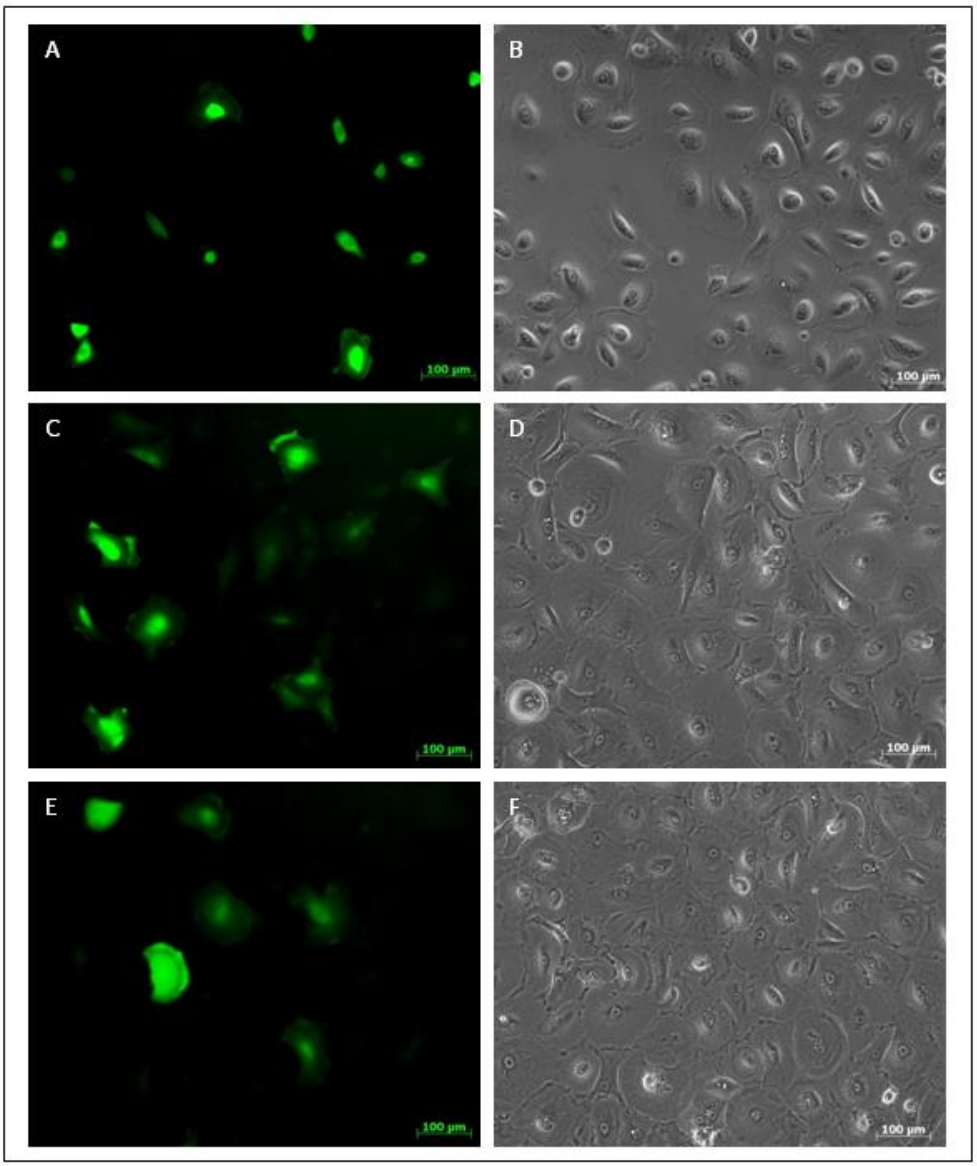

Figure 3.25 Fluorescent and phase contrast microscopic observations of hEKs subjected to a second round of nucleofection with GFP-P (**A**-**B**) 5 days; (**C**-**D**) 7 days; (**E**-**F**) 9 days post-nucleofection, same field of view for each given time point, scale bar represents 100µm

Flow cytometry of hEKs undergoing a second round of nucleofection with GFP-P was performed to quantify successfully nucleofected hEKs. This revealed an increase in the number of hEKs incorporating GFP-P and mirrored previous results with a decrease over time and persistence at high levels between 5-7 days post-nucleofection (Figure 2.26).

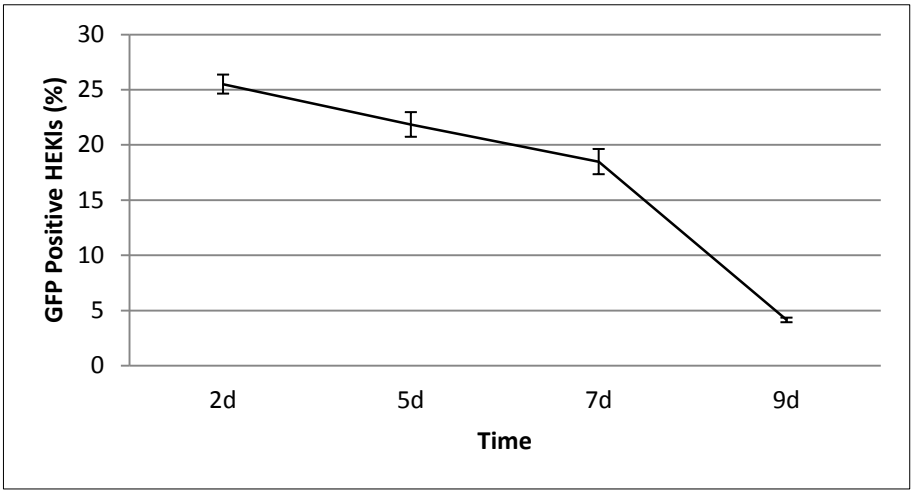

Figure 3.26 Nucleofection efficiency second round of nucleofection GFP-P. Points plotted represent the mean number of hEKs successfully nucleofected with GFP-P quantified using flow cytometry at specific time points post-nucleofection, error bars represent standard error of the mean, n=3

hEKs nucleofected with miRNA inhibitor control were also harvested after 5 days and subjected to further rounds of nucleofection. This revealed a number of successfully nucleofected hEKs compared to nucleofected in the absence of miRNA inhibitor control, which failed to maintain miRNA inhibitor expression (Figure 3.27).

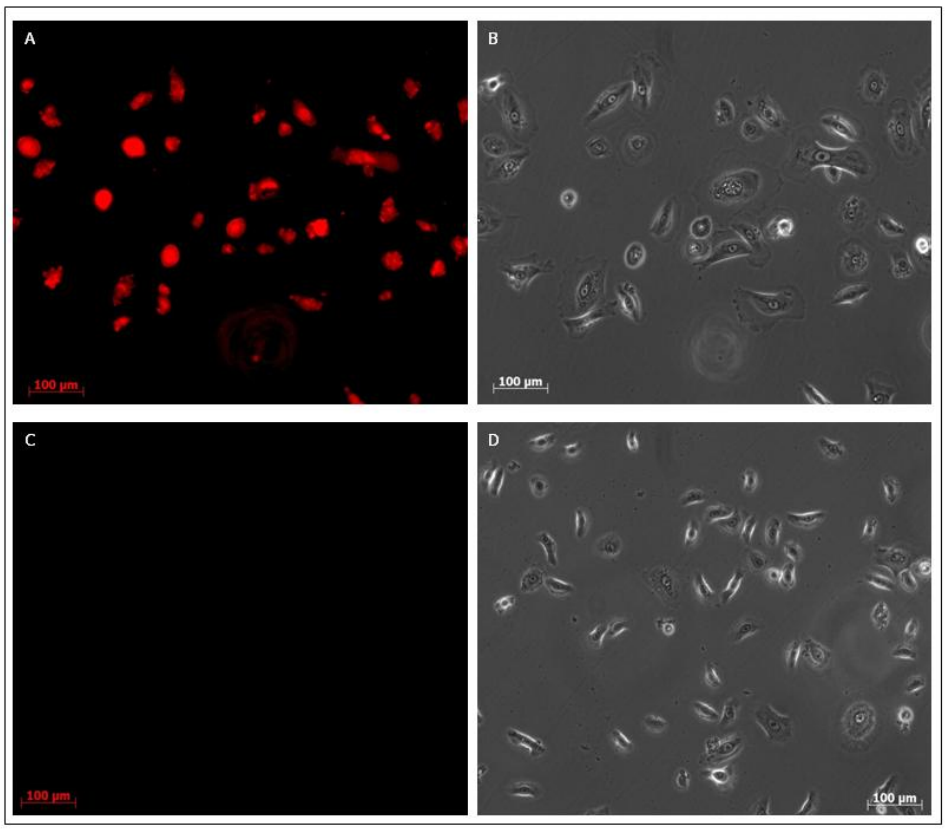

Figure 3.27 Fluorescent and phase contrast microscopic observations of hEKs subjected to second round of nucleofection after 48 hours (**A–B**) with miRNA inhibitor control; (**C-D**) without of miRNA inhibitor control, same field of view for each sample, scale bar represents 100µm

hEKs which had undergone a second round of nucleofection in the presence of miRNA inhibitor control were maintained for a further 9 days, a total of 14 days since the initial round of nucleofection and observed using fluorescent and transmitted light microscopy after 5, 7 and 9 days. This revealed the persistence of miRNA inhibitor control in a number of hEKs during this culture period (Figure 3.28).

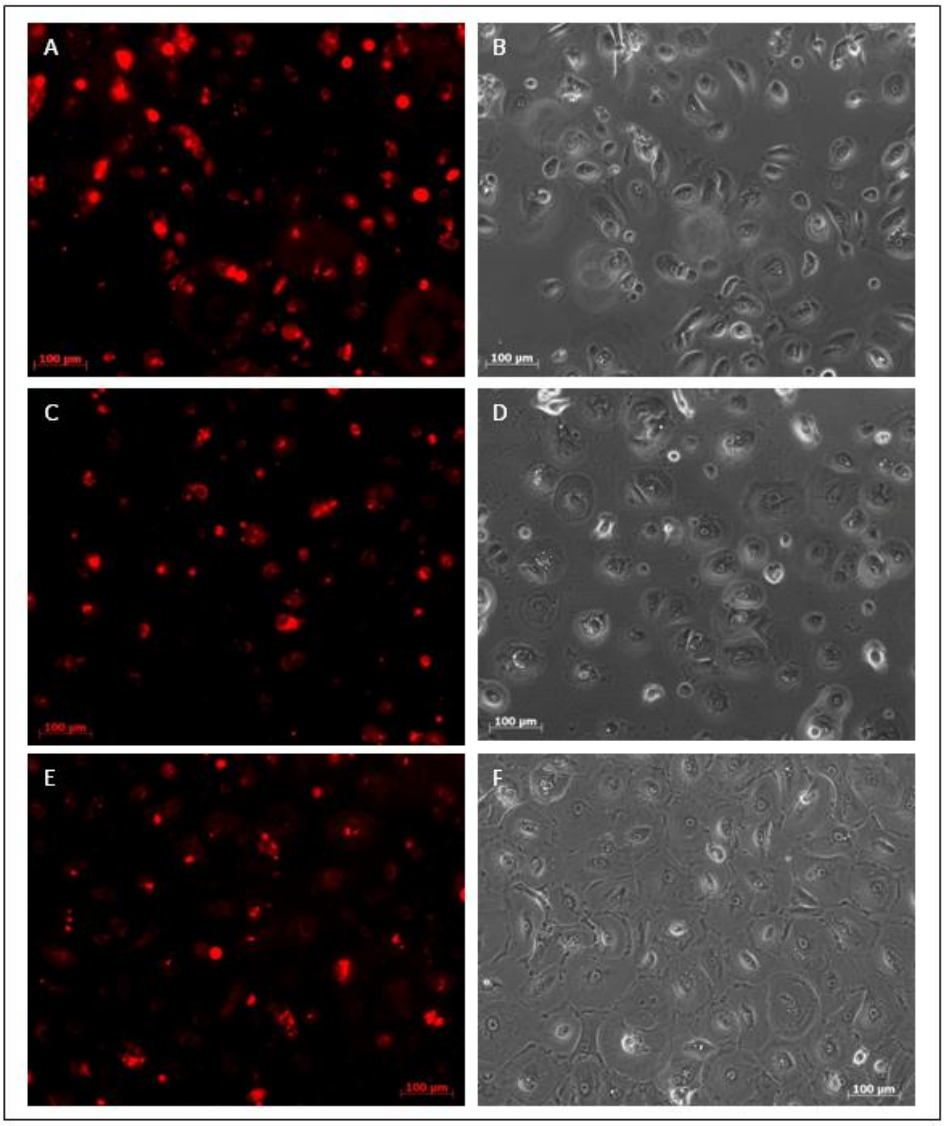

Figure 3.28 Fluorescent and phase contrast microscopic observations of hEKs subjected to a second round of nucleofection with miRNA inhibitor control (**A-B**) 5 days; (**C-D**) 7 days; (**E-F**) 9 days post-nucleofection, same field of view for each given time point, scale bar represents 100µm

Flow cytometry demonstrated that a second round of nucleofection resulted in an increase in hEKs successfully incorporating the miRNA inhibitor control and mirrored previous results with a gradual decrease in miRNA inhibitor control over time (Figure 3.29). However, despite a decrease,

transcription of miRNA inhibitor control remained high throughout the culture period.

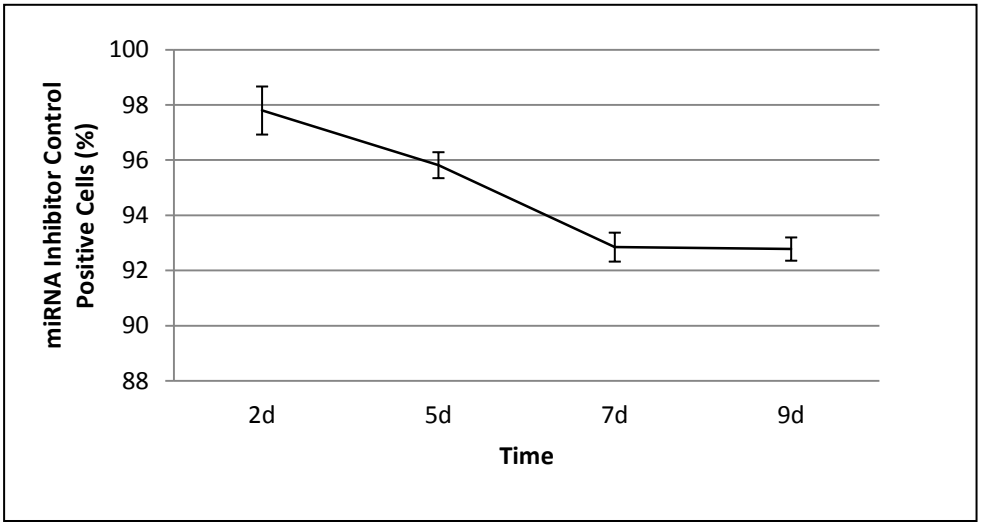

Figure 3.29 Nucleofection efficiency second round of nucleofection miRNA inhibitor control. Points plotted represent mean number of hEKs successfully nucleofected with miRNA inhibitor control quantified using flow cytometry at specific time points post-nucleofection, error bars represent standard error of the mean, n=3

This data showed increased fluorescence intensity when hEKs had undergone a further round of nucleofection (Figure 3.30). The red area represents hEKs after a second round of nucleofection with miRNA inhibitor control while the blue line indicates hEKs after an initial round of nucleofection with miRNA inhibitor control. The shift in fluorescence suggests increased miRNA inhibitor present in these cells.

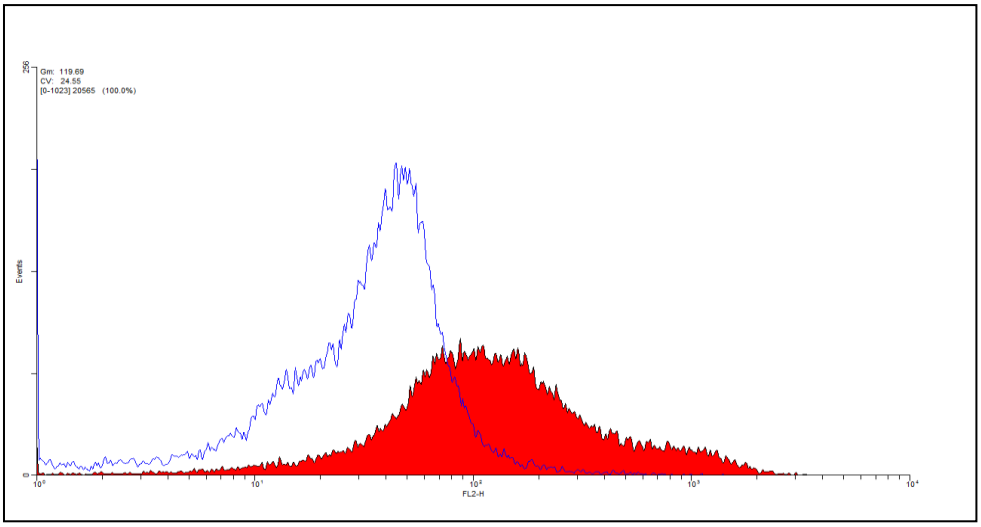

Figure 3.30 Representative histogram of hEKs nucleofected with miRNA inhibitor control. Blue line represents initial round of nucleofection. Red area represents second round of nucleofection 24 hours post-nucleofection

3.3.5 Co-Nucleofection

Nucleofection is a flexible non-viral method of delivering both plasmid DNA and miRNA inhibitors to primary cells. In order to develop an effective reprogramming strategy it was necessary to establish whether plasmid DNA and miRNA inhibitors could be delivered in combination. hEKs were subject to nucleofection with GFP-P and microRNA inhibitor control at previously optimised concentrations (section 3.3.3) and characterised. Nuclear transfer of both substrates was visible after 24 hours using fluorescent microscopy. As expected, the majority of cells had incorporated miRNA inhibitor control compared to a much smaller number incorporating GFP-P (Figure 3.31). It was also evident that that a number of hEKs had been successfully nucleofected with both GFP-P and miRNA inhibitor control.

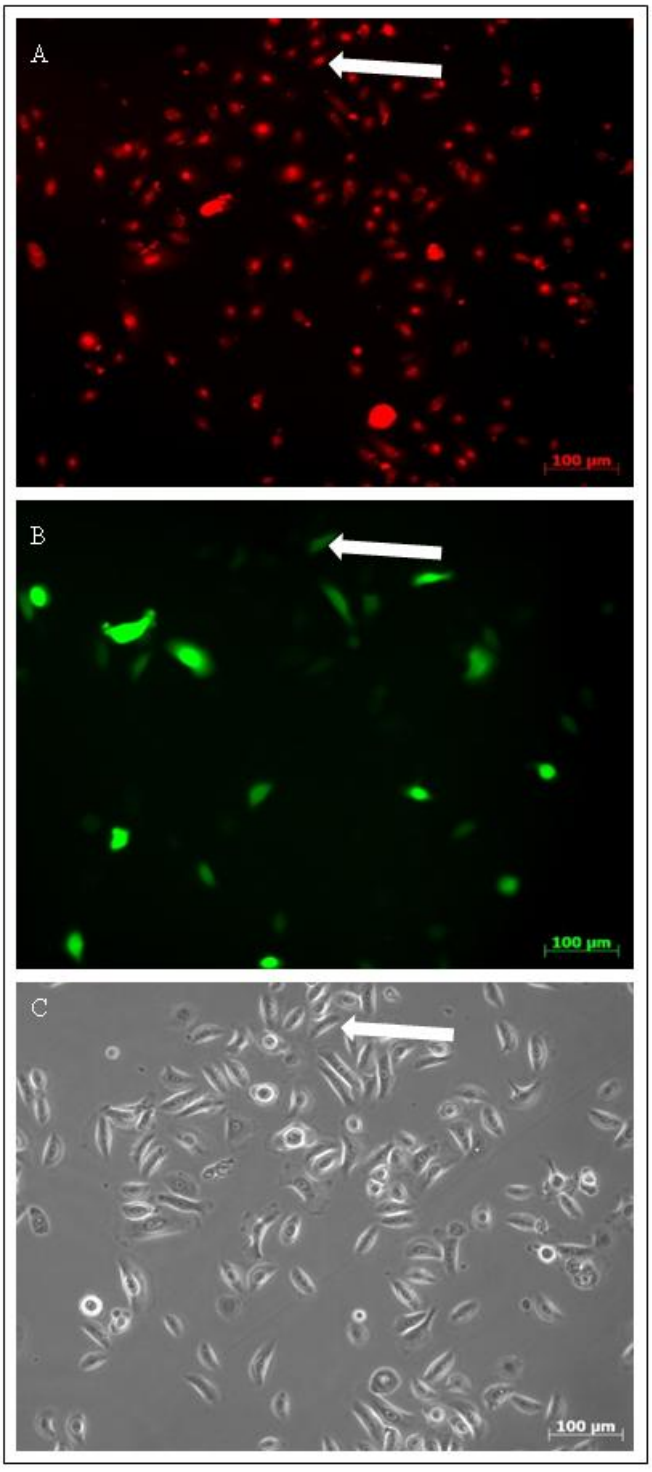

Figure 3.31 Co-nucleofection of hEKs **A**: miRNA inhibitor control fluorescent microscopic observation 24 hours post nucleofection. **B:** GFP-P fluorescent microscopic observation. **C**: Light microscopic observation. Arrow indicates cell that has received both substrates, same field of view

Flow cytometry of co-nucleofected hEKs after 24 hours revealed the vast majority had incorporated miRNA inhibitor control, 59.68% ± 3.03, n=3, whilst 11% ± 1.69, n=3 received GFP-P. It could also be deduced that 7.64% ± 0.76, n=3 of hEKs had successfully incorporated both miRNA inhibitor control and GFP-P (Figure 3.32).

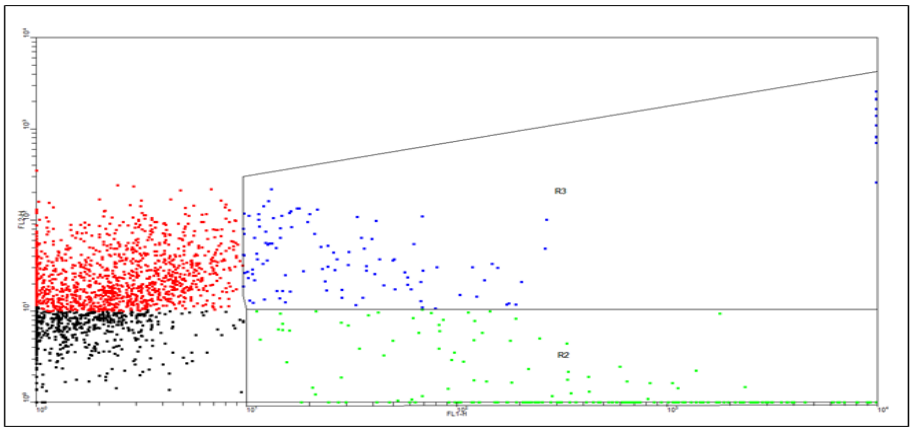

Figure 3.32 Representative dot plot of hEKs 24 hours post-co-nucleofection. **Red**: miRNA inhibitor control, **Green**: GFP-P, **Blue**: miRNA inhibitor control and GFP-P

3.4 Nucleofection of miR-145 Inhibitor

As detailed previously, miR-145, has been highlighted due to its relationship with major pluripotency genes. To conclude effects of this specific miRNA on the major regulators of a pluripotent phenotype, we established a knock-out study whereby the function of this miRNA could be deduced by studying the effects of its inhibition on cell phenotype.

To assess the effect of miR-145 inhibition, hEKs were nucleofected with an miR-145 antisense inhibitor and the genomic effects of forced inhibition evaluated by quantifying expression of an array of genes known to influence somatic cell reprogramming. So that an accurate analysis of miR-145 inhibited hEKs could be achieved, a number of controls were included. A

negative control was established whereby the miR-145 inhibitor was replaced with a scrambled miRNA inhibitor, which does not compliment any native miRNA or mRNA sequence in mouse, rat or human and is therefore non-effective in influencing gene pathways. A mock-treated control sample was included whereby cells were subjected to all of the experimental conditions in the absence of a miRNA inhibitor such that non-specific effects conferred solely as a consequence of transfection biochemistry could be monitored. In conjunction, untreated controls were included which comprised of cells which had not undergone nucleofection to give a baseline of cellular activity. Total RNA was subsequently isolated from hEKs at 1, 3, 5, 7 and 9 days post-nucleofection.

qRT-PCR analysis revealed that inhibition of miR-145, resulted in significant changes in expression of key pluripotency-associated genes (section 2.10.5). Figure 3.33 illustrates RT–PCR analysis of the pluripotency marker, *Oct4*, following miR-145 inhibition relative to hEKs nucleofected in the absence of miR-145, showing significant upregulation 3 days post-nucleofection. Most significant was the increase in *Oct4* expression, in excess of 10 fold, detected 5 days post-nucleofection with miR-145 inhibitor. Expression of *Oct4* subsequently decreased however 9 days post-nucleofection *Oct4* expression remained significantly elevated compared to hEKs nucleofected in the absence of miR-145 inhibitor.

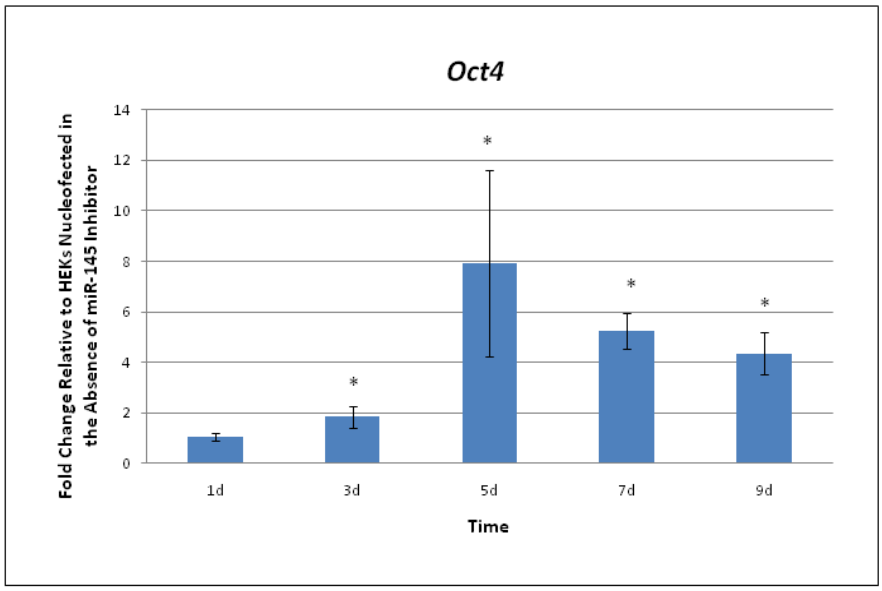

Figure 3.33 qRT-PCR analysis of hEKs nucleofected with miR-145 inhibitor over time. Bars represent mean fold change of *Oct4* expression relative to hEKs nucleofected in the absence of miR-145 inhibitor. Error bars represent the standard error of the mean, n=3. Mann Whitney U statistical test *p-value = 0.05

Another key mediator of a pluripotency is *Sox2*, which is closely associated with neural development and differentiation. It was possible to observe an increase in the expression of *Sox2* following nucleofection with miR-145 inhibitor. A significant increase in *Sox2* expression was detected as early as 1 day post-nucleofection and increased in excess of 30 fold 9 days post-miR-145 inhibition (Figure 3.34). A similar pattern of expression was also noted for *Klf4* with a significant increase exceeding 25 fold 9 days post-miR-145 inhibition (Figure 3.35) relative to hEKs nucleofected in the absence of miR-145.

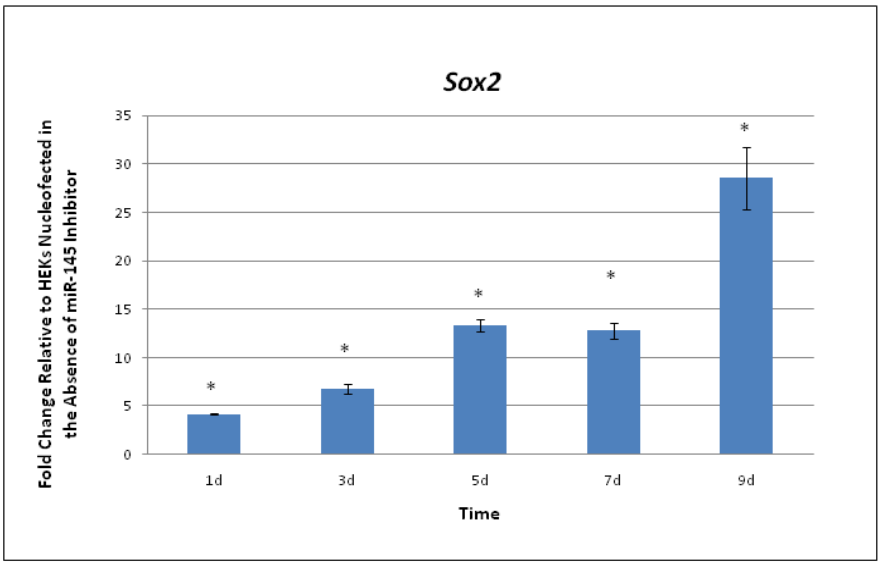

Figure 3.34 qRT-PCR analysis of hEKs nucleofected with miR-145 inhibitor over time. Bars represent the mean fold change of *Sox2* expression relative to hEKs nucleofected in the absence of miR-145 inhibitor. Error bars represent the standard error of the mean, n=3. Mann Whitney U statistical test *p-value = 0.05

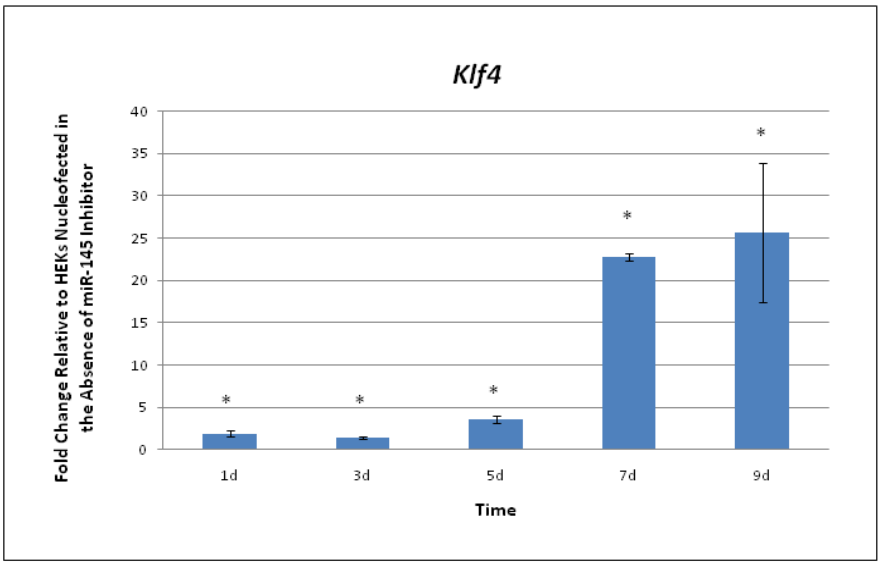

Figure 3.35 qRT-PCR analysis of hEKs nucleofected with miR-145 inhibitor over time. Bars represent the mean fold change of *Klf4* expression relative to hEKs nucleofected in the absence of miR-145 inhibitor. Error bars represent the standard error of the mean, n=3. Mann Whitney U statistical test *p-value = 0.05

Inhibition of miR-145 also corresponded to an increase in *c-Myc* expression with more than 10 fold upregulation detected 5 days post-nucleofection with miR-145 inhibitor (Figure 3.36).

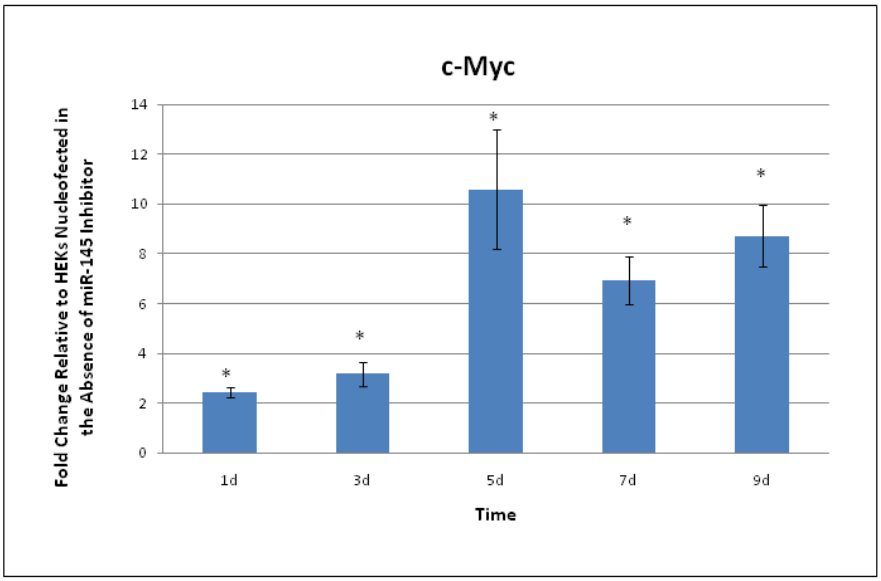

Figure 3.36 qRT-PCR analysis of hEKs nucleofected with miR-145 inhibitor over time. Bars represent the mean fold change of *c-Myc* expression relative to hEKs nucleofected in the absence of miR-145 inhibitor. Error bars represent the standard error of the mean, n=3. Mann Whitney U statistical test *p-value = 0.05

Although *Nanog* expression was also altered following miR-145 inhibition, effects were more difficult to interpret. Initially following nucleofection *Nanog* expression was significantly upregulated however this was followed by a significant decrease in expression. Between days 3 and 5 post-nucleofection *Nanog* expression increased again but was not found to be statistically significant. The most significant increase in *Nanog* expression was 7 days post-nucleofection with more than a 5 fold increase however once again *Nanog* expression decreased after this point (Figure 3.37).

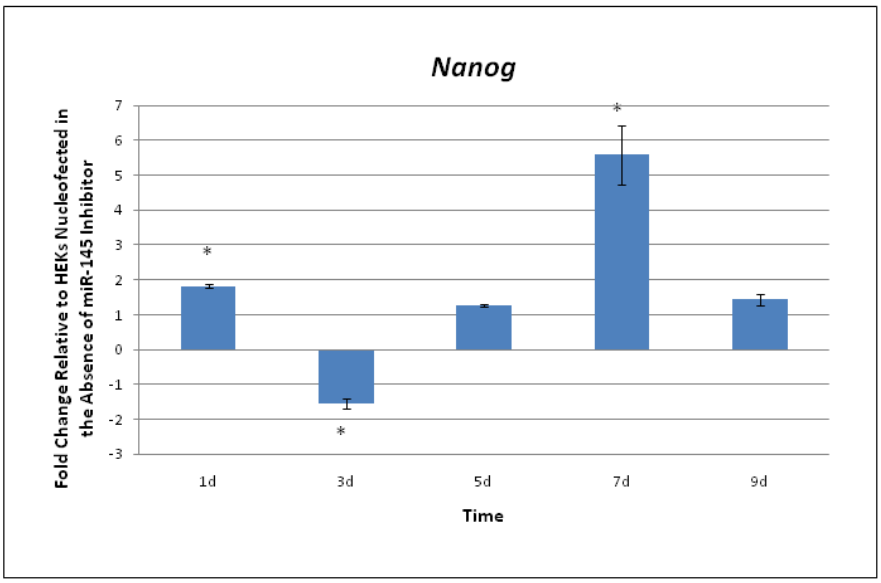

Figure 3.37 qRT-PCR analysis of hEKs nucleofected with miR-145 inhibitor over time. Bars represent the mean fold change of *Nanog* expression relative to hEKs nucleofected in the absence of miR-145 inhibitor. Error bars represent the standard error of the mean, n=3. Mann Whitney U statistical test *p-value = 0.05

To detect whether activation of pluripotency associated genes affected expression of hEK specific genes, qRT-PCR analysis of *cytokeratin14* expression was performed. A significant decrease in *cytokeratin14* expression was detected 1 day following nucleofection with miR-145 inhibitor however over the period of culture *cytokeratin14* expression returned to basal levels (Figure 3.38).

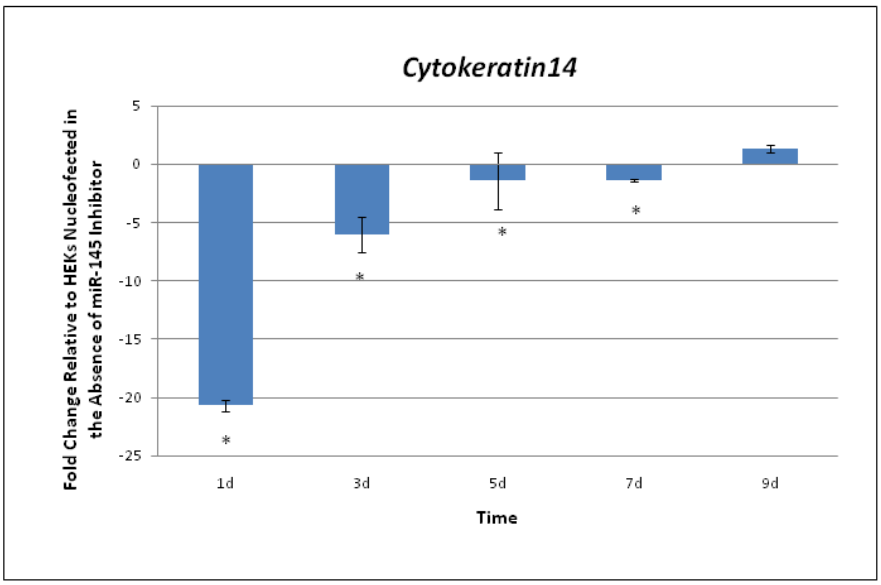

Figure 3.38 qRT-PCR analysis of hEKs nucleofected with miR-145 inhibitor over time. Bars represent the mean fold change of *cytokeratin14* expression relative to hEKs nucleofected in the absence of miR-145 inhibitor. Error bars represent the standard error of the mean, n=3. Mann Whitney U statistical test *p-value = 0.05

3.5 hESC Media to Promote Pluripotency

Considering miR-145 inhibition is capable of activating expression of normally silenced pluripotency genes in hEKs it was hypothesised that a reprogramming strategy could be developed based upon miR-145 inhibition. To provide hEKs with an environment to promote expression of pluripotency genes it was hypothesised that serum-free media, typically used for the routine culture of hESCs without feeder cells, may provide stimulatory growth factors to promote a more plastic genotype, facilitating reprogramming. hEKs were taken from passage 2-5, nucleofected with miR-145 inhibitor and 24 hours post-nucleofection hEK media was replaced with hESC media.

This resulted in a rapid morphological change with miR-145 inhibited hEKs maintained under hESC culture conditions forming distinct colonies, a characteristic of hESCs. hEKs which had also received the miR-145 inhibitor and were subsequently maintained in hEK media remained as a monolayer (Figure 3.39).

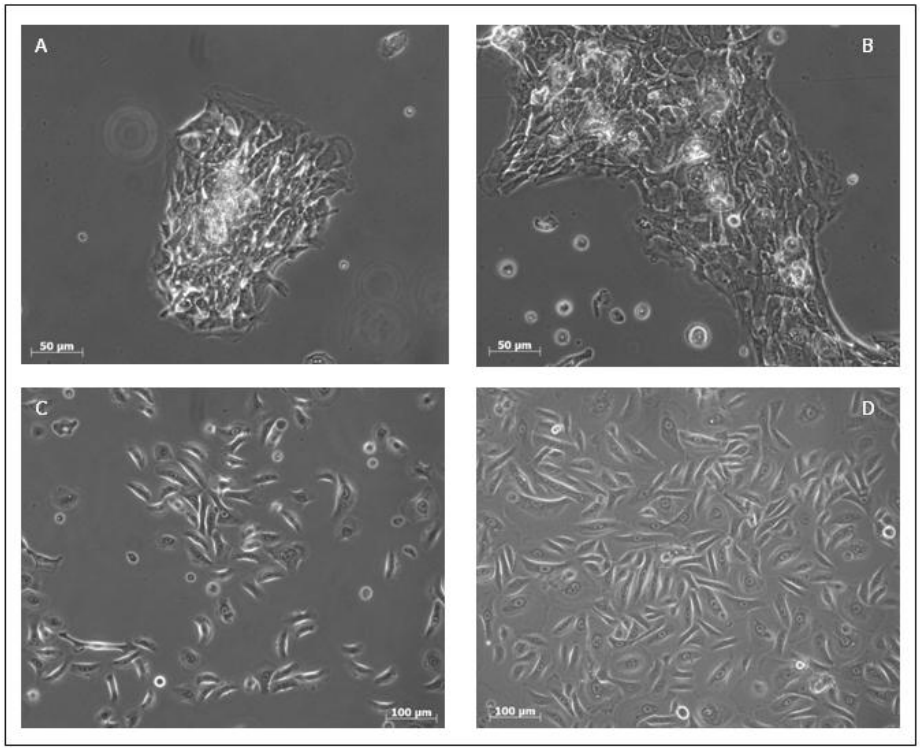

Figure 3.39 Morphology of miR-145 inhibited hEKs maintained either in hESC media (top) or hEK media (bottom). Phase contrast microscopic observation **A-C**: 1 day post-nucleofection. **B-D**: 5 days post-nucleofection

To investigate effects of hESC media at a genomic level qRT-PCR analysis was performed on hEKs nucleofected with miR-145 inhibitor and subsequently maintained in either hESC or hEK media post-nucleofection. Concordant with previous results 5 days was selected as a significant time point with *Oct4* expression found to peak at this time following miR-145

inhibition. Gene expression was analysed after hEKs received the miR-145 inhibitor and were cultured in hESC or hEK media for 5 days. The data presented here represent the fold change in gene expression relative to hEKs which had undergone nucleofection in the absence of the miR-145 inhibitor.

It was possible to detect a significant increase in *Oct4* expression when miR-145 inhibited hEKs were maintained in either hESC or hEK media compared to hEKs nucleofected in the absence of miR-145 inhibitor.

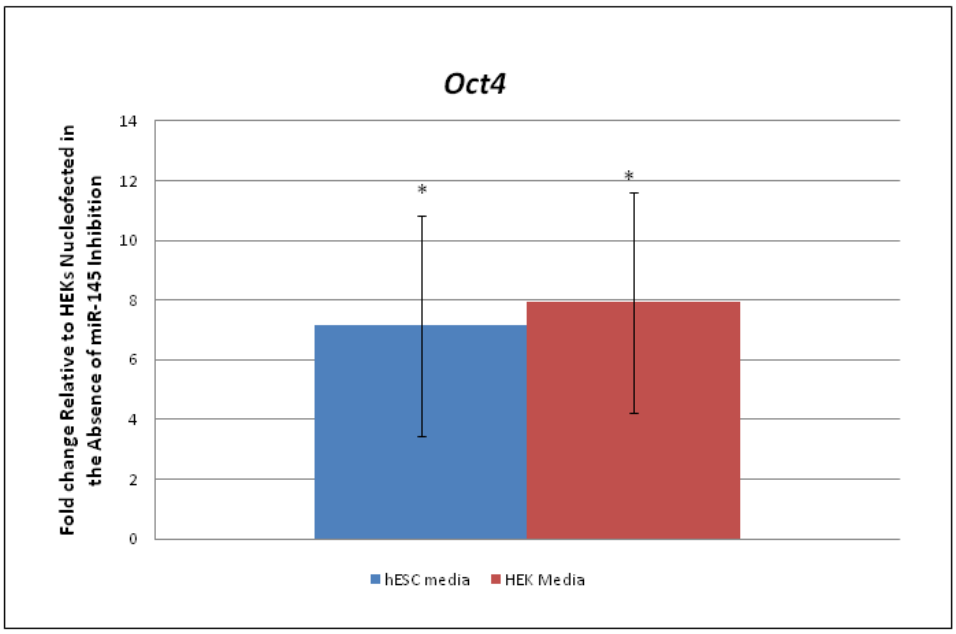

Figure 3.40 qRT-PCR analysis of hEKs 5 days post-nucleofection with miR-145 inhibitor maintained in either hESC (blue) or hEK (red) media. Bars represent the mean fold change of *Oct4* expression relative to hEKs nucleofected in the absence of miR-145 inhibitor. Error bars represent the standard error of the mean, n=3. Mann Whitney U statistical test *p-value = 0.05

To observe Oct4 at the proteomic level both hEKs, nucleofected with miR-145 inhibitor and subsequently cultured in either hESC or hEK media were subject to immunohistochemistry (Section 2.3). In both cases re-expression of this pluripotency master regulator led to successful translation of the Oct4 protein (Figure 3.41).

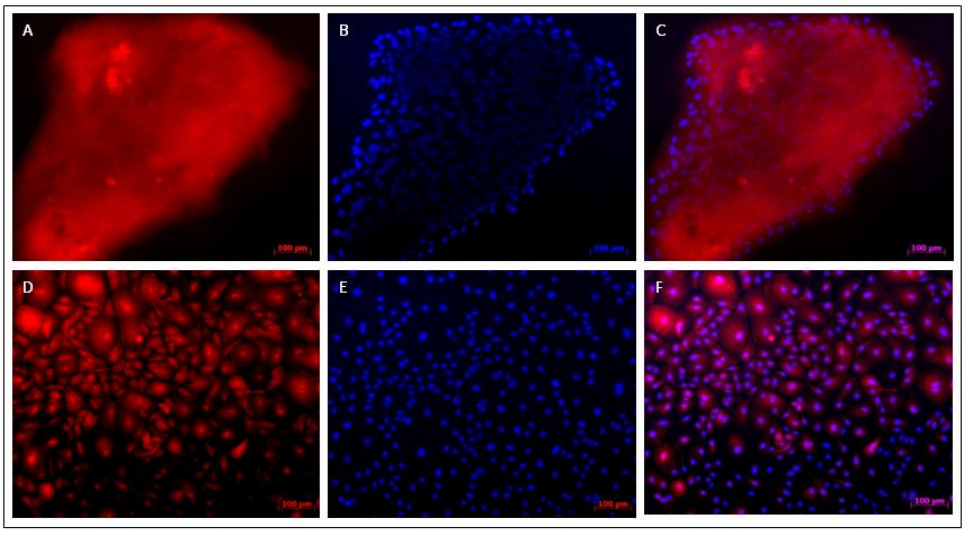

Figure 3.41 *Oct4* protein expression 5 days post-nucleofection with miR-145 inhibitor. Fluorescent microscopic observation of **Oct4**, **DAPI** miR-145 inhibited hEKs maintained in (**A-C**): hESC media. (**D-F**): hEK media.

qRT-PCR analysis showed that in the case of miR-145 inhibited hEKs cultured in hESC media, *Sox2* expression had risen more than 70 fold compared to the 10 fold increase detected when maintained in hEK media (Figure 3.42). Furthermore qRT-PCR revealed that *Nanog* expression had also risen significantly when miR-145 inhibited hEKs were maintained under hESC conditions with more than a 7 fold expression increase compared to approximately 1 fold in the case of miR-145 inhibited hEKs maintained in hEK media (Figure 3.43), again representing a significant difference in pluripotency gene expression between the two culture systems.

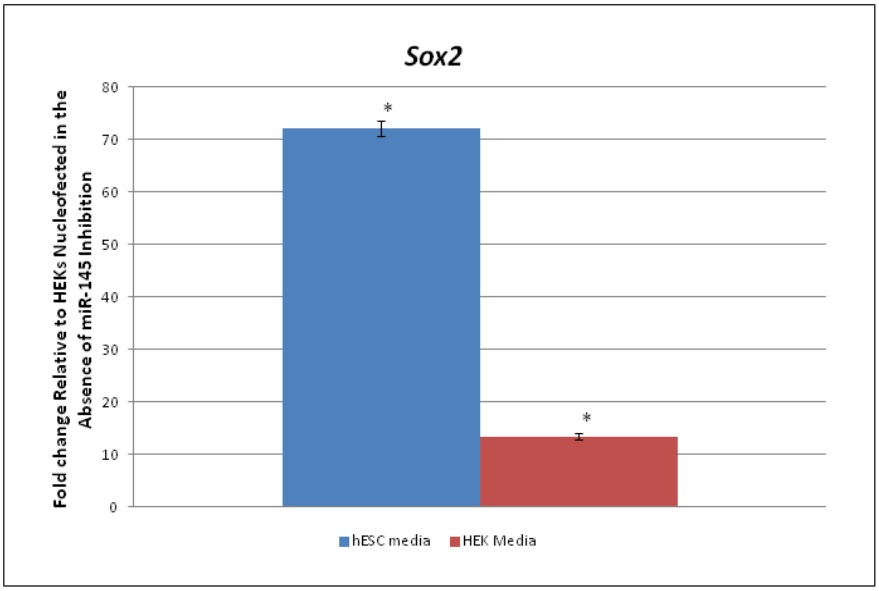

Figure 3.42 qRT-PCR analysis of hEKs 5 days post-nucleofection with miR-145 inhibitor maintained in either hESC (blue) or hEK (red) media. Bars represent the mean fold change of *Sox2* expression relative to hEKs nucleofected in the absence of miR-145 inhibitor. Error bars represent the standard error of the mean, n=3. Mann Whitney U statistical test *p-value = 0.05

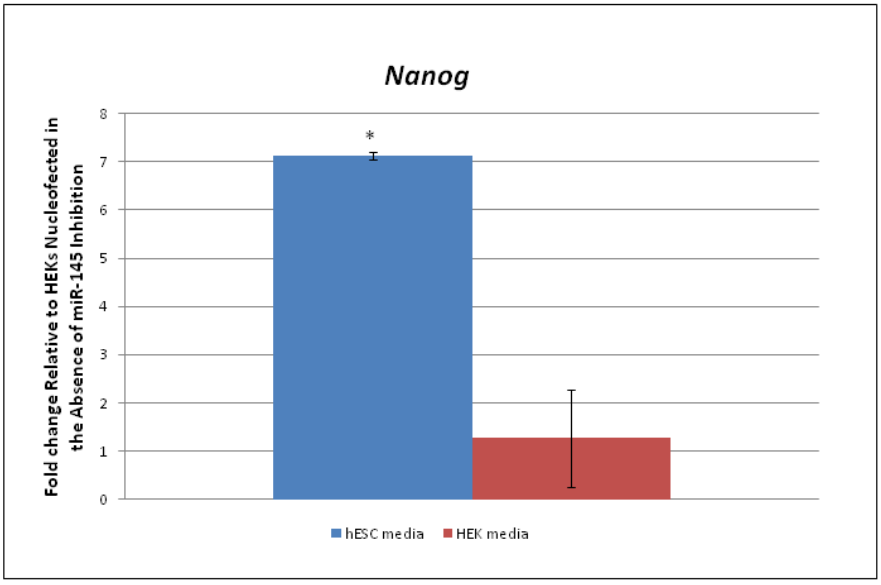

Figure 3.43 qRT-PCR analysis of hEKs 5 days post-nucleofection with miR-145 inhibitor maintained in either hESC (blue)or hEK (red) media. Bars represent the mean fold change of *Nanog* expression, error bars represent the standard error of the mean, n=3. Mann Whitney U statistical test *p-value = 0.05

Immunohistochemistry was performed to observe how altered gene expression affects synthesis of both Sox2 and Nanog proteins confirming translation of Sox2 (Figure 3.44) and Nanog (Figure 3.45) in miR-145 inhibited hEKs maintained in both hEK and hESC media.

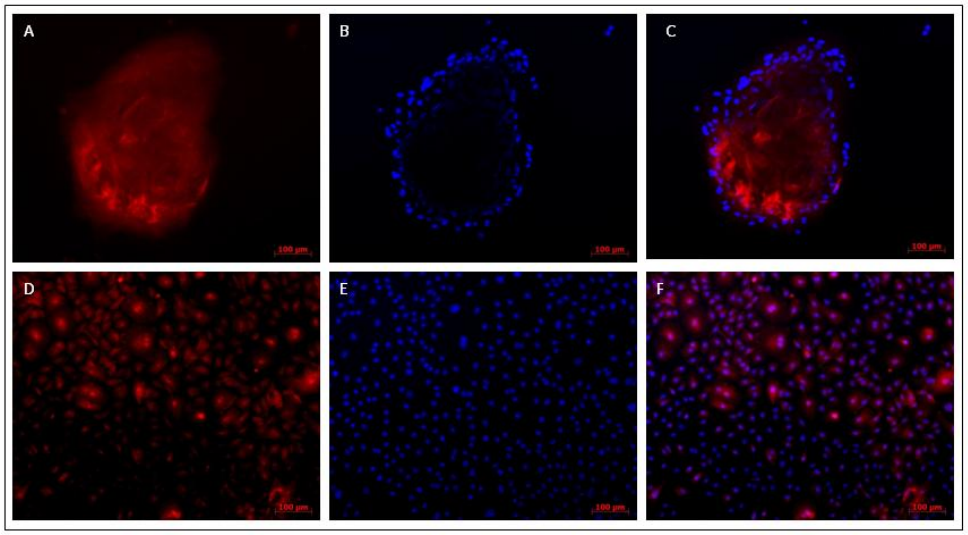

Figure 3.44 Sox2 protein expression 5 days post-nucleofection with miR-145 inhibitor. Fluorescent microscopic observation of **Sox2**, **DAPI** miR-145 inhibited hEKs maintained in (**A-C**): hESC media. (**D-F**): hEK media.

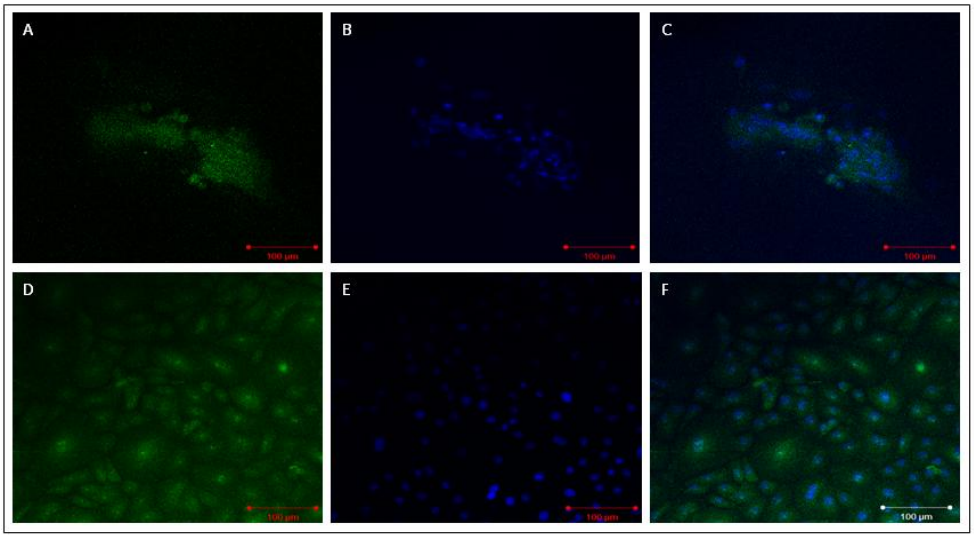

Figure 3.45 Nanog protein expression 5 days post-nucleofection with miR-145 inhibitor. Fluorescent microscopic observation of **Nanog**, **DAPI** miR-145 inhibited hEKs maintained in (**A-C**): hESC media. (**D-F**): hEK media.

Expression of *Klf4* and *c-Myc* were also increased significantly when hEKs were maintained under hESC culture conditions. Figure 3.46 demonstrates that under hESC culture conditions *Klf4* expression increased more than 7 fold compared to less than 4 fold when maintained in hEK media post-nucleofection. Furthermore, Figure 3.47 illustrates a significant increase in *c-Myc* expression following maintenance of miR-145 inhibited hEKs in hESC media almost doubling the fold change compared to those maintained in hEK media for 5 days.

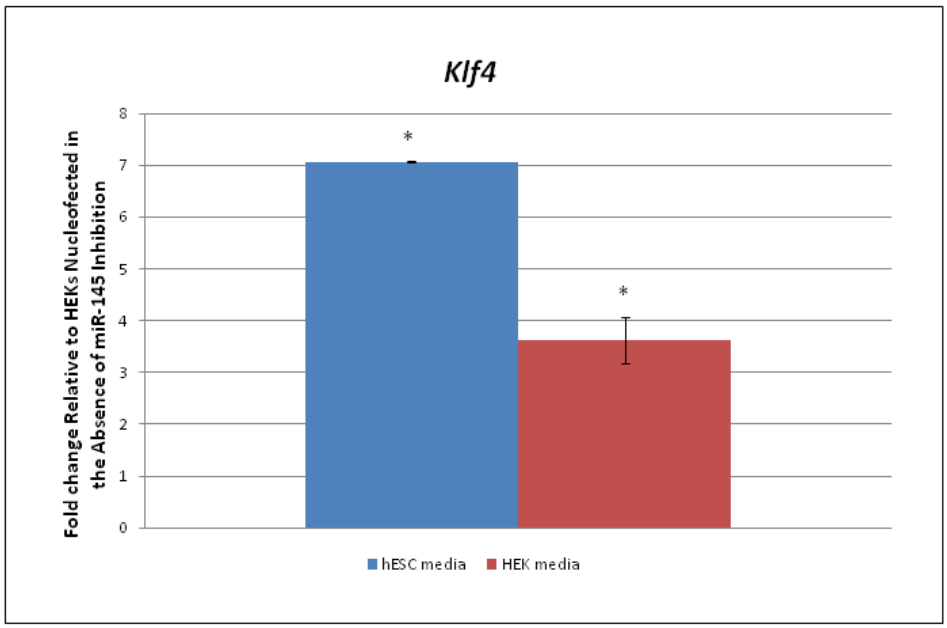

Figure 3.46 qRT-PCR analysis of hEKs 5 days post-nucleofection with miR-145 inhibitor maintained in either hESC (blue) or hEK (red) media. Bars represent the mean fold change of *Klf4* expression relative to hEKs nucleofected in the absence of miR-145 inhibitor. Error bars represent the standard error of the mean, n=3. Mann Whitney U statistical test *p-value = 0.05

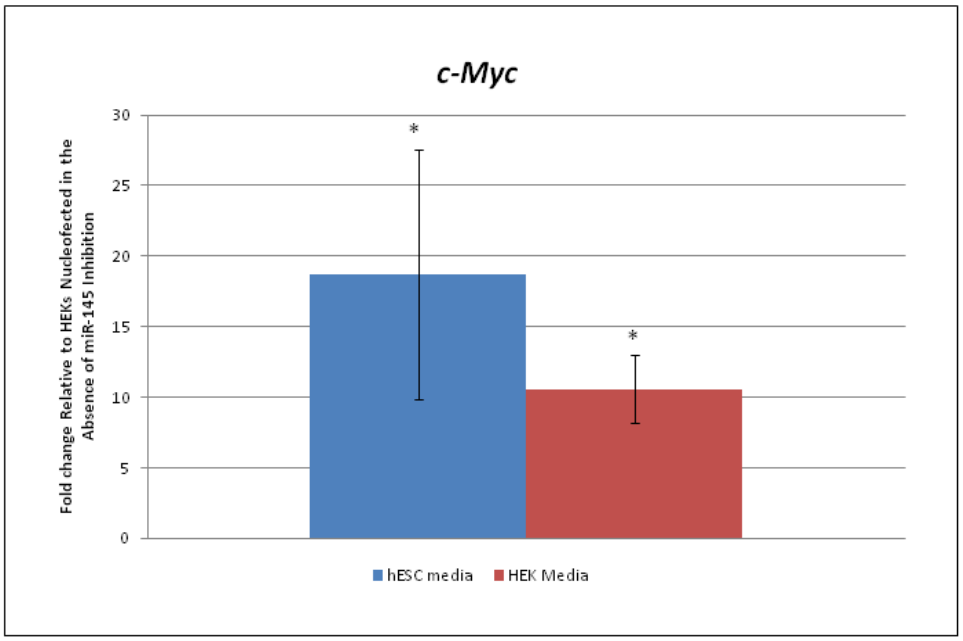

Figure 3.47 qRT-PCR analysis of hEKs 5 days post-nucleofection with miR-145 inhibitor maintained in either hESC (blue) or hEK (red) media. Bars represent the mean fold change of *c-Myc* expression relative to hEKs nucleofected in the absence of miR-145 inhibitor. Error bars represent the standard error of the mean, n=3. Mann Whitney U statistical test **p*-value = 0.05

The expression of *cytokeratin14* was also investigated to identify an altered genotype following miR-145 inhibition and culture in hESC media. We had previously identified that *cytokeratin14* expression decreased upon inhibition of miR-145 followed by maintenance in hEK media (Figure 3.35). Substituting hEK media with hESC media provided more profound effects on *cytokeratin14* expression, with a mean fold change of -8 $x10^3$ (Figure 3.48) strongly suggesting an altered phenotype, which may have lead to the distinct change in cell morphology.

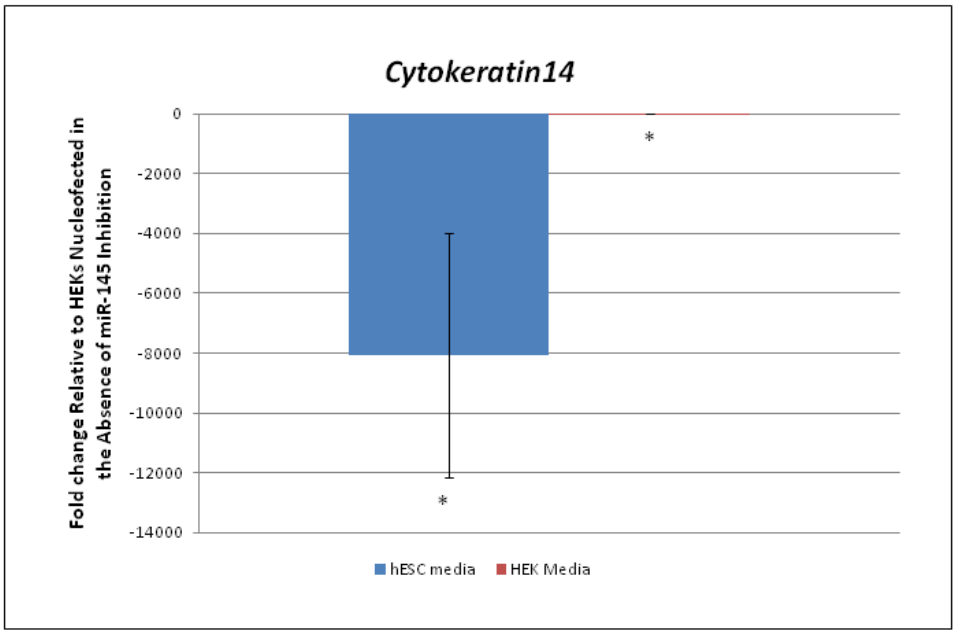

Figure 3.48 qRT-PCR analysis of hEKs 5 days post-nucleofection with miR-145 inhibitor maintained in either hESC (blue) or hEK (red) media. Bars represent the mean fold change of *cytokeratin-14* expression relative to hEKs nucleofected in the absence of miR-145 inhibitor. Error bars represent the standard error of the mean, n=3. Mann Whitney U statistical test **p*-value = 0.05

3.6 Direct Reprogramming of miR-145 Inhibited hEKs

To establish whether miR-145 inhibited hEKs remained lineage committed, they were subject to defined differentiation parameters to orchestrate phenotype changes toward functional lineages. *In vitro* differentiation of adult stem cells into osteoblasts, chondrocytes and adipocytes is a gold standard experiment for concluding cell plasticity [172]. Therefore we subjected cells to established tri-lineage differentiation criteria to demonstrate acquired plasticity of miR-145 inhibited hEKs.

hEKs were nucleofected with miR-145 inhibitor and subsequently cultured in either hEK or hESC media for 5 days before being subject to tri-lineage differentiation using defined osteogenic, chondrogenic and adipogenic

media formulations (section 2.13). hEKs nucleofected in the absence of miR-145 inhibitor were also subject to the same differentiation parameters as a negative control while tri-lineage differentiation of hMSCs was conducted using the same media formulations as a positive control.

3.6.1 Osteogenic Differentiation

One of the earliest indicators of osteogenesis is the osteogenic master gene; core binding factor α1 (*CBFA1/RUNX2*). All samples, except for hEKs nucleofected without miR-145 inhibitor, were found to express *CBFA1* when observed immunohistochemically 5 days post-directed differentiation (Figure 3.49). The induction of osteogenic phenotype was further confirmed by observation of osteocalcin 21 days post-induction (Figure 3.50).

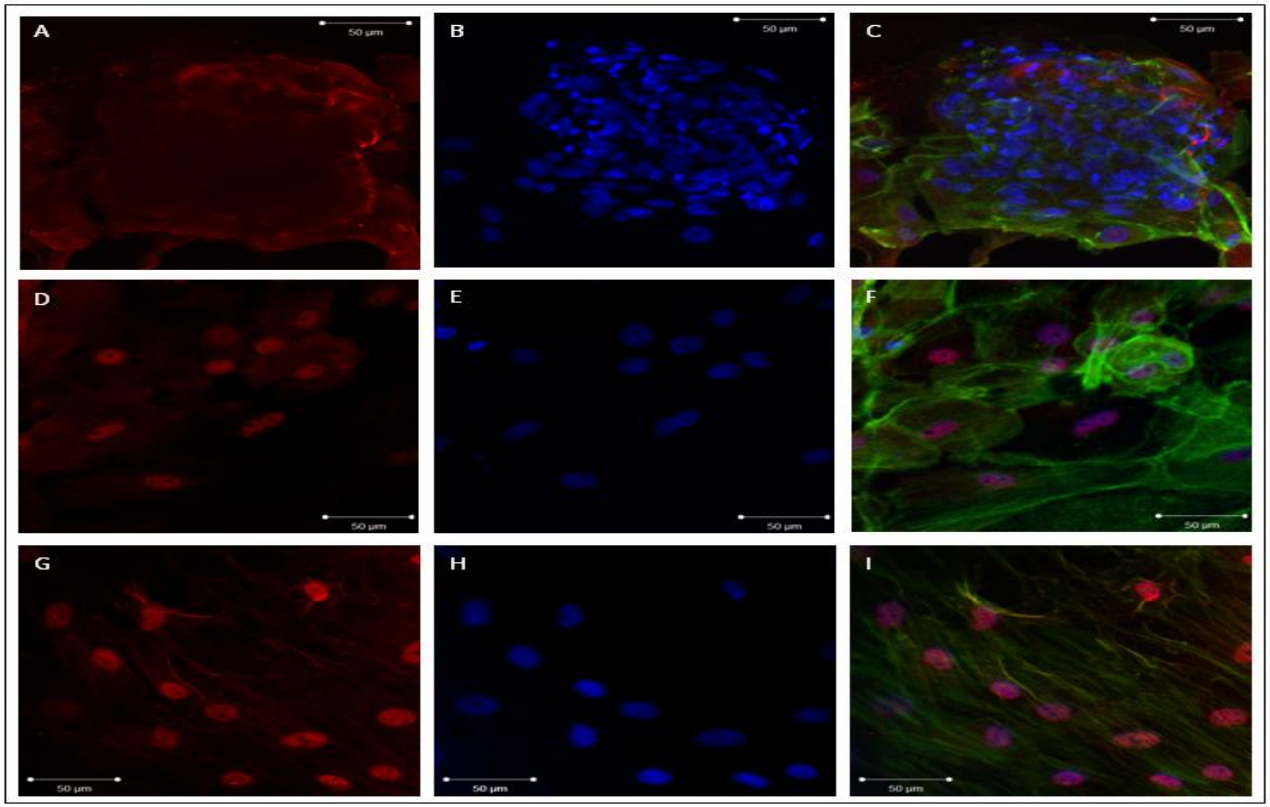

Figure 3.49 Fluorescent microscopic observation of hEKs stained for **CBFA1**, **DAPI**, **F-Actin** after 5 days directed osteogenic differentiation (**A-C**): miR-145 inhibited hEKs maintained in hESC media prior to osteogenic differentiation. (**D-F**): miR-145 inhibited hEKs maintained in hEK media prior to osteogenic differentiation. (**G-I**): hMSCs

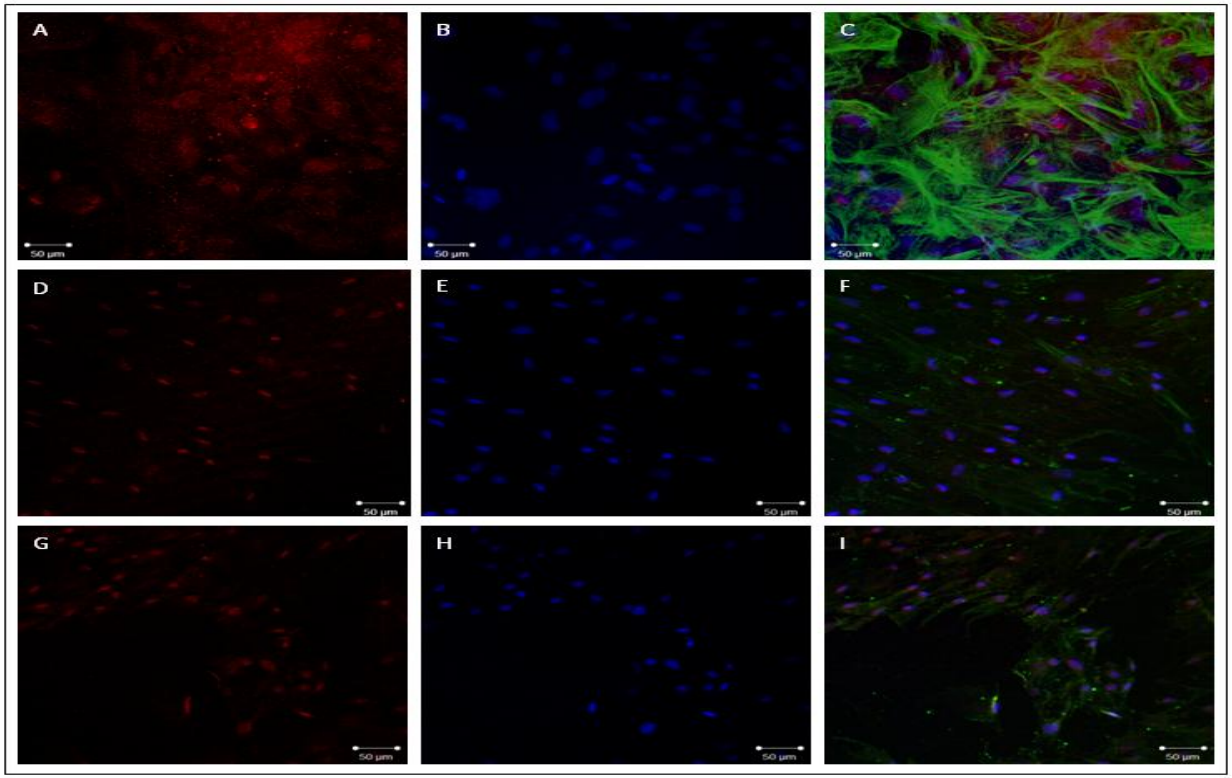

Figure 3.50 Fluorescent microscopic observation of hEKs stained for **Osteocalcin**, **DAPI**, **F-Actin** after 21 days directed osteogenic differentiation (**A-C**): miR-145 inhibited hEKs maintained in hESC media prior to osteogenic differentiation. (**D-F**): miR-145 inhibited hEKs maintained in hEK media prior to osteogenic differentiation. (**G-I**): hMSCs

Von Kossa and Alizarin Red S staining were also performed and provided further confirmation of terminal functional osteogenesis (Figures 3.51- 3.52)

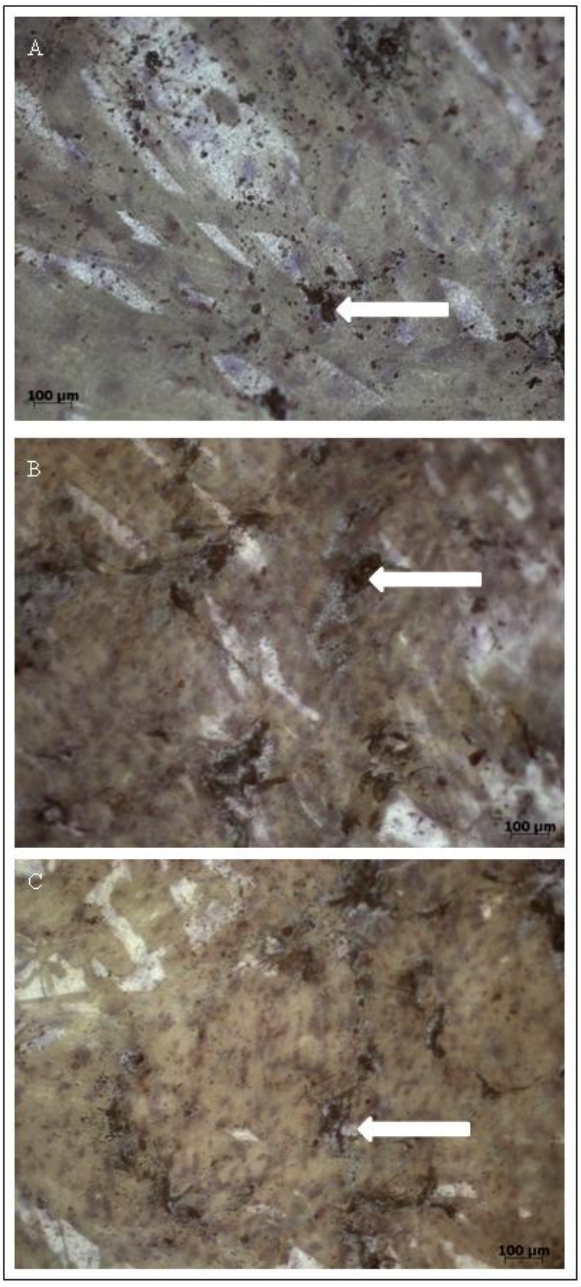

Figure 3.51 Histological observation of Von Kossa staining *in situ* after 21 days directed osteogenic differentiation (**A**): miR-145 inhibited hEKs maintained in hESC media prior to osteogenic differentiation. (**B**): miR-145 inhibited hEKs maintained in hEK media prior to osteogenic differentiation. (**C**): hMSCs, arrows indicate mineralisation, scale bar represents 100µm

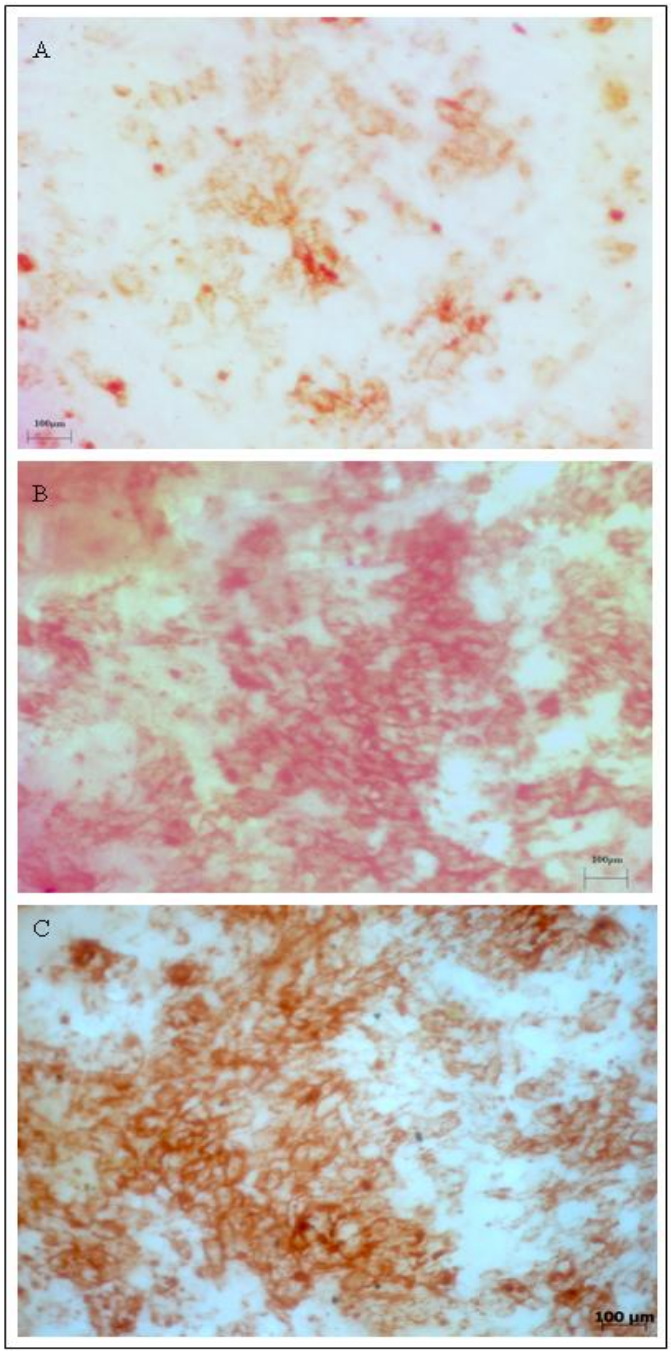

Figure 3.52 Histological observation of Alizarin Red S staining *in situ* after 21 days directed osteogenic differentiation (**A**): miR-145 inhibited hEKs maintained in hESC media prior to osteogenic differentiation. (**B**): miR-145 inhibited hEKs maintained in hEK media prior to osteogenic differentiation. (**C**): hMSCs, scale bar represents 50µm

qRT-PCR analysis provided further insight into genomic changes occurring during osteogenesis. *CBFA1* expression increased significantly between 1 and 3 days, in the case of hMSCs and miR-145 inhibited hEKs pre-incubated in hESC media following osteogenic induction. In both cases *CBFA1* expression peaked after 5 days with more than a 200 fold increase detected when miR-145 inhibited hEKs had been pre-incubated in hESC media compared to hEKs nucleofected without miR-145 prior to osteogenic differentiation. This was followed by a progressive decrease in *CBFA1* expression for both hMSCs and miR-145 inhibited hEKs pre-incubated in hESC media. In the case of miR-145 inhibited hEKs pre-incubated in hEK media, *CBFA1* expression was also found to significantly increase, reaching a maximum at the later time point of 7 days. This increase in *CBFA1* expression was the lowest of the three groups investigated, nevertheless a significant change exceeding 100 fold was detected after 7 days of directed osteogenic differentiation compared to hEKs nucleofected in the absence of miR-145 inhibitor subjected to the same osteo-induction parameters (Figure 3.53).

An increase in *osteonectin* expression was detected between 14 and 21 days for both miR-145 inhibited hEKs and hMSCs (Figure 3.54). This indicated a shift in expression of early osteogenic transcription factors, such as *CBFA1*, to genes responsible for the induction of terminal functional osteogenesis. This was further emphasised by an increase in *osteocalcin* expression, which is also involved in calcium ion binding and subsequent ossification and matrix mineralisation, detected after 21 days of defined osteogenic differentiation (Figure 3.55).

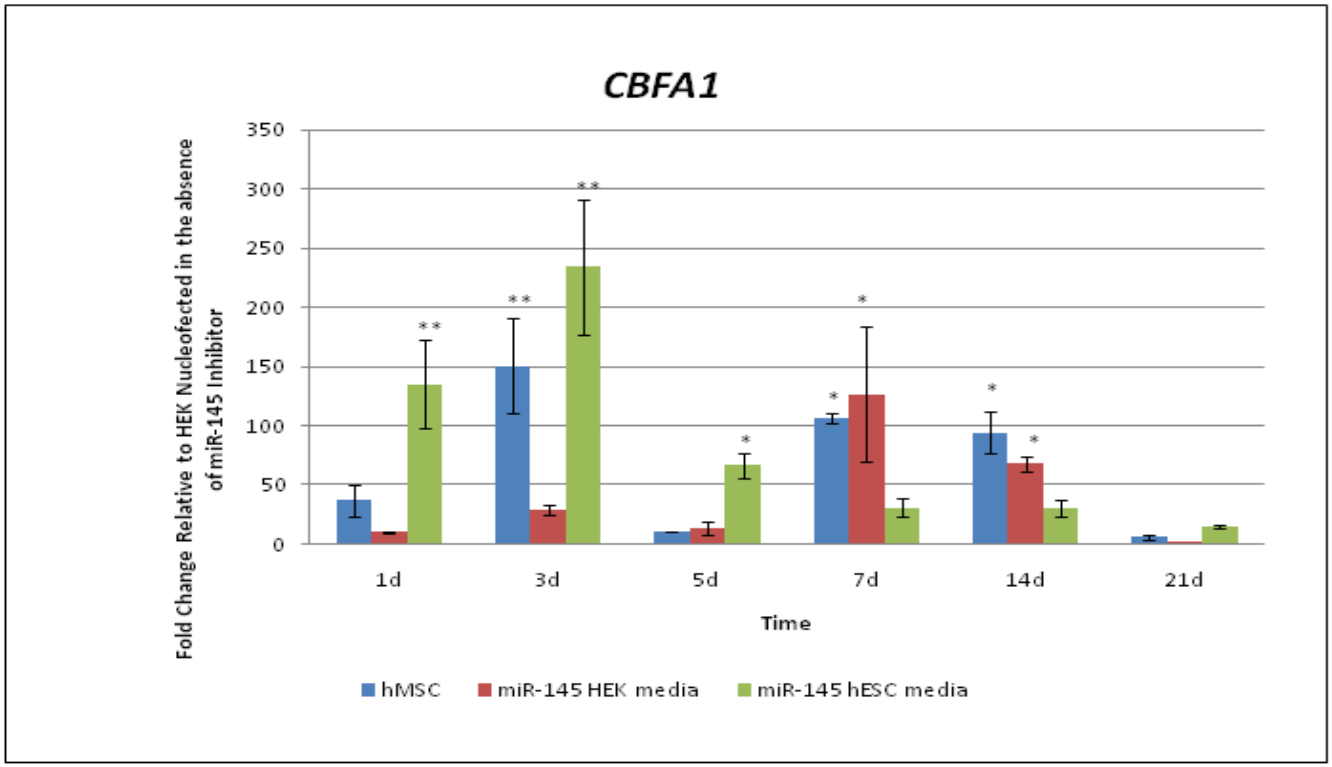

Figure 3.53 qRT-PCR analysis of hEKs nucleofected with miR-145 inhibitor pre-incubated in either hESC or hEK media and hMSCs subjected to defined osteogenic differentiation. Bars represent the mean fold change of *CBFA1* expression relative to hEKs subjected to the same experimental parameters except for miR-145 inhibition, error bars represent the standard error of the mean, n=3. Two-way ANOVA statistical test *p<0.05, **p<0.01

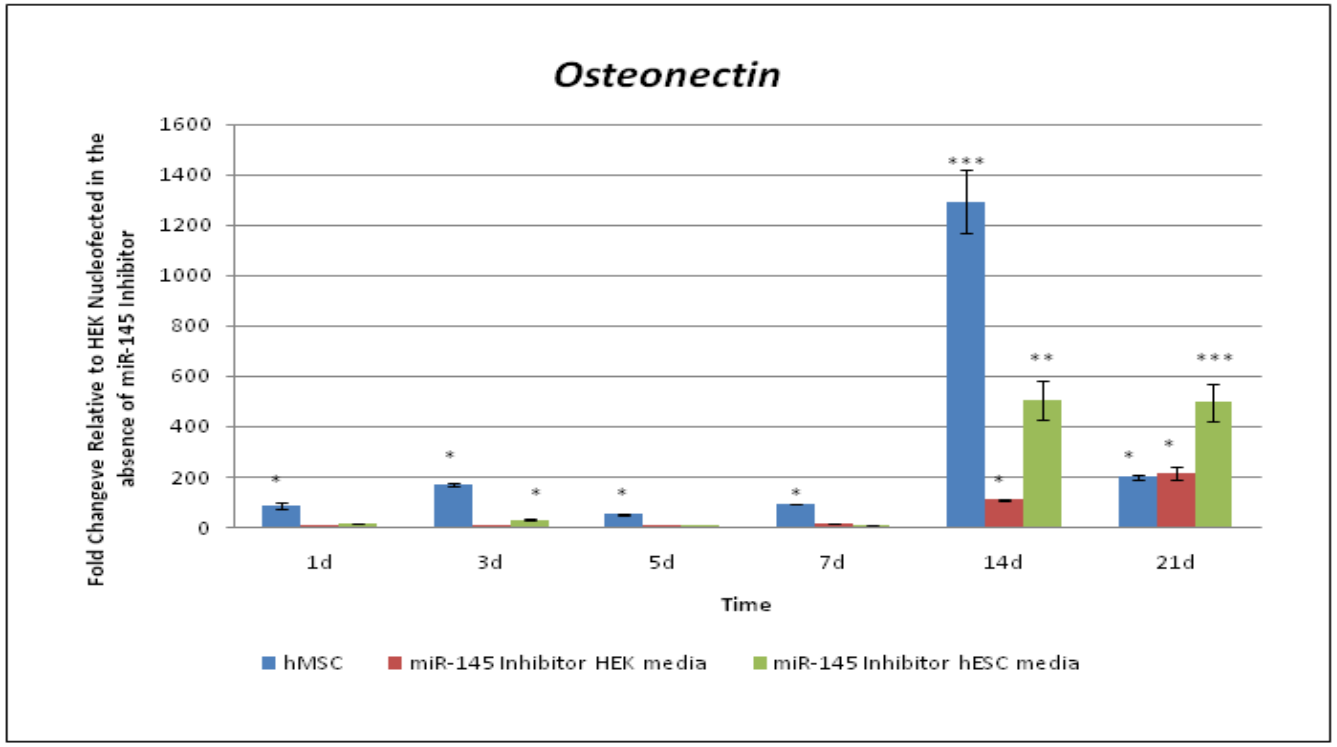

Figure 3.54 qRT-PCR analysis of hEKs nucleofected with miR-145 inhibitor pre-incubated in either hESC or hEK media and hMSCs subjected to defined osteogenic differentiation. Bars represent the mean fold change of *Osteonectin* expression relative to hEKs subjected to the same experimental parameters except for miR-145 inhibition, error bars represent the standard error of the mean, n=3. Two-way ANOVA statistical test *p<0.05, **p<0.01, ***p<0.001

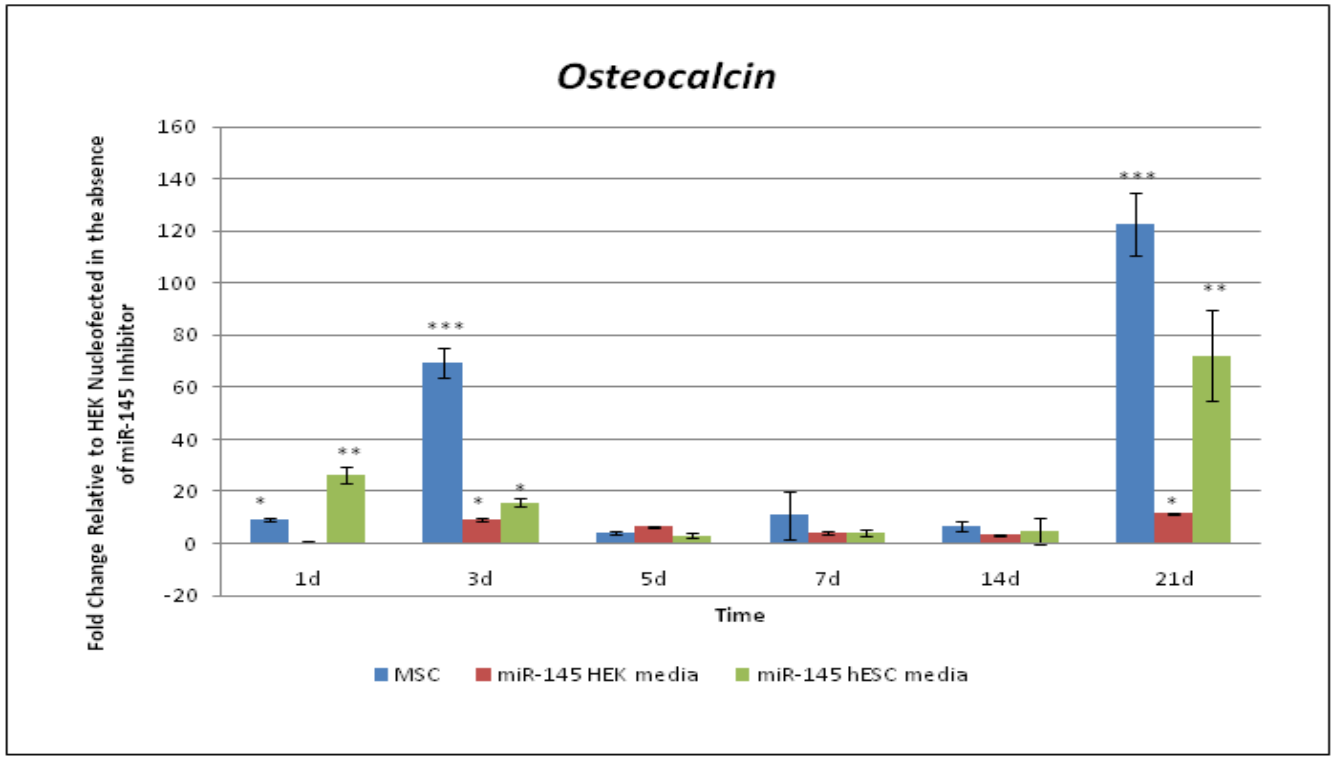

Figure 3.55 qRT-PCR analysis of hEKs nucleofected with miR-145 inhibitor pre-incubated in either hESC or hEK media and hMSCs subjected to defined osteogenic differentiation. Bars represent the mean fold change of *Osteocalcin* expression relative to hEKs subjected to the same experimental parameters except for miR-145 inhibition, error bars represent the standard error of the mean, n=3. Two-way ANOVA statistical test *p<0.05, **p<0.01, ***p<0.001

Following qRT-PCR, amplicons were subject to gel electrophoresis to confirm their identity. All amplicons were represented by a single band ranging between 100-200 bp (Figure 3.56).

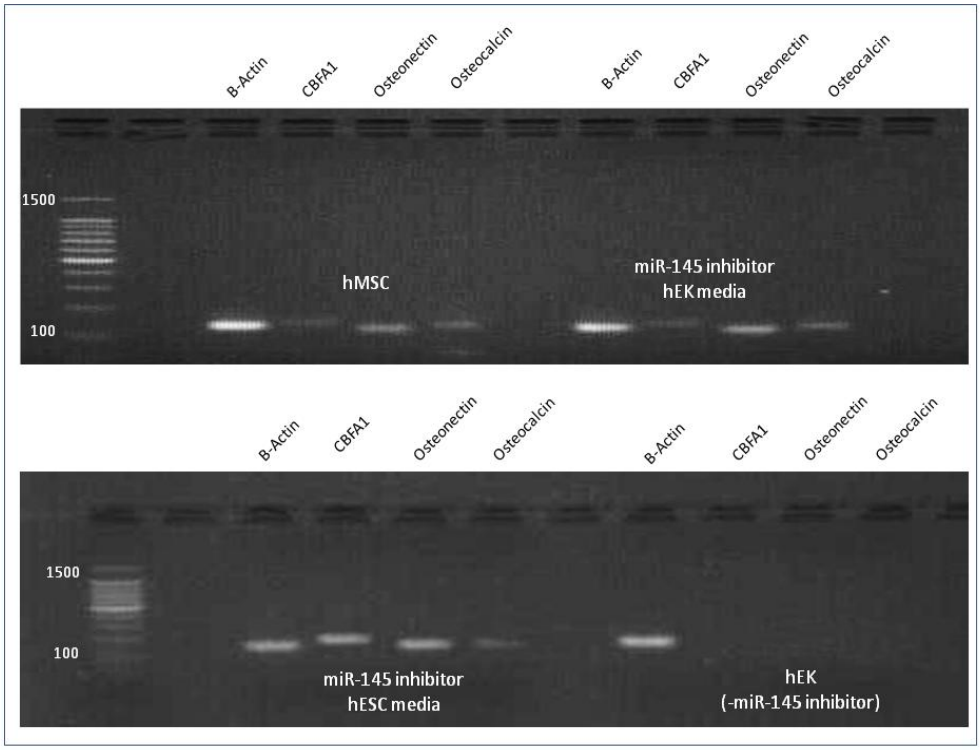

Figure 3.56 Osteogenic PCR product validation. Agarose gel electrophoresis of osteogenic PCR products was performed stained with ethidium bromide and visualised under UV light

3.6.2 Chondrogenic Differentiation

The same transfection variables were introduced to defined chondrogenic differentiation stimuli (Table 2.3). Aggrecan is an early marker of chondrogenic differentiation; 7 days post-chondrogenic induction, aggrecan was clearly observed in most samples with the exception being hEKs that had not received the miR-145 inhibitor prior to chondrogenic differentiation (Figure 3.57).

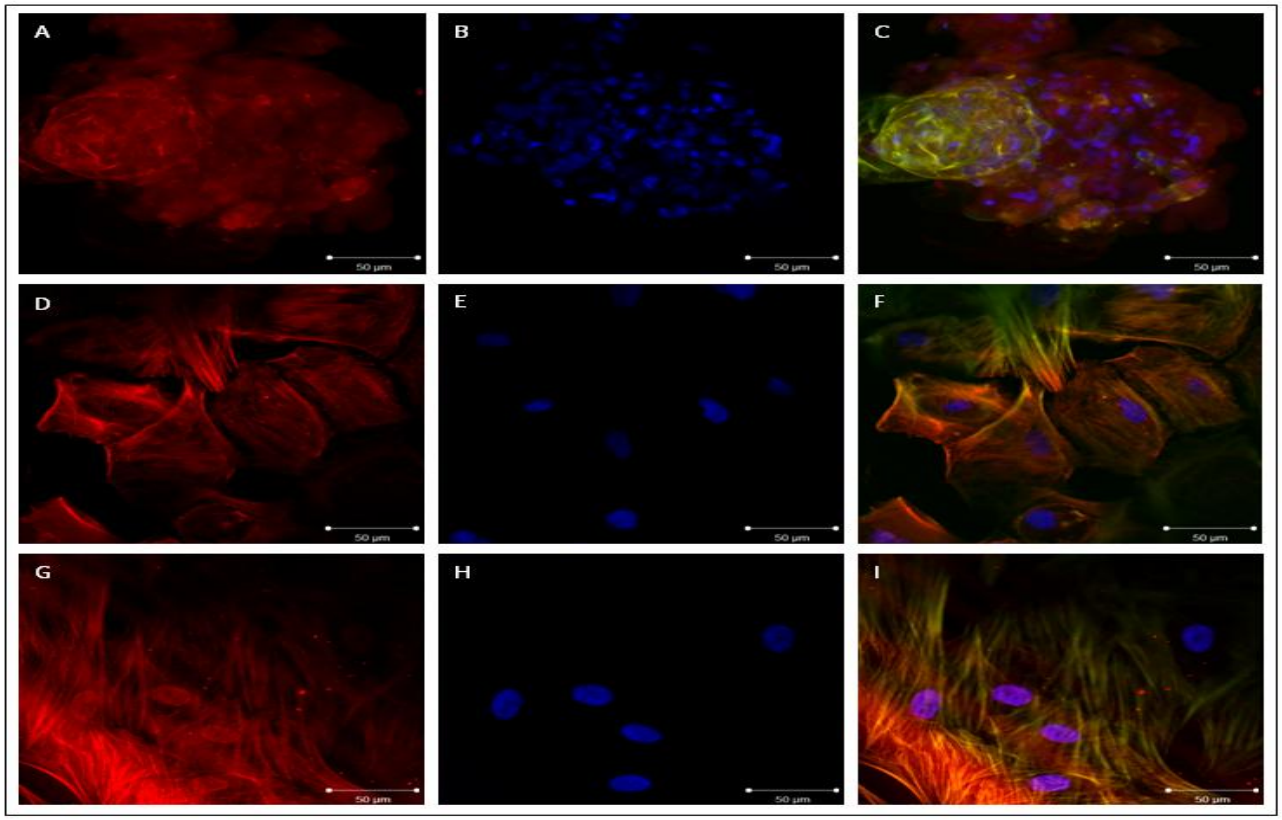

Figure 3.57 Fluorescent microscopic observation of (**A-C**): miR-145 inhibited hEKs pre-incubated in hESC media. (**D-F**): miR-145 inhibited hEKs pre-incubated in hEK media (**G-I**): hMSCs stained for **Aggrecan**, **DAPI**, **F-Actin** after 7 days directed chondrogenic differentiation, scale bar represents 50µm

After 21 days of defined chondrogenic culture immunohistochemical analysis of type II collagen (Col II) was performed. Col II is highly prevalent in chondrocyte ECM occupying 50% total matrix protein and 70-80% total collagen [173]. Immunohistochemistry revealed an abundance of Col II (Figure 3.58).

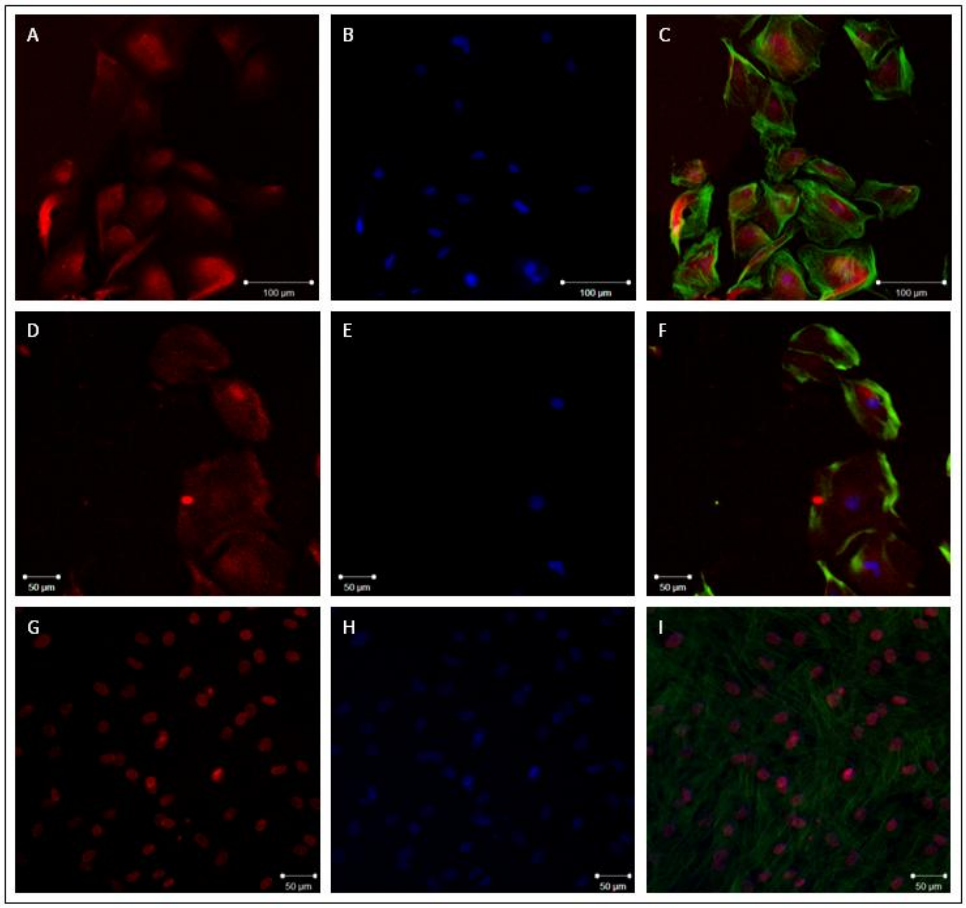

Figure 3.58 Fluorescent microscopic observation of (**A-C**): miR-145 inhibited hEKs pre-incubated in hESC media. (**D-F**): miR-145 inhibited hEKs pre-incubated in hEK media. (**G-I**): hMSCs stained for **Col II**, **DAPI**, **F-Actin** after 21 days of defined chondrogenic stimulation, scale bar represents 100µm (A-C) 50µm (D-H)

Van Gieson staining was performed in order to confirm chondrogenic differentiation histologically (Section 2.8). This protocol stains collagen indicated as pink/red staining shown in Figure 3.59.

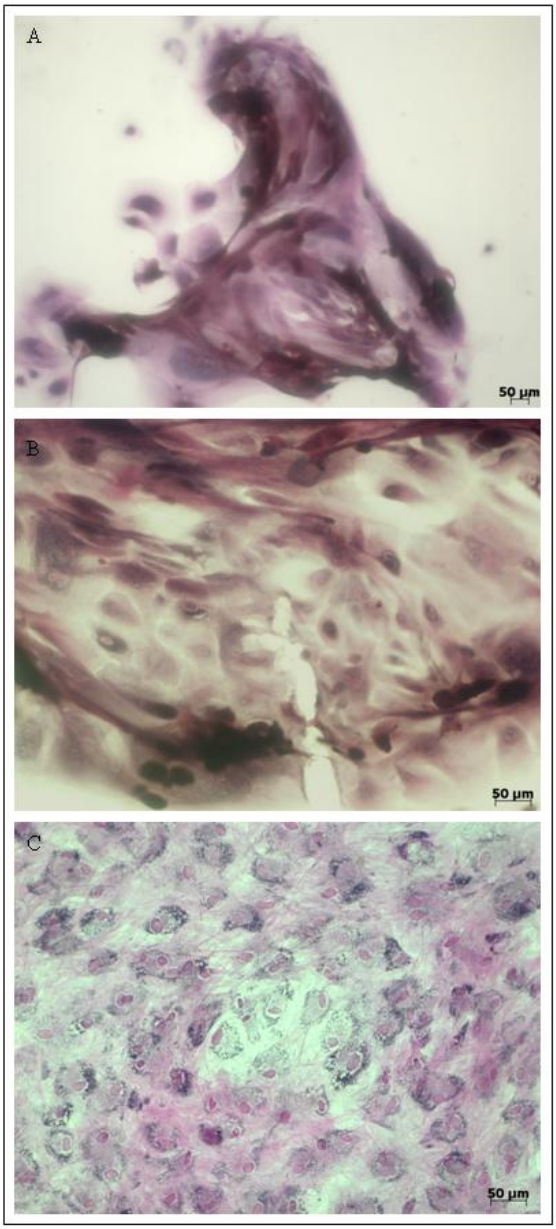

Figure 3.59 Histological observation of Van Gieson staining *in situ* indicating an abundance of collagen after 21 days directed chondrogenic differentiation (**A**): miR-145 inhibited hEKs maintained in hESC media prior to chondrogenic differentiation. (**B**): miR-145 inhibited hEKs maintained in hEK media prior to chondrogenic differentiation. (**C**): hMSCs, scale bar represents 50µm

To gain insight into genomic changes occurring during chondrogenesis, qRT-PCR was performed to investigate Col II gene expression. A significant increase in Col II was detected in hMSCs subject to defined chondrogenic culture with expression reaching a maximum after 21 days (Figure 3.60). Col II expression was also found at high levels where miR-145 inhibited hEKs had been subject to defined chondrogenic differentiation. A significant increase in Col II expression was detected at all time points except for 7 days where miR-145 inhibited hEKs had been pre-incubated in hESC media. Col II expression also significantly increased where miR-145 inhibited hEKs had been pre-incubated in hEK media at days 1 and 14 (Figure 3.61).

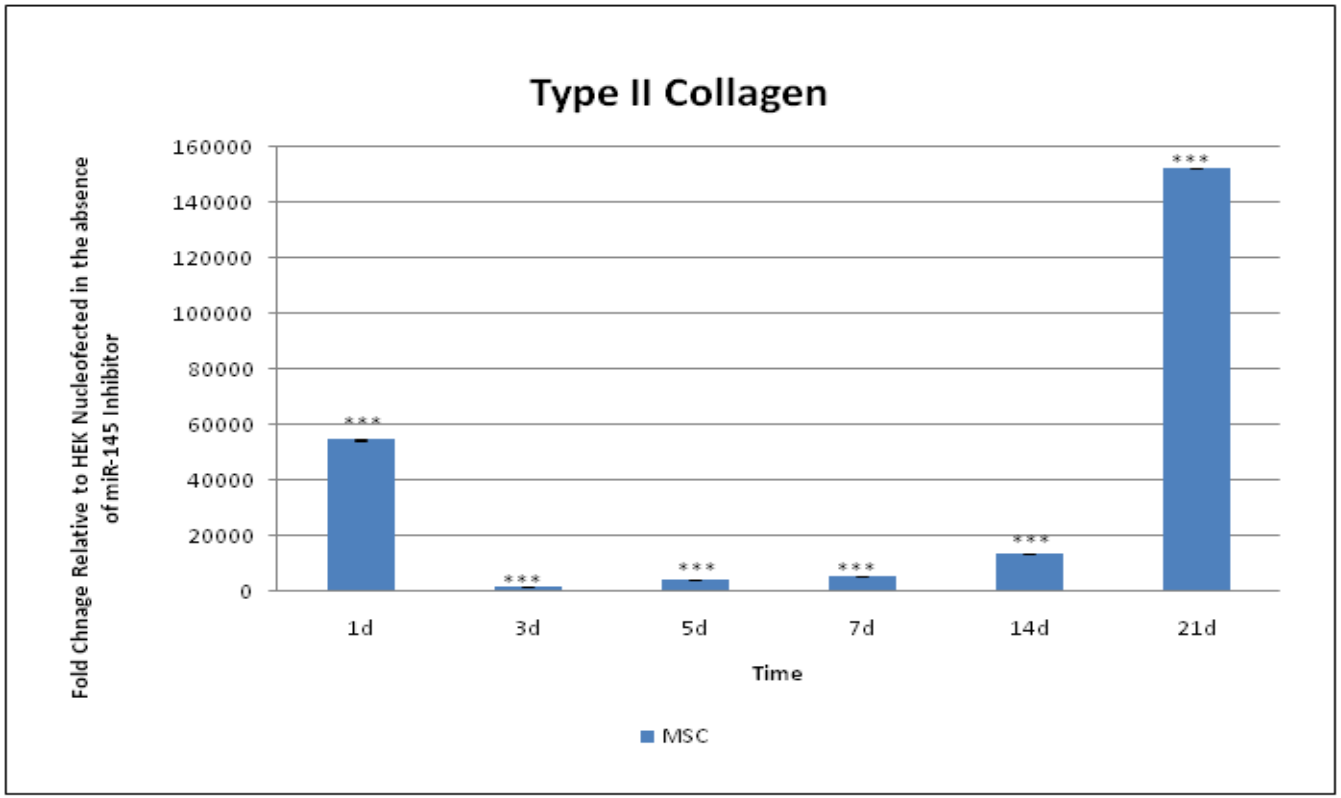

Figure 3.60 qRT-PCR analysis of hMSCs subjected to defined chondrogenic differentiation. Bars represent the mean fold change of hCol II expression relative to hEKs subjected to the same experimental parameters except for miR-145 inhibition, error bars represent the standard error of the mean, n=3. Two-way ANOVA statistical test *p<0.05, **p<0.01, ***p<0.001

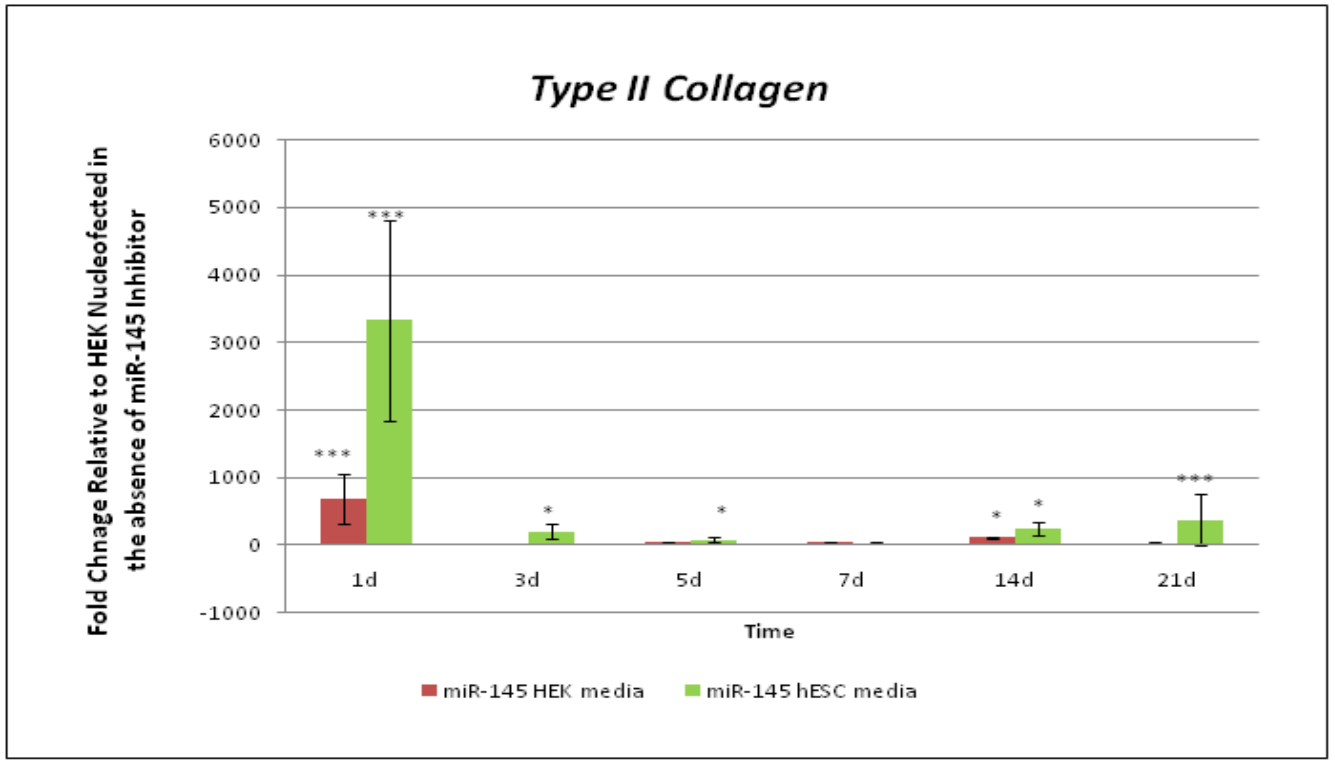

Figure 3.61 qRT-PCR analysis of hEKs nucleofected with miR-145 inhibitor pre-incubated in either hESC or hEK media then subjected to defined chondrogenic differentiation. Bars represent the mean fold change of *hCol II* expression relative to hEKs subjected to the same experimental parameters except for miR-145 inhibition, error bars represent the standard error of the mean, n=3. Two-way ANOVA statistical test *p<0.05, **p<0.01, ***p<0.001

Following qRT-PCR, amplicons were subject to gel electrophoresis to confirm their identity. Together this data provides confirmation of the directed reprogramming of miR-145 inhibited hEKs towards a chondrogenic phenotype (Figure 3.62).

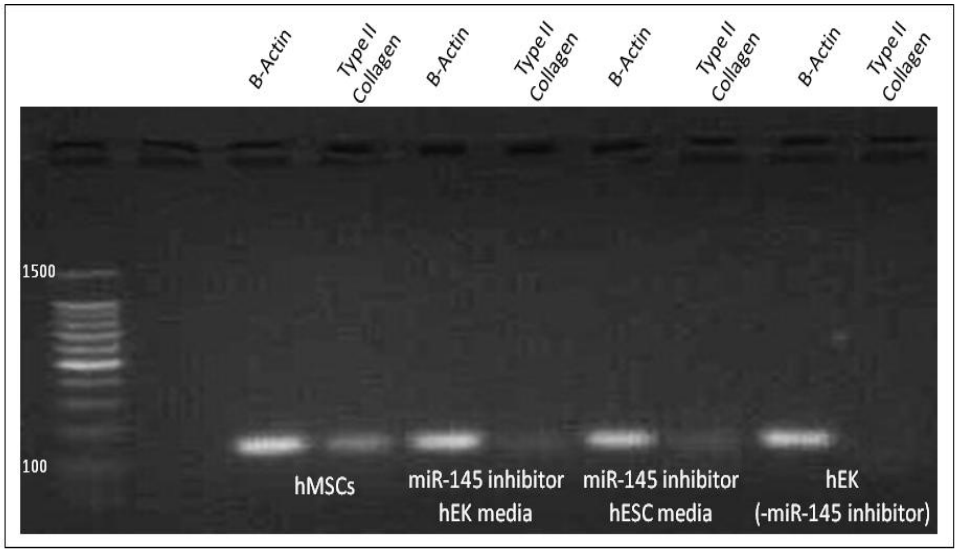

Figure 3.62 Chondrogenic PCR product validation. Agarose gel electrophoresis of chondrogenic PCR products was performed stained with ethidium bromide and visualised under UV light

3.6.3 Adipogenic Differentiation

To complete demonstration that miR-145 inhibited hEKs can be directed through tri-lineage commitment, adipogenic differentiation was conducted by replacing either hEK or hESC media with the adipogenic media (table 2.4), 5 days post-nucleofection with miR-145 inhibitor. In addition to miR-145 inhibited hEKs, hMSCs were also subject to adipogenic differentiation as a positive control. Furthermore hEKs nucleofected in the absence of miR-145 inhibitor prior to adipogenic culture allowed us to establish baseline data.

The gold standard for identifying adipocytes is histological staining with Oil Red O (Section 2.9). Cells were subject to Oil Red O staining throughout the culture period and lipid encapsulation was visualised as early as 3 days post-induction. By day 14 lipid droplets were clearly visible in a large number of cells (Figure 3.63).

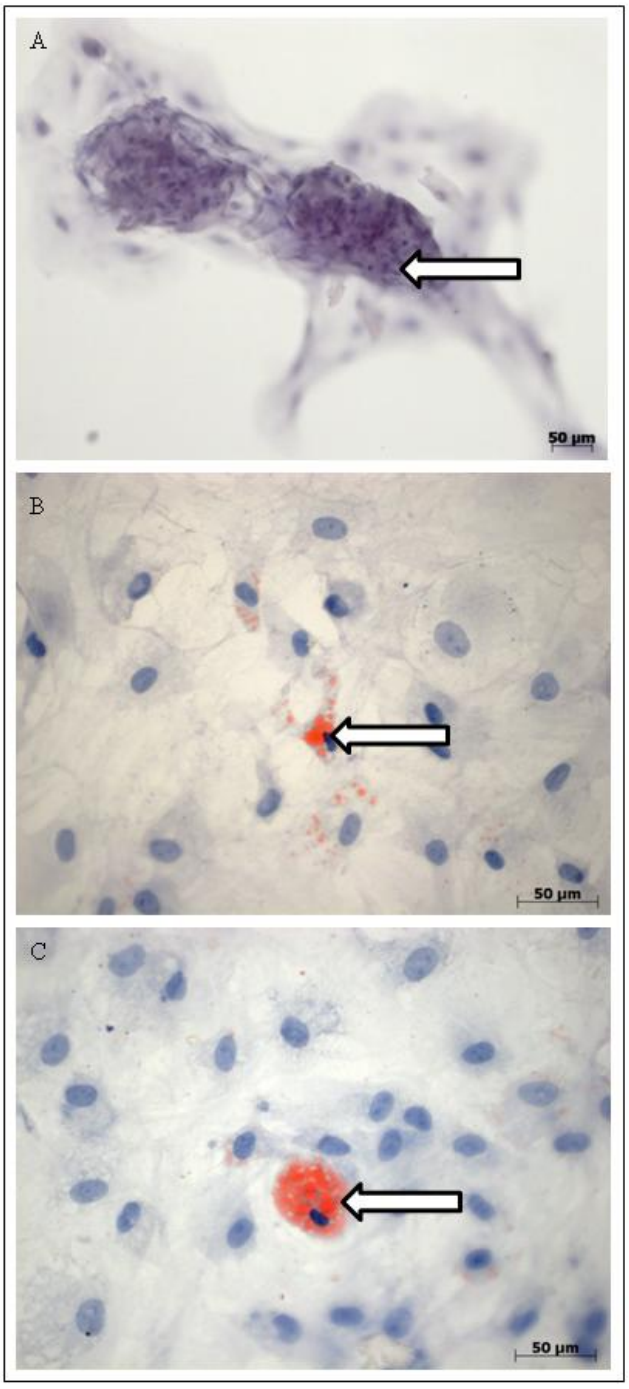

Figure 3.63 Histological observation of Oil Red O staining *in situ* after 14 days directed adipogenic differentiation (**A**): miR-145 inhibited hEKs maintained in hESC media prior to adipogenic differentiation. (**B**): miR-145 inhibited hEKs maintained in hEK media prior to adipogenic differentiation. (**C**): hMSCs, arrows indicate lipid filled vacuoles, scale bar represents 50µm

To identify expression of key adipogenic associated genes, qRT-PCR analysis was also performed. The expression of periosome proliferator-activated receptor γ (PPARγ) was investigated due to the role of this receptor complex in adipogenesis. Activation of PPARγ results in homodimerisation with the retinoid X receptor (RXR) to form a transcription factor complex, which promotes transcription of genes responsible for adipogenic development [174]. Initiation of adipogenesis was therefore characterised by an increase in PPARγ observed after 1 day of adipogenic culture (Figure 3.64). PPARγ was significantly upregulated in the majority of samples with the exception of hEKs nucleofected in the absence of miR-145 inhibitor prior to adipogenic differentiation. PPARγ expression decreased after 1 day in all samples consistent with its role in early adipogenesis.

Adiponectin is abundant in terminal adipose tissue and has a functional role in glucose and lipid metabolism. A significant increase in adiponectin was detected at 1, 5, 7 and 14 days post-adipogenic differentiation, in the case of hMSCs, exceeding 100 fold after 1 day. miR-145 inhibited hEKs pre-incubated in hESC media prior to defined differentiation significantly increased adiponectin expression after 1, 3 and 21 days to a reduced extent with maximum expression at 35 fold after 1 day. Where miR-145 inhibited hEKs had been pre-incubated in hEK media prior to adipogenic differentiation, considerably lower levels of adiponectin were observed peaking after 21 days (Figure 3.65). The levels observed indicated no statistically significant upregulation in adiponectin expression in the case of miR-145 inhibited hEKs pre-incubated in hEK media.

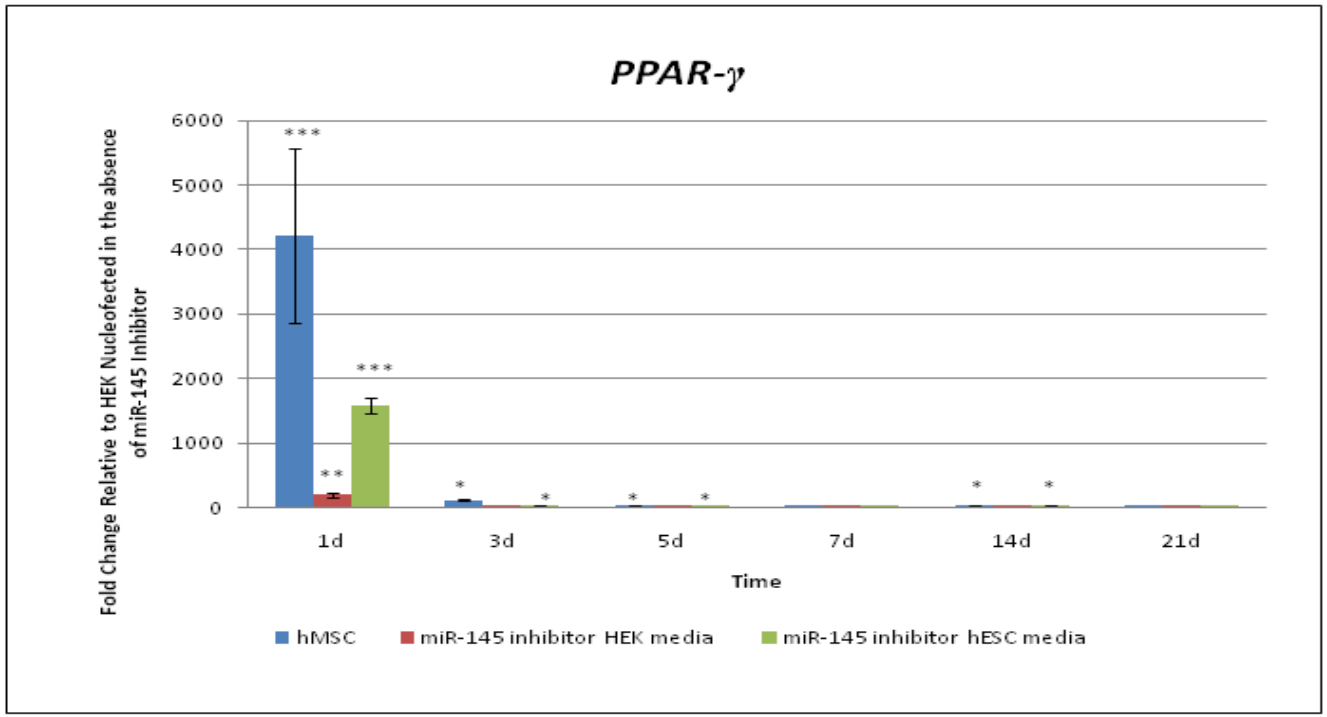

Figure 3.64 qRT-PCR analysis of hEKs nucleofected with miR-145 inhibitor pre-incubated in either hESC or hEK media and hMSCs subjected to defined adipogenic differentiation. Bars represent the mean fold change of *PPARγ* expression relative to hEKs subjected to the same experimental parameters except for miR-145 inhibition, error bars represent the standard error of the mean, n=3. Two-way ANOVA statistical test *p<0.05, **p<0.01, ***p<0.001

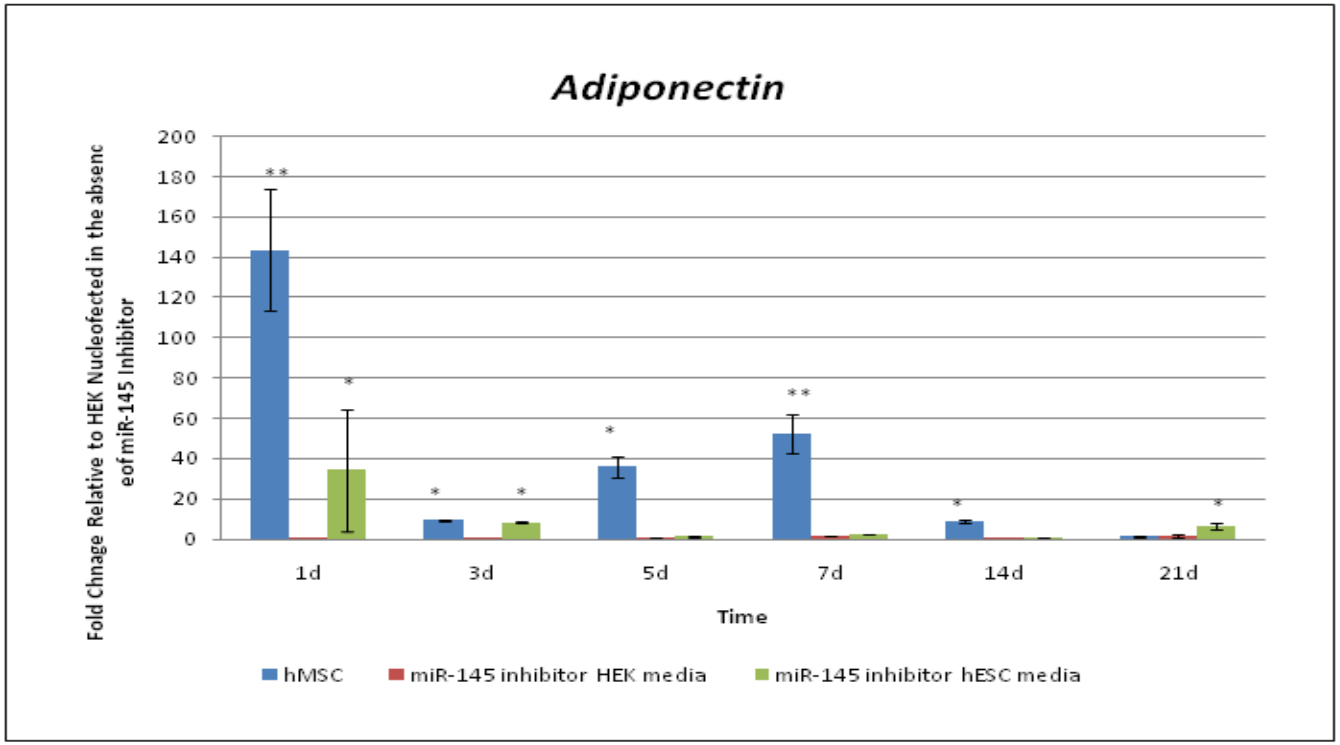

Figure 3.65 qRT-PCR analysis of hEKs nucleofected with miR-145 inhibitor pre-incubated in either hESC or hEK media and hMSCs subjected to defined adipogenic differentiation. Bars represent the mean fold change of *Adiponectin* expression relative to hEKs subjected to the same experimental parameters except for miR-145 inhibition, error bars represent the standard error of the mean, n=3. Two-way ANOVA statistical test *p<0.05, **p<0.01, ***p<0.001

A selection of the amplicons produced from qRT-PCR experiments were subject to gel electrophoresis. Together this data suggests the direct reprogramming of miR-145 inhibited hEKs towards an adipogenic phenotype, with miR-145 inhibited hEKs pre-incubated in hESC media having an increased efficacy compared to miR-145 inhibited hEKs pre-incubated in hEK media (Figure 3.66).

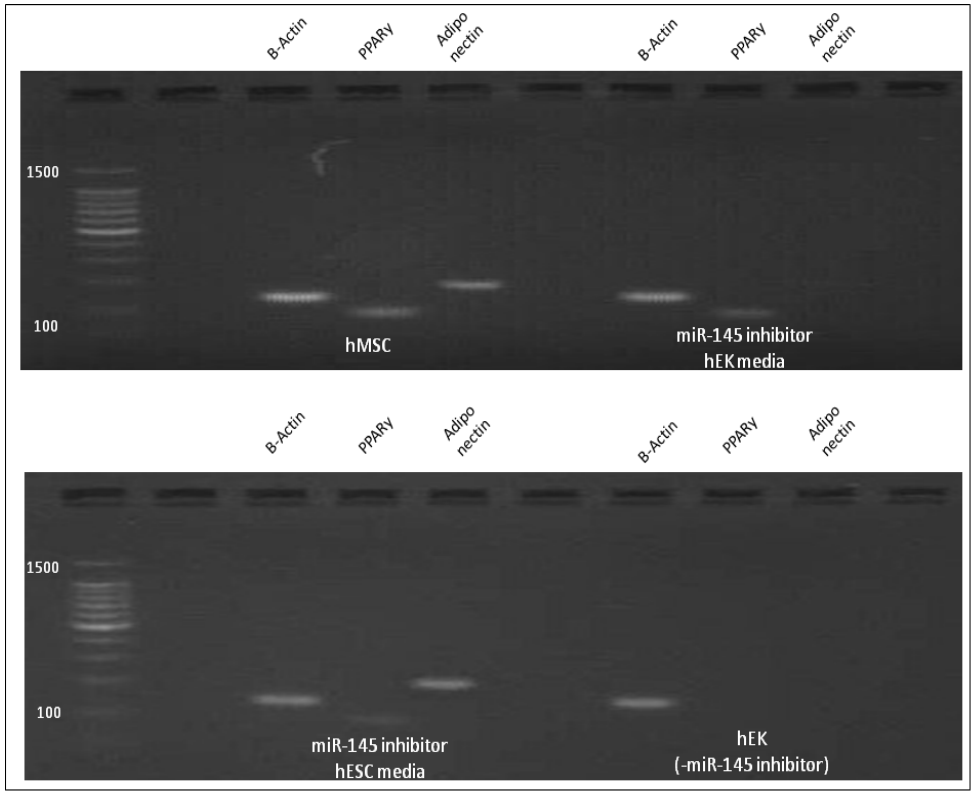

Figure 3.66 Adipogenic PCR product validation. Agarose gel electrophoresis of adipogenic PCR products was performed, stained with ethidium bromide and visualised under UV light

3.6.4 Neurogenic Differentiation

To assess the differentiation potential of miR-145 inhibited hEKs, neural differentiation was selected. Neurogenic differentiation was chosen given the high levels of *Sox2* expressed by miR-145 inhibited hEKs, a master regulator of neural stem cells. In line with previous experiments hEKs were subject to nucleofection with miR-145 inhibitor and cultured in either hEK or hESC media. Basal media was replaced after 5 days with neural differentiation media supplemented with 300ng/mL all-trans retinoic acid to induce neurogenesis.

Nestin was selected as an early marker of neurogenesis, as it is widely regarded as being ubiquitously expressed in neural precursor cells [175]. *Nestin* expression is notoriously transient and due to the rapid switching and termination of translation can often be difficult to detect. Nevertheless *Nestin* was successfully observed in the majority of samples (Figure 3.67), with expression maxima after 3 days for hMSCs and miR-145 inhibited hEKs pre-incubated in hESC media while miR-145 inhibited hEKs pre-incubated in hEK media demonstrated delayed expression after 5 days. The most significant increase in *Nestin* expression was noted for miR-145 inhibited hEKs pre-incubated in hESC media, demonstrating more than 30 fold increase in expression after 3 days neural induction, perhaps not surprising given the increased expression of *Sox2* observed prior to neurogenic induction.

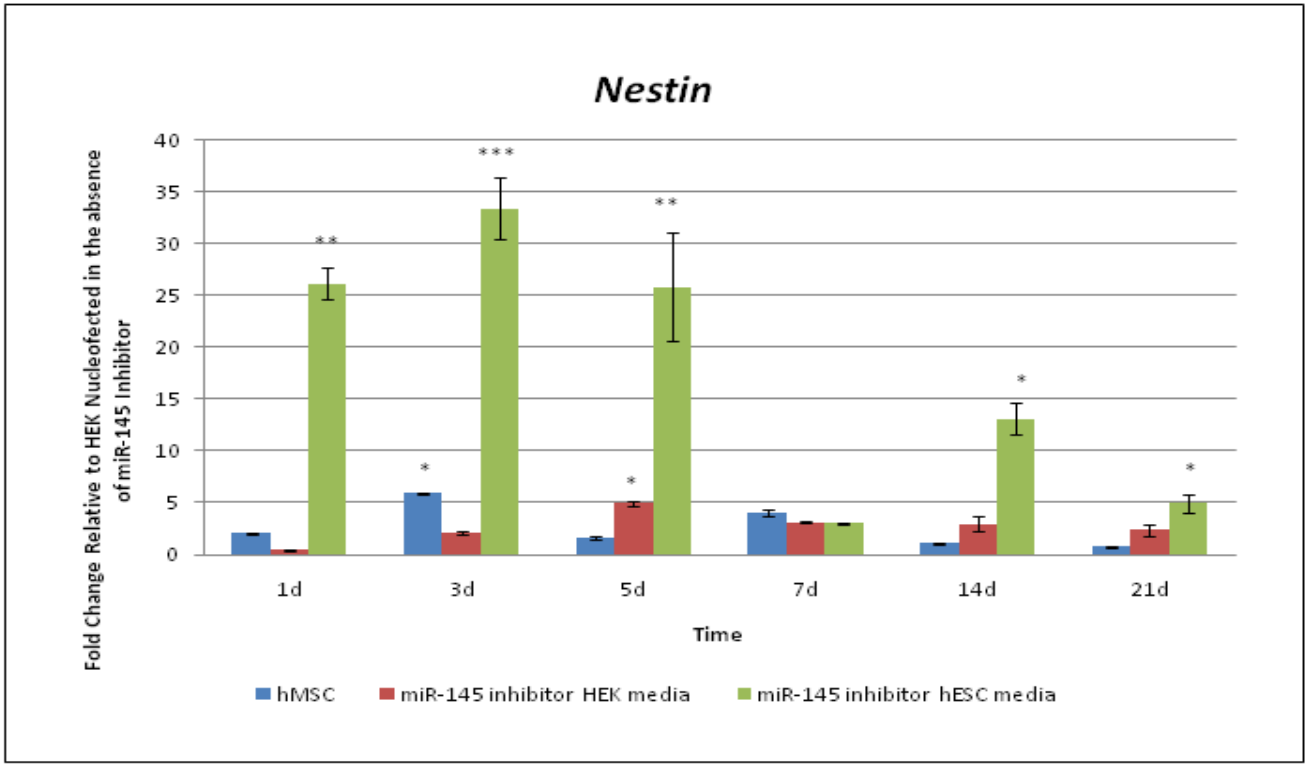

Figure 3.67 qRT-PCR analysis of hEKs nucleofected with miR-145 inhibitor pre-incubated in either hESC or hEK media and hMSCs subjected to defined neurogenic differentiation. Bars represent the mean fold change of *Nestin* expression relative to hEKs subjected to the same experimental parameters except for miR-145 inhibition, error bars represent the standard error of the mean, n=3. Two-way ANOVA statistical test *p<0.05, **p<0.01, ***p<0.001

During neurogenesis *Nestin* is replaced with tissue-specific intermediate filament proteins, such as neurofilament and βIII-tubulin. Immunohistochemistry provided evidence of neurogenesis through detection of neurofilament (Figure 3.68) and βIII-tubulin (Figure 3.69) after 21 days of defined neural differentiation. The expression of neurofilament was confirmed using qRT-PCR, which showed significant elevation of this gene between 14 and 21 days post-neurogenic differentiation in all cases (Figure 3.70).

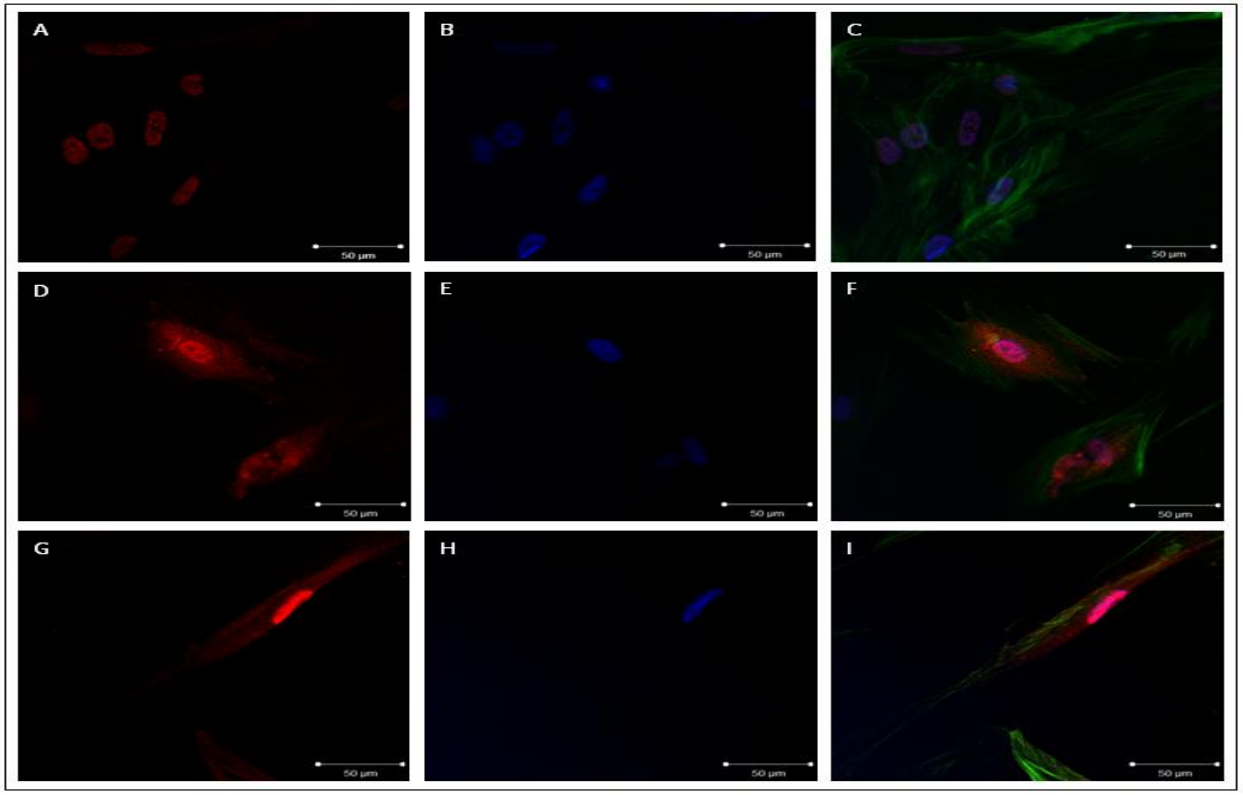

Figure 3.68 Fluorescent microscopic observation of hEKs after 21 days of defined neurogenic stimulation. (**A-C**): miR-145 inhibited hEKs pre-incubated in hESC media. (**D-F**): miR-145 inhibited hEKs pre-incubated in hEK media. (**G-I**): hMSCs **Neurofilament**, **DAPI**, **F-Actin**, scale bar represents 50µm

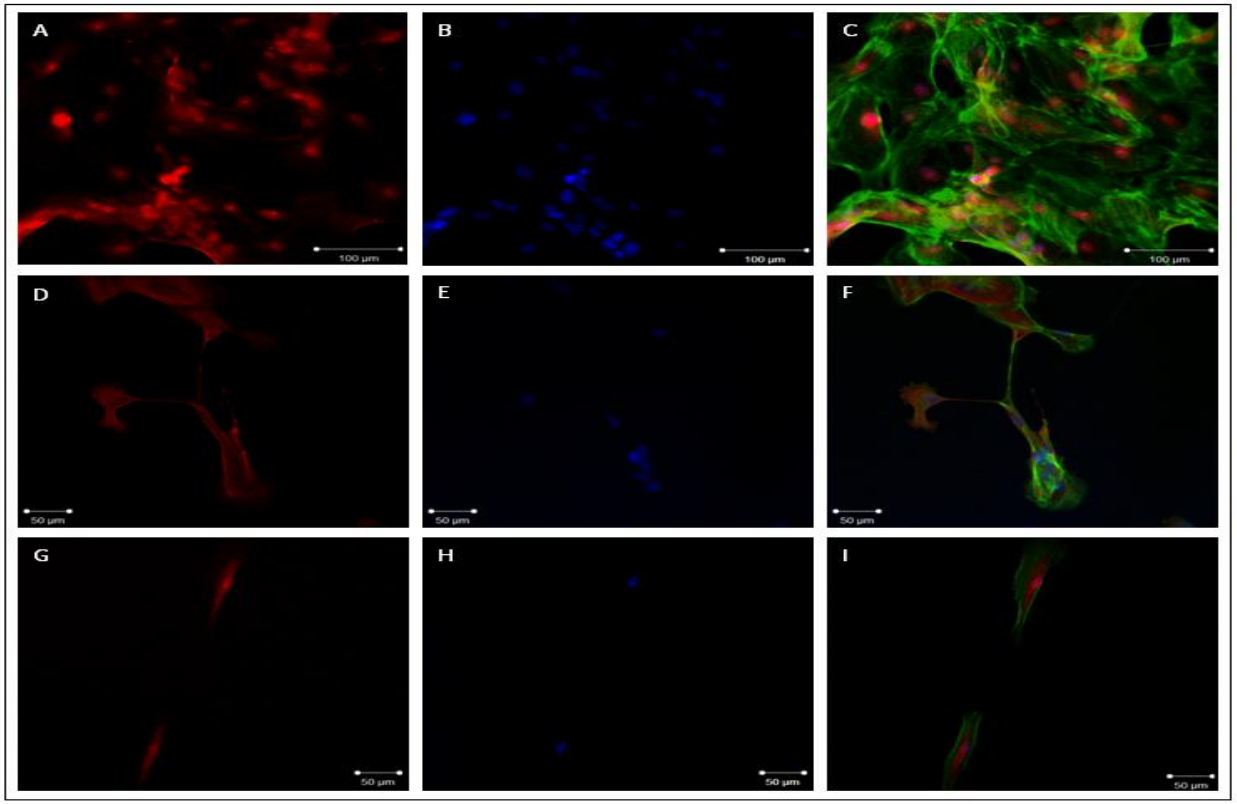

Figure 3.69 Fluorescent microscopic observation of hEKs after 21 days of defined neurogenic stimulation. (**A-C**): miR-145 inhibited hEKs pre-incubated in hESC media. (**D-F**): miR-145 inhibited hEKs pre-incubated in hEK media. (**G-I**): hMSCs **βIII tubulin**, **DAPI**, **F-Actin**, scale bar represents 50µm

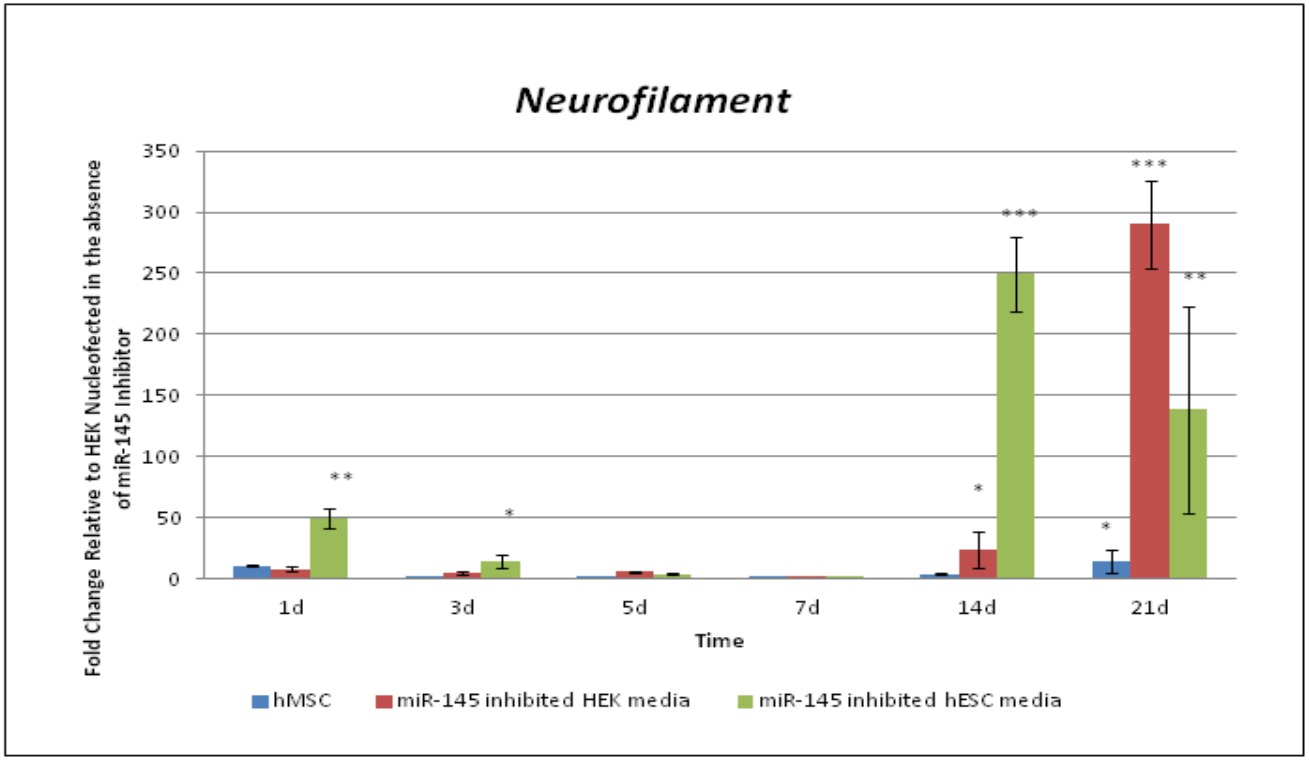

Figure 3.70 qRT-PCR analysis of hEKs nucleofected with miR-145 inhibitor pre-incubated in either hESC or hEK media and hMSCs subjected to defined neurogenic differentiation. Bars represent the mean fold change of *Neurofilament* expression relative to hEKs subjected to the same experimental parameters except for miR-145 inhibition, error bars represent the standard error of the mean, n=3. Two-way ANOVA statistical test *p<0.05, **p<0.01, ***p<0.001

Appropriate wells were selected following qRT-PCR and amplified products subjected to gel electrophoresis to confirm their identity. Together this data provides confirmation of the directed reprogramming of miR-145 inhibited hEKs towards a neurogenic phenotype (Figure 3.71).

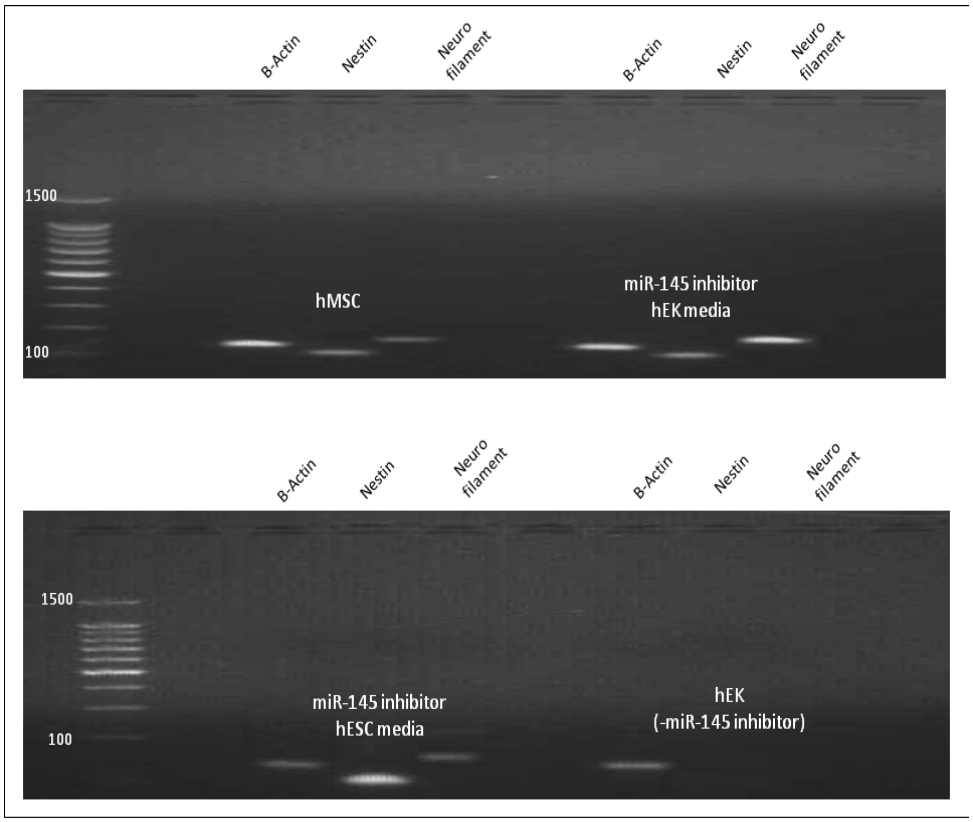

Figure 3.71 Neurogenic PCR product validation. Agarose gel electrophoresis of neurogenic PCR products, stained with ethidium bromide and visualised under UV light

3.7 Ectopic Bone Formation Model

We hypothesised that miR-145 inhibited hEKs, which demonstrated osteogenic differentiation *in vitro,* could differentiate to a functional osteoblast lineage *in vivo* and when delivered with an appropriate scaffold give rise to ectopic mineralised tissue.

One group of polymeric materials, which has shown excellent promise in the field of biomaterials and regenerative medicine, are hydrogels. Hydrogels are a class of hydrophilic cross-linked polymers, produced from either organic or inorganic components. Foremost, this class of materials is renowned for their cellular compliance, in the case of proteinaceous hydrogels, providing a matrix mimetic substrate on which primary cells can adhere and proliferate [176]. Additionally, hydrogels can be delivered via minimally invasive procedures in a liquid phase, often engineered to use a patient's autologous physiology to facilitate gellation, allowing scaffold assembly *in situ* [177].

Therefore for the purpose of this investigation we adopted a host-derived blood plasma approach to generate a completely autologous matrix for cell delivery and expansion, which is able to overcome the post-surgical complications associated with a lack of scaffold histocompatibility [178]. The exogenous array of growth factors, cytokines and other regulatory peptides found within plasma removes the dependency on xenogenic animal serum from the cell culture matrix.

3.7.1 Validation of PPP-Hydrogel for Maintenance of Pluripotency

HESCs were chosen as a candidate for the validation of a PPP-derived hydrogel as a supportive matrix for the maintenance of a pluripotent, self-renewing phenotype. Expansion and phenotype of hESCs has conventionally been maintained though co-culture with feeder cells, typically MEFs [179]. While MEFs provide contact signalling and secreted solutes, which hESCs require to expand and self renew, this method is a double edged sword exposing hESCs to potential xeno-contaminants. Ideally pharmacopeia-grade hESCs should be maintained in xeno-free culture using materials of human or completely synthetic origin in order to increase their clinical potential. Therefore this PPP-derived hydrogel derived in conjunction with chemically defined medium, would be particularly attractive to cell based therapies. To validate whether a PPP hydrogel was able to maintain a pluripotent self-renewing phenotype, hESCs were taken from passage 8 and embedded within a 4mm hydrogel layer at a density of $5.0x10^3$cells/cm^2. HESCs were also maintained on TCP coated with 5µg/mL of hFN and maintained using the same media formulation detailed in section 2.1.2 as a positive control.

A fundamental feature of any culture system is its cytocompatibility, therefore to validate whether the hydrogel was able to provide an environment capable of maintaining cell viability a live/dead assay was performed. To confirm whether components of this assay were first able to diffuse throughout the hydrogel to successfully interact with the cells encapsulated within, a control was established whereby hESCs embedded within the hydrogel were subject to 70% ethanol for 10 minutes, at room temperature, inducing cell death. Upon staining, hESCs were found to exclusively fluoresce red (Ex510, Em595) indicating that the hydrogel permits diffusion of assay reagents. Viability tests confirmed that hESCs

cultured within PPP-derived hydrogel remained viable after 72 hours in culture (Figure 3.72).

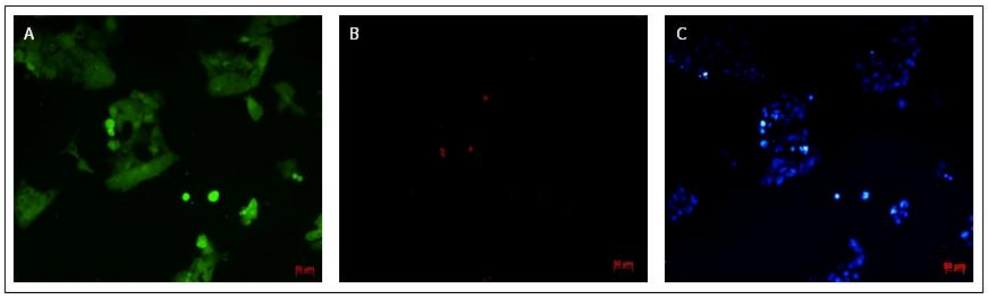

Figure 3.72 Cytotoxicity of PPP-derived hydrogel. Live/dead staining of hESCs embedded within PPP-derived hydrogel after 72 hours in culture A: Live cells. B: Dead cells. C: Nuclei, same field of view. Scale bar represents 50µm

Undifferentiated hESCs typically exhibit a high nucleus to cytoplasm ratio and form tightly packed colonies. hESCs embedded within the hydrogel were observed to proliferate and successfully formed colonies displaying typical hESC morphology. Expansion of hESC populations continued until reaching confluency after 72 hours (Figure 3.73).

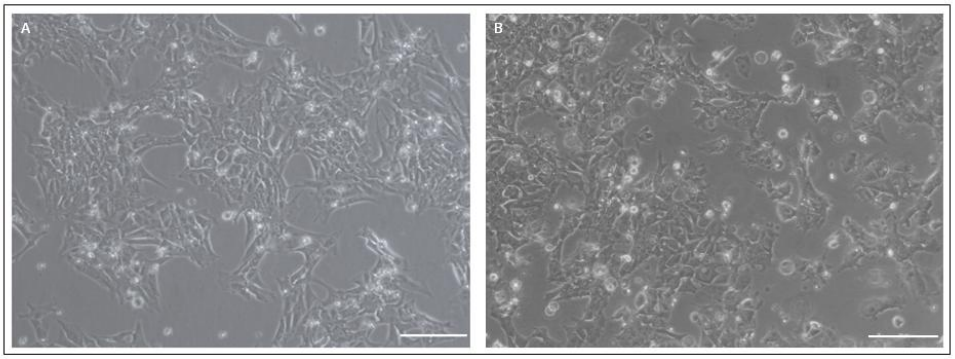

Figure 3.73 Cell morphology of hESCs maintained under PPP-hydrogel conditions. Phase contrast light microscopic observation of hESCs after 72 hours of culture **A**: hFN. **B**: PPP-derived hydrogel. Scale bars represent 200µm

This confirmed that PPP hydrogel was capable of maintaining hESC expansion. While morphological analysis of hESCs embedded within the hydrogel suggested hESCs remained undifferentiated, to confirm this observation immunohistochemistry was performed. Transcription factors *Oct4*, *Nanog* and *Sox2*, all of which are typically expressed by hESCs in standard culture [58, 180, 181] were selected as indicators of pluripotency. After 72 hours in culture, all nuclear transcription factors were clearly identified in all experimental samples after 10 passages (Figure 3.74).

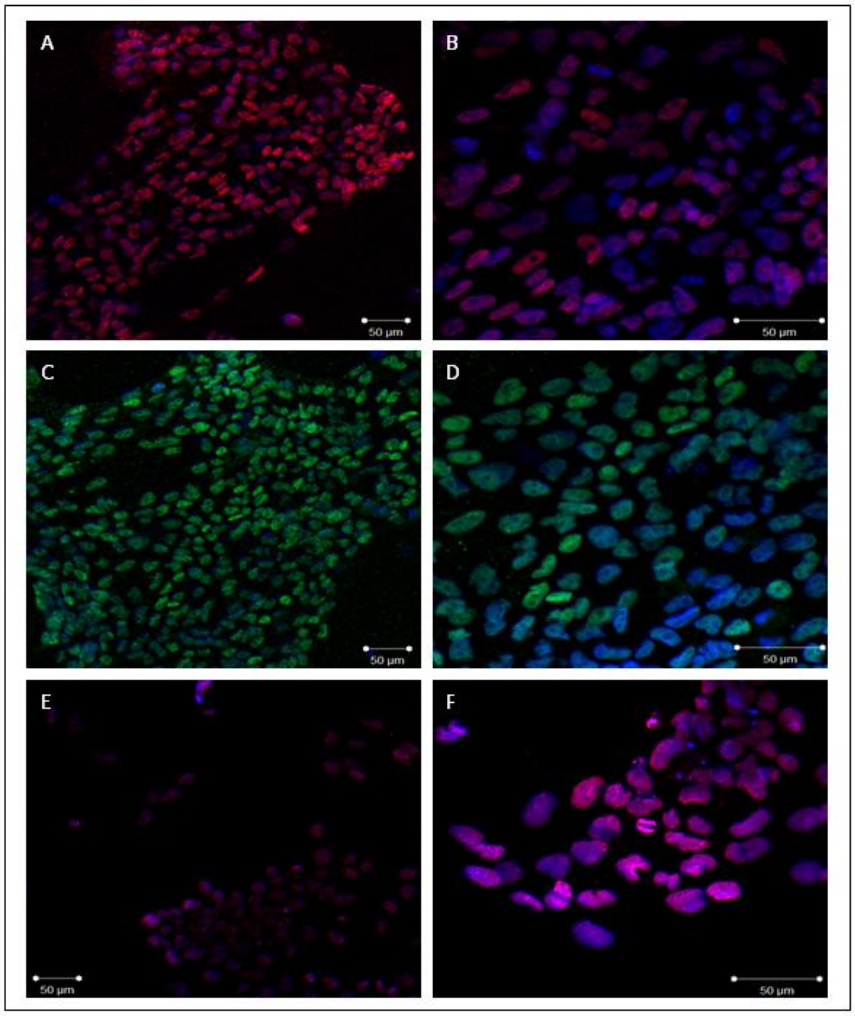

Figure 3.74 Fluorescent microscopic observation of hESCs stained within PPP hydrogel after 10 passages. **A-B** **Oct4**, **DAPI**. **C-D** **Nanog**, **DAPI**. **E-F** **Sox2**, **DAPI** Scale bars represent 50µm

Expression of pluripotency markers *Oct4*, *Nanog* and *Sox2*, were also analysed up to 10 passages using qRT-PCR. Significant levels of each of these markers were identified for hESCs maintained on hFN or embedded within PPP-derived hydrogels. The expression of Oct4, Nanog and Sox2 was comparable over a number of passages with no significant difference in expression (Figures 3.75 - 3.77).

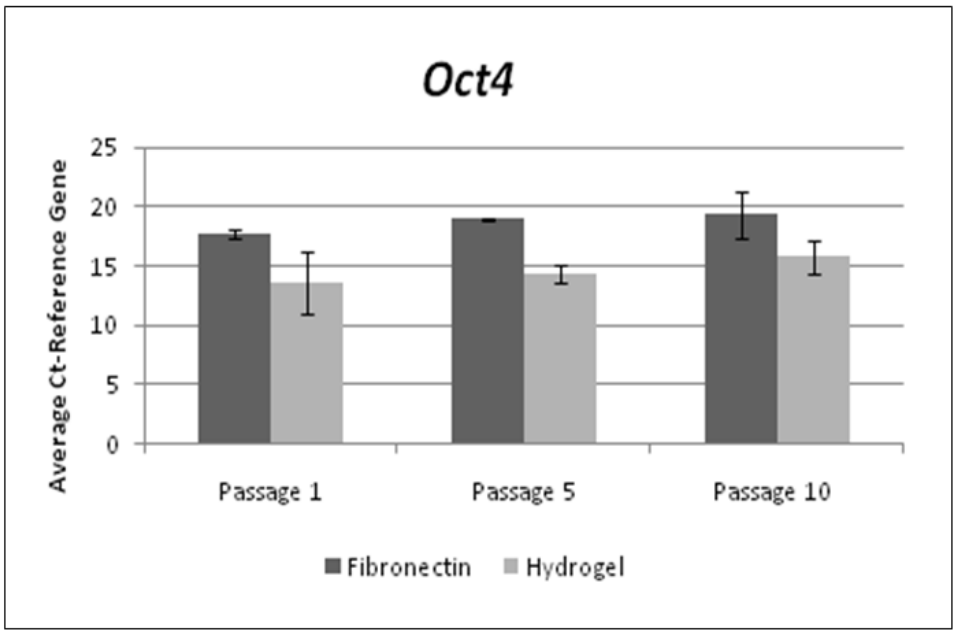

Figure 3.75 qRT-PCR analysis of hESC maintained under PPP-derived hydrogel conditions. Bars represent the mean fold change of *Oct4* expression relative to hESCs maintained on hFN, error bars represent the standard error of the mean, n=3

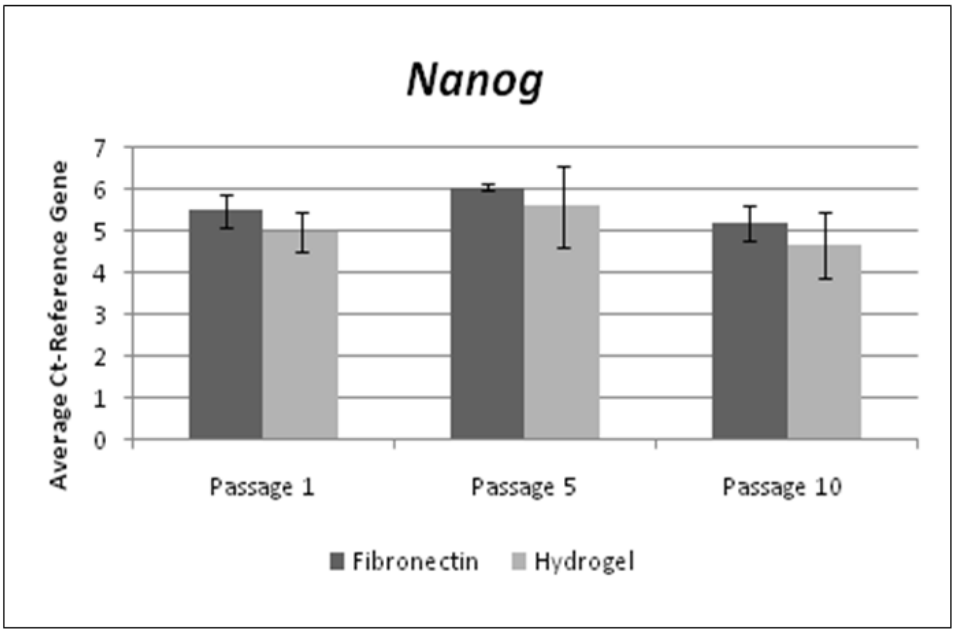

Figure 3.76 qRT-PCR analysis of hESC maintained under PPP-derived hydrogel conditions. Bars represent the mean fold change of *Nanog* expression relative to hESCs maintained on hFN, error bars represent the standard error of the mean, n=3

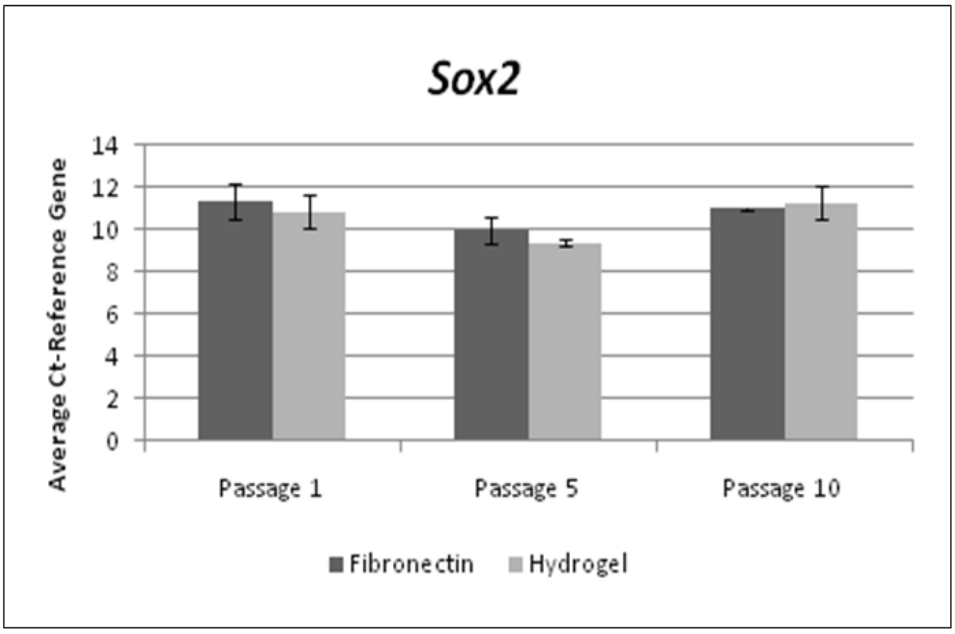

Figure 3.77 qRT-PCR analysis of hESC maintained under PPP-derived hydrogel conditions. Bars represent the mean fold change of *Sox2* expression relative to hESCs maintained on hFN, error bars represent the standard error of the mean, n=3

To establish whether this matrix was capable of maintaining hESC phenotype over an extended period of culture, hESCs embedded within the PPP hydrogel construct were cultured through 25 passages (section 2.1.2). No changes in morphology, viability or phenotype were observed over the extended culture period thus the ability of the PPP-hydrogel to maintain undifferentiated expansion of hESCs *in vitro* was confirmed (Figure 3.78).

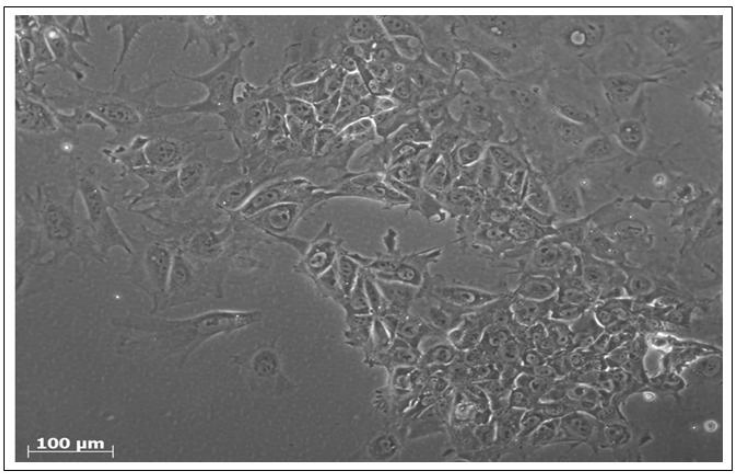

Figure 3.78 Long-term maintenance of hESCs using PPP-derived hydrogel system. Phase contrast microscopic observation of hESCs after 10 passages cultured within the PPP-derived hydrogel

Teratomas were induced 6 weeks post-injection and observed both macroscopically and microscopically following H&E staining of explanted tissue. Structures derived from all three germ layers of the developing organism were identified, confirming that the hESCs maintain their differentiation potential when maintained within this PPP-derived hydrogel (Figure 3.79).

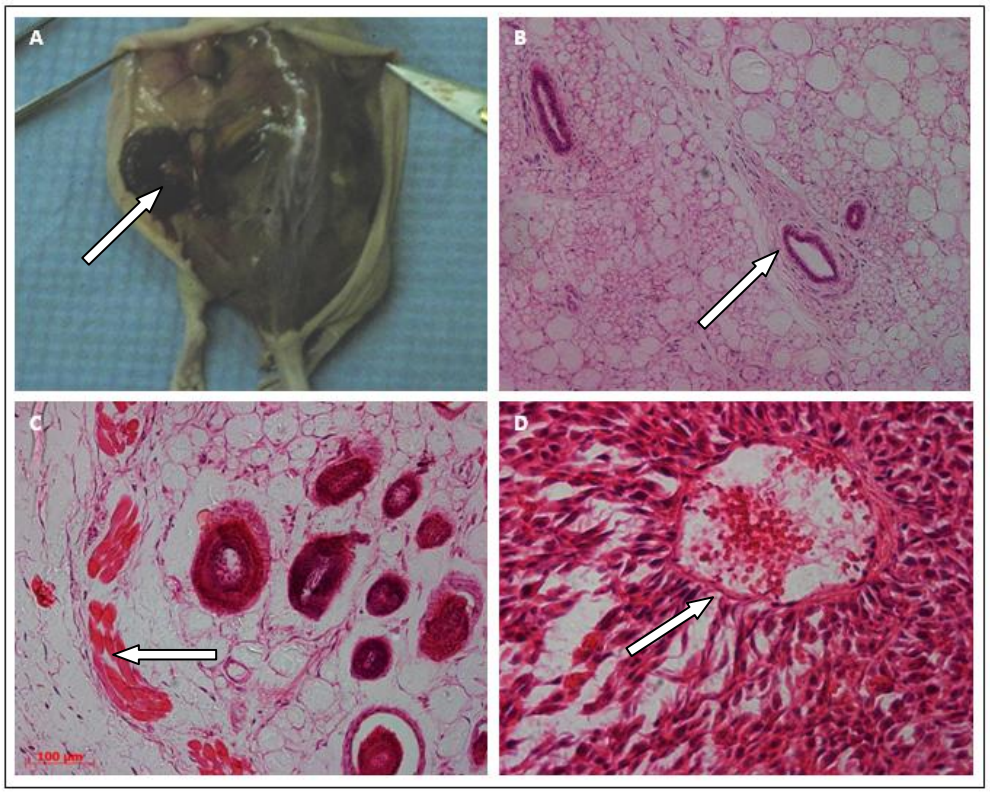

Figure 3.79 Teratoma formation indicates differentiation into derivatives of the three germ layers. A: Macroscopic observation of teratoma formation. B: Endoderm (arrow indicates glandular structure) C: Mesoderm and ectoderm (black arrow indicates myofibres and white arrow hair follicle) . D: Mesoderm (arrow indicates blood vessel.

3.6.2 Validation of Hydroxyapatite Hydrogel

To investigate whether reprogrammed hEKs were capable of differentiating towards osteogenic lineages *in vivo* an ectopic bone formation model was designed to include the incorporation of hydroxyapatite (HA) in order to promote osteogenesis. To determine an appropriate concentration HA to incorporate into PPP hydrogels, concentrations ranging from 0.5% to 10% (w/v) were prepared and gellation time monitored. Stable hydrogel formation was concluded when the polymeric solution no longer flowed when inverted.

Hydrogels infused with 0.5% to 1% HA formed stable hydrogels when incubated at 37°C after 5 minutes while an increased concentration of 3% HA resulted in an increased gellation time of 10 minutes. Higher HA concentrations of 5% and 10% took significantly longer to gellate with hydrogel formation occurring after 20 and 30 minutes respectively. The increase in gellation time correlated with an increase in HA concentration, which is unusual as it was hypothesised that the abundance of calcium in HA would decrease gellation time however this may be ascribed to HA intervening in the crosslinking process thus weakening this process. As gellation should occur at a sufficiently rapid rate for clinical use concentrations ranging from 3% to 10% were eliminated.

Prior to delivery hydrogels infused with 0.5% to 1% HA were compared by performing an *in vitro* cytocompatibility test. hMSCs were embedded within the HA-hydrogels at a density of $1x10^4$ cells per mL of HA-hydrogel suspension and incubated at 37°C, 5% CO_2. Viability was evaluated using a live/dead cytotoxicity assay at 1, 3 and 5 days.

Viability after 1 day embedded within the hydrogel appeared to favour a HA concentration of 0.5% over 1% HA and HA-free hydrogels (Figure 3.80).

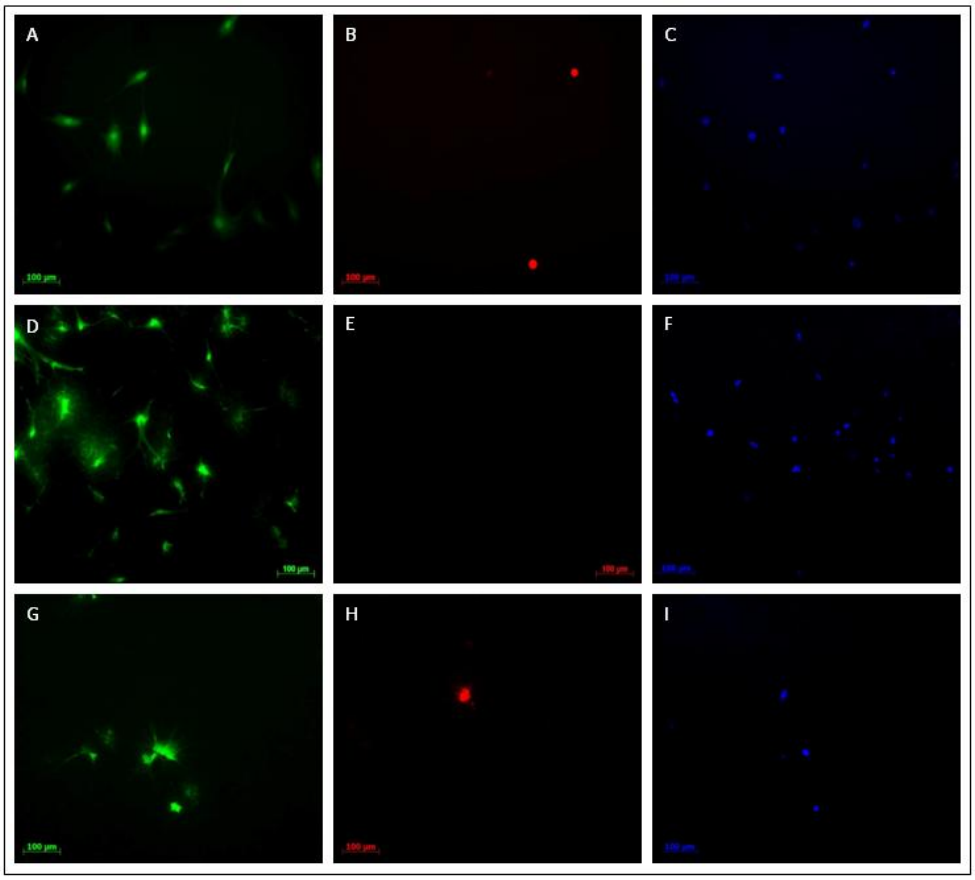

Figure 3.80 Fluorescent microscopic observation of **live**, **dead,** **nuclei** hMSCs after 24 hours of culture, embedded in PPP-derived hydrogel (**A-C**) HA-free. (**D-F**): 0.5% HA. (**G-I**): 1% HA

Upon maintaining hMSCs for a further 2 days it was possible to observe an increase in viable cells within all hydrogel constructs. In terms of the number of dead cells the 0.5% hydrogel appeared superior with a noticeable reduction in the number of dead cells compared to 1% and HA-free hydrogels (Figure 3.81).

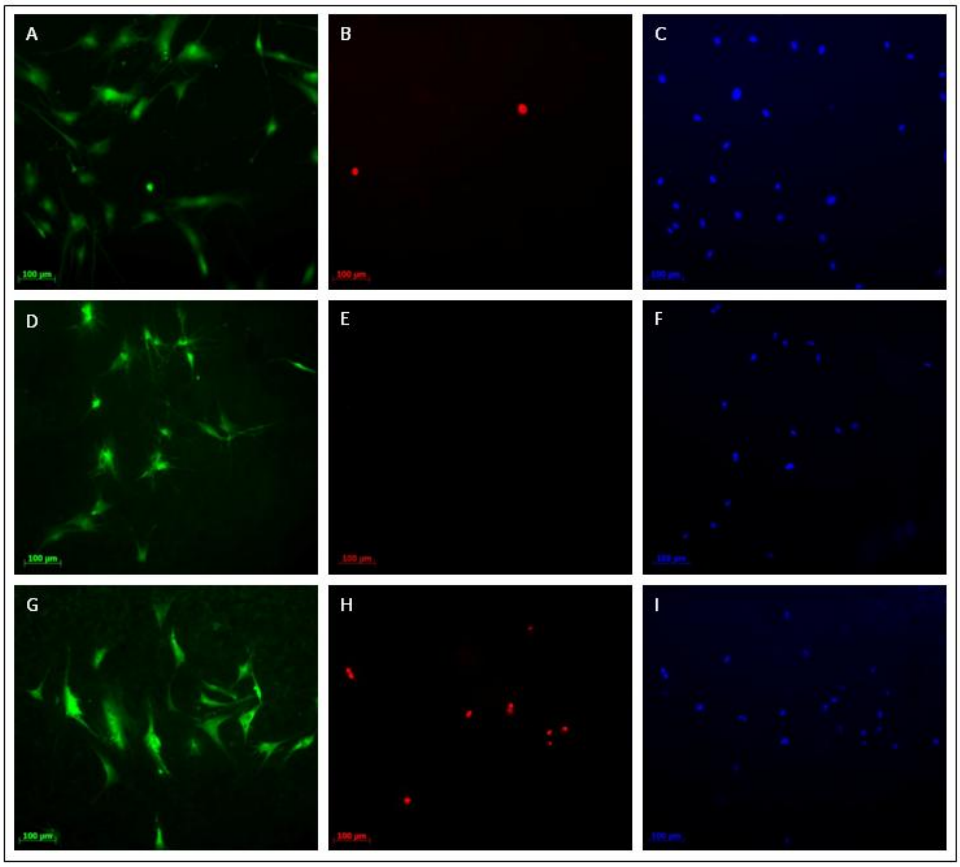

Figure 3.81 Fluorescent microscopic observation of **live**/ **dead, nuclei** hMSCs after 72 hours of culture, embedded in PPP-derived hydrogel (**A-C**) HA-free. (**D-F**): 0.5% HA. (**G-I**): 1% HA

After 5 days embedded within the hydrogel constructs hMSCs proliferated and maintained high viability (Figure 3.82).

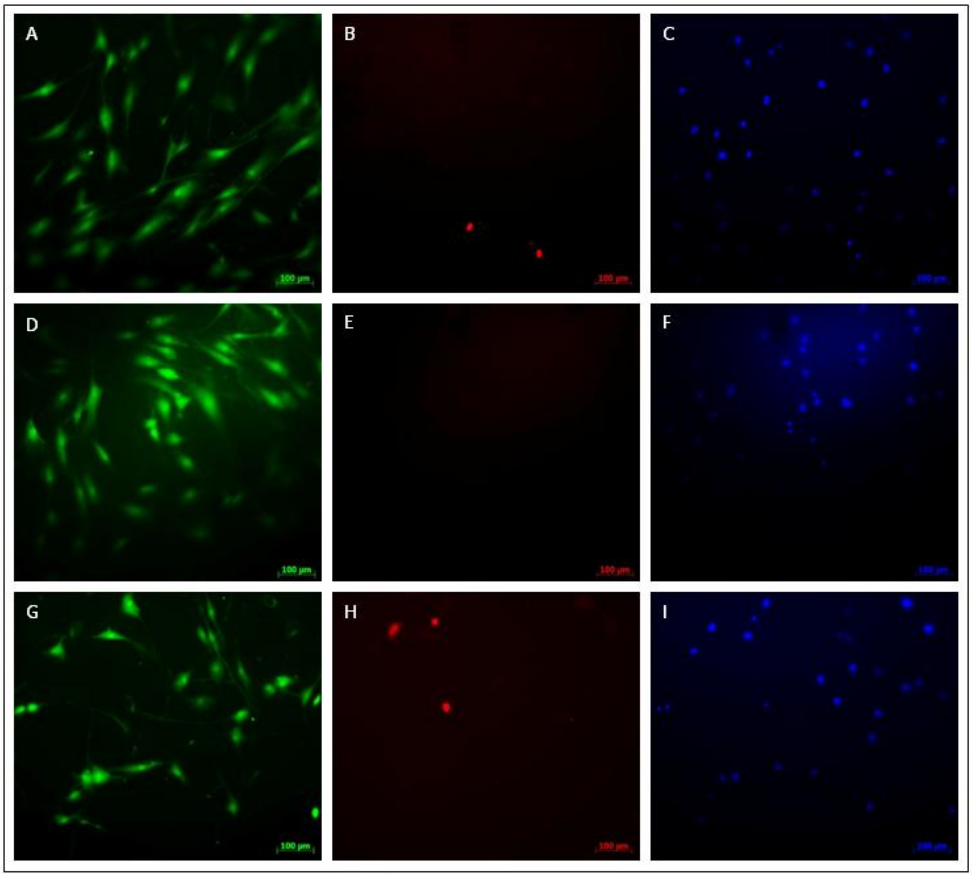

Figure 3.82 Fluorescent microscopic observation of **live**/ **dead, nuclei** hMSCs after 5 days of culture, embedded in PPP-derived hydrogel **A-C**) HA-free. (**D-F**): 0.5% HA. (**G-I**): 1% HA

The PPP hydrogel was therefore validated as an appropriate scaffold capable of maintaining hMSCs *in vitro*. When considering the incorporation of HA within the hydrogel a concentration of 0.5% was selected for subsequent investigations as it demonstrated superiority in promoting hMSC viability.

3.7.3 Ectopic Tissue Formation Model

Four cell types of interest: miR-145 inhibited hEKs maintained in either hEK or hESC media for 5 days prior to implant, hEKs taken at passage 3 that had been nucleofected without miR-145 inhibitor and hMSCs taken at passage 4 were delivered in PPP-derived hydrogel with and without HA into 6 week old SCID mice. Animals were sacrificed four weeks post-implantation and tissue formation was initially observed macroscopically. At each of the sites receiving either miR-145 inhibited hEKs or hMSCs with and without HA soft white tissue was identified (Figure 3.83). No macroscopic tissue formation was observed at sites receiving hEKs nucleofected without miR-145 implanted with or without HA.

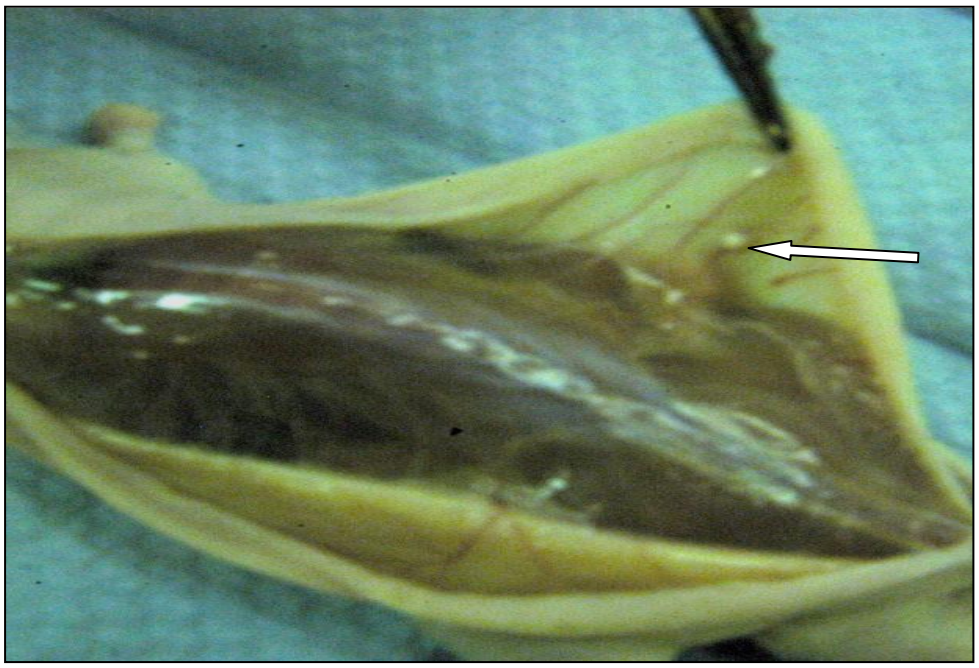

Figure 3.83 Macroscopic observation of tissue formation at site receiving miR-145 inhibited hEKs pre-incubated in hESC media implanted without HA. Arrow indicates *de novo* ectopic tissue

Tissue was dissected from each of the implanted sites, which were then prepared as detailed in section 2.14). Samples were subject to tinctural histopathology using H&E (section 2.16). Atypical glandular-like structures were identified in a number of samples, which received hMSCs or miR-145 inhibited hEKs implanted with and without HA.

In an attempt to characterise *de novo* tissue, samples were subjected to CBFA1 and osteocalcin immunohistochemical staining, however staining for both was negative so proved inconclusive that implanted cells had undergone osteogenesis as hypothesised. As such, further characterisation will need to be conducted in order to identify the *de novo* tissue formed upon implantation *in vivo*.

4.0 Discussion

Somatic cell reprogramming has developed rapidly over the past decade with research focusing on establishing safer, more efficient methods. The main objective of this study was to establish a successful, non-viral method of delivering reprogramming stimuli to replace oncogenic transcription factors. To avoid unpredictable exogenous reprogramming factor reactivation, a transient strategy was sought and ultimately direct reprogramming was pursued to yield functional cells.

4.1 Basal characterisation of hESCs

To establish baseline data, pluripotent stem cells were maintained and characterised. The hESC line, HUES7, was selected as it has been extensively characterised [182-184]. Throughout extended culture, hESCs demonstrated prominent nucleoli, high ratio of nucleus to cytoplasm and displayed compact colony morphology. In addition, hESCs were positive for molecular markers of an undifferentiated pluripotent phenotype; including *Oct4*, *Nanog*, *Sox2*, *SSEA3*, *SSEA4*, *TRA-1-60*, *TRA-1-81* and alkaline phosphatase (Figures 3.2-3.4). This is consistent with the literature, which details these markers as a prerequisite of pluripotency [185]. In order to compare hEK and hESC genotypes, qRT-PCR of total cDNA was performed. Interestingly, this revealed that while hEKs did not express *Oct4*, *Nanog* or *Sox2*, they did express moderate levels of *Klf4* and to a much lesser extent *c-Myc*, which is in agreement with published data reporting that keratinocytes express higher levels of *Klf4* and *c-Myc* compared to other somatic cells, such as fibroblasts [128]. As expected, hEKs expressed high levels of *Cytokeratin-14* therefore a panel of markers was established to distinguish pluripotent hESC from differentiated hEK phenotypes (Figure 3.5).

4.2 Deriving a mimetic pluripotent stem cell microenvironment

It is well documented that the cellular microenvironment greatly influences lineage specification and cell behavior [186, 187]. If we consider the embryonic microenvironment we deduce that the ECM is an important source of regulatory signals that influence pluripotent cells to adopt specific fates. Research has elucidated many cell-cell and cell-matrix interactions occurring between embryonic stem cells and their microenvironment, however mimicking this complexity *in vitro* has yet to be achieved. Nevertheless, exciting studies have shown that signals derived from the microenvironment influence fate of both ESCs and adult progenitor cells [168, 188]. Considering the powerful role that the microenvironment plays in influencing plasticity and lineage determination, it was proposed that providing hEKs with an ECM homologue known to support a pluripotent, self-renewing phenotype may promote hyperplasia.

The feeder-free system used in this study for maintenance of hESCs is composed of two distinct components, a hFN substrate and serum-free media, containing growth factors previously validated for maintenance of hESC phenotype [168]. Initially hFN was considered for the maintenance of hEKs to provide an environment known to promote repogramming. It was rational that hEKs would adhere to hFN as they possess $\alpha_5\beta_1$ integrins, which mediate attachment to fibronectin [167, 189]. As predicted, hEKs adhered to a range of hFN concentrations and cell counts revealed that hEKs preferentially adhered to a concentration of 5µg/mL (Figure 3.6), which is routinely used for the feeder-free maintenance of hESCs [168]. Whilst a large proportion of hEKs successfully adhered to hFN, initial attachment was impaired compared to hCol I (Figure 3.9), which is commonly used for the culture of hEKs *in vitro,* facilitating attachment via $\alpha_2\beta_1$ integrins [167, 190]. It is recognised that cell attachment occurs through interactions between integrins, cell adhesion receptors and extracellular proteins

therefore a number of factors could affect the attachment of hEKs to hFN. One suggestion is that hEKs possess an increased number of integrins, such as $\alpha_2\beta_1$ thus increasing attachment to hCol I. Despite an initial reduction in attachment, hEKs seeded on hFN proliferated at a similar rate to hCol I, demonstrating that hFN is capable of sustaining hEKs over an extended culture period, validating the possibility of incorporating this substrate in hEK reprogramming.

4.3 Identification and validation of a non-viral method of delivering inducing stimuli

Due to the risk of insertional mutagenesis, non-viral methods for somatic cell reprogramming are increasingly sought. When developing this novel strategy for directly reprogramming hEKs, one of the main priorities was to establish a non-viral method of delivering inducing stimuli. Previous non-viral and non-integrating methods have included adenoviruses [136], plasmids [191], excision of reprogramming factors using Cre-loxP [139] or piggyBac transposition [84]. However, as detailed in chapter 1 these techniques often suffer from low efficiencies therefore an alternative solution was sought.

A number of alternative non-viral transfection methods were considered including electroporation and liposomal delivery. These approaches are limited by low efficiency, high cytotoxicity and inability to deliver nucleic acids past the nuclear envelope. Nucleofection however was identified as a promising method of intracellular molecular delivery. Nucleofection is based on electroporation whereby application of voltage temporarily compromises the integrity of the plasma membrane allowing extracellular molecules to enter. Unlike traditional electroporation, nucleofection is based on cell–type specific, high voltage pulses created by a nucleofector

device. This facilitates transitory creation of small pores in the nuclear envelope. In combination with cell-type specific reagents this allows efficient transfer of nucleic acids directly into the nuclei with minimal cytotoxicity [148, 192]. Proprietary reagents consist of modular protein complexes that combine with charged particles, such as nucleic acids, to form a nucleoprotein complex. Different protein, complexes facilitate separate functions, such as cell membrane association, endosomal release and nuclear transport [193].

Two prominent studies which have also successfully utilised nucleofection for delivery of their reprogramming stimuli include reprogramming of human adipose stem cells using a minicircle vector [144] and reprogramming of human embryonic fibroblasts using a piggyBac transposon system [84]. The first study utilised minicircle vectors consisting of supercoiled DNA molecules containing *Oct4, Sox2, Lin28* and *Nanog* while the piggyBac transposon system makes use of a single vector containing OKSM. In both cases each of the reprogramming factors were separated by the self-cleaving peptide 2A, which allowed subsequent excision of exogenous genes following reprogramming. Whilst both studies demonstrate significant advances in reprogramming facilitated by nucleofection both rely heavily on large amounts of foreign DNA including the known oncogenes, *c-Myc* and *Klf4* while the novel strategy detailed herein addresses these issues through a miRNA approach.

Prior to delivery of inducing factors it was necessary to optimise a number of outcomes, such as viability, efficiency and persistence of inducing stimuli.

4.3.1 Viability post-nucleofection

Quantification of hEK viability post-nucleofection was performed using a combination of live/dead staining and trypan-blue dye exclusion. Whole well analysis assessed cells residing both in the adherent monolayer and supernatant compared to hEKs which had undergone identical trypsinisation and centrifugation procedures to ascertain viability as a direct result of nucleofection. Both assays confirmed increased apoptosis compared to non-nucleofected controls with approximately 25% remaining viable post-nucleofection (table 3.2). This level of viability is relatively low, levels as high as 40-60% have been previously reported [194]. However the viability reported here is not unusual with other studies reporting hEK viability of 23% post-nucleofection [195] and in one case 14% [196].

One variable known to considerably affect viability is media composition. The media formulation, KGM-Gold (Lonza, UK), is suggested for optimal viability post-nucleofection [194], however this media was not adopted in this strategy. Deviation from the suggested media may have led to a decrease in the overall cell viability, however despite increased cell death hEKs proliferated and demonstrated typical morphology following nucleofection (Figure 3.8). This is likely to be a result of the high number of cells used in each nucleofection, which meant the significant cell death incurred did not detrimentally affect subsequent culture of hEKs. Nucleofection was subsequently performed many times throughout this investigation and the level of viability remained constant, successfully demonstrating the repeatability of this technique.

4.3.2 Optimising reprogramming microenvironment

As identified previously hFN was considered as a substrate to promote the reprogramming of hEKs. As such, hFN was investigated post-nucleofection

to establish the feasibility of utilising this substrate in this reprogramming strategy. Consistent with earlier experiments a decreased number of hEKs attached to hFN compared to hCol I following nucleofection (table 3.2). In addition, when evaluating adherent hEKs following GFP-P nucleofection, hFN significantly reduced the percentage of GFP^{bright} cells from approximately 20% to 8%, suggesting that a number of nucleofected hEKs failed to attach to the substrate and remained in the supernatant. This was confirmed by whole well analysis, which revealed that the total number of GFP^{bright} cells was comparable between the two systems (Figure 3.15). Onset of terminal differentiation is known to result in decreased fibronectin binding due to loss of $\alpha_5\beta_1$ integrin from the cell surface [197]. Reduced attachment post-nucleofection may therefore have been exacerbated due to the induction of terminal differentiation. It was concluded from this series of experiments that hColI was the optimal substrate post-nucleofection for increasing efficiency of the reprogramming strategy.

4.3.3 Phenotype post-nucleofection

Commonly used transfection methods, such as liposome-mediated DNA transfer can induce the terminal differentiation of somatic cells [198] and these alterations in differentiation state may affect the response of transfected hEKS to the investigated gene product. Therefore prior to delivery of inducing stimuli phenotypic analysis of hEKs post-nucleofection was undertaken. Cytokeratin-14 and involucrin were highlighted as markers of hEK lineage commitment [171, 197, 198]. To establish a positive control, hEKs were subject to suspension culture. This model increases expression of involucrin and subsequently induces terminal differentiation [197, 199]. Cytokeratin-14 was found to be abundant in hEKs maintained under adherent culture and also following nucleofection whilst hEKs maintained in suspension demonstrated considerably reduced expression of

this protein. In addition, a number of hEKs maintained in suspension became hypertrophic and demonstrated positive staining for involucrin, confirming that this culture system had resulted in terminal differentiation of the majority of hEKs, consistent with previous literature [200]. hEKs subject to nucleofection displayed only a few involucrin positive cells suggesting this procedure had not considerably altered their phenotype. This was further confirmed through qRT-PCR, which revealed that nucleofection alone did not alter hEK genotype with both hEK specific genes, such as *cytokeratin-14* and pluripotency genes, such as *Oct4*, *Sox2* and *Nanog* remaining unaltered.

4.3.4 Nucleofection efficiency

Upon establishing the viability and phenotype of hEKs post-nucleofection, it was crucial that the feasibility of delivering inducing stimuli was investigated. It was hypothesised that combinations of plasmid DNA and miRNA may provide a compelling approach for reprogramming hEKs therefore delivery of both substrates needed to be evaluated. A range of appropriate parameters were available for the nucleofection of plasmid DNA [194], however delivery of miRNA required further optimisation, which ultimately identified a favourable concentration of 100nM (Figure 3.20). In both cases the same electrical pulse parameters were used in order to maintain consistency between samples.

Remarkable differences were noted in terms of both DNA and miRNA delivery. Both were rapidly incorporated into the nuclei of hEKs however distinct differences were noted in copy number/cell and delivery efficiency. In the case of GFP-P, a range of cellular fluorescence intensities were detected (Figure 3.14). Reference to previous literature confirmed that this was not an unusual phenomenon with one publication reporting an average

of 1000 plasmid copies per cell following nucleofection, however the standard deviations of these measurements were large suggesting that there can be huge variation in copy number/cell [201]. The efficiency of GFP-P delivery was reproducible with 19.82% ± 2.45, n=6 hEKs successfully nucleofected after 24 hours. The literature indicates that transfection efficiency of hEKs varies considerably with some studies reporting similarly low efficiencies between 5-20% [195, 202] however several studies report much higher efficiencies between 50-60% [202]. If we compare the efficiency of nucleofection reported herein to other non-viral transfection methods, the efficiency of plasmid nucleofection is relatively high with reported efficiencies of 0.1 - 11% using liposomal based transfection reagents [202, 203]

Delivery of miRNA inhibitors provided somewhat different results. Flow cytometric data showed a distinct peak and decrease in fluorescence intensity compared to GFP-P nucleofection (Figure 3.21). In addition, the number of hEKs successfully incorporating the miRNA inhibitor was significantly increased, with a mean efficiency of 88.58% compared to 19.82% detected 24 hours post-nucleofection. The number of studies describing nucleofection of miRNA is limited, however existing reports detail similar efficiencies of 90% [204]. The increased efficiency of miRNA inhibitor delivery suggests uptake is more consistent in terms of the quantity however the difference in fluorescent intensity could be attributed to the difference in fluorochrome labelling each substrate,

4.3.5 Stable or transient transfer?

To investigate longevity of both substrates and ascertain whether transfer is stable or transient, hEKs were maintained in their original wells for 10 days following nucleofection. A similar pattern emerged between the two

substrates with expression peaking for both constructs after 3 days and decreasing over time. When hEKs received miRNA inhibitor, this molecule remained in approximately 80% hEKs after 10 days, while GFP-P had largely been cleared by this point. This may be due to the initially increased cytoplasmic concentration of miRNA inhibitor retaining detectable intensity after several round of mitosis.

To confirm transfer was transient and also assess the feasibility of successive rounds of nucleofection, hEKs were subject to a further round of nucleofection. hEKs that received either GFP-P or miRNA inhibitor demonstrated an increased number of successfully nucleofected cells and in the case of miRNA inhibitor, an increase in fluorescence was also observed. This suggests an increase in substrate transferred to each cell and that hEKs nucleofected during initial nucleofection were more amenable to receiving substrates during serial nucleofections. In addition, hEKs nucleofected in the absence of either GFP-P or miRNA inhibitor during the second round demonstrated an absence of either substrate, providing confirmation that transfer is transient and substrates are eventually cleared through mitosis if not repeatedly transfected [205].

Co-nucleofection has been adopted by many groups as an effective way of delivering a number of substrates [206-208] and it was hypothesised that to develop an effective reprogramming strategy it may be necessary to deliver a number of inducing stimuli. During this investigation it was possible to demonstrate successful delivery of both GFP-P and miRNA inhibitor to hEKs. Flow cytometry revealed that 7.64% of adherent hEKs received both constructs. Considering the low levels of nucleofection reported in other strategies, with only 10.8% of hASCs receiving the minicircle vector before undergoing reprogramming [144] it is not unreasonable to consider co-nucleofection of plasmid DNA and miRNA inhibitors as a practicable strategy for reprogramming hEKs.

4.4 Inhibition of miR-145

miR-145 was highlighted early in this study as a potential mediator of pluripotency [119]. It was hypothesised that modulating its expression may alter the expression of key pluripotency regulators. This investigation successfully demonstrated that inhibition of miR-145 activated pluripotency genes in hEKs that are normally silenced. In the case of *Oct4*, expression was significantly upregulated following miR-145 inhibition, with an expression peak after 5 days. Previous studies have focused on initiating reprogramming through introduction of a number of genes with the vast majority including *Oct4 [45, 144]*. Another study, which mirrors the level of transcriptional regulation described herein, utilised small interfering RNA (siRNA) to mediate expression of scaffold attachment factor A (SAF-A) [209]. This study demonstrates that decreasing SAF-A mRNA through siRNA transfection subsequently decreased *Oct4* expression and vice versa This supports the findings presented in this thesis, which suggest that indirect activation of *Oct4* expression can replace exogenous *Oct4*. The majority of reprogramming strategies involve the induction of *Oct4*, consistent with its role as a mediator of a pluripotent state suggesting that *Oct4* is involved in transcriptional activation of itself or as a heterodimer with *Sox2*.

Literature has shown that miR-145 is associated with both *Oct4* and *Sox2* [119] therefore discovery that miR-145 is capable of activating *Oct4* expression in hEKs suggested that miR-145 may mediate expression of other pluripotency associated genes. As hypothesised, expression of *Sox2* was found to have significantly increased upon miR-145 inhibition. The pattern of expression was different to that observed for *Oct4* with a progressive increase peaking at 9 days, with more than a 25 fold increase detected compared to hEKs nucleofected in the absence of miR-145 inhibitor. If we consider another direct target of miR-145, *Klf4*, we

observed a similar pattern of re-expression to that of *Sox2*. Expression gradually increased over time and peaked at more than 25 fold after 9 days, which is distinctly similar to *Sox2* re-expression. With previous studies highlighting miR-145 as directly targeting *Oct4*, *Sox2* and *Klf4* 3' UTRs [119] it is not surprising that miR-145 inhibition produced this biologically significant effect. Whilst miR-145 directly targets all three genes, the fact that *Oct4* does not follow the same pattern of re-expression nor reaches the same level is not surprising given the tight multifactorial regulation that this gene demonstrated in previous studies [62, 210].

The interaction between miR-145 and *c-Myc* has not received as much attention as its effect on *Oct4*, *Sox2* and *Klf4*. However, miR-145 has been shown to directly silence *c-Myc*, an oncogenic phosphoprotein, which plays a key role in regulating cell cycle progression, apoptosis and transformation [211]. Inhibition of miR-145 resulted in a significant increase in *c-Myc* expression, which peaked after 5 days and exceeded more than 10 fold upregulation. This echoes another study whereby miR-145 inhibition enhanced *c-Myc* expression. This study demonstrated the link between p53 and *c-Myc* by identifying that p53 transcriptionally induces expression of miR-145 through interaction with a p53 response element in the miR-145 promoter. miR-145 then proceeds to silence *c-Myc*, however this process is reversible demonstrated by miR-145 inhibition upregulating *c-Myc* expression via p53 [212].

There have been no reports of miR-145 directly targeting *Nanog*, however it was hypothesised that *Nanog* expression may be significantly altered as a result of increased levels of *Oct4* and *Sox2* given the intrinsic, cooperative regulation of these master regulators [181]. Gene expression data did not conclusively indicate Nanog re-expression, despite a statistically significant upregulation in *Nanog* expression detected after 1 and 7 days. This suggests that miR-145 inhibition alone is not sufficient to induce pluripotency.

To ascertain whether miR-145 inhibition had altered the genotype of hEKs, the expression of the ubiquitously expressed *cytokeratin-14*, was investigated. qRT-PCR analysis revealed an initial decrease in expression, which increased over time resuming to basal levels after 9 days. This reflects the transient nature of miRNA inhibition and provides further evidence that miR-145 inhibition is insufficient to induce a pluripotent state.

4.5 hESC media formulation promotes pluripotency gene expression

To promote increased expression of pluripotency associated genes it was hypothesised that the reprogramming microenvironment should mimic that of the embryo as far as possible. miR-145 inhibited hEKs were provided with media (section 2.1.2), routinely used for culture of hESCs, providing growth factors known to promote pluripotency.

One growth factor of particular relevance is FGF2, which is thought to maintain the pluripotency transcription program via activation of the MAPK pathway [213]. Also incorporated in this media is Activin A, a key regulator in the maintenance of stemness in hESCs, known to induce expression of *Oct4* and *Nanog*, promote Wnt3 and suppress BMP signals [214]. This media formulation has previously been validated for use in the absence of feeder cells in combination with hFN substrates [168].

Upon providing miR-145 inhibited hEKs with growth factor supplemented hESC media, a rapid morphological change occurred. Cells maintained in hESC media clustered together to form distinct colonies whilst those maintained in hEK media remained as a monolayer (Figure 3.39). This distinctive morphological change suggested that miR-145 inhibited hEKs maintained in hESC media had undergone noteworthy biological changes.

In order to investigate these changes at the genomic level, qRT-PCR analysis was performed to compare the two culture systems. In terms of *Oct4* there was little change in expression between the two systems and proteomic analysis demonstrated successful translation of *Oct4* in both cases (Figure 3.41).

There were however differences in *Sox2* expression between the two systems. miR-145-inhibited hEKs maintained in hESC media post-nucleofection displayed increased *Sox2* expression, of 70 fold relative to hEKs nucleofected in the absence of miR-145 inhibitor (Figure 3.42). This profound increase in expression may be attributed to the neural supplements included in this hESC media formulation, N2 and B27. These are known to promote a neural precursor phenotype, however they are also often employed for the maintenance of undifferentiated hESCs [168, 215]. In both cases *Sox2* expression was successfully translated as validated using immunohistochemistry (Figure 3.43).

As discussed earlier, *Nanog* expression failed to reach the same levels as the other pluripotency associated genes. Upon providing miR-145 inhibited hEKs with hESC media *Nanog* expression was upregulated. Despite this statistically significant upregulation, *Nanog* expression remained lower than other pluripotency-associated genes however successful translation was identified by immunohistochemistry (Figure 3.45).

Both *c-Myc* and *Klf4* underwent further upregulation in the presence of hESC media confirming the original hypothesis that providing miR-145 inhibited hEKs with growth factors found in the embryonic microenvironment would increase expression of pluripotency-associated genes.

In order to assess whether genomic changes were extended to hEK-specific genes, *cytokeratin14* expression was evaluated under hESC conditions.

This revealed a prominent decrease in *cytokeratin14* expression of $8x10^3$ fold, strongly suggesting a transformed phenotype. Therefore it was concluded that inhibition of miR-145 combined with growth factor stimulation was capable of activating normally silenced pluripotency genes, promoting acquisition of a stem cell-like phenotype.

The benefits of gaining a fully reprogrammed state were at this point re-evaluated. Whilst pluripotent stem cells are unsurpassed in their differentiation capabilities, they come with their own set of limitations as the extensive differentiation capabilities demonstrated *in vitro* translates to undesirable tumorigenesis *in vivo*. While iPSCs provide an opportunity to derive patient-specific stem cells for use in cell replacement therapies and generate new models for human disease this requires establishment of defined differentiation strategies. Despite substantial progress during the previous decade to optimise generation of functionally competent cells from a variety of pluripotent sources, it remains technically difficult to obtain a homogenous population of lineage-specific cells from a pluripotent stem cell. It was proposed that devising a strategy to direct hEK fate into desirable, functional cell lineages rather than completely reversing their phenotype through a pluripotent intermediate would be more advantageous in many respects.

4.6 Direct reprogramming of miR-145 inhibited hEKs

To direct reprogramming, a series of differentiation media formulations were established (table 2.4). These media formulations have previously been validated for directed differentiation of hMSCs [216-219], which display a number of stemness properties exhibited by miR-145 inhibited hEKs, such as *Oct4* expression [220]. Therefore it was proposed that these formulations may stimulate differentiation of hEKs into desirable lineages.

This novel direct reprogramming approach demonstrated that miR-145 inhibited hEKs underwent functional osteogenic differentiation. This was initially demonstrated through identification of the earliest and most specific marker of osteoblast differentiation, Cbfa1, after 5 days of differentiation culture (Figure 3.49). Forced expression of Cbfa1 in hMSCs leads to osteoblastic differentiation highlighting the influential role of this master regulator in orchestrating osteogenesis [221]. qRT-PCR analysis, indicated an increase in *Cbfa1* expression after 3 days directed osteogenic differentiation in hMSCs and miR-145 inhibited hEKs pre-incubated in hESC media and at the later time point of 7 days for miR-145 inhibited hEKs pre-incubated in hEK media (Figure 3.53). This is similar to data obtained in a previous study, which reports detection of *Cbfa1* after 2 days where hMSCs are subject to identical osteogenic differentiation parameters [216]. Other studies report maximal upregulation of *Cbfa1* after 7 days of directed differentiation confirming that early upregulation of this osteogenic master gene is typical [222]. Similarities in *Cbfa1* expression profiles suggest miR-145 inhibited hEKs cultured in hESC media share a phenotype more akin to hMSCs than miR-145 inhibited hEKs maintained in hEK media.

CBFA1 acts upstream of *osteocalcin* and *osteonectin* [223] therefore it was hypothesised that upregulation of *CBFA1* would induce these genes. Gene expression data revealed an upregulation of both *osteonectin* and *osteocalcin* after 14 and 21 days respectively (Figures 3.54-3.55). This is consistent with previous studies reporting *osteonectin* expression maxima after 14 days [224, 225]. *Osteocalcin* expression also increases in a time-dependent manner and is often only upregulated after 21 days of osteogenic differentiation [222] confirming the development of an osteoblastic phenotype [225]. Changes reported herein for all osteogenic genes were relatively high, often exceeding 100 fold at the maxima, compared to other studies, typically between 10-50 fold [226]. This can be attributed to the

genomic data described herein being presented relative to lineage committed hEKs nucleofected in the absence of miR-145 inhibitor rather than multipotent hMSCs. There are no previous reports of osteogenic, chondrogenic, adipogenic or neurogenic differentiation of miR-145 inhibited cells therefore it is impossible to draw any direct comparison. However this data provides an indication of the genomic changes occurring compared to hMSCs and along with immunohistochemical and histological staining provides confirmation of directed differentiation into multiple lineages. To conclude osteoblast functionality, histological staining was performed. A combination of Von Kossa and Alizarin Red S staining were able to provide confirmation of extracellular mineralisation after 21 days (Figures 3.51-3.52).

Application of defined chondrogenic differentiation media was also able to direct the differentiation of miR-145-inhibited hEKs identified by a number of chondrocyte-specific markers. Initially this was demonstrated through the identification of aggrecan, an early marker of chondrogenesis, after 7 days directed differentiation (Figure 3.57). This is consistent with previous literature, which details a time dependent accumulation of aggrecan between 6-12 days [227]. In addition, this direct reprogramming strategy was able to induce markers associated with terminal chondrogenesis, such as Col II. hMSCs demonstrated typical Col II expression profile with a gradual increase in expression, peaking after 21 days, except for an increase after 1 day (Figure 3.60). miR-145 inhibited hEKs demonstrated reduced expression of this marker compared to hMSCs however the expression profile did follow the same pattern with a peak in expression after 1 day followed by a general increase in Col II expression over time (Figure 3.1). This observation does not exactly replicate that found in the literature with chondrogenic differentiation typically characterised by detection between 7-14 days followed by a peak in expression after 21 days [228]. However different media formulations can provide distinctly different chondrogenic

potential, which may alter the pattern of expression. What this clearly demonstrates is the acquisition of a chondrogenic phenotype with consistency between hMSCs and miR-145 inhibited hEKs. Van Gieson staining also identified the abundance of collagen present in both miR-145 inhibited hEKs and hMSCs providing further evidence for the acquisition of a chondrogenic phenotype (Figure 3.59).

To further probe the stem cell-like phenotype of miR-145 inhibited hEKs adipogenic differentiation media was applied. *PPARγ*, an early initiator of adipogenesis [174, 229], was detected after 1 day in hMSCs and miR-145 inhibited hEKs. *PPARγ* expression decreased after this point, however it remained significantly upregulated until day 14 in the case of hMSCs and miR-145 inhibited hEKs pre-incubated in hESC media (Figure 3.64), which correlates with previous reports, which also indicate early initiation of this gene [230, 231]. *Adiponectin* is also heavily implicated in adipogenesis and is often associated with later stages of differentiation [232]. Gene expression data revealed an increase in adiponectin after 1 day, which subsequently decreased but remained significantly upregulated at 14 days in the case of hMSCs and 21 days in miR-145 inhibited hEKs pre-incubated in hESC media (Figure 3.65). qRT-PCR analysis therefore revealed an increased affinity of these two groups to undergo adipogenesis compared to miR-145 inhibited hEKs pre-incubated in hEK media, perhaps due to the increased expression of pluripotency associated genes in the first instance. To confirm adipocyte functionality, Oil Red O staining was performed, which clearly identified lipid droplets after 3 days in both hMSCs and miR-145 inhibited hEKs subject to adipogenic differentiation. The abundance of lipid droplets increased up to 14 days (Figure 3.63), consistent with previous studies, which detail time dependent accumulation of lipid filled vacuoles [233].

Finally, to demonstrate the differentiation potential of miR-145 inhibited hEKs, a neurogenic differentiation strategy was selected. The high levels of the neural precursor gene, *Sox2,* demonstrated by miR-145 inhibited hEKs in hESC media led to the hypothesis that these cells may be directed towards a neural phenotype. Expression of the early neural marker *nestin* provided evidence of the neurogenic differentiation of miR-145 inhibited hEKs pre-incubated in hESC media [175]. *Nestin* expression was found to be significantly elevated throughout the culture period decreasing in a time dependent manner, which is consistent with other reports of neurogenesis [234].

hMSCs also demonstrated significant expression of this early marker after 3 days, however at reduced levels compared to miR-145 inhibited hEKs pre-incubated in hESC media. This is consistent with previous literature, which widely characterises hMSCs according to their 'tri-lineage' potential. However reports of neural differentiation are far less common suggesting increased restrictions in achieving neural transdifferentiation. If we consider the expression of *nestin* in miR-145 inhibited hEKs pre-incubated in hEK media, a similar increase was observed after 5 days as detected for hMSCs after 3 days. The delayed expression of lineage specific genes for miR-145 inhibited hEKs pre-incubated in hEK media is a consistent theme throughout this investigation suggesting the initial decreased expression of pluripotency associated genes may have imparted restrictions on subsequent differentiation.

Terminal markers of neurogenesis, neurofilament and βIII-tubulin, were detected at the later time points of 14 to 21 days. Gene expression data indicated significant upregulation of *neurofilament* in miR-145 inhibited hEKs pre-incubated in hESC and hEK media after 14 and 21 days respectively (Figure 3.70). Although hMSCs demonstrated significant upregulation of *neurofilament* after 21 days, the level of expression was

reduced compared to miR-145 inhibited hEKs supporting an increased ability of reprogrammed cells to undergo neurogenesis. Despite varying levels of neural-specific genes all three cell types were βIII-tubulin positive confirming successful acquisition of a neuronal phenotype after 21 days directed neurogenic culture (Figure 3.69) consistent with other reports, which verify a neuronal phenotype based on the identification of βIII-tubulin [235].

4.7 Maintenance of a hESC phenotype using PPP-derived hydrogel

To evaluate the effect of an *in vivo* environment on stem cell phenotypes an appropriate implantation model was formulated, incorporating a PPP-derived hydrogel, which had previously been validated in terms of its ability to maintain human MSCs, dermal fibroblasts, articular chondrocytes and osteoblasts [178].

Considering the native 3D microenvironment of hESCs it was hypothesised that they required a structural framework and morphogenic cues to mediate cell fate and function. The PPP-derived hydrogel possesses many ideal characteristics with its 3D composition, mechanical integrity and excellent mass transport properties contributing to its cytocompatibility. Prior to implantation, the ability of this PPP-derived hydrogel to maintain a self-renewing, undifferentiated hESC phenotype was evaluated. Both cell viability and morphological analysis suggested that this matrix was capable of supporting a hESC phenotype *in vitro* (3.72-3.73). hESCs primarily express integrins recognising the RGD peptide sequence present in most ECM proteins. It is likely that fibronectin within the PPP-derived hydrogel played an important role in promoting maintenance of hESCs through facilitating attachment via integrin binding to RGD sequences [236, 237]. The main component of the matrix is fibrin, which also has multiple

interacting sites that serve as adhesion motifs, including binding sites for $\alpha_5\beta_1$ integrins [237], it is therefore possible that the abundance of fibrin within the hydrogel may also have served to mediate attachment and proliferation of hESCs. In addition, the conversion of the soluble protein fibrinogen to the insoluble protein fibrin during gellation, generates a network of fibres comparable to that found within natural ECM. In combination with soluble growth factors supplied in the culture media this system provides a microenvironment, which promotes a self-renewing, undifferentiated phenotype .

This novel, feeder-free, PPP-derived hydrogel system was used to culture hESCs up to 25 passages demonstrating the ability of this system to support the long-term maintenance of an undifferentiated phenotype. Throughout the culture period their pluripotent phenotype was validated through a combination of qRT-PCR and immunohistochemical staining of the pluripotency markers *Oct4*, *Sox2* and *Nanog* consistent with validation of other feeder-free culture systems [238, 239]. This was directly compared to the previously reported fibronectin, feeder-free system [168] with no significant differences in pluripotency gene expression noted between both systems. In addition, hESCs implanted within PPP-derived hydrogels *in vivo* demonstrated successful teratoma formation, the gold standard for confirming a pluripotent phenotype [240]. Together these data demonstrate a new platform for studying pluripotent stem cell biology both *in vitro* and *in vivo*.

4.8 Ectopic Tissue Formation Model

To provide miR-145 inhibited hEKs with stimulation to direct their differentiation *in vivo,* an ectopic bone formation model was formulated to incorporate HA within cell-loaded hydrogels. This is consistent with other

ectopic bone formation strategies, which make use of the osteoinductive properties of HA to promote osteogenesis [241]. To determine an optimal concentration of HA, an *in vitro* viability assay was performed, which revealed that a concentration of 0.5% HA promoted hMSC growth. This is comparable to a previous study which demonstrated a high level of hMSC cytocompatibility using 1% HA poly(ethylene glycol) dimethacrylate (PEGDMA) hydrogels [242].

Previous studies describing hydrogel-derived bone tissue typically use stem cells, such as hMSCs directed into critically sized bone defects rather than generating bone ectopically. One such example used a hyaluronic acid polymer in conjunction with BMP-2 and hMSCs implanted into a rat calvarial defect of critical size. This demonstrated complete healing of the defect after 4 weeks, the neo-bone being difficult to discern from the host tissue [243]. An ectopic bone formation strategy was adopted in this investigation to aid clear indication of donor-derived tissue formation.

Implantation into NOD/SCID mice provided evidence that both hMSCs and miR-145 inhibited hEKs contributed to *de novo* tissue formation *in vivo*, identified macroscopically as white tissue masses in both HA and HA-free implanted groups (Figure 3.83). Histological staining identified atypical glandular structures in a number of samples, which received either hMSCs or miR-145 inhibited hEKs, while these structures were absent at sites that had received untreated hEKs (Figure 3.84) providing further evidence that the stem cell characteristics of miR-145 inhibited hEKs and hMSCs had resulted in *de novo* tissue formation *in vivo*.

To characterise this tissue a number of markers associated with an osteogenic phenotype were selected with previous studies reporting identification of both CBFA1 and Osteocalcin after 4 weeks confirming ectopic bone formation [244]. Negative detection of these markers suggested that these cells had not undergone osteogenesis as hypothesised.

Considering the stem cell-like phenotype of miR-145 inhibited hEKs it is possible that the *in vivo* microenvironment may have stimulated these cells into a number of possible lineages therefore further characterisation of the tissue will be required to elucidate their *in vivo* differentiation capabilities.

5.0 Conclusions

This investigation successfully validated nucleofection as an effective method of introducing both plasmid DNA and miRNA inhibitors to hEKs; avoiding many of the complications associated with viral-mediated transfection. This non-viral technique has previously been reported for the reprogramming of human progenitor cells, however in both cases plasmid DNA was utilised. This is the first report of nucleofection-mediated, miRNA inhibitor delivery facilitating the reprogramming of human lineage committed cells.

Inhibition of miR-145 successfully activated silenced pluripotency genes in hEKs. The activation of *Oct4* is of considerable significance as this transcription factor is considered to be a proxy for stemness and a prerequisite for pluripotency. The results detailed herein demonstrated that inhibition of miR-145 indirectly activated expression of endogenous *Oct4* while also significantly upregulating *Sox2, Klf4* and *c-Myc* expression.

Growth factor supplemented media routinely used for the maintenance of hESCs was found to further stimulate expression of pluripotency associated genes *Sox2, Nanog, Klf4* and *c-Myc* however did not alter the expression of *Oct4*. In addition the hEK marker, *cytokeratin14* was found to have notably decreased under these culture conditions. This altered genotype was reflected in a rapid morphological change with cells clustering together to form colonies strongly suggestive of a distinct phenotypic change.

Direct reprogramming of miR-145 inhibited hEKs towards tri-lineage and transgermal fates was successfully achieved using defined differentiation media formulations previously validated for the directed differentiation of hMSCs. Osteogenic, chondrogenic, adipogenic and neurogenic lineages were confirmed using an array of proteomic and genomic markers. This

novel, non-viral, miRNA approach for the direct reprogramming of somatic cells yielded transdifferentiated functional cells offering significant advances for clinical translation.

References

1. Langer, R. and J. Vacanti, *Tissue engineering.* Science, 1993. **260**(5110): p. 920-926.
2. Alison, M.R., et al., *Markers of adult tissue-based stem cells.* Handb Exp Pharmacol, 2006(174): p. 185-227.
3. de Wynter, E.A., Emmerson A.J., Testa N.G. , *Properties of peripheral blood and cord blood stem cells.* Bailliere's Best Pract Res Clin Haematol, 1999. **12**: p. 1-17.
4. Dua, H., Azuara-Blanco A., *Limbal stem cells of the corneal epithelium.* Surv Ophthalmol, 2000. **44**: p. 415-425.
5. Beresford, J.N., *Osteogenic stem cells and the stromal system of bone and marrow.* Clin Orthop Relat Res, 1989(240): p. 270-80.
6. Gregg, C.T., T. Shingo, and S. Weiss, *Neural stem cells of the mammalian forebrain.* Symp Soc Exp Biol, 2001(53): p. 1-19.
7. Jo, Y.Y., et al., *Isolation and characterization of postnatal stem cells from human dental tissues.* Tissue Eng, 2007. **13**(4): p. 767-73.
8. Grove, J.E., E. Bruscia, and D.S. Krause, *Plasticity of bone marrow-derived stem cells.* Stem Cells, 2004. **22**(4): p. 487-500.
9. Heike, T. and T. Nakahata, *Stem cell plasticity in the hematopoietic system.* Int J Hematol, 2004. **79**(1): p. 7-14.
10. Osterziel, K.J., *Improved clinical outcome after intracoronary administration of bone-marrow-derived progenitor cells in acute myocardial infarction: final 1 year results of the REPAIR-AMI trial.* European Heart Journal 2007. **28**(5): p. 638.
11. Strauer, B.E., Yousef, M., Schannwell, C.M., *The acute and long-term effects of intracoronary stem cell transplantation in 191 patients with chronic heart failure: the STAR-heart study.* American Journal of Cardiology, 2010. **12**(7): p. 721-729.
12. Meyer, G.P., Wollert, K.C., Lotz, J., *Intracoronary bone marrow cell transfer after myocardial infarction: 5-year follow-up from the*

randomized BOOST trial. European Heart Journal, 2009. **30**(24): p. 2978-2984.

13. Bolli, R., Chugh, A.R., D'Amario, D., Loughran, J.H., Stoddard, M.F., Ikram, S., Beache, G.M., Wagner, S.G., Leri, A., Hosada, T., Sanada, F., Elmore, J.B., Goichberg, P., Cappetta, D., Solankhi, N.K., Fahsah, I., Rokosh, D.G., Slaughter, M.S., Kajstura, J., Anversa, P., *Cardiac stem cells in patients with ischaemia cariomyopathy (SCIPIO): Initail results of a randomised phase I trial.* The Lancet, 2011. **378**(9806): p. 1847-1857.
14. Voltarelli, J.C., Couri, C.E., Stracieri, A.B., *Autologous Nonmyeloblative Hematopoietic Stem Cell Transplantation in Newly Diagnosed Type I Diabetes Mellitus.* JAMA, 2007. **297**(14): p. 1568-1576.
15. Couri, C.E.B., Oliveira, M.C.B., Stracieri, A.B.P.L., Moraes, D.A., Pieroni, F., Barros, G.M.N., Madeira, M.I.A., Malmegrim, K.C.R., Foss-Freitas, M.C., Simones, B.P., Martinez, E.Z., Foss, M.C., Burt, R.K., Voltarelli, J.C., *C-Peptide Levels and Insulin Independence Following Autologous Nonmyeloablative Hematopoietic Stem Cell Transplantation in Newly Diagnosed Type I Diabetes Mellitus.* JAMA, 2009. **301**(15): p. 1573-1579.
16. Till, J.E., McCulloch, E.A., *A Direct Measurement of the Radiation Sensitivity of Normal Mouse Bone Marrow Cells.* Radiat. Res, 1961. **14**: p. 2213-222.
17. Thomas, E.D., *Bone Marrow Transplantation: a Review.* Semin. Hematol, 1999. **36**: p. 95-103.
18. Gratwohl, A., Baldomero H., Aljurf, M., Pasquini, M.C., Bouzas, L.F., Yoshimi, A., Szer, J., Lipton, J., Schwendener, A., Gratwohl, M., Frauendorfer, K., Niederwieser, D., Horowitz, M., Kodera, Y., *Hematopoietic Stem Cell Transplantation: A Global Perspective.* JAMA, 2010. **303**(16): p. 1617-1624.

19. Rietze, R.L., et al., *Purification of a pluripotent neural stem cell from the adult mouse brain.* Nature, 2001. **412**(6848): p. 736-739.
20. Harris, D.T. and I. Rogers, *Umbilical Cord Blood: A Unique Source of Pluripotent Stem Cells for Regenerative Medicine.* Current Stem Cell Research & Therapy, 2007. **2**: p. 301-309.
21. Parker, A.M. and A.J. Katz, *Adipose-derived stem cells for the regeneration of damaged tissues.* Expert Opin Biol Ther, 2006. **6**(6): p. 567-78.
22. Kerkis, I., et al., *Isolation and characterization of a population of immature dental pulp stem cells expressing OCT-4 and other embryonic stem cell markers.* Cells Tissues Organs, 2006. **184**(3-4): p. 105-16.
23. Thomson, J.A., et al., *Embryonic stem cell lines derived from human blastocysts.* Science, 1998. **282**(5391): p. 1145-7.
24. Amit, M., et al., *Clonally Derived Human Embryonic Stem Cell Lines Maintain Pluripotency and Proliferative Potential for Prolonged Periods of Culture.* Developmental Biology, 2000. **227**(2): p. 271-278.
25. Chidgey, A.P. and R.L. Boyd, *Immune Privilege for Stem Cells: Not as Simple as It Looked.* Cell Stem Cell, 2008. **3**(4): p. 357-358.
26. BioWorld, *Economy's to Blame: hESC Pioneer Geron Abandons Stem Cell R&D.* www.bioworld.com/content/economys-blame-hesc-pioneer-geron-abandons-stem-cel-rd, 2011.
27. Briggs, R. and T.J. King, *Transplantation of living nuclei from blatula cells into enucleated frog's eggs.* Proc Natl Acad Sci U S A, 1952. **38**: p. 455-463.
28. Gurdon, J.B., *The developmental capacity of nuclei taken from intestinal epithelium cells of feeding tadpoles.* J Embryol Exp Morphol, 1962. **10**: p. 622-640.

29. Wilmut, I., et al., *Viable offspring derived from fetal and adult mammalian cells.* Nature, 1997. **385**(6619): p. 810-813.
30. Stevens, L.C., Little, C.C., *Spontaneous testicular teratomas in an inbred strain of mice.* Proc Natl Acad Sci 1954. **40**: p. 1080-1087.
31. Cowan, C.A., et al., *Nuclear Reprogramming of Somatic Cells After Fusion with Human Embryonic Stem Cells.* Science, 2005. **309**(5739): p. 1369-1373.
32. Do, J.T. and H.R. Scholer, *Nuclei of Embryonic Stem Cells Reprogram Somatic Cells.* Stem Cells, 2004. **22**(6): p. 941-949.
33. Miller, R.A., Ruddle, F.H., *Pluripotent tetracarcinomathymus somatic cell hybrids.* Cell, 1976. **9**: p. 45-55.
34. Evans, M.J., Kaufman, M.H., *Establishment in culture of pluripotential cells from mouse embryos.* Nature, 1981. **292**: p. 154-156.
35. Matsui, Y.Z., K., Hogan, B.L., *Derivation of pluripotential embryonic stem cells from murine primordial germ cells in culture.* Cell, 1992. **70**: p. 841-847.
36. Brons, I.G., Smithers, L.G., Trotter, M.W.,Rugg-Gunn, P., Sun, B., Chuva de Sousa Lopes, S.M., Howlett, S.K., Clarkson, A., Arhlund-Richter, L., Pederson, R.A., *Derivation of pluripotent epiblast cells from mammalian embryos.* Nature, 2007. **448**: p. 191-195.
37. Taranger, C.K., et al., *Induction of dedifferentiation, genomewide transcriptional programming, and epigenetic reprogramming by extracts of carcinoma and embryonic stem cells.* Mol Biol Cell, 2005. **16**(12): p. 5719-35.
38. Hansis, C., et al., *Nuclear reprogramming of human somatic cells by xenopus egg extract requires BRG1*. Curr Biol, 2004. **14**(16): p. 1475-80.

39. Davis, R.L., Weintraub, H., Lasser, A.B., *Expression of a single transfected cDNA converts fibroblasts to myoblasts.* Cell, 1987. **51**: p. 987-1000

40. Xie, H., Ye, M., Feng, R., Graf, T. , *Stepwise reprogramming of B cells into macrophages.* Cell, 2004. **117**: p. 663-676.

41. Takahashi, K. and S. Yamanaka, *Induction of pluripotent stem cells from mouse embryonic and adult fibroblast cultures by defined factors.* Cell, 2006. **126**(4): p. 663-76.

42. Yamanaka, S., *Induction of pluripotent stem cells from mouse fibroblasts by four transcription factors.* Cell Proliferation, 2008. **41**: p. 51-56.

43. Meissner, A., M. Wernig, and R. Jaenisch, *Direct reprogramming of genetically unmodified fibroblasts into pluripotent stem cells.* Nat Biotech, 2007. **25**(10): p. 1177-1181.

44. Maherali, N., et al., *Directly Reprogrammed Fibroblasts Show Global Epigenetic Remodeling and Widespread Tissue Contribution.* Cell Stem Cell, 2007. **1**(1): p. 55-70.

45. Takahashi, K., et al., *Induction of Pluripotent Stem Cells from Adult Human Fibroblasts by Defined Factors.* Cell, 2007. **131**(5): p. 861-872.

46. Okita, K., T. Ichisaka, and S. Yamanaka, *Generation of germline-competent induced pluripotent stem cells.* Nature, 2007. **448**(7151): p. 313-317.

47. Wernig, M., et al., *In vitro reprogramming of fibroblasts into a pluripotent ES-cell-like state.* Nature, 2007. **448**(7151): p. 318-324.

48. Li, W., Wei, W., Zhu, S., Shi, Y., Lin, T., Hao, E. Hayek, A., Deng, H., Ding, S., *Generation of human and rat induced pluripotent stem*

cells by combining genetic reprogramming and chemical inhibitors. Cell Stem Cell, 2009. **4**: p. 16-19.

49. Lui, H., Zhu, F., Yong, J., Zhang, P., Hou, P., Li, H., Jiang, W., Cai, J., Lui, M., Cui, K., *Generation of induced pluripotent stem cells from adult rhesus monkey fibroblasts.* Cell Stem Cell, 2008. **3**: p. 587-590

50. Nakagawa, M., et al., *Generation of induced pluripotent stem cells without Myc from mouse and human fibroblasts.* Nat Biotech, 2008. **26**(1): p. 101-106.
51. Yu, J., et al., *Induced Pluripotent Stem Cell Lines Derived from Human Somatic Cells.* Science, 2007. **318**(5858): p. 1917-1920.
52. Viswanathan, S.R., Daley, G.Q., Gregory, R.I., *Selective blockade of microRNA processing by Lin28.* Science, 2008. **320**: p. 97-100.
53. Kim, H.H., Kuwano, Y., Srikantan, S., Lee, E.K., Martindale, J.L., Gorospe, M., *HuR recruits let-7/RISC to repress C-Myc expression.* Genes Dev, 2009. **23**: p. 1743-1748.
54. Huangfu, D., Osafune, K., Maehr, R., Guo, W., Eijkelenboom, A., Chen, S., Muhlestein, W., Melton, D. A., *Induction of pluripotent stem cells from primary human fibroblasts with only Oct4 and Sox2.* Nat Biotech, 2008. **26**: p. 1269-1275.
55. Kim, J.B., et al., *Oct4-Induced Pluripotency in Adult Neural Stem Cells.* Cell, 2009. **136**(3): p. 411-419.
56. Nakagawa, M., Koyanagi, M., Tanabe, K., Takahashi, K., Ichisaka, T., Aoi, T., Okita, K., Mochiduki, Y., Takizawa, N., Yamanaka, S., *Generation of induced pluripotent stem cells without Myc from mouse and human fibroblasts.* Nat Biotech, 2008. **26**: p. 101-106.
57. Heng, J.C., Feng, B., Han, J., Jiang, J., Kraus, P., Ng, J.H., Orlov, Y.L., Huss, M., Yang, L., Lufkin, T., Lim, B., Ng, H.H., *The nuclear receptor Nr5a2 can replace Oct4 in the reprogramming of murine*

somatic cells to pluripotent cells. Cell Stem Cell, 2010. **6**(2): p. 167-174.

58. Scholer, H.R., et al., *New type of POU domain in germ line-specific protein Oct-4.* Nature, 1990. **344**(6265): p. 435-439.
59. Nichols, J., et al., *Formation of pluripotent stem cells in the mammalian embryo depends on the POU transcription factor Oct4.* Cell, 1998. **95**(3): p. 379-91.
60. Palmieri, S.L., et al., *Oct-4 Transcription Factor Is Differentially Expressed in the Mouse Embryo during Establishment of the First Two Extraembryonic Cell Lineages Involved in Implantation.* Developmental Biology, 1994. **166**(1): p. 259-267.
61. Pesce, M. and H.R. Scholer, *Oct-4: Gatekeeper in the Beginnings of Mammalian Development.* Stem Cells, 2001. **19**(4): p. 271-278.
62. Niwa, H., J.-i. Miyazaki, and A.G. Smith, *Quantitative expression of Oct-3/4 defines differentiation, dedifferentiation or self-renewal of ES cells.* Nat Genet, 2000. **24**(4): p. 372-376.
63. Niwa, H., *Molecular mechanism to maintain stem cell renewal of ES cells.* Cell Struct Funct, 2001. **26**(3): p. 137-48.
64. Boyer, L., et al., *Core transcriptional regulatory circuitry in human embryonic stem cells.* Cell, 2005. **122**(6): p. 947 - 56.
65. Loh, Y.H., et al., *The Oct4 and Nanog transcription network regulates pluripotency in mouse embryonic stem cells.* Nature Genetics, 2006. **38**(4): p. 431-440.
66. Avilion, A.A., et al., *Multipotent cell lineages in early mouse development depend on SOX2 function.* Genes Dev, 2003. **17**(1): p. 126-40.
67. Chew, J.-L., et al., *Reciprocal Transcriptional Regulation of Pou5f1 and Sox2 via the Oct4/Sox2 Complex in Embryonic Stem Cells.* Mol. Cell. Biol., 2005. **25**(14): p. 6031-6046.

68. Masui, S., et al., *Pluripotency governed by Sox2 via regulation of Oct3/4 expression in mouse embryonic stem cells.* Nat Cell Biol, 2007. **9**(6): p. 625-635.
69. Adhikary, S. and M. Eilers, *Transcriptional regulation and transformation by Myc proteins.* Nat Rev Mol Cell Biol, 2005. **6**(8): p. 635-645.
70. Cartwright, P., et al., *LIF/STAT3 controls ES cell self-renewal and pluripotency by a Myc-dependent mechanism.* Development, 2005. **132**(5): p. 885-896.
71. Rohan, K.H., et al., *Maintenance of pluripotency in human embryonic stem cells is STAT3 independent.* Stem Cells, 2004. **22**(4): p. 522-30.
72. Cotterman, R., et al., *N-Myc Regulates a Widespread Euchromatic Program in the Human Genome Partially Independent of Its Role as a Classical Transcription Factor*. Cancer Res, 2008. **68**(23): p. 9654-9662.
73. Marson, A., et al., *Wnt Signaling Promotes Reprogramming of Somatic Cells to Pluripotency.* Cell Stem Cell, 2008. **3**(2): p. 132-135.
74. Li, Y., et al., *Murine embryonic stem cell differentiation is promoted by SOCS-3 and inhibited by the zinc finger transcription factor Klf4.* Blood, 2005. **105**(2): p. 635-637.
75. Nakatake, Y., et al., *Klf4 Cooperates with Oct3/4 and Sox2 To Activate the Lefty1 Core Promoter in Embryonic Stem Cells.* Mol. Cell. Biol., 2006. **26**(20): p. 7772-7782.
76. McCarthy, N., *Look both ways.* Nat Rev Cancer, 2005. **5**(12): p. 917-917.
77. Pan, G. and J.A. Thomson, *Nanog and transcriptional networks in embryonic stem cell pluripotency.* Cell Res, 2007. **17**(1): p. 42-9.

78. Stadtfeld, M., et al., *Defining Molecular Cornerstones during Fibroblast to iPS Cell Reprogramming in Mouse.* Cell Stem Cell, 2008. **2**(3): p. 230-240.
79. MacArthur, B.D., C.P. Please, and R.O.C. Oreffo, *Stochasticity and the Molecular Mechanisms of Induced Pluripotency.* PLoS ONE, 2008. **3**(8): p. e3086.
80. Panopoulos, A.D., et al., *Rapid and Highly Efficient Generation of Induced Pluripotent Stem Cells from Human Umbilical Vein Endothelial Cells.* PLoS ONE, 2010. **6**(5): p. e19743.
81. Marion, R.M., Strati, K.M., Li, H., Tejera, A., Schoeftner, S., Ortega, S., Serrano, M., Blasco, M.A., *Telomeres aquire embryonic stem cell characteristics in induced pluripotent stem cells.* Cell Stem Cell, 2009. **4**: p. 141-154.
82. Chin, M.H., Mason, M.J., Xie, W., Volinia, S., Singer, M., Peterson, C., Ambartsumyan, G., Aimiuwan, O.,Richter, L., Zhang, J., *Induced pluripotent stem cells and embryonic stem cells are distinguished by gene expression signatures.* Cell Stem Cell, 2009. **5**: p. 111-123.
83. Polo, J.M., Liu, S., Figueroa, M.E., Kulalert, W., Eminli, S., Tan, K.Y., Apostolou, E., Stadtfeld, M., Li, Y., Shioda, T., *Cell type of origin influences the molecular and functional properties of mouse induced pluripotent stem cells.* Nat Biotech, 2010. **28**: p. 848-855.
84. Woltjen, K., Michael, I.P., Mohseni, P., Desai, R., Mileikovsky, M., Hàmàlàinen, R., Cowling, R., Wang, W., Liu, P., Gertsenstein, M., Kaji, K., Sung, H., Nagy, A., *piggyBac transposition reprograms fibroblasts to induced pluripotent stem cells.* nature, 2009. **458**: p. 766-770.
85. Zhou, W. and C.R. Freed, *Adenoviral Gene Delivery Can Reprogram Human Fibroblasts to Induced Pluripotent Stem Cells.* Stem Cells, 2009. **27**(11): p. 2667-2674.

86. Zhou, H., Wu, S., Joo, J.Y., Zhu, S., Han, D.W., Lin, T., Trauger, S., Bien, G., Yao, S, Zhu, Y., *Generation of induced pluripotent stem cells using recombinant proteins.* Cell Stem Cell, 2009. **4**: p. 381-384.
87. Edwards, R.G. and H.K. Beard, *Oocyte polarity and cell determination in early mammalian embryos.* Molecular Human Reproduction, 1997. **3**(10): p. 863-905.
88. Morgan, H.D., et al., *Epigenetic reprogramming in mammals.* Human Molecular Genetics, 2005. **14**(suppl 1): p. R47-R58.
89. Fedor, M.J., *Chromatin structure and gene expression.* Current Opinion in Cell Biology, 1992. **4**(3): p. 436-443.
90. Fukuda, H., et al., *Simple histone acetylation plays a complex role in the regulation of gene expression.* Briefings in functional genomics & proteomics, 2006. **5**(3): p. 190-208.
91. Meshorer, E. and T. Misteli, *Chromatin in pluripotent embryonic stem cells and differentiation.* Nat Rev Mol Cell Biol, 2006. **7**(7): p. 540-546.
92. Sun, F., et al., *Nuclear reprogramming: the zygotic transcription program is established through an 'erase-and-rebuild' strategy.* Cell Res, 2007. **17**(2): p. 117-134.
93. Huangfu, D., et al., *Induction of pluripotent stem cells by defined factors is greatly improved by small-molecule compounds.* Nat Biotech, 2008. **26**(7): p. 795-797.
94. Shi, Y., et al., *A Combined Chemical and Genetic Approach for the Generation of Induced Pluripotent Stem Cells.* Cell Stem Cell, 2008. **3**(1): p. 119-119.
95. Shi, Y., et al., *Induction of Pluripotent Stem Cells from Mouse Embryonic Fibroblasts by Oct4 and Klf4 with Small-Molecule Compounds.* Cell Stem Cell, 2008. **3**(5): p. 568-574.

96. Huelsken, J. and J. Behrens, *The Wnt signalling pathway.* Journal of cell science, 2002. **115**(21): p. 3977-3978.

97. Li, W., et al., *Generation of Human-Induced Pluripotent Stem Cells in the Absence of Exogenous Sox2.* Stem Cells, 2009. **27**(12): p. 2992-3000.

98. Silva, J., Barrandon, O., Nichols, J., Kawaguchi, J., Theunissen, T.W., Smith, A., *Promotion of reprogramming to ground state pluripotency by signal inhibition.* PLoS Biol, 2008. **6**(10).

99. Ying, Q.-L., et al., *The ground state of embryonic stem cell self-renewal.* Nature, 2008. **453**(7194): p. 519-523.

100. Choi, J., Costa, M.L., Mermelstein, C.S., Chagas, C., Holtzer, H., *MyoD converts primary dermal fibroblasts, chondroblasts, smooth muscle, and retinal pigmented epithelial cells into striated mononucleated myoblasts and multinucleated myotubes.* Proc Natl Acad Sci, 1990. **87**: p. 7988-7992.

101. Vierbuchen, T., Ostermeier, A., Pang, Z.P., Kokubu, Y., Sudhof, T.C., Wernig, M., *Direct conversion of fibroblasts to functional neurons by defined factors.* Nature, 2010. **463**: p. 1035-1041.

102. Leda, M., Fu, J.D., Delgado-Oluguin, P., Vedantham, V., Hayashi, Y., Bruneau, B.G., Srivastava, D., *Direct reprogramming of fibroblasts into functional cardiomyocytes by defined factors.* Cell, 2010. **142**(3): p. 375-386.

103. Szabo, E., Rampalli, S., Risueno, R.M., Schnerch, A., Mitchell, R., Fiebigcomyn, A., Levadoux-Martin, M., Bhatia, M., *Direct conversion of human fibroblasts to multilineage blood progenitors.* Nature, 2010. **468**: p. 521-526.

104. Kim, J., Efe, J.A., Zhu, S., Talantova, M., Yuan, X., Wang, S., Lipton, S.A., Zhang, K., Ding, S., *Direct reprogramming of mouse fibroblasts to neural progenitors.* PNAS, 2011. **108**: p. 7838-7843.

105. Efe, J.A., Hilcove, S., Kim, J., Zhou, H., Ouyang, K., Wang, G., Chen, J., Ding, S., *Conversion of mouse fibroblasts into cardiomyocytes using a direct reprogramming strategy.* Nature Cell Biology, 2011. **13**: p. 215-222.
106. Chalfie, M., H.R. Horvitz, and J.E. Sulston, *Mutations that lead to reiterations in the cell lineages of C. elegans.* Cell, 1981. **24**(1): p. 59-69.
107. Bartel, D.P., *MicroRNAs: Genomics, Biogenesis, Mechanism, and Function.* Cell, 2004. **116**(2): p. 281-297.
108. Doench, J.G. and P.A. Sharp, *Specificity of microRNA target selection in translational repression.* Genes & Development, 2004. **18**(5): p. 504-511.
109. Kirton, L., *Analysis of miRNA and mRNA associated with Epithelial Mesenchymal Transition.* http://cnx.org/content/m36053/1.2/, 2010.
110. Denli, A.M., et al., *Processing of primary microRNAs by the Microprocessor complex.* Nature, 2004. **432**(7014): p. 231-235.
111. Lund, E., et al., *Nuclear Export of MicroRNA Precursors.* Science, 2004. **303**(5654): p. 95-98.
112. Hutvagner, G., et al., *A Cellular Function for the RNA-Interference Enzyme Dicer in the Maturation of the let-7 Small Temporal RNA.* Science, 2001. **293**(5531): p. 834-838.
113. www.ambion.com/techlib/resources/miRNA/mirna_pro.html, 2011.
114. Visvanathan, J., Lee, S., Lee, B., Lee, J.W., Lee, S.K. , *The microRNA miR-124 antagonizes the anti-neural REST/SCP1 pathway during embryonic CNS development.* Genes Dev, 2007. **21**: p. 744-749.
115. Judson, R.L., Babiarz, J.E., Venere, M., Belloch, R., *Embryonic stem cell-specific microRNAs promote induced pluripotency.* Nat Biotech, 2009. **27**: p. 459-461.

116. Anokye-Danso, F., Trivedi, C.M., Juhr, D., Gupta, M., Cui, Z., Tian, Y., Zhang, Y., Yang, W., Gruber, P.J., Epstein, J.A., *Highly efficient miRNA-mediated reprogramming of mouse and human somatic cells to pluripotency.* Cell Stem Cell, 2011. **8**: p. 376-388.
117. Miyoshi, N., et al., *Reprogramming of Mouse and Human Cells to Pluripotency Using Mature MicroRNAs.* Cell Stem Cell, 2011. **8**(6): p. 633-638.
118. Pillai, R., *MicroRNA function: multiple mechanisms for a tiny RNA?* RNA, 2005. **12**: p. 1753-61.
119. Xu, N., Papagiannakopoulos, T., Pan, G., Thomson, J.A., Kosik, K.S., *MicroRNA-145 Regulates OCT4, SOX2, and KLF4 and Represses Pluripotency in Human Embryonic Stem Cells.* Cell, 2009. **137**(4): p. 647-658.
120. Neveu, P., et al., *MicroRNA Profiling Reveals Two Distinct p53-Related Human Pluripotent Stem Cell States.* Cell Stem Cell. **7**(6): p. 671-681.
121. Zhao, Y., et al., *Two Supporting Factors Greatly Improve the Efficiency of Human iPSC Generation.* Cell Stem Cell, 2008. **3**(5): p. 475-479.
122. Kawamura, T., et al., *Linking the p53 tumour suppressor pathway to somatic cell reprogramming.* Nature, 2009. **460**(7259): p. 1140-1144.
123. Suzuki, H.I., Yamagata, K., Sugimoto, K., Iwamoto, T., Kato, S., Miyazono, K. , *Modulation of microRNA processing by p53.* Nature, 2009. **460**: p. 529-533.
124. Loh, Y., Agarwal, S., Park, I., Urbach, A., Hongguang Huo, H., Garrett C. Heffner, G.C., Kim, K., Miller, J.D., Ng, K., Daley, G.Q., *Generation of induced pluripotent stem cells from human blood.* Hematopoiesis and Stem Cells, 2009. **113**(22): p. 5476-5479.

125. Song, B., Niclis, J.C., Alikhan, M.A., Sakkal, S., Sylvain, A., Kerr, P.G., Lasett, A.L., Bernard, C.A., Ricardo, S.D., *Generation of induced pluripotent stem cells from human kidney mesangial cells.* J Am Soc Nephrol, 2011. **22**: p. 1213-1220.

126. Anchan, R.M., Quaas, P., Gerami-Naini, B., Bartake, H., Griffin, A., Zhou, Y., Day, D., Eaton, J.L., George, L.L., Naber, C., Turbe-Doan, A., Park, P.J., Hornstein, M.D., Maas, R.L., *Amniocytes can serve dual function as a source of iPS cells and feeder layers.* Human Molecular Genetics, 2011. **20**(5): p. 962-974.

127. Brown, M.E., Rondon, E., Rajesh, D., Mack, A., Lewis, R., Feng, X., Zitur, L.J., *Derivation of induced pluripotent stem cells from human peripheral blood T lymphocytes.* PLoS ONE, 2010. **5**(6).

128. Aasen, T., Raya, A., Barrero, M. J., Garreta, E., Consiglio, A., Gonzalez, F., Vassena, R., Bilic, J., Pekarik, V., Tiscornia, G., Edel, M., Boue, S., Izpisua Belmonte, J. C., *Efficient and rapid generation of induced pluripotent stem cells from human keratinocytes.* Nat Biotech, 2008. **26**(11): p. 1276-1284.

129. Haase, A., et al., *Generation of Induced Pluripotent Stem Cells from Human Cord Blood.* Cell Stem Cell, 2009. **5**(4): p. 434-441.

130. Weiss, R., Teich, N., Varmus, H., Coffin, J., *RNA tumor viruses.* Cold Spring Harbour Laboratories, 1982. **2**.

131. Okano, M., et al., *DNA Methyltransferases Dnmt3a and Dnmt3b Are Essential for De Novo Methylation and Mammalian Development.* Cell, 1999. **99**(3): p. 247-257.

132. Jahner, D., et al., *De novo methylation and expression of retroviral genomes during mouse embryogenesis.* Nature, 1982. **298**(5875): p. 623-628.

133. Kustikova, O., et al., *Clonal Dominance of Hematopoietic Stem Cells Triggered by Retroviral Gene Marking.* Science, 2005. **308**(5725): p. 1171-1174.

134. Hockemeyer, D., et al., *A Drug-Inducible System for Direct Reprogramming of Human Somatic Cells to Pluripotency.* Cell Stem Cell, 2008. **3**(3): p. 346-353.
135. Aoi, T., et al., *Generation of Pluripotent Stem Cells from Adult Mouse Liver and Stomach Cells.* Science, 2008: p. 1154884.
136. Stadtfeld, M., et al., *Induced Pluripotent Stem Cells Generated Without Viral Integration.* Science, 2008. **322**(5903): p. 945-949.
137. He, T.-C., et al., *A simplified system for generating recombinant adenoviruses.* Proceedings of the National Academy of Sciences, 1998. **95**(5): p. 2509-2514.
138. Yu, J., Hu, K., Smuga-Otto, K., Tian, S., Stewart, R., Slukvin, I.I., Thomson, J.A., *Human induced pluripotent stem cells free of vector and transgene sequences.* Science, 2009. **324**: p. 797-801.
139. Soldner, F., Hockemeyer, D., beard, C., Gao, Q., Bell, G.W., Cook, E.G., Hargus, G., Blak, A., Cooper, O., Mitalipova, M., Isacson, O., Jaenisch, R., *Parkinson's disease patient-derived induced pluripotent stem cells free of viral reprogramming factors.* Cell, 2009. **136**(5): p. 964-977.
140. Kim, D., et al., *Generation of Human Induced Pluripotent Stem Cells by Direct Delivery of Reprogramming Proteins.* Cell Stem Cell, 2009. **4**(6): p. 472-476.
141. Cho, H.J., Lee, C.S., Kwon, Y.W., Paek, J.S., Lee, S.H., Hur, J., Lee, E.J., Roh, T.Y., Chu, I.S., Leem, S.H., , *Induction of pluripotent stem cells from adult somatic cells by protein-based reprogramming without genetic manipulation.* Blood, 2010. **116**: p. 386-395.
142. Warren, L., Manos, P.D., Ahfeldt, T., Loh, Y., Li, H., Lau, F., Ebina, W., Smith Z.D., Meissner, A., Daley, G.Q., *Highly efficient reprogramming to pluripotency and directed differentiation of human cells using synthetic modified mRNA.* Cell Stem Cell, 2010. **7**(5): p. 618-630.

143. Yusa, K., Rad, R., Takeda, J., Bradley, A., *Generation of transgene-free induced pluripotent mouse stem cells by the piggyBac transposon.* Nature, 2009. **6**: p. 363-369.
144. Jia, F., Wilson, K.D., Sun, N., Gupta, D.M., Huang, M., Li, Z., Panetta, N.J., Chen, Z.Y., Robbins, R.C., Kay, M.A., Longaker, M.T., Wu, J.C., *A nonviral minicircle vector for deriving human iPS cells.* Nature, 2010. **7**(3): p. 197-199.
145. Felgner, P.L., et al., *Lipofection: a highly efficient, lipid-mediated DNA-transfection procedure.* Proceedings of the National Academy of Sciences, 1987. **84**(21): p. 7413-7417.
146. Weisman, S., *Lipoplexes*, in *Nanotechnologies for the Life Sciences*. 2007, Wiley-VCH Verlag GmbH & Co. KGaA.
147. Sakurai, F., Nishioka, T., Saito, H., Baba, T., Okuda, A., Matsumoto, O., Taga, T., Yamashita, F., Takakura, Y., Hashida, M., *Interaction between DNA-cationic liposome complexes and erythrocytes is an important factor in systemic gene transfer via the intravenous route in mice: the role of the neutral helper lipid* Gene Therapy, 2001. **8**: p. 677-686.
148. Gresch, O., et al., *New non-viral method for gene transfer into primary cells.* Methods, 2004. **33**(2): p. 151-163.
149. Schofield, J.P. and C.T. Caskey, *Non-viral approaches to gene therapy.* British Medical Bulletin, 1995. **51**(1): p. 56-71.
150. Haber, J.E., *DNA repair: Gatekeepers of recombination.* Nature, 1999. **398**(6729): p. 665-667.
151. Quenneville, S.P., et al., *Nucleofection of Muscle-Derived Stem Cells and Myoblasts with [phi]C31 Integrase: Stable Expression of a Full-Length-Dystrophin Fusion Gene by Human Myoblasts.* Mol Ther, 2004. **10**(4): p. 679-687.
152. Lakshmipathy, U., et al., *Efficient Transfection of Embryonic and Adult Stem Cells.* Stem Cells, 2004. **22**(4): p. 531-543.

153. Balasubramaniyan, V., et al., *Transient Expression of Olig1 Initiates the Differentiation of Neural Stem Cells into Oligodendrocyte Progenitor Cells.* Stem Cells, 2004. **22**(6): p. 878-882.

154. Jörg H. W. Distler, A.J., Mariola Kurowska-Stolarska, Beat A. Michel, Renate E. Gay, Steffen Gay, Oliver Distler,, *Nucleofection: a new, highly efficient transfection method for primary human keratinocytes*.* Experimental Dermatology, 2005. **14**(4): p. 315-320.

155. Chang, C.J., Mitra, K., Koya, M., Velho, M., Desprat, R., Bouhassira, E.E., *Production of embryonic and fetal-like red blood cells from human induced pluripotent stem cells.* PLoS ONE, 2011. **6**(10).

156. Kokkinaki, M., Sahibzada, N., Golestaneh, N., *Human induced pluripotent stem-derived retinal pigment epithelium (RPE) cells exhibit ion transport, membrane potential, polarized vacular endothelial growth factor secretion, and gene expression pattern similar to native RPE.* Stem Cells, 2011. **29**(5): p. 825-835.

157. Jung, Y., Bauer, G., Nolta, J.A., *Induced pluripotent stem cell-derived mesenchymal stem cells: Progress toward safe clinical products.* Stem Cells, 2011. **Epub ahead of print**.

158. Espejel, S., Roll, G.R., MsLaughlin, K.J., Lee, A.Y., Zhang, J.Y., Laird, D.J., Okita, K., Yamanaka, S., Willenberg, H., *Induced pluripotent stem cell-derived hepatocytes have the functional and proliferative capabilities needed for liver regeneration in mice.* J Clin Invest, 2010. **120**(9): p. 3120-3126.

159. Somers, A., Jean, J., Sommer, C.A., Omari, A., Ford, C.C., Mills, J.A., Ying, L., Sommer, A.G., Jean, J.M., Smith B.W., Lafyatis, R., Demierre, M., Weiss, D.J., French, D.L., Gadue, P., Murphy, G.J., Mostoslavsky, G., Kotton, D.N., *Generation of transgene-free lung disease-specific human induced pluripotent stem cells using a single*

excisable lentiviral stem cell cassette. Stem Cells, 2010. **28**: p. 1728-1740.

160. Ye, Z., Zhan, H., Mali, P., Dowey, S., Williams, D.M., Jang, Y.Y., Dang, C.V., Spivak, J.L., Moliterno A.R., Cheng, L., *Human induced pluripotent stem cells from blood cells of healthy donors and patients with acquired blood disorders.* Blood, 2009. **114**: p. 5473-5480.
161. Carvajal-Vergara, X., Sevilla, A., D'Souza, S.L., Ang, Y., Schaniel, C., Lee, D., Kaplan, A.D., Adler, E.D., Rozov, R., Ge, Y., Cohen, N., Edelmann, L.J., Chang, B., Waghray, A., Su, J., Pardo, S., Lichtenbelt, K.D., Tartaglia, M., Gelb, B.D., Lemischka, I.R., *Patient-specific induced pluripotent stem-cell-derived models of LEOPARD syndrome.* Nature, 2010. **465**: p. 808-812.
162. Ma, J., Guo, L., Fiene, S.J., Anson, B.D., Thomson, J.A., Kamp, T.J., Kolaja, K.L., Swanson, B.J., January, C.T., *High purity human induced pluripotent stem cell (hiPSC) derived cardiomyocytes: Electrophysiological properties of action potentials and ionic currents.* Am J Physiol Heart Circ Physiol, 2011. **301**(5): p. Epub ahead of print.
163. Anson, B., Nuwaysir, E., Wang, W.B., Swanson, B., *Industrialized production of human iPSC-derived cardiomyocytes for use in drug discover and toxicity testing.* BioPharm International, 2011. **24**(3): p. 58-67.
164. Gonzales, K.A.U., Ng, H, *Choreographing pluripotency and cell fate with transcription factors.* Biochimica et Biophysica Acta, 2011. **1**(1809): p. 337-349.
165. Adewumi, O., et al., *Characterization of human embryonic stem cell lines by the International Stem Cell Initiative.* Nat Biotechnol, 2007. **25**(7): p. 803-16.

166. Streuli, C.H., Schmidhauser, C., Kobrin, M., Bissell, M., Derynck, R., *Extracellular matrix regulates expression of the TGF-β1 gene.* J Cell Biol, 1993. **120**: p. 253-260.

167. Adams, J.C., Watt, F. M., *Expression of β1, β3, β4 and β5 integrins by human epidermal keratincytes and non-differentiating keratinocytes.* J. Cell Biol., 1991. **115**: p. 829-841.

168. Baxter, M.C., M. Bates, N. Small, F. Murray, P. Edgar, D. Kimber, S.J., *Analysis of the distinct functions of growth factors and tissue culture substrates necessary for the long-term self-renewal of human embryonic stem cell lines.* Stem Cell Research, 2009. **3**(1): p. 28-38.

169. Uchida, E.M., H. Ishii-Watabe, A. Hayakawa, T., *Comparison of the efficiency and safety of non-viral vector-mediated gene transfer into a wide range of human cells.* Biol Pharm Bull, 2002. **25**: p. 891-897.

170. Rice, R.H., Green, H., *Presence in human epidermal cells of a soluble protein presursor of the cross-linked envelope: activation of the cross-linking calcium ions.* Cell, 1979. **18**: p. 681-694.

171. Watt, F.M., *Involucrin and other markers of keratinocyte terminal differentiation.* Journal of Investigative Dermatology, 1983. **81**: p. 100-103.

172. Yang, Z., Schmitt, J.F., Lee, E.H., *Immunohistochemical analysis of human mesenchymal stem cells differentiating into chondrogenic, osteogenic and adipogenic lineages.* Methods in Molecular Biology, 2011. **698**: p. 353-366.

173. Eyre, D.R., *The collagens of articular cartilage.* Semin Arthritis Rheum, 1991. **21**: p. 2-11.

174. Yang, W., rachez, C., Freedman, L.P., *Dicrete roles for perioxisome proliferator-activated receptor y and retinoid X receptor in recruiting nuclear receptor coactivators.* Molecular and Cellular Biology, 2000. **20**: p. 8008-8017.

175. Lendahl, U., Zimmerman, L.B., McKay, R.D., *CNS stem cells express a new class of intermediate filament protein.* Cell, 1990. **60**(4): p. 585-595.

176. Peppas, N.A.H., J.Z. Khademhosseini, A. Langer, R, *Hydrogels in Biology and Medicine: From Molecular Principles to Bionanotechnology.* Advanced Materials, 2006. **18**(11): p. 1345-1360.

177. Monlinaro, G., Leroux, J.C., Damas, J., Adam, A., *Biocompatibility of thermosensitive chitosan-based hydrogels:an in vivo experimental approach to injectable biomaterials.* Biomaterials, 2002(23): p. 2717-2722.

178. Bryan, N., N.P. Rhodes, and J.A. Hunt, *Derivation and performance of an entirely autologous injectable hydrogel delivery system for cell-based therapies.* Biomaterials, 2009. **30**(2): p. 180-188.

179. Richards, M. and A. Bongso, *Propagation of Human Embryonic Stem Cells on Human Feeder Cells*, in *Methods of Molecular Biology*. 2006. p. 23-41.

180. Mitsui, K., et al., *The Homeoprotein Nanog Is Required for Maintenance of Pluripotency in Mouse Epiblast and ES Cells.* Cell, 2003. **113**(5): p. 631-642.

181. Rodda, D.J., et al., *Transcriptional regulation of nanog by OCT4 and SOX2.* J Biol Chem, 2005. **280**(26): p. 24731-7.

182. Cowan, C.A., Klimanskaya, I., McMahon, J., Atienza, J., Witmyer, J., Zucker, J.P., Wang, S., Morton, C.C., McMahon, A.P., Powers, D., Melton, D.A., *Derivation of embryonic stem-cell lines from human blastocysts.* N Engl J Med, 2004. **350**: p. 1353-1356.

183. Braam, S.R., Denning, C., Van den Brink, S., Kats, P., Hochstenbach, R., Passier, R., Mummery, C.L., *Improved genetic manipulation of human embryonic stem cells.* Nature Methods, 2008. **5**: p. 389-392.

184. Osafune, K., Caron, L., Borowiak, M., Martinez, R.J., Fitz-Gerald, C.S., Sato, Y., Cowan, C.A., Chien K.R., Melton, D.A., *Marked differences in differentiation propensity among human embryonic stem cells lines* Nature Biotechnology, 2008. **26**: p. 313-315.

185. Hoffman, L.M., Carpenter M.K., *Characterization and culture of human embryonic stem cells.* Nat Biotech, 2005a. **23**: p. 699-708.

186. Metallo, C.M., Mohr, J.C., Detzel, C.J., dePablo, J.J., van Wie, B.J., Palecek, S.P., *Engineering the stem cell microenvironment.* Biotechnology Prog, 2007. **23**(1): p. 18-23.

187. Fuchs, E., Tumbar, T., Guasch, G., *Socializing with the neighbours: stem cells and their niche.* Cell, 2007. **116**(6): p. 769-778.

188. Booth, B.W., Mack, D.L., Androutsellis-Theotokis, A., McKay, R.D.G., Boulanger, C.A., Smith, G.H., *The mammary micorenvironment alters the differentiation repertoire of neural stem cells.* PNAS, 2008. **105**(39): p. 14891-14896.

189. Adams, J.C., Watt, F.M., *Expression of beta 1, beta 3, beta 4, and beta 5 integrins by human epidermal keratinocytes and non-differentiating keratinocytes.* J Cell Biol, 1991. **115**(3): p. 829-841.

190. Fujisaki, H., Hattori, S., *Keratinocye apoptosis on type I collagen gel caused by lack of laminin 5/10/11 deposition and Akt signalling.* Experimental Cell Research, 2002. **280**(2): p. 255-269.

191. Okita, K., et al., *Generation of Mouse Induced Pluripotent Stem Cells Without Viral Vectors.* Science, 2008. **322**(5903): p. 949-953.

192. Maasho, K., Marunsina, A., Reynolds, N.M., Coligan, J.E., Borrego, F., *Efficient gene transfer into the human natural killer cell line, NKL, using the Amaxa nucleofection system* Journal Of Immunological Methods, 2004. **284**: p. 133-140.

193. Schmidt, H., Altrogge, L., Lenz, D., Riemen, G., Brosterhus, H., Lorbach, E., Helfrich, J., Hein, K., Gremse, M., Males, T., Christine, R., Siebenkotten, G., Ortmann, B., Turbanski, T., Klaes, A.,

Modular Transfection Systems. United States Patent and Trademark Office (US Patent ed), 2008. **7320859**.

194. Lonza, *Optimized protocol for human keratinocytes-adult.* 2011.
195. Jacobsen, F., Mertens-Rill, J., Beller, J., Hirsch, T., Daigeler, A., Langer, S., Lehnhardt, M., Steinau, H., Steinstraesser, L., *Nucleofection: A new method for cutaneous gene transfer?* J Biomed Biotechnol, 2006. **2006**(5): p. 1-8.
196. Lenz, P., Bacot, S.M., Frazier-Jessen, M.R., Feldman, G.M., *Nucleoporation of dendritic cells: efficient gene transfer by electroporation into human monocyte-derived dendritic cells.* FEBS Lett, 2003. **538**(1-3): p. 149-154.
197. Adams, J.C., Watt, F.M., *Changes in keratinocyte adhesion during termianl differentiation: reduction in fibronectin binding preceds alpha 5 beta 1 integrin loss from cell surface.* Cell, 1990. **63**: p. 425-435.
198. Jensen, U.B., Peterson, M.S., Lund, T.B., Jensen, T. G., Bolund, L., *Transgene expression in human epidermal keratinocytes: cell cycle arrest of productively transfected cells.* Exp Dermatol, 2000. **9**: p. 298-310.
199. Schweizer, J., Bowden, P.E., Coulombe, P.A., Langbein, L., Lane, E.B., Magin, T.M., Maltais, L., Omary, M.B., Parry, D.A., Rogers, M.A., Wright, M.W., *New consensus nomenclature for mammalian keratins.* J Cell Biol, 2006. **174**(2): p. 169-174.
200. Luowei, L., Tennenbaum, T., Yuspa, S.H., *Suspension-induced murine keratinocyte differentiation is mediated by calcium.* Journal of Investigative Dermatology, 1995. **106**: p. 254-260.
201. Johnson, B.D., Gershan, J.A., Natalia, N., Zujewski, H., Weber, J.J., Yan, X., Orentas, R.J., *Neuroblastoma cells transiently transfected to simultaneously express the co-stimulatory molecules CD54,*

CD80, CD86, and CD137L generate antitumor immunity in mice. Journal of Immunotherapy, 2005. **28**(5): p. 449-460.

202. Distler, J.H., Jungel, A., Kurowska-Stolarska, M., Michel, B.A., Gay, R.E., Distler, O., *Nucleofection: a new, highly efficient transfection method for primary human keratinocytes.* Exp Dermatol, 2005. **14**(4): p. 315-320.
203. Dickens, S., Van den Berge, S., Hendrickx, B., Verdonck, K., Luttun, A., Vranckx, J.J., *Nonviral transfection strategies for keratinocytes, fibroblasts and endothelial progenitor cells for ex vivo gene transfer to skin wounds.* Tissue Engineering Part C: Methods, 2010. **16**(6): p. 1601-1608.
204. Igoucheva, O., Alexeev, V., *MicroRNA-dependent regulation of cKit in cutaneous melanoma.* Biochemical and Biophysical Research Communications, 2008. **379**(3): p. 790-794.
205. Schulz, T.C., Palmarini, G.M., Noggle, S.A., Weiler, D.A., Mitalipova, M.M., Condie, B.G., *Directed neuronal differentiation of human embryonic stem cells.* BMC Neuroscience, 2003. **4**: p. 27-28.
206. Keravala, A., Ormerod, B.K., Palmer, T.D., Calos, M.P., *Long-Term transgene expression in mouse neural progenitor cells modified with PhiC31 integrase.* J Neurosci Methods, 2008. **173**(2): p. 299-305.
207. Gaughwin, P., Ciesla, M., Yang, H., Lim, B., Brundin, P., *Stage-specific modulation of cortical neuronal development by mmu-miR-134.* Cereb Cortex, 2011. **21**(8): p. 1857-1869.
208. Vo, N., Klein, M.E., Varlamova, O., Keller, D.M., Yamamoto, T., Goodman, R.H., Impey, S., *A cAMP-reponse element binding protein-induced mircoRNA regulates neuronal morphogenesis.* PNAS, 2005. **102**(45): p. 16426-16431.

209. Vizlin-Hodzic, D.J., H., Ryme, J., Simonsson, T., Simonsson, S., *SAF-A has a role in transcriptional regulation of Oct4 in ES cells through promoter binding.* Cell Reprogram, 2011. **13**(1): p. 13-27.
210. Nichols, J., et al., *Formation of Pluripotent Stem Cells in the Mammalian Embryo Depends on the POU Transcription Factor Oct4.* Cell, 1998. **95**(3): p. 379-391.
211. Hermeking, H. and D. Eick, *Mediation of c-Myc-induced apoptosis by p53.* Science, 1994. **265**(5181): p. 2091-2093.
212. Sachdeva, M., Zhu, S., Wu, F., Wu, H., Walia, V., Kumar, S., Elble, R., Watabe, K., Mo, Y., *p53 represses c-Myc through induction of the tumor suppressor miR-145.* PNAS, 2008. **106**(9): p. 3207-3212.
213. Eiselleova, L., Matulka, K., Kriz, V., Kunova, M., Schmidtova, Z., Neradil, J., Tichy, B., Dvorakova, D., Pospisilova, S., Hampl, S., Dvorak, P., *A complex role for FGF-2 in self-renewal, survival, and adhesion of human embryonic stem cells.* Stem Cells, 2009. **27**(8): p. 1847-1857.
214. Xiao, L., Yuan, X., Sharkis, S.J., *Activin A maintains self-renewal and regulates fibroblast growth factor, wnt and bone morphogenetic protein pathways in human embryonic stem cells.* Stem Cells, 2006. **24**(6): p. 1476-1486.
215. Yao, S., Chen, S., Clark, J., Hao, E., Beattie, G.M., Hayek, A., Ding, S., *Long-term self-renewal and directed differentiation of human embryonic stem cells in chemically defined media.* PNAS, 2006. **103**(18): p. 6907-6912.
216. Curran, J.M., Chen, R., Hunt, J.A., *The guidance of human mesenchymal stem cell differentiation in vitro by controlled modifications to the cell substrate.* Biomaterials, 2006. **27**(27): p. 4783-4793.
217. Jaiswal, N., Haynesworth, S.E., Caplan, A.I., Bruder, S.P., *Osteogenic differentiation of purified, culture-expanded human*

mesenchymal stem cells in vitro. J Cell Biochem, 1997. **64**(2): p. 295-312.

218. Yoo, J.U., Barthel, T.S., Nishimura, K., Solchaga, L., Caplan, A.I., Goldberg, V.M., Johnstone, B., *The chondrogenic potential of human bone-marrow derived mesenchymal progenitor cells.* J Bone Joint Surg Am, 1998. **80**: p. 1745-1757.
219. Lecka-Czernik, B., Gubrij, I., Moerman, E.J., Kajkenova, O., Lipschitz, D.A., Manolagas, S.C., Jilka, R.L., *Inhibition of Osf2/Cbfa1 expression and terminal osteoblast differentiation by PPARgamma2.* J Cell Biochem, 1999. **74**(3): p. 357-371.
220. Sung, H., Hong, S., Yoo, J., Oh, J., Shin, H., Choi, I., Ahn, K., Kim, S., Park, Y., Kim, B., *Stemness evaluation of mesenchymal stem cells from placentas according to devlopmental stage: Comparison to those from adult bone marrow.* J Korean Med Sci, 2010. **25**(10): p. 1418-1426.
221. Ducy, P., Zhang, R., Geoffrroy, V., Ridall, A.L., Karsenty, G., *Osf2/CBFA1: A transcriptional activator of osteoblast differentiation.* Cell, 1997. **89**: p. 747-754.
222. Tataria, M., Quarto, N., Longaker, M.T., Sylvester, K.G., *Absence of the p53 tumor suppressor gene promotes osteogenesis in mesenchymal stem cells.* Journal of pediatric surgery, 2006. **41**(4): p. 624-632.
223. Harada, H., Tagashira, S., Fukiwara, M., Ogawa, S., Katsumata, T., Yamaguchi, A., Komori, T., Nakatsuka, M., *Cbfa1 isoforms exert functional differences in osteoblast differentiation.* J Biol Chem, 1999. **274**: p. 2972-6978.
224. Dyson, J.A., Genever, P.G., Dalgarno, K.W., Wood, D.J., *Development of custom-built scaffolds using mesenchymal stem cells and apatite-wollastonite glass-ceramics.* Tissue Eng, 2007. **13**(12): p. 2891-2901.

225. Long, M.W., *Ostoegenesis and bone-marrow-derived stem cells.* Blood Cells Mol Dis, 2001. **27**: p. 677-690.

226. Friedman, M.S., Long, M.W., Hankenson, K.D., *Osteogenic differentiation of human mesenchymal stem cell is regulated by bone morphogenetic protein-6.* Journal Of Cellular Biochemistry, 2006. **98**: p. 538-554.

227. Xu, J., Wang, W., Ludeman, M., Cheng, K., Hayami, T., Lotz, J.C., Kapila, S., *Chondrogenic differentiation of humanmesenchymal stem cells in three-dimensional alginate gels.* Tissue Engineering Part A, 2008. **14**(5): p. 667-680.

228. Mais, A., et al., *Prostanoid pattern and iNOS expression during chondrogenic differentiation of human mesenchymal stem cells.* J Cell Biochem, 2006. **98**(4): p. 798-809.

229. Rosen, E.D., Sarraf, P., Troy, A.E., Bradwin, G., Moore, K., Milstone, D.S., *PPAR gamma is required for the differentiation of adipose tissue in vivo and in vitro.* Mol Cell, 1999. **4**: p. 611-617.

230. Janderova, L., McNeil, M., Murrell, A.N., Mynatt, R.L., Smith, S.R., *Human mesenchymal stem cells as an in vitro model for human adipogenesis.* Obesity research, 2003. **11**: p. 65-74.

231. Zhang, L., Su, P., Xu, C., Chen, C., Liang, A., Du, K., Peng, Y., Huang, D., *Melatonin inhibits adipogenesis and enhance osteogenesis of human mesenchymal stem cells by suppressing PPARy expression and enhancing Runx2 expression.* Journal of Pineal Research, 2010. **49**(4): p. 364-372.

232. Gregoire, F.M., Smas, C.M., Sul, H.S., *Understanding adipocyte differentiation* Physiol Rev, 1998. **78**: p. 783-809.

233. Yang, X., He, X., He, J., Zhang, L., Su, X., Dong, Z., Xu, Y., Li, Y., Li, Y., *High efficient isolation and systematic identification of human adipose-derived stem cells.* Journal of Biomedical Science, 2011. **18**(1): p. 59.

234. Gu, H., Yue, Z., Leong, W.S., Nugraha, B., Tan, L.P., *Control of in vitro neural differentiation of mesenchymal stem cells in 3D macroporous, cellulosic hydrogels.* Regen Med, 2010. **5**(2): p. 245-253.

235. Kim, S.J., Lee. J.K., Kim, J.W., Jung, J.W., Seo, K., Park, S.B., Roh, K.H., Lee, S.R., Hong, Y.H., Kim, S.J., *Surface modification of polydimethylsiloxane (PDMS) induced proliferation and neural-like cells differentiation of umbilical cord blood-derived mesenchymal stem cells.* J Mater Sci Mater Med, 2008. **19**: p. 2953-2962.

236. Midwood, K.S.M., Y. Hsia, H.C. Valenick, L.V. Schwarzbauer, J.E., *Modulation of cell-fibronectin matrix interactions during tissue repair*. Journal of Investigative Dermatology, 2006. **11**: p. 73-78.

237. Marshall, J.F.R., D.C. McCartney, A.C. Mitjans, F. Goodman, S.L. Hart, I.R., *Alpha 5 beta 1 is a receptor for vitronectin and fibrinogen, and acts with alpha 5 beta 1 to mediate spreading on fibronectin.* Journal of cell science, 1995. **108**(3): p. 1227-1238.

238. Ludwig, T.E., Levenstein, M.E., Jones, J.M., Berggren, W.T., Mitchen, E.R., Frane, J.L., Crandall, L.J., Daigh, C.A., Conard, K.R., Piekarczyk, M.S., Llanas, R.A., Thomson, J.A., *Derivation of human embryonic stem cells in defined conditions.* Nature Biotechnol, 2006. **24**: p. 185-187.

239. Klimanskaya, I., Chung, Y., Meisner, L., Johnson, J., West, M.D., Lanza, R., *Human embryonic stem cells derived without feeder cells.* The Lancet, 2005. **365**(9471): p. 1636-1641.

240. Lensch, M.W., Schalaeger, T.M., Zon, L.I., Daley, G.Q., *Teratoma formation assays with human embryonic stem cells: A rationale for one type of human-animal chimera.* Cell Stem Cell, 2007. **1**(3): p. 253-258.

241. Lin, L., Chow, K.L., Leng, Y., *Study of hydroxyapatite osteoinductivity with an osteogenic differentiation of mesenchymal stem cells.* J Biomed Mater Res A, 2009. **89**(2): p. 326-335.

242. Zhou, Z., Yang, D., Nie, J., Ren, Y., Cui, F., *Injectable Poly(ethylene glycol) Dimethacrylate-based hydrogels with hydroxyapatite.* Journal of Bioactive and Compatible Polymers, 2009. **24**: p. 405-423.

243. Kim, J., Kim, I.S., Cho, T.H., Lee, K.B., Hwang, S.J., Tae, G., Noh, I., Lee, S.H., Park, Y., *Bone regeneration using hyaluronic acid-based hydrogel with bone morphogenic protein-2 and human mesenchymal stem cells.* Biomaterials, 2007. **28**(10): p. 1830-1837.

244. Mai, R., Hagedorn, M.G., Gelinsky, M., Werner, C., Turhani, D., Spath, H., Gedrange, T., Lauer, G., *Ectopic bone formation in nude rats using human osteoblasts seeded poly(3)hydroxybutyrate embroidery and hydroxyapatite-collagen tapes constructs.* Journal of Cranio-Maxillofacial Surgery, 2006. **34**: p. 101-109.